

https://dspace.org/

Environmental Reconstruction at Nahoon Point during MIS 5e: Contextualising Human Occupation using a Geoarchaeological Approach

Morrissey, Peter

2019
https://hdl.handle.net/10539/28765

Downloaded from a DSpace repository. https://dspace.org/

Environmental Reconstruction at Nahoon Point during MIS 5e: Contextualising Human Occupation using a Geoarchaeological Approach



Peter Morrissey

676930

A Dissertation submitted to the Faculty of Science, University of the Witwatersrand, Johannesburg, in fulfilment of the requirements for the degree of Master of Science

FACULTY OF SCIENCE

UNIVERSITY OF THE WITWATERSRAND, JOHANNESBURG

2019

DECLARATION

I, Peter Morrissey, declare that this dissertation "*Environmental Reconstruction at Nahoon Point during MIS 5e: Contextualising Human Occupation using a Geoarchaeological Approach*" is my own unaided work. It is being submitted for the Degree of Master of Science at the University of the Witwatersrand, Johannesburg. It has not been submitted before for any degree or examination at any other University.



Peter Morrissey

11 March 2019, East London

ABSTRACT

Several published sites – the Nahoon Point footprint site, Blind River and Bats Cave – and a number of previously unreported artefactual deposits indicate human occupation around East London, Eastern Cape, South Africa, during Early Marine Isotope Stage (MIS) 5 (130–105 ka). These finds are within aeolianite deposits of the Nahoon Formation and shallow marine deposits of the Salnova Formation. Past research has mainly focussed on dating the deposits and on analysing the anatomical details preserved in the human footprints and the Blind River femur. Published work on the stratigraphy and sedimentology of these deposits has been limited in both geographic scale and detail. Depositional and erosional features in the area have been considered to represent both of the two MIS 5e sea-level highstands that are known from global and South African records. However, this argument is undermined by significant uncertainties about stratigraphic relationships between different deposits. The goal of this study was to reconstruct the palaeoenvironmental conditions associated with human occupation during this time period, with a particular focus on resolving stratigraphic uncertainties and determining how many highstands are represented in the local sequence. To this end, logging and sampling of 20 profiles was conducted along several kilometres of coastline around the published sites. The stratigraphic sequence in the study area records the interplay between, and changes in the relative dominance of, aeolian and marine depositional processes and their respective environments of deposition. Two distinct phases of aeolian deposition are preserved in the aeolianites. High-angle cross-bedding and low-angle convex-upwards lamination are the dominant depositional structures. Winds from between the south and the northwest were primarily responsible for dune formation in both phases. This pattern is most similar to the present winter wind regime in the area. Depositional and erosional features in the study area indicate the occurrence of a sea level transgression phase between the two phases of aeolian deposition. This stepped highstand reached a peak of up to 7.82 ± 0.82 m above present mean sea level at around 117.3 ± 6.2 ka. The updated stratigraphy, combined with the dates previously obtained for various deposits, indicate that the Phase 1 aeolianites correlate broadly with the mid-MIS 5e relative lowstand and that the Phase 2 marine deposits formed during the second MIS 5e highstand, while the Phase 3 aeolianites were deposited during late MIS 5e and MIS 5d. No evidence for

the first MIS 5e highstand was found in the study area, although this may have been overprinted by later events. The presence of lithic artefacts in coastal marine deposits at several locations indicates human activity within the intertidal and supratidal zones. Palaeoenvironmental data and trace fossil evidence, from both this work and previous studies, suggest that a variety of marine and terrestrial species were (or may have been) present in the area. The available archaeological information on early MIS 5 human subsistence strategies indicates that human populations would have been able to exploit available food and water resources. Therefore, it is not surprising that the distribution of archaeological deposits within the stratigraphic sequence suggests fairly continuous human occupation of this changing landscape despite environmental variations during early MIS 5.

ACKNOWLEDGEMENTS

This research project would not have been possible without financial support from The Palaeontological Scientific Trust (PAST), The Department of Science and Technology-National Research Foundation (DST-NRF), and the University of the Witwatersrand's Postgraduate Merit Award programme. I wish to acknowledge and thank these bodies for their contributions.

I thank Wendy, Jason and Lily Koll for accommodating me in their home while I conducted my fieldwork. Kevin Cole of the East London Museum and the rangers at the Nahoon Point Nature Reserve provided vital logistical assistance during the fieldwork. Kevin also helped with his extensive knowledge of the area and access to various sources of information. I wish to acknowledge and thank all of them for their help.

Dr Marine Wojcieszak of the Evolutionary Studies Institute at the University of the Witwatersrand conducted FTIR analysis of several samples from Nahoon Point. I am grateful to her for her time and expertise in conducting the analysis and interpreting the FTIR spectra.

My family and friends provided considerable support to me throughout the course of this research. I cannot possibly express my gratitude for all they have done. Kelita Shadrach helped with a great deal of emotional support, proof-reading, figure editing, keeping me fed, and countless small tasks that kept me able to focus on writing this dissertation. I could never thank her enough for all she has done.

Finally, I wish to acknowledge the contribution made to this project by my supervisors: Prof. Jasper Knight and Dr Dominic Stratford. Over the past few years, they have spent a great deal of time training and mentoring me. Their comments and guidance have improved this dissertation enormously. This study would not have been possible without them, and I am forever grateful to them.

DEDICATION

This dissertation is dedicated to my late father, Norman Alan Morrissey (3.10.1949 – 23.7.2017), who passed away while I was conducting the research that is presented here.

He always encouraged my curiosity and taught me the joy of learning about the world. As a poet and a former game ranger, he taught me a unique appreciation for nature in all its beauty and its harshness. He showed me the importance of recognising the complexity that is all around us, in all things. I will always be grateful that he knew Nahoon Point and that I could share some of my work with him before he died.

Thank you for everything Dad!

TABLE OF CONTENTS

ABSTRACT ii

ACKNOWLEDGEMENTS iv

DEDICATION v

LIST OF FIGURES x

LIST OF TABLES xiii

1. INTRODUCTION 1

1.1. RATIONALE 5

1.2. RESEARCH QUESTION AND AIMS 6

1.2.1. Research question 6

1.2.2. Aims 6

1.3. STRUCTURE 7

2. SITE DESCRIPTION 8

2.1. PHYSICAL SETTING AND ENVIRONMENT 8

2.1.1. Climate 8

2.1.2. Geology 10

2.1.3. Geomorphology 13

2.1.4. Flora and Fauna 15

2.2. HUMAN AND FAUNAL TRACKWAYS 17

2.3. DATING 20

2.3.1. Radiocarbon dating by Deacon (1966) 20

2.3.2. Luminescence subtraction dating by Vogel et al. (1999) 20

2.3.3. Optically stimulated luminescence dating by Jacobs & Roberts (2009) 21

2.3.4. Dates for related deposits 23

2.4. ARCHAEOLOGY 23

2.4.1. Bats Cave 24

2.4.2. Blind River 25

2.5. PALAEOENVIRONMENT 26
2.5.1. Palaeoenvironmental models and hypotheses 26
2.5.2. Critique of existing model 29
3. LITERATURE REVIEW 32
3.1. COASTAL AEOLIANITE 32
3.1.1. Aeolian processes 32
3.1.2. Aeolianite cementation 35
3.2. BEACHROCK 37
3.2.1. Coastal marine deposition 37
3.2.2. Beachrock cementation 38
3.3. SOUTH AFRICAN COASTAL AEOLANITES AND BEACHROCK 40
3.3.1. Coastal aeolianites and dunes in South Africa 40
3.3.2. Early MIS 5 sea levels 42
3.4. EARLY MIS 5 ARCHAEOLOGY OF SOUTH AFRICA 45
4. METHODOLOGY 51
4.1. FIELD METHODS 51
4.1.1. Survey and Mapping 51
4.1.2. Logging 53
4.1.3. Sampling 54
4.2. LABORATORY ANALYSIS 55
4.2.1. Treatment of Samples 55
4.2.2. Density and Porosity 55
4.2.3. Carbonate Content 56
4.2.4. Particle Size 57
4.2.5. Thin Section Analysis 59
4.2.6. Fourier Transform Infrared Analysis 61
4.3. INTERPRETATION OF RESULTS 62

5. RESULTS 64
5.1. FIELD RESULTS 64
5.1.1. Profile location description 64
5.1.2. Sedimentary Logs 67
5.1.3. Artefact deposits 120
5.2. LABORATORY RESULTS 126
5.2.1. Density and Porosity 126
5.2.2. Carbonate content 126
5.2.3. Thin section analysis 129
5.2.4. Fourier Transform Infrared Analysis 132
6. DISCUSSION 135
6.1. STRATIGRAPHY 135
6.1.1. Stratigraphic sequence 135
6.1.2. Sedimentary facies 140
6.1.3. Comparison to previous model 148
6.2. AEOLIAN LANDFORMS 150
6.2.1. Phase 1 150
6.2.2. Phase 3 151
6.3. PALAEO-WIND 152
6.4. CEMENTATION OF DEPOSITS 155
6.4.1. Aeolianite 155
6.4.2. Beachrock 156
6.5. SEA LEVEL 158
6.6. HUMAN OCCUPATION 163
6.6.1. Human presence and behaviour 163
6.6.2. Coastal resource availability and exploitation 166
7. CONCLUSIONS 170

7.1. STRATIGRAPHY & CHRONOLOGY 170
7.2. PALAEOENVIRONMENTS 170
7.3. HUMAN-ENVIRONMENTAL INTERACTIONS 172
REFERENCES 174

LIST OF FIGURES

Figure 1.1. The four major sea level 'events' during MIS 5e and early MIS 5d.. 3

Figure 2.1. The Nahoon Point Nature Reserve and immediate surrounds. Inset: the location of East London within South Africa. 9

Figure 2.2. Annual and seasonal wind roses for East London. 11

Figure 2.3. The geology of the area around Nahoon Point.. 12

Figure 2.4. The bathymetry of the nearshore area along the coastline around Nahoon Point. 15

Figure 2.5. The five trackways on the panel in 1964 when it was still *in-situ* at Nahoon Point. 18

Figure 2.6. The sedimentary profiles from which dating samples were taken by Jacobs and Roberts (2009) 22

Figure 2.7. The sedimentary profile at Blind River, the dating sample locations and their respective age determinations 24

Figure 3.1. A cross section schematic of idealised dunes 34

Figure 3.2. A cross-section through a generalised shoreline profile 37

Figure 3.3. The distributions of different calcium carbonate cement types and their fabrics within the coastal zone 39

Figure 3.4. The locations of South African MIS 5e/5d (130 – 105 ka) archaeological and palaeoanthropological sites and the current extent of the major biomes within South Africa. 49

Figure 4.1. The study area within the Nahoon Point Nature Reserve 52

Figure 5.1. The locations within the study area of the 20 profiles logged for this project 65

Figure 5.2. The logged sequence of Profile 1 69

Figure 5.3. A photograph of Profile 1 with the units marked. 70

Figure 5.4. Several examples of disturbed bedding in Unit 3 of Profile 1 71

Figure 5.5. The logged sequence of Profile 2 73

Figure 5.6. A photograph of Profile 2 with the units marked. Inset: close-up photograph of a rhizolith in Unit 5 75

Figure 5.7. The logged sequence of Profile 3 76

Figure 5.8. A photograph of Profile 3 with the units marked. 77

Figure 5.9. The logged sequence of Profile 4 79

Figure 5.10. A photograph of Profile 4 with the units marked. 80

Figure 5.11. The logged sequence of Profile 5 81

Figure 5.12. A photograph of Profile 5 with the units marked. 82

Figure 5.13. Beachrock conglomerate lying unconformably on an eroded aeolianite deposit on Nahoon Point 83

Figure 5.14. The logged sequence of Profile 6 85

Figure 5.15. A photograph of Profile 6 86

Figure 5.16. The logged sequence of Profile 7. 87

Figure 5.17. A photograph of Profile 7 with the units marked 88

Figure 5.18. The logged sequence of Profile 8 89

Figure 5.19. A photograph of Profile 8 with the units marked 90

Figure 5.20. The logged sequence of Profile 9 91

Figure 5.21. A photograph of Profile 9 with the units marked. Inset: close-up photograph of a rhizolith in Unit 1 92

Figure 5.22. The logged sequence of Profile 10. 94

Figure 5.23. A photograph of Profile 10 with the units marked. Inset: a close-up photograph of several rhizoliths in Unit 3 95

Figure 5.24. The logged sequence of Profile 11 96

Figure 5.25. A photograph of Profile 11 with the units marked. 97

Figure 5.26. The logged sequence of Profile 12. 99

Figure 5.27. A photograph of Profile 12 with the units marked 100

Figure 5.28. The logged sequence of Profile 13. 102

Figure 5.29. A photograph of Profile 13 with the units marked. 103

Figure 5.30. The logged sequence of Profile 14. 104

Figure 5.31. A photograph of Profile 14 with the units marked. 105

Figure 5.32. The logged sequence of Profile 15. 107

Figure 5.33. A photograph of Profile 15 with the units marked. 108

Figure 5.34. The logged sequence of Profile 16. 110

Figure 5.35. A photograph of Profile 16 with the units marked 111

Figure 5.36. The logged sequence of Profile 17. 112

Figure 5.37. A photograph of Profile 17 with the units marked. 113

Figure 5.38. The logged sequence of Profile 18. 114

Figure 5.39. A photograph of Profile 18 with the units marked. 115

Figure 5.40. The logged sequence of Profile 19. 116

Figure 5.41. A photograph of Profile 19 with the units marked. 117

Figure 5.42. The logged sequence of Profile 20. 119

Figure 5.43. A photograph of Profile 20 with the units marked. 120

Figure 5.44. Map of the Nahoon Point Nature Reserve indicating the locations of artefact-bearing deposits discovered and/or recorded during the survey of the study area and several previously reported sites 121

Figure 5.45. A relatively well preserved blade photographed *in situ*, cemented to the conglomerate around Nahoon Point.. 123

Figure 5.46. The two artefacts discovered at Profile 15 123

Figure 5.47. Examples of artefacts discovered in aeolianite units in Profile 16. A) the single lithic in Unit 1. B) relatively large overshot flake found at the contact between Unit 1 and Unit 2. C) small flake found at the contact between Unit 1 and Unit 2 124

Figure 5.48. A blade (A) and a flake (B) (arrowed) photographed *in situ* within the conglomerate deposit near Bats Cave.. 125

Figure 5.49. Photomicrographs of sample P1U5.4 taken under cross-polarised light 130

Figure 5.50. Photomicrographs of sample P2U5.2 taken under cross-polarised light 131

Figure 5.51. Concentrations of clay (the brown to reddish-brown in these images) within both rim cements and pore-filling cements and in the form of obviously altered sand-sized grains: A) sample P1U5.4. B) sample P2U5.2 under cross-polarised light. 133

Figure 5.52. The ATR-FTIR spectra for the four analysed samples.. 134

Figure 6.1. Stratigraphic correlation of the logged profiles across the study area. The locations of the profiles within the reserve and within the study area are indicated in the inset map. 137

Figure 6.2. A generalised stratigraphic cross-section of the aeolianite and beachrock deposits in the study area. 139

Figure 6.3. The facies identified in the three depositional phases within the profiles at the study area 141

Figure 6.4. Comparison between a track observed at Nahoon Point and published real-world and theoretical examples of similar tracks. 143

Figure 6.5. Wind roses for Phase 1 and Phase 3 based on dune bedding dip orientation measurements collected from the 20 logged profiles. 153

Figure 6.6. A generalised geological cross-section of the deposits in the study area with the sea level estimates for various features indicated. Inset: An MIS 5e global sea level graph 162

LIST OF TABLES

Table 2.1. A summary of ages and sea level estimates for the phases identified in the MIS 5e palaeoenvironmental model developed by Roberts (2008) and Jacobs & Roberts (2009). 29

Table 3.1. Published dates/date ranges for South African archaeological and palaeoanthropological sites with evidence for human presence or occupation during Early MIS 5 48

Table 3.2. A summary of the known palaeoenvironmental conditions at South African Early MIS 5 sites. 50

Table 4.1. Example of the table used to record data during the analysis of carbonate content through Loss on Ignition. 57

Table 4.2. The standard operating procedure settings used on the Mastersizer 3000 for particle size analysis. 59

Table 5.1. The co-ordinates of each logged profile, the elevations relative to high tide level for the bases of the profiles, and the logged height of each profile. 66

Table 5.2. The stratigraphic position and sedimentary/geomorphic context of the evidence for human presence within the study area. 122

Table 5.3. The porosity, density and carbonate content of the 68 bulk samples collected from the study area..... 127

Table 6.1. A summary of the evidence for local sea level during Phase 2 collected from the study area and the estimates made from this evidence.. 159

1. INTRODUCTION

In 1964, three *Homo sapiens* footprints were found preserved in coastal aeolianite at Nahoon Point near East London, Eastern Cape Province, South Africa (Mountain 1966; Roberts 2008). The tracks of at least three other vertebrate species were found in association with the human footprints (Mountain 1966). The faunal trackways have been identified to various degrees of taxonomic resolution, but as the taxa have fairly broad environmental ranges, they provide only very general palaeoenvironmental information (K. Cole pers. comm. 2016).

Coastal aeolianite, sometimes (but not in this dissertation) referred to as dune-rock or dune calcarenite, is a type of rock that is formed through the cementation of sand within sand dunes and related aeolian deposits as a result of the dissolution and re-precipitation of calcium carbonate ($CaCO_3$) by water (Fairbridge & Johnson 1978; Brooke 2001; McLaren 2007). These rocks are composed of relatively well-sorted sands and preserve depositional features characteristic of aeolian deposits, such as high-angle cross-bedding (Fairbridge & Johnson 1978; Brooke 2001; McLaren 2007). Dunes and other accumulations of wind-blown sand are common in coastal areas due to the presence of strong winds and the availability of sediment on the coastal margin (Tinley 1985; Abegg *et al*. 2001; Bateman *et al*. 2004, 2011; Roberts *et al*. 2014). Bioclasts (fragmentary remains of marine shells) in the sediment commonly provide the $CaCO_3$ required to cement the aeolian deposits (Gardner & McLaren 1994; Brooke 2001; McLaren 2007).

Beachrock and pedogenic calcrete are also present within the sequence on Nahoon Point, often in contact with aeolianite deposits (Mountain 1966; Roberts 2008). Beachrocks form through the lithification of beach deposits as a result of the precipitation of calcium carbonate cements around and between grains and clasts (up to large boulders) within the deposits (Hopley 1986; Gischler 2007; Vousdoukas *et al*. 2007; Mauz *et al*. 2015). Beachrock is distinguishable from aeolianite due to a lack of aeolian bedding structures, relatively poorly sorted grain size profiles, and differences in the types of calcium carbonate cements (Hopley 1986; Gischler 2007; Vousdoukas *et al*. 2007; Mauz *et al*. 2015). Around Nahoon Point specifically, beachrock can be distinguished from aeolianite due to the presence of clasts larger

than sand (up to and including boulders) and relatively large shell fragments (Mountain 1966; Roberts 2008; Jacobs & Roberts 2009).

Calcrete is a calcium carbonate-rich rock type which forms below the landscape surface through the precipitation of calcium carbonate cement into soils or other sediments by saturated groundwater to such a degree that the original grains are displaced and replaced (Goudie 1973; Watts 1980; Wright 2007). In sharp contrast to aeolianite and beachrock, calcretes form during periods of limited physical deposition when landscapes are relatively stable (Wright 2007). Pedogenic calcrete can be distinguished from aeolianite in the field by the lack of aeolian bedding structures and the fact that it is significantly more strongly cemented – which can be observed in the hardness of the rock, much higher visible calcium carbonate content in the calcretes, and notably lower visible porosity than aeolianite (e.g. Butzer 2004; Wright 2007; Roberts *et al*. 2009; Lipar *et al*. 2017).

The aeolianite at the footprint site has been dated using Optically Stimulated Luminescence to between 128 000 and 120 000 years ago (128 and 120 ka) (Jacobs & Roberts 2009), which falls within Marine Isotope Stage (MIS) 5e (130 – 115 ka), the last interglacial (Shackleton *et al*. 2003). At a location several kilometres to the west of Nahoon Point, a marine deposit on a raised bench in aeolianite similar to that at the footprint site was dated to between 123.5 and 111.1 ka (Jacobs & Roberts 2009). An overlying bioturbated aeolianite deposit was found to date between 123.3 and 108.3 ka (Jacobs & Roberts 2009).

The sea level history of MIS 5e can be divided into four ‘events’ (Figure 1.1), including two highstands, a relative lowstand and an eventual regression (Wilson *et al*. 1998; Zazo 1999; Dumas *et al*. 2006; Hearty *et al*. 2007; Kopp *et al.* 2009, 2013; Thompson *et al*. 2011; O’Leary *et al*. 2013; Gischler 2014). The precise timing and magnitude of these events are still subject to some debate, but can be assigned to rough time periods. The early MIS 5e highstand (Figure 1.1) occurred between ~132 ka and ~126 ka, and was followed by the mid-MIS 5e lowstand (Figure 1.1) from ~126 ka to ~122 ka. The late MIS 5e highstand (Figure 1.1) began ~122 ka and ended ~118 ka with the start of the late MIS 5e/MIS 5d regression (Figure 1.1). The

terms defined here (and their rough ages) will be used throughout this dissertation. The nature of these events will be considered in greater detail in following chapters.

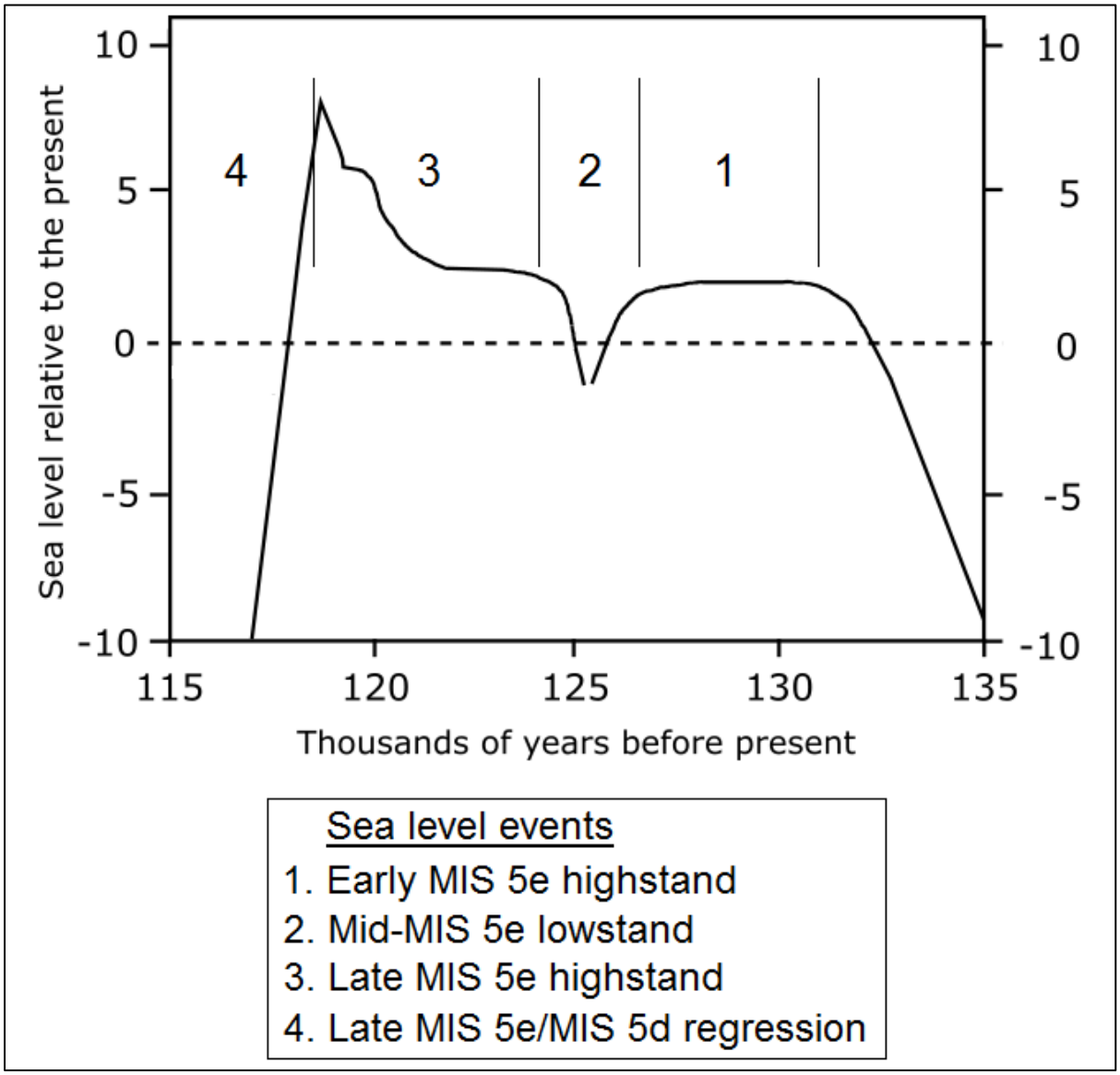


Figure 1.1. The four major sea level 'events' during MIS 5e and early MIS 5d (after Hearty *et al*. 2007). Age ranges for the events are presented in the text above. Note that the relative sea levels reached during the first and second highstands may have been more similar to one another than reflected in this particular diagram.

The date ranges obtained by Jacobs and Roberts (2009) are fairly wide, but the sequence has been argued to indicate the interruption of dune formation during the mid-MIS 5e lowstand by the late MIS 5e transgression (generally argued to have peaked at ~120 ka) followed by the resumption of aeolian deposition during late MIS 5e and early MIS 5d (115 – 105 ka) (Jacobs & Roberts 2009). The palaeo-dunes

preserved in the aeolianite at Nahoon Point indicate that sea level was similar to present during their formation because the shoreline was close enough for marine sediment to be blown to, and deposited at the Point, but far enough away from this location that dune formation was not prevented by storm waves (Roberts 2008; Jacobs & Roberts 2009).

The pedogenic calcrete which caps the aeolianite in places (Roberts 2008) indicates a period of landscape stability after the formation of the aeolianite. As the calcrete most likely formed during a cooler period well after the MIS 5e interglacial (Butzer 2004; Roberts *et al*. 2009, 2014; Lipar *et al*. 2017) and thus, will provide little palaeoenvironmental information about this period of time, the calcretes will receive limited attention in this dissertation.

The published sites of Blind River and Bats Cave, both within a few kilometres of Nahoon Point, provide evidence for human occupation of the area during the MIS 5e transgression (Deacon 1966; Wang *et al*. 2008; Jacobs & Roberts 2009). Several small previously-unreported assemblages of lithic artefacts (stone tools) found in the vicinity of Nahoon Point also indicate some degree of occupation during other periods of MIS 5e or MIS 5d. Altogether, the footprints and the artefactual deposits suggest that the landscape around Nahoon Point was occupied and utilised fairly continuously (at least at the available temporal resolution) during different environmental stages (including at least one sea level highstand and two periods of relatively low sea level [Roberts 2008; Jacobs & Roberts 2009]) within MIS 5e, and possibly MIS 5d.

The archaeological record of the Middle Stone Age (MIS 9 – 2: ~300 ka - ~20 ka) provides evidence for human occupation of a wide range of physical environments (Wadley 2015; Carr *et al*. 2016). The ability of Middle Stone Age humans to adapt culturally to a range of environments has been argued to be a potential indicator of cognitive modernity (McBrearty & Brooks 2000; Henshilwood & Marean 2003; McBrearty 2007; Marean 2014, 2016). Only nine archaeological sites and two palaeoanthropological sites in South Africa have yielded deposits which date to MIS 5e and/or MIS 5d. The sites utilised in this study are among a handful of sites that

preserve evidence for human occupation of coastal environments during this period (Wadley 2015).

1.1. RATIONALE

Past research at Nahoon Point has focused on dating the footprints (Deacon 1966; Vogel *et al*. 1999; Jacobs & Roberts 2009), identifying the species responsible for the faunal trackways (Mountain 1966; Roberts 2008; K. Cole pers. comm. 2016), and analysing the anatomical details preserved in the human footprints (Roberts 2008). To date, work on the geology of the site has been largely descriptive and has focused on the lithology and general geomorphology of the deposits (Mountain 1966; Le Roux 1989a, b; Roberts 2008). Therefore, there is currently only a limited understanding of the geological and environmental context of the Nahoon footprints (Mountain 1966; Roberts 2008). Consequently, the environmental context of human occupation at Nahoon during MIS 5e and (potentially) MIS 5d is poorly known.

Coastal environments are affected by a wide range of terrestrial and oceanic processes (Brooke 2001; Shaw *et al*. 2001; Bateman *et al*. 2004). Various factors, such as the prevailing wind and wave climate, sea level, the existing geology, and geomorphological processes, control the formation and dynamics of the physical environment (Cooper & Flores 1991; Miller & Mason 1994; Illenberger 1996; Brooke 2001; Bateman *et al*. 2004, 2011; Chase & Thomas 2006). Factors such as distance from the sea and topography can result in important differences between local environments over very short distances within the coastal zone (Bird 2008; Davidson-Arnott 2010). Therefore, the exact nature of the physical characteristics and ecology of coastal environments can differ considerably over space and time.

This project focuses on understanding the palaeoenvironmental context of the Nahoon site using an integrated geoarchaeological approach. This integrated approach involved contextualising evidence for human occupation (including both the Nahoon Point footprints and newly-discovered lithic artefacts) within the physical environment, and the ecosystem/s that existed at the time. This required reconstruction of the palaeoenvironments associated with the human footprints and artefact deposits. Of particular interest was testing the assumption (detailed in

Chapter 2) that the sequence at and around Nahoon Point records both of the MIS 5e sea-level highstands. The reconstruction was achieved through sedimentological analysis of the aeolianite strata (and other relevant sedimentary features) using both field and laboratory-based techniques.

Unlike previous studies, which have focused on individual outcrops in varying degrees of detail and at a relatively low stratigraphic resolution (Mountain 1966; Le Roux 1989a, b; Roberts 2008), this study was based on the detailed stratigraphic and sedimentological analysis of 20 profiles spread across several kilometres of coastline around Nahoon Point. Therefore, this work provides considerably more information on spatial and temporal patterns within the aeolianite sequence.

1.2. RESEARCH QUESTION AND AIMS

1.2.1. Research question

This research project is framed around a single research question:

What were the local physical environmental conditions within the study area during the time period when the footprints were formed and lithic artefacts were discarded?

1.2.2. Aims

This project has three aims, which address the research question stated above.

1. To clarify the stratigraphic history of, and relationships between, the aeolianite and deposits of other sedimentary rocks (such as beachrock and calcrete) at Nahoon Point and the surrounding area. This allows for the determination of the relative ages of the different geomorphological features in the study area and thus, the use of these features as evidence for palaeoenvironmental conditions during various parts of the sequence.

2. To determine what processes formed the sand dunes that the human footprints were preserved in, and any contemporaneous geomorphological features (e.g. inter-dune deposits).

3. To reconstruct the local environment within the study area during the period of interest based on the clarified understanding of the formation processes that produced the aeolianite strata and any contemporaneous geomorphological features.

1.3. STRUCTURE

This dissertation is divided into seven chapters, including this one. Chapter Two will be focused on providing background on the site, including the current environment and climate of the area and the existing literature on the footprints and palaeoenvironments at Nahoon Point. Chapter Three considers the context of Nahoon Point and the other sites in the study area within our current understanding of the archaeological, geological, and palaeoenvironmental records of southern Africa and the world. A section of this chapter is focused on reviewing research relevant to understanding aeolianite formation and diagenesis. Chapter Four details the field and laboratory methods and techniques utilised for this study. The results of the project will be presented in Chapter Five. Discussion of the results will follow in Chapter Six. Finally, the conclusions of the project will be stated in Chapter Seven.

2. SITE DESCRIPTION

The purpose of this chapter is to describe the climate, geology, geomorphology, and flora and fauna of Nahoon Point and its surrounds; the existing research on the human and animal trackways found at the site; the dating of the footprints; the archaeology of the area; and what is currently known about the palaeoenvironment of Nahoon Point.

2.1. PHYSICAL SETTING AND ENVIRONMENT

Nahoon Point is located near the city of East London, Eastern Cape Province on the northeastern end of South Africa's southern coast (which extends from Cape Agulhas to a little north of East London) (Figure 2.1). The Point falls within the Nahoon Point Nature Reserve, a small coastal protected area that is centred on the Point but includes several kilometres of coastline south of the Nahoon River and east of the urban centre of East London.

2.1.1. Climate

East London (based on the period 1961 – 1990) has a warm-temperate to sub-tropical climate with relatively high average annual rainfall of 921 mm (South African Weather Service 2012). Rainfall is year-round, but is strongly bimodal, occurring mostly in the autumn and in the spring and early summer (Wiseman *et al*. 1993; South African Weather Service 2012). On average, July is the driest month (16 mm) and March is the wettest (79 mm) (South African Weather Service 2012). There is considerable inter-annual variability in monthly rainfall, which is partly due to the occurrence of cut off-lows which produce periods of extreme rainfall (Wiseman *et al*. 1993). During such an event in 1970, 853 mm of rain fell in a week; 200 mm of which was in a period of 11 hours (Wiseman *et al*. 1993). Temperatures are relatively stable due to the regulating effect of the Agulhas Current, which flows past East London (Wiseman *et al*. 1993). Average monthly minima range between 9.3°C in July and 18°C in February, while average monthly maxima range from 20°C in July to 26°C in February (South African Weather Service 2012).

East London experiences strong winds throughout the year, with calm conditions occurring as little as 1.5% of the year (Wiseman *et al*. 1993; Theron 2004). Based on

data collected from the weather station at the East London airport for the decade 2008-2017, average wind speed for the area is 8.87 knots (MIDAS Global Weather Observation 2018). Further examination of these data indicates seasonal variation in wind speed. Average wind speeds are lower in autumn (8 knots) and winter (8.58 knots) and higher in spring (9.79 knots) and summer (9.14 knots). These relatively high average wind speeds indicate that there is potential for aeolian transport (and eventual deposition) of sand-sized grains throughout the year.

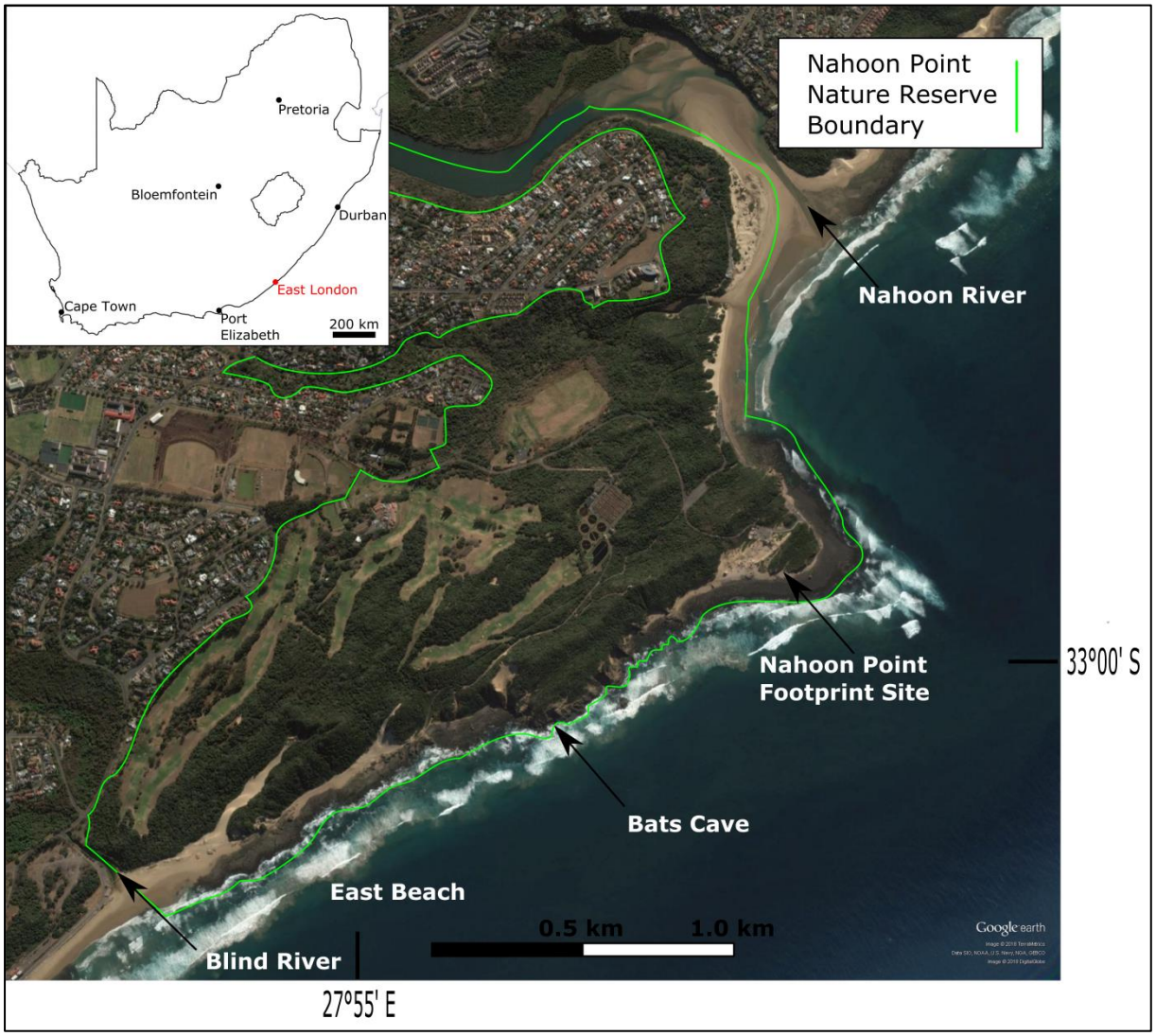


Figure 2.1. The Nahoon Point Nature Reserve and immediate surrounds (Imagery: Google Earth, 23 July 2017). Locations within or near the reserve referred to in this chapter are indicated. The East London city centre is to the West of this map. The visible development is within several of East London's suburbs. Inset: the location of East London within South Africa.

There is considerable seasonal variation in wind directions at East London (Figure 2.2). Summer winds are predominantly from the northeast and, to a markedly lesser

degree, from the southwest (Figure 2.2b). Southerly and south-easterly winds are rare but do occur in this season. In the autumn, the dominant winds are from the west and southwest, while north-easterlies are still fairly common (Figure 2.2c). North-westerly and south-easterly winds occur, but are far less common. During winter, westerly and south-westerly winds dominate (Figure 2.2d). North-westerly winds are fairly common, while north-easterlies are far rarer than in other seasons. Spring winds are mostly from the west and southwest, with a lesser but significant component from the northeast (Figure 2.2e).

Throughout the year, winds are approximately coast-parallel (south-westerlies and north-easterlies) much of the time (Wiseman *et al*. 1993; Theron 2004). Offshore winds (northerlies and north-westerlies) are far more common than onshore winds (southerlies and south-easterlies), although both are relatively minor components of the wind regime (Figure 2.2). During autumn and winter offshore winds are markedly more common than onshore winds; in spring and summer offshore winds are very rare and onshore winds are more likely to occur (Figure 2.2).

2.1.2. Geology

Nahoon Point is formed by a sill of Jurassic-age Karoo dolerite that intruded into the Beaufort series sandstones that dominate the geology of the East London area (Mountain 1945) (Figure 2.3). This sill is exposed in several places on the point and along the shoreline to the southwest of the point (Mountain 1945). The dolerite is overlain by Late Pleistocene-age (130 ka to 11.7 ka [Cohen et al. 2013]) Nahoon Formation aeolianites (Mountain 1945; Roberts 2008; Jacob & Roberts 2009). However, the aeolianites are generally covered by unconsolidated aeolian sediments of varying thickness and are seldom exposed except along the shoreline (Mountain 1945; Roberts 2008). These unconsolidated deposits are Holocene-age (11.7 ka to present [Walker *et al*. 2009]) aeolian sediments of the Schelm Hoek Formation (Illenberger 1992; Roberts *et al*. 2006).

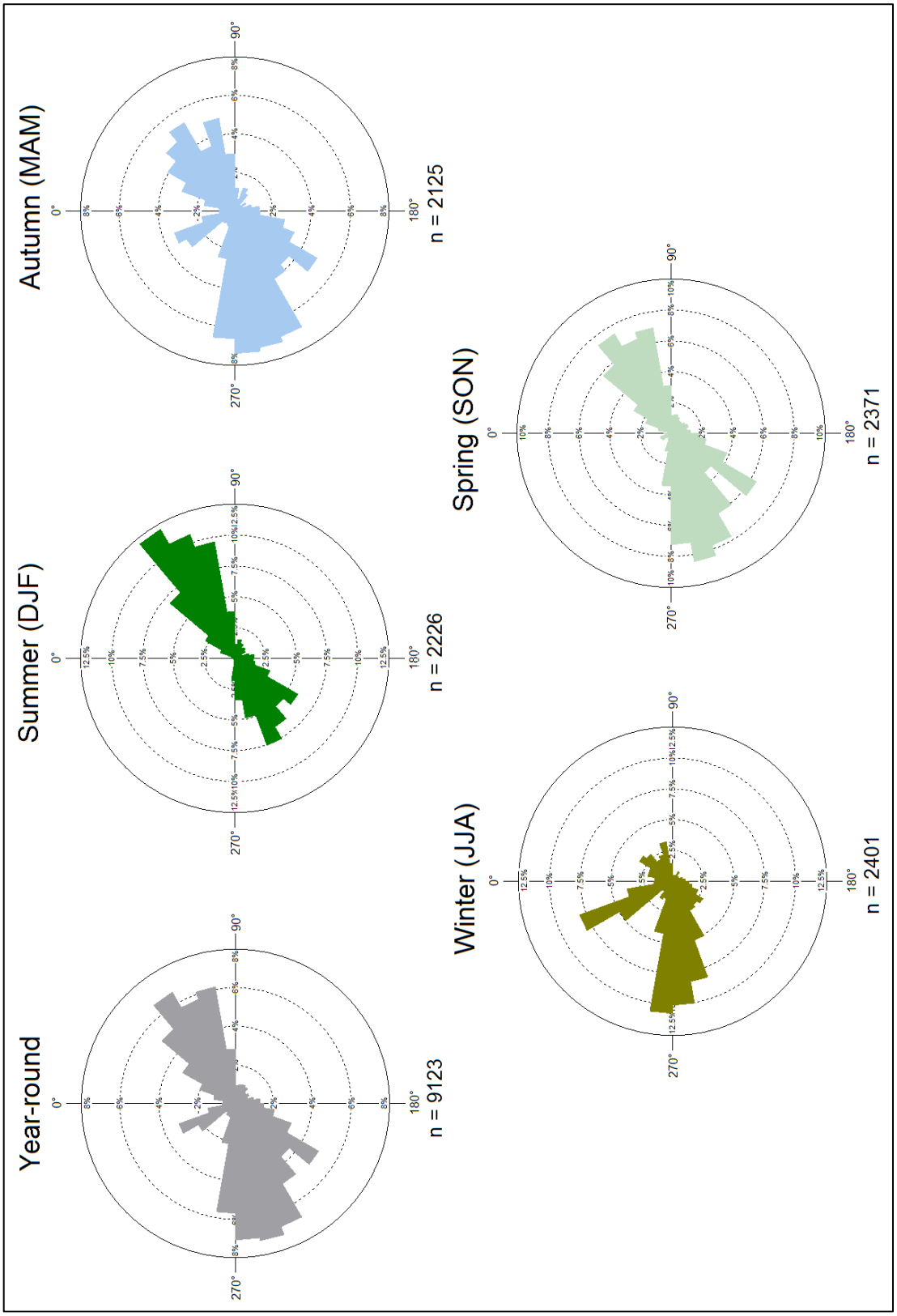


Figure 2.2. Annual and seasonal wind roses for East London based on data for 2008-2017 from the Met Office MIDAS Global Weather Observation Data catalogue. Only measurements with velocities exceeding or equal to 5.5 knots were included.

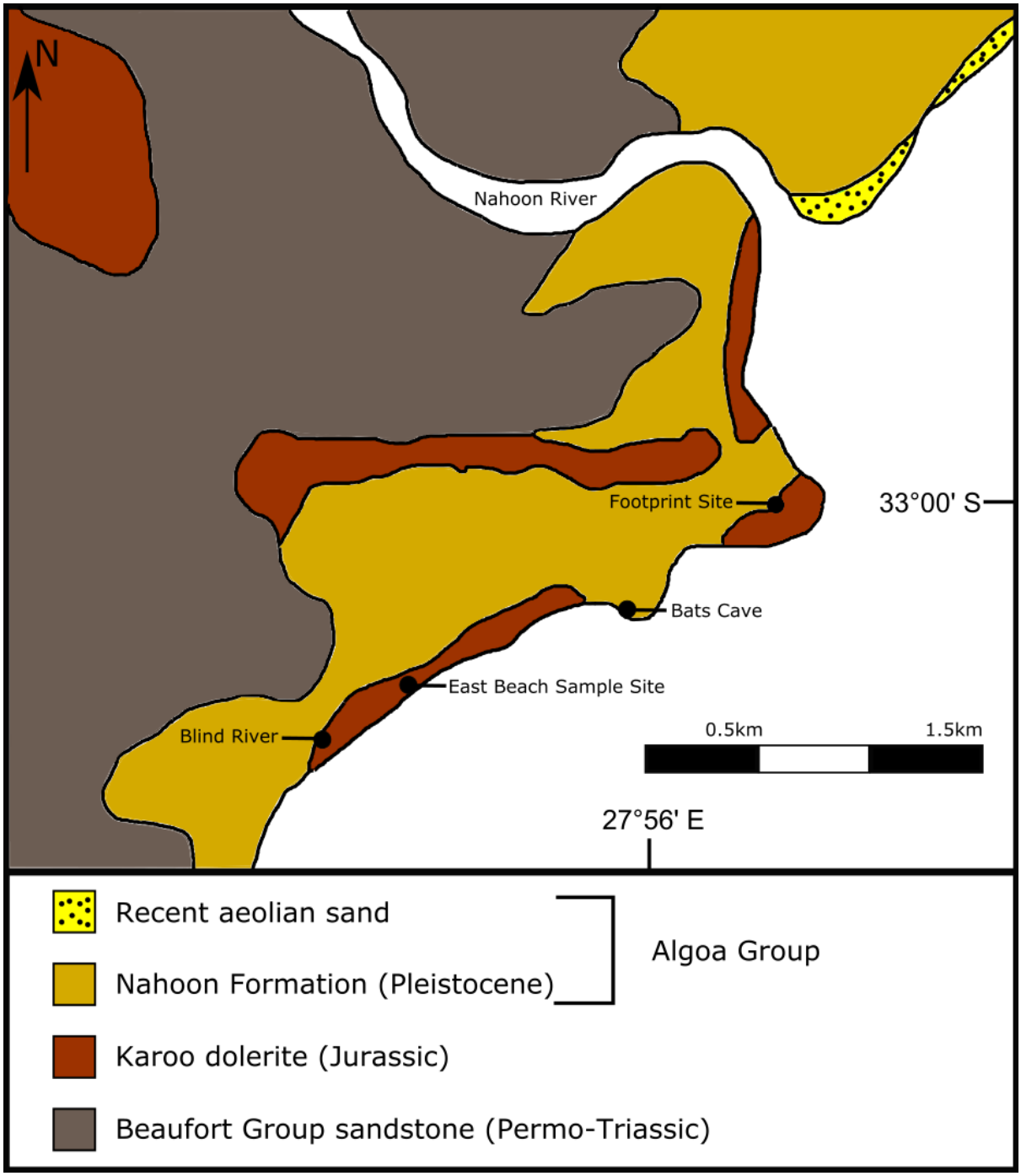


Figure 2.3. The geology of the area around Nahoon Point (modified from Roberts 2008). Note that the marine and estuarine deposits of the Pleistocene Salnova Formation are not mapped. Roberts (2008) did not state why they were not mapped. The recent aeolian sand deposits are of the Schelm Hoek Formation.

The aeolianites are well-sorted medium-grained calcareous sandstones cemented by calcium carbonate ($CaCO_3$) that was dissolved out of marine shell fragments by water movement within the deposits (Mountain 1966; Le Roux 1989a, b). High-angle

cross-bedding structures and the degree of sorting and rounding of grains have been used as evidence for their deposition by aeolian processes (Le Roux 1989a, b). Therefore, the aeolianites represent ancient dunes and associated features, such as interdune deposits (Mountain 1966; Le Roux 1989b; Roberts 2008).

Exposures of conglomeritic and sandstone deposits of the marine and estuarine Salnova Formation (which dates stratigraphically to the Middle and Late Pleistocene across its reported geographic distribution ([Le Roux 1991]) have been reported from various locations along the East London coastline, including at Nahoon Point (Mountain 1945, 1966; Deacon 1966; Roberts 2008; Wang *et al*. 2008). These have been deposited on Beaufort sandstones, on dolerite, and on aeolianite (Mountain 1945; Roberts 2008; Jacobs & Roberts 2009).

2.1.3. Geomorphology

The coastline around Nahoon Point is mixed, with both sandy and rocky features (Figure 2.1). Both sandy beaches and boulder beaches are present, and these sometimes grade into one another, with the sandy beaches at higher elevations. Loose boulders are present up to 1.5 m above high tide level, and may represent either modern storm deposits or the remains of Holocene raised beach deposits. A prominent raised marine bench is visible along rocky sections of the coast at elevations of 4 m to 6 m above mean sea level (Davies 1971; Jacobs & Roberts 2009). This feature is argued to date to MIS 5e (130 – 115 ka) (Roberts 2008; Jacobs & Roberts 2009). A fossilised boulder beach (beachrock) made up of dolerite and sandstone clasts and calcareous sandstone matrix is present within the current intertidal zone up to ~1 m above mean sea level (Mountain 1966; Davies 1971, 1980; Roberts 2008). This deposit rests on aeolianite in places, but is most commonly observed overlying the dolerite (Davies 1980; Roberts 2008).

The modern dunes around Nahoon Point are retentive, shore parallel cordons (Roberts 2008). These dunes range in height from less than a metre to 20 – 30 m high. Most are vegetated to varying degrees (see section 2.1.4.); the only non-vegetated dunes are found to the east of the Nahoon River mouth. Fossil dunes up

to 20 m high are preserved along the coastline as aeolianite. The aeolianite is generally exposed in sea cliffs and in stacks (Roberts 2008).

The major depositional structure in the aeolianite is northerly-dipping high-angle cross-stratification (Le Roux 1989b; Roberts 2008; Jacobs & Roberts 2009). However, low-angle convex-upward laminated bottomsets are fairly common, as are interdune deposits (Roberts 2008; Jacobs & Roberts 2009). The original bedding or lamination has been disturbed in many places by slumping or by root action (Roberts 2008). At the footprint site the aeolianite is overlain unconformably by a pedogenic calcrete (Roberts 2008).

The mouth of the Nahoon River is approximately 1.5 km to the north of Nahoon Point (Figure 2.1). The terraced valley through which the river flows developed during alternating periods of fluvial deposition and incision throughout the Quaternary (Mountain 1974; Rust *et al*. 1985; Reddering & Esterhuysen 1987). Deposition took place during interglacial sea-level highs (valley drowning), while incision of these deposits occurred when sea levels dropped during glacial periods (Rust *et al*. 1985). Regular flooding events in the river alter the morphology of the deposits in the tidal portion of the estuary, particularly near the mouth (Reddering & Esterhuysen 1987). The effects of flooding are considerably less severe higher up the river course (Reddering & Esterhuysen 1987). The average tidal range in the area is 1.63 m, falling within the classification of micro-tidal (Bursey & Wooldridge 2002).

The Agulhas Current flows past East London towards the southwest (Flemming 1978, 1980). Whilst this current flows strongly all along South Africa's eastern coastline, it is fastest (2.5 m/s at the surface) at East London (Flemming 1978). However, due to the influence of coastline morphology (especially features like Nahoon Point) and underwater topography, inshore currents around East London tend to flow north or northeast (Whillier 1962; Theron 2004). Waves in the area are predominantly from the south or southwest (Wiseman *et al*. 1993; Cooper 2001). As a result, longshore drift is generally from southwest to northeast (Wiseman *et al*. 1993; Bursey & Woodridge 2002; Theron 2004).

The coastal shelf at East London is approximately 25 km wide and the shelf-break occurs at about 140 m depth (Flemming 1980, 1981). The seabed reaches a depth of 30 m within approximately 1 km of the coast (Figure 2.4). The nearshore undersea topography around Nahoon Point is very rough, with many irregular features especially within a few hundred metres of the shoreline (see Figure 2.4). This is due to the presence of extensive aeolianite and dolerite outcrops on the seabed, which are known collectively as the Nahoon Reef. The seabed around these outcrops is generally sandy and has considerably smoother topography.

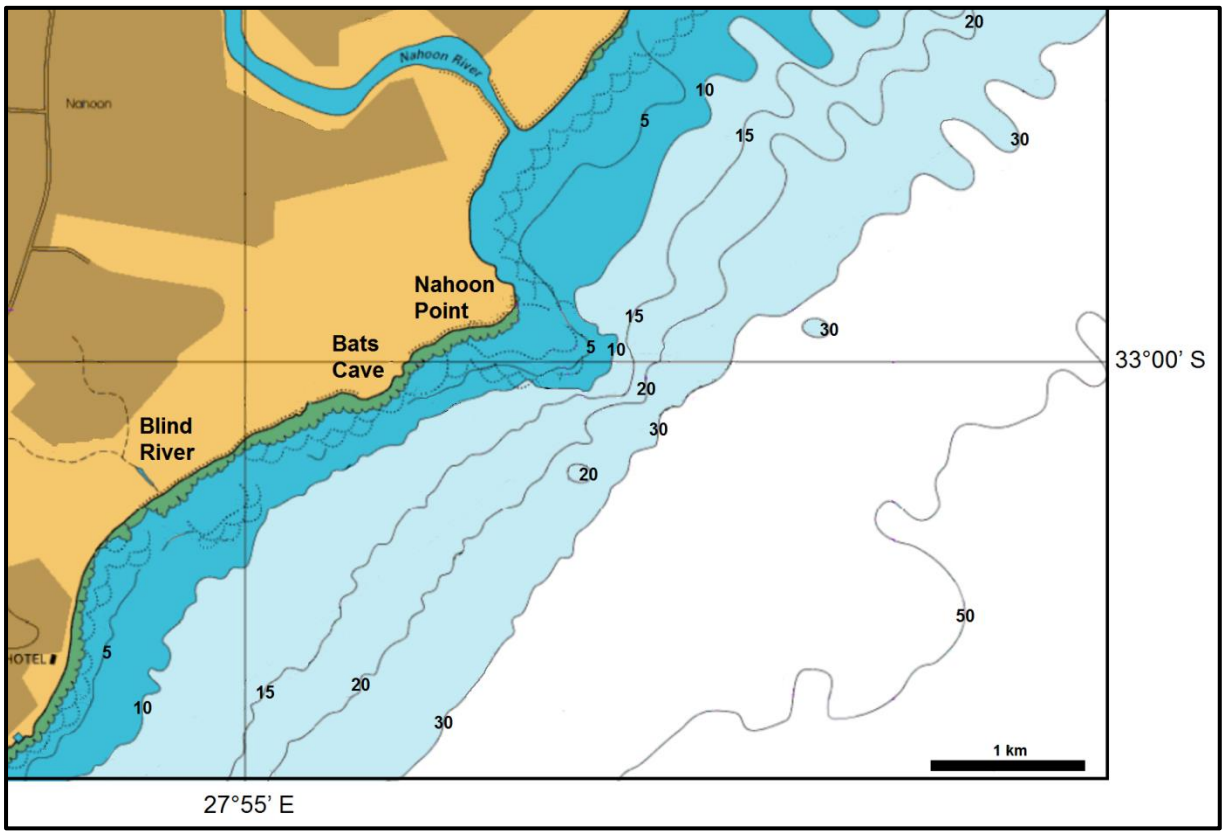


Figure 2.4. The bathymetry of the nearshore area along the coastline around Nahoon Point (after Admiralty 2005). The contours are in metres. The semi-circles in the shallowest areas indicate the positions of known rocky outcrops on the seabed.

2.1.4. Flora and Fauna

As Nahoon Point is very near the urban centre of East London, there has been considerable human impact on the ecosystems in the area (Wiseman et al. 1993). Therefore, it is difficult to determine the pristine natural flora and fauna of the area. However, research using both historical sources and more recent sightings allows for a reasonable, if imperfect, understanding of the natural biota.

East London is located within the Albany Thicket biome (Potts *et al*. 2015). The natural floral communities within the area around Nahoon Point are dominated by thicket species, but the exact composition varies considerably (Wiseman *et al*. 1993). There is a general progression of three communities moving inland from the sea. There are no clear boundaries between these communities as they grade into one another (Wiseman *et al*. 1993).

On the exposed seaward slopes of the dunes, there is a low and dense thicket, stunted by wind and spray (Wiseman *et al*. 1993). The density and size of the vegetation increases considerably up the dune slopes (Wiseman *et al*. 1993). The most common species are dune kokboom *Maytenus procumbens*, bietou *Chrysanthemoides monilifera*, dune crow-berry *Rhus crenata*, gonna *Passerina rigida*, baboon grape *Rhoicissus digitate* and klimop *Cynanchum natalitium*. From the dune crests and down the landward slopes, there is dense thicket, with trees and shrubs up to 5 m high (Wiseman *et al*. 1993). The following species dominate: red milkwood *Mimusops caffra*, boer-bean *Schotia afra*, koeboebessie *Cassine aethiopica*, Natal guarri *Euclea natalensis* and coast olive *Olea exasperata*. In the sheltered valleys behind the dunes, the trees reach up to 10 m high, and undergrowth is relatively thin due to the shade of the canopy (Wiseman *et al*. 1993). The dominant species are jackal-berry *Diospyros natalensis*, white milkwood *Sideroxylon inerme*, wild plum *Harpephyllum caffrum*, koeboebessie *Cassine aethiopica*, dune poison-bush *Acokanthera oblongifolia* and dune soap-berry *Deinbollia oblongifolia*.

Comprehensive lists of faunal species known to occur in the vicinity of the Nahoon River (in all its stages) in historic and recent times can be found in the appendices to Wiseman *et al*. (1993). Although this source is somewhat outdated, few species have been added to the list kept by the East London Museum since its publication (K. Cole pers. comm. 2016). As there are a number of distinct terrestrial and marine environments around East London, a fairly wide range of species are reported (Wiseman *et al*. 1993). The most commonly sighted bird species include the African Black Oystercatcher *Haematopus moquini*, the Ringed Plover *Charadrius hiaticula* and the Common Sandpiper *Tringa hypoleucos*. Recorded mammal species inlcude:

Vervet monkey *Cercopithecus aethiops*, Scrub hare *Lepus saxatilis*, Vlei rat *Otomys irroratus*, Cape clawless otter *Aonyx capensis*, Large grey mongoose *Herpestes ichneumon*, Water mongoose *Atilax paludinosis*, Aardvark *Orycteropus afer*, Rock dassie *Procavia capensis*, Hippopotamus *Hippopotamus amphibius*, Bushbuck *Tragelaphus scriptus*, Common duiker *Sylvicapra grimmia* and Blue duiker *Philantomba monticola*.

2.2. HUMAN AND FAUNAL TRACKWAYS

The Nahoon Point footprints were discovered in 1964 by R. Kaiser and W. Hartley who noticed them in an overhang in a small aeolianite cliff on the southern end of Nahoon Point while checking sewage pipes in the area. The human and animal trackways were preserved as infilled casts of the original tracks (Figure 2.5). The negatives (the tracks themselves) were lost when the aeolianite panel they were preserved in fell away (in 1964), exposing the overlying panel that contained the positives. The upper panel collapsed not long after its discovery and broke into two pieces. These are currently on display in the East London Museum.

The panel sloped up towards the south (seaward) at around 17°, and was on the leeward (north-facing) slope of a sand dune (Mountain 1966; Roberts 2008). Five distinct trackways were identified, produced by four or five individuals representing four species.

The first trackway comprises three human footprints (a left, right, left sequence) which head directly up the slope of the palaeodune, heading south towards the sea (Mountain 1966). Only two of the footprints have been analysed because the third was lost during the curation process after the aeolianite panel collapsed in 1964 (Roberts 2008). Of these two (a left and right set), most of the analysis was conducted on the left print as it preserved considerably more anatomical detail. Roberts (2008) argues the footprints were made by a *Homo sapiens* individual because the left footprint displays the following modern anatomical characteristics: “hallux aligned with the other toes; digits 1–4 short and straight and not of greatly dissimilar length; hallux tip bulbous; and a prominent medial longitudinal arch” (Roberts 2008: 199–200).

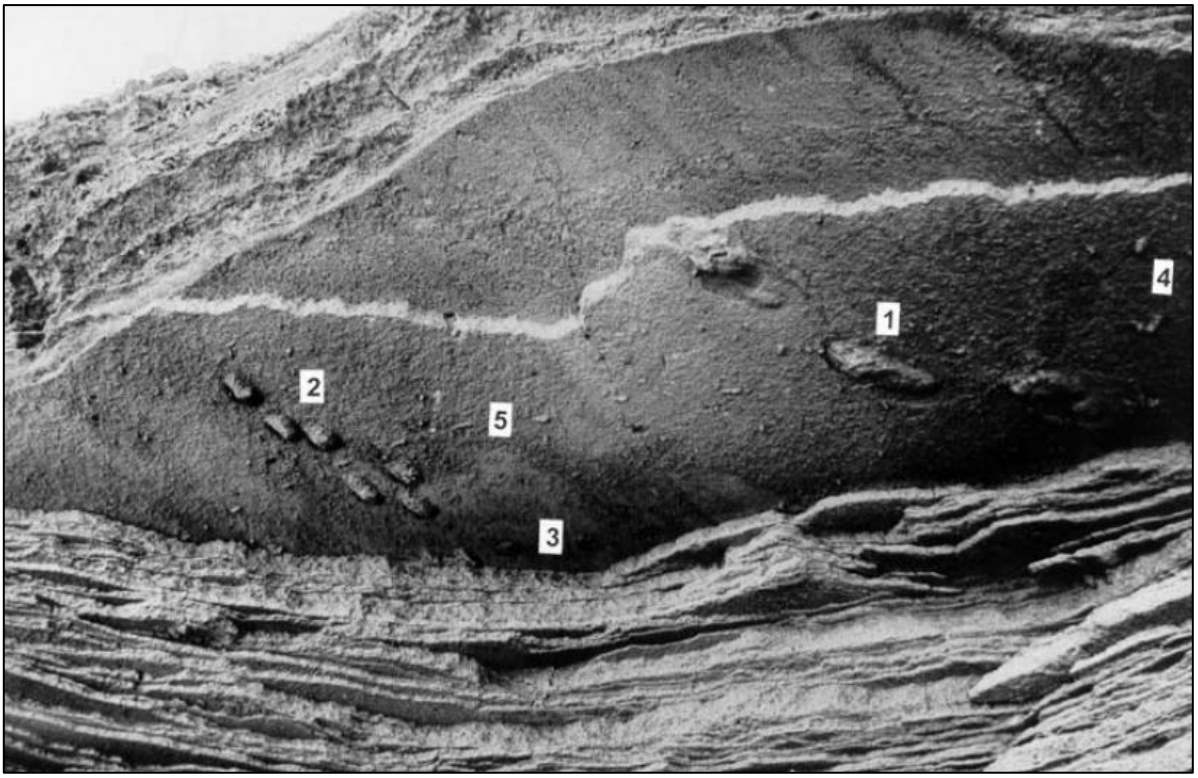


Figure 2.5. The five trackways (marked 1 to 5) on the panel in 1964 when it was still *in-situ* in the aeolianite cliff at Nahoon Point (Roberts 2008).

Human footprints of a similar age have been reported from Langebaan Lagoon, on South Africa's west coast (Roberts & Berger 1997; Roberts 2008). While these tracks preserve less detail of the anatomy of their maker, there is enough evidence to determine that they were also made by a *Homo sapiens* individual (Roberts 2008).

Roberts (2008) used the size of the footprints from Nahoon (19.2 cm long) to estimate the height of the individual at ~127 cm. Comparison to modern data on the stature of Khoi-San populations suggests that the individual may have been a juvenile, but likely more than 10 years old (Roberts 2008). In contrast, the larger Langebaan footprints (22.8 cm) were likely produced by an adult with similar body dimensions to a modern Khoi-San individual (Roberts 2008).

The second trackway at Nahoon Point is roughly parallel to trackway 1, but goes the other way – northwards, down the slope (Roberts 2008: 204). The tracks, six in total, are fairly large (~8.0 cm long and ~3.0-4.5 cm wide) impressions with obvious claw marks (Roberts 2008: 203 – 204). It was initially suggested that they were produced

by a hyena (Mountain 1966: 106). However, Roberts (2008: 204) contests this attribution due to the lack of the clear size difference between front and back paws that hyenas display (Skinner & Chimimba 2005: 365 – 378). Recent analysis of the impressions, including an experimental replication, indicates that this trackway was produced by a scrub hare *Lepus saxatilis* individual (K. Cole pers. comm. 2016). The bounding motion of the animal downslope would have led to the production of impressions far larger than the actual size of the animal's feet (K. Cole pers. comm. 2016).

The third trackway comprises two small (3.6 cm) round impressions, spaced 18 cm apart, heading up the slope towards the west (Roberts 2008: 204). One print preserves the marks of four toes, while the other only preserves three (Roberts 2008: 204). Based on the size of the prints, and the lack of claw marks, it was initially argued that they were produced by a small felid (Mountain 1966: 106). However, the morphology of the tracks is not consistent with a felid, and they have now been attributed to a mongoose (K. Cole pers. comm. 2016). It is not possible to definitively say which species of mongoose produced the tracks, but based on their size, it is either the large grey mongoose *Herpestes ichneumon* or the water mongoose *Atilax paludinosus* (K. Cole pers. comm. 2016).

The fourth trackway is a well-preserved set of three-toed bird tracks, with a spacing of 18-20 cm, which cross the slope diagonally (Roberts 2008: 203). Skead (pers. comm. in Mountain 1966) stated that they could have been produced by an oystercatcher, a crane, or a dikkop. Based on the size of the tracks and the spacing between them, they have now been attributed to the African black oystercatcher *Haematopus moquini* (K. Cole pers. comm. 2016).

The fifth trackway is a set of narrow linear impressions which form a line of approximately 1.2 m length across the slope, perpendicular to the dip (Mountain 1966: 106). Comparison of the width, length, and spacing of these impressions with the bird tracks (described above) revealed that the impressions were made by the central digit of a bird's foot (Roberts 2008: 203). The other digits may not have left impressions, or their impressions may have been destroyed by erosion (Roberts

2008: 203). The size and spacing of the impressions suggests that they were also made by an *H. moquini* individual (K. Cole pers. comm. 2016).

2.3. DATING

Three attempts have been made to date the sediments in which the Nahoon Point footprints were preserved. These attempts used different materials (aeolianite samples from different parts of the profile at the footprint site) and different dating techniques. Unsurprisingly, the studies yielded different results for the age of the footprints.

2.3.1. Radiocarbon dating by Deacon (1966)

A sample of bioclastic carbonate material taken from within the aeolianite footprint panel yielded an uncalibrated radiocarbon age of between 28.7 and 29.5 ka (Deacon 1966). Despite efforts to only use apparently unaltered shell fragments for this dating, there was considerable potential for contamination. The bioclastic carbonate in aeolianite is easily dissolved and reprecipitated by diagenetic processes, allowing the introduction of younger carbon into a sample (Jacobs & Roberts 2009: 162). As a result, this date is considered to be methodologically invalid.

2.3.2. Luminescence subtraction dating by Vogel et al. (1999)

The second dating attempt was undertaken by Vogel *et al*. (1999), who used thermoluminescence (TL) and infrared stimulated luminescence (IRSL) to date a sample of aeolianite from Nahoon Point. No specific details of the sample's provenance have been published. The results from these two techniques (TL: 236 ± 12 ka and IRSL: 144 ± 7.5 ka) were combined using a luminescence subtraction method to yield an age of 75 ± 9 ka. No information was provided on the exact location from which the dating sample was taken and therefore it is difficult to determine how this date actually relates to the footprints. Huntley (2002) argues that the environmental dose rates (how much radiation the sediment grains were exposed to after burial) used by Vogel *et al*. (1999) for their Nahoon samples were calculated incorrectly due to an underestimation of anomalous fading. This casts doubt on the accuracy of the dating results.

In a reply to Huntley (2002), the authors agree that it is possible that their estimations were inaccurate (Vogel *et al*. 2002). A new date of 125 ka (no error range was presented) was given for the sample based on "the revised IRSL equivalent dose" (Vogel *et al*. 2002: 561). No details were given for the data used in the calculation of the new dose rate (Vogel *et al*. 2002).

2.3.3. Optically stimulated luminescence dating by Jacobs & Roberts (2009)

The third dating attempt involved the use of the optically stimulated luminescence (OSL) method on a sample taken from the aeolianite at the footprint site (Jacobs & Roberts 2009). The sample was taken in direct association to the former location of the footprints (Figure 2.6). This sample yielded a date of 122 ± 6 ka (Jacobs & Roberts 2009). This result was then combined with a revised date of 128 ± 9 ka for the IRSL sample dated by Vogel *et al*. (1999) [the revision was made based on Huntley (2002) and Vogel *et al*. (2002)] to yield a final result of 124 ± 4 ka (Jacobs & Roberts 2009). This date falls within the last interglacial period, Marine Isotope Stage 5e, dated to 130 – 115 ka (Shackleton *et al*. 2003).

Of the three attempts at dating the site, the study by Jacobs & Roberts (2009) is here considered to be the most methodologically-sound. Therefore, it is seen as the most accurate estimate of the age of the footprints. The geology at Nahoon Point supports a mid-MIS 5e date for the footprint site (Roberts 2008; Jacobs & Roberts 2009). The erosion of the aeolianite above the footprints (evidenced by a marked unconformity) bears witness to a sea-level highstand (estimated to have been at least 6 m above present) after the production of the footprints (Roberts 2008; Jacobs & Roberts 2009).

As will be discussed further in Chapter 3, MIS 5e coastal deposits in South Africa and abroad have been found to record two sea-level transgressions within a period of about 10 000 years (Cooper & Flores 1991; Ramsay & Cooper 2002; Hearty *et al*. 2007; Carr *et al*. 2010, 2016; Cawthra *et al*. 2018). The most securely dated evidence in South Africa indicates sea levels between 6 m and 8.5 m above present during early and late MIS 5e (Carr *et al*. 2010; Roberts *et al*. 2012; Cawthra *et al*. 2018). The available evidence suggests that the earlier MIS 5e highstand was lower

than the later one (Hearty *et al*. 2007; Carr *et al*. 2010: 362). The mid-Holocene transgression could not have created the unconformity above the footprints as it reached only 2 to 3 m above present sea level on the southern coast (Miller *et al*. 1993). Therefore, the most likely scenario is that the footprints were emplaced in mid-MIS 5e before the dune was truncated by the (minimum) +6 m subsequent highstand.

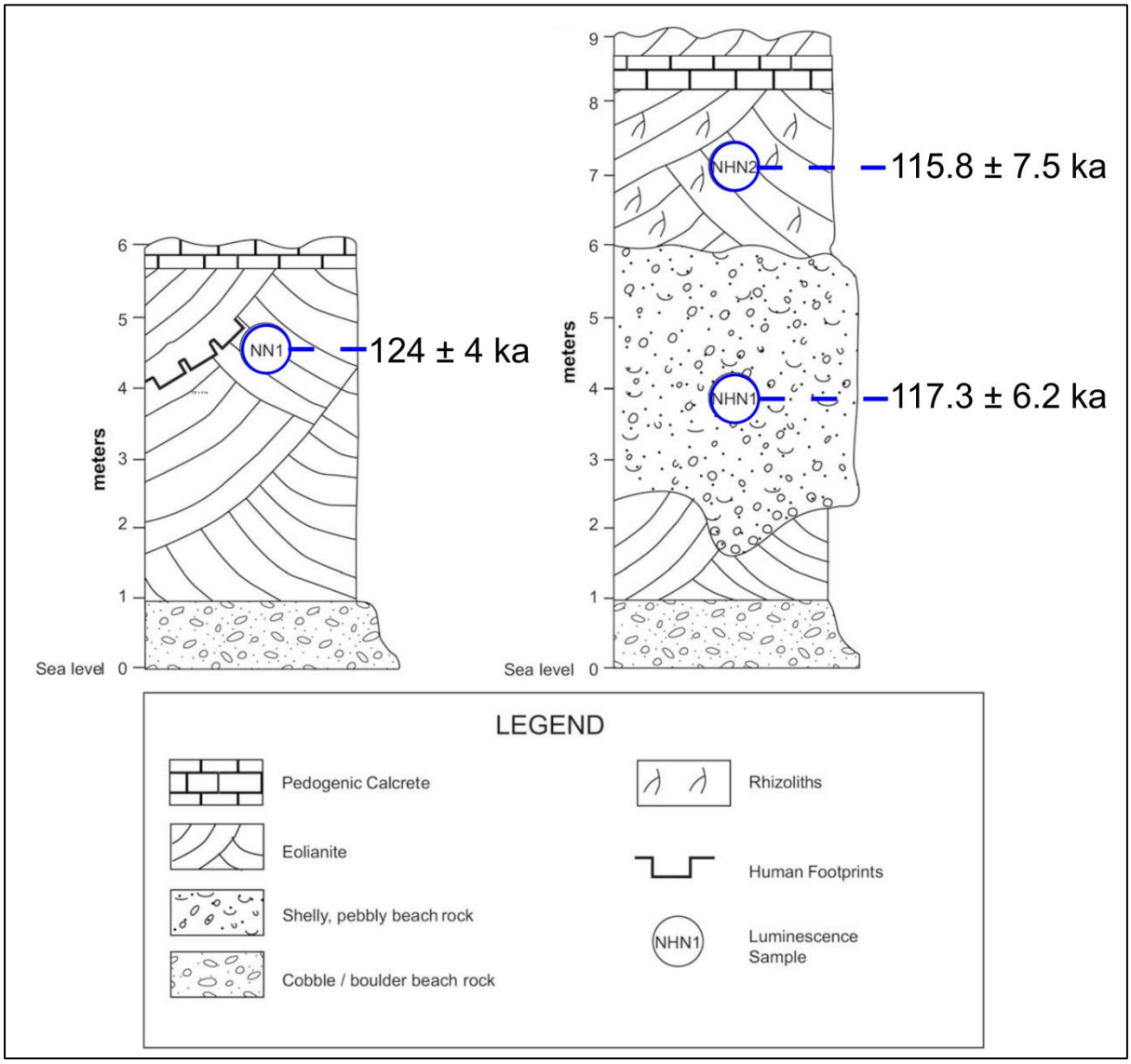


Figure 2.6. The sedimentary profiles from which dating samples were taken by Jacobs and Roberts (2009). The sample locations within the profiles and the ages determined for each sample are indicated. Left: the profile at the footprint site on Nahoon Point. Right: the East Beach profile. Note that in both cases the stratigraphic relationship with the underlying beachrock was inferred rather than observed.

2.3.4. Dates for related deposits

Jacobs and Roberts (2009) also conducted OSL dating on samples taken from deposits at East Beach, several kilometres to the west of Nahoon Point (Figures 2.1 and 2.5). The first sample (NHN1) was taken from a shelly, pebbly marine deposit that overlies aeolianite similar to that which contained the footprints. This sample was dated to 117.3 ± 6.2 ka. Middle Stone Age artefacts found within this deposit support a Late Pleistocene date for this transgressive event (Jacobs & Roberts 2009). The second sample (NHN2) was taken from rhizolith-rich aeolianite that overlies the beachrock. It was dated to 115.8 ± 7.5 ka.

The archaeological site of Blind River, roughly 2.5 km from Nahoon Point (Figure 2.1) was recently dated using OSL. Artefacts have been recovered from two sedimentary units at the site (Figure 2.7), an estuarine calcarenite, and an overlying marine gravel deposit with a maximum elevation of 10 m above present sea level (Wang *et al*. 2008). Two samples were taken for OSL dating from within the estuarine deposit, at 5 m and 3.5 m below the top of the marine/estuarine sequence (Wang *et al*. 2008). The samples were dated to 119 ± 9 ka and 118 ± 7 ka respectively (Wang *et al*. 2008). As the peak of MIS 5e was around 120 ka, and the samples were taken well below the marine gravel, the authors argue that the samples' true ages are probably older than their median ages. They suggest ages around 122 ka would be most likely. This would make the main artefactual deposit closer to 120 ka.

Based on these dates, it appears that the formation of these marine and estuarine deposits took place after the footprints were made, during late MIS 5e. The subsequent formation of terrestrial aeolian deposits occurred during late MIS 5e/early MIS 5d (Shackleton *et al*. 2003).

2.4. ARCHAEOLOGY

Two Middle Stone Age (MSA) archaeological assemblages (at Bats Cave and Blind River) have been reported from the coastline near Nahoon Point. As the artefacts from these sites have not been analysed in detail, they currently provide little information other than evidence for human occupation of the area during the MSA.

However, based on their geological context and the typological characteristics of the assemblages, they appear to relate to the period of MIS 5e.

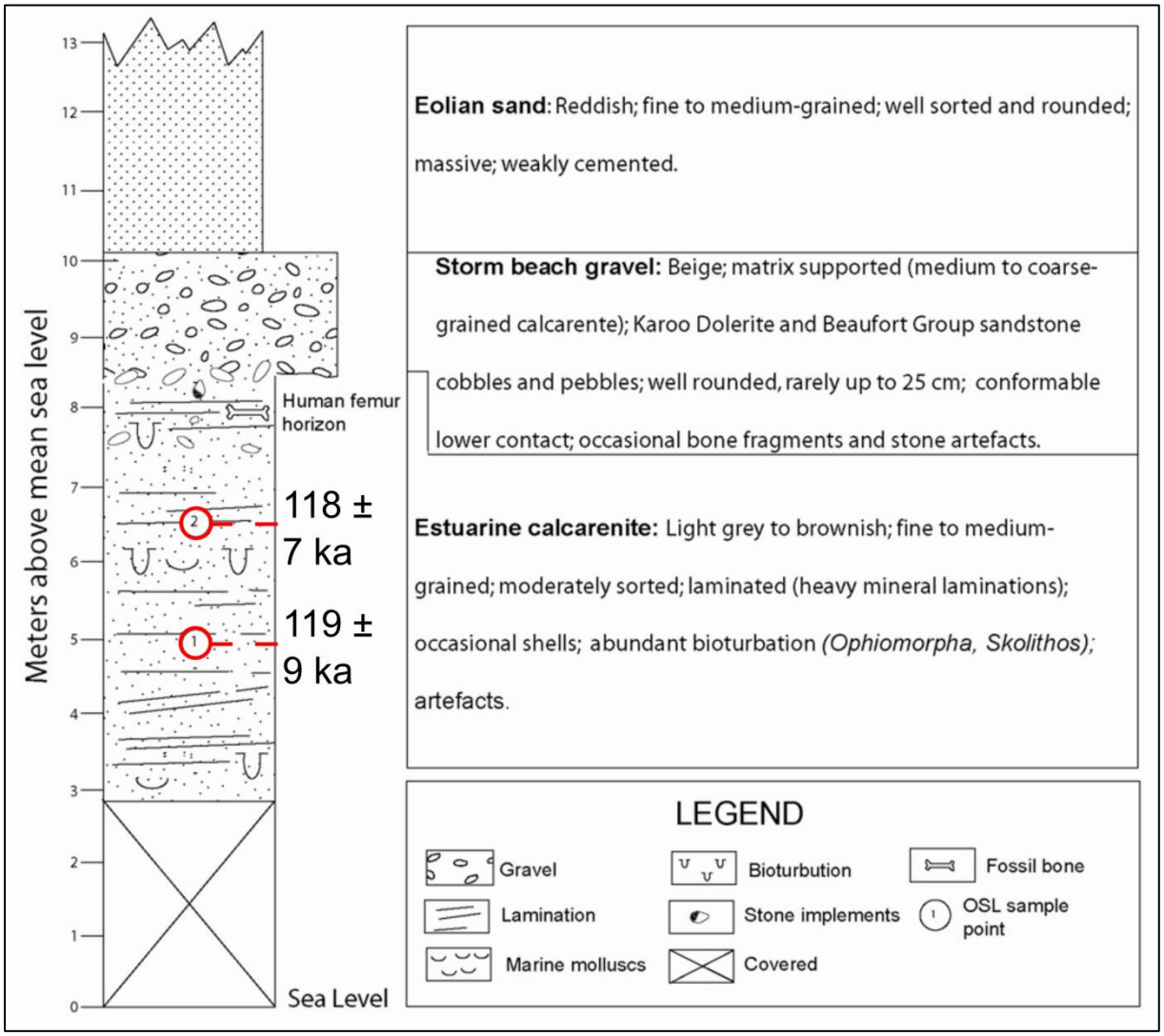


Figure 2.7. The sedimentary profile at Blind River, with the dating sample locations and their respective age determinations indicated (after Wang *et al*. 2008).

2.4.1. Bats Cave

A small assemblage of lithic artefacts was recovered from a beachrock deposit in the vicinity of Bats Cave (Figure 2.1), about 1.5 km to the west of Nahoon Point (Deacon 1966). The typological characteristics of the assemblage allowed Deacon (1966) to attribute it to the MSA. The small lithic sample size (28) prevented classification of the assemblage to a specific industry within the MSA. The lithology of the artefacts was not reported. Very limited context is given for the beachrock within which the

artefacts were found (Deacon 1966), which makes it difficult to determine how they relate stratigraphically to the aeolianite and, thus, the footprints.

Lithic artefacts have also been reported from a shelly beachrock deposit at East Beach (Figures 2.1 & 2.5), near to Bats Cave (Jacobs & Roberts 2009). This deposit lies between two aeolianite deposits, but these have yet to be linked stratigraphically to the aeolianite at the footprint site.

It has been argued that there are two known periods of Late Pleistocene beachrock deposition in the area, one pre-dating, and the other post-dating the production of the footprints (Roberts 2008; Jacobs & Roberts 2009). Both of these depositional events appear to have taken place during MIS 5e (Jacobs & Roberts 2009). Therefore, this assemblage may be broadly similar in age to the Nahoon Point footprints. However, the stratigraphic relationship between the artefact-bearing beachrock and the footprint-bearing aeolianite is currently too poorly understood for chronostratigraphic correlation.

2.4.2. Blind River

Construction work near the mouth of Blind River, roughly 2 km from Nahoon Point (Figure 2.1), during the early 1930s exposed an archaeological deposit which was excavated by Laidler (1933, 1934) and MacFarlane (1937). Artefacts were found within two distinct sedimentary units – a lower sandy deposit and an upper gravel unit (Figure 2.7). The artefacts in both units were classified as belonging to the MSA based on their typological characteristics (Laidler 1934; MacFarlane 1937). An initial suggestion that they shared an affinity with the Fauresmith Industry did not appear in subsequent interpretations (Laidler 1933, 1934; MacFarlane 1937). A partial human femur was found in association with the lithic artefacts, and based on its morphology it was attributed to an adult *Homo sapiens* (Wells 1935). Analysis of the femur by Wang *et al*. (2008) confirmed this attribution.

As discussed above (in Section 2.3.4) a combination of OSL dating and geomorphological analysis indicates that the artefacts date to around the peak of MIS 5e, at approximately 120 ka (Wang *et al*. 2008). Several authors have argued

that the Blind River deposit dates to around 405 ka (Bednarik 2003; Beaumont & Vogel 2006; Beaumont & Bednarik 2013). However, the means by which this relative date was obtained are problematic. The artefacts were erroneously attributed to the Fauresmith Industry, and this poorly-defined and inadequately-dated archaeological entity (Herries 2011; Underhill 2011) was used to indicate an apparent age-range for the site. The gravel deposit, with a maximum elevation of +11 m, was assumed to have formed during a period of time when sea level was at least that high above present. The most recent highstand within the assumed (but highly problematic) age-range for the Fauresmith to have reached this level was during MIS 11, at around 405 ka. However, this is based on a misinterpretation of the sedimentology and geomorphology of the gravel deposit, which is actually a storm beach deposit which would have formed well above mean sea level (Wang *et al*. 2008). Therefore, this date (405 ka) is entirely invalid, while the OSL dates, indicating an MIS 5e age, are considered accurate in this study.

As the Blind River deposits are within a few kilometres of Nahoon Point, and are (relatively speaking) only a little younger than the footprints, it is surprising that past researchers have made no attempt to link the sites. Part of the problem, perhaps, is the lack of a landscape-scale stratigraphic model to accommodate these sites and the area between them (including the artefact-bearing conglomerate around Bats Cave).

2.5. PALAEOENVIRONMENT

2.5.1. Palaeoenvironmental models and hypotheses

Almost all that is currently known or hypothesised about the environment at (and around) Nahoon Point during MIS 5e is based on the geomorphological or sedimentological properties of the Nahoon Formation aeolianites or marine deposits of the Salnova Formation. Only a single hypothesis has been developed from the faunal trackways found with the human footprints.

Mountain (1966) suggested that the occurrence of so many trackways on the landward slope of a palaeodune could be evidence for the presence of a dune slack. Dune slacks are relatively low-lying areas between dune cordons in which water can

be found at or near the surface seasonally (Ranwell 1959). As a source of fresh water in the coastal zone, a dune slack is an attractive location. Dune slacks have been recorded along the Eastern Cape coast in recent times (Avis & Lubke 1996). This hypothesis is compelling, but currently impossible to test without finding sedimentary or geomorphological evidence for such a feature.

Roberts (2008) used an experimental approach to identify the weather conditions at the time of the production of the trackways. He made footprints on dunes in a range of different weather conditions while controlling for slope angle and other substrate properties and compared the tracks he had produced to the Nahoon Footprints. The lack of cracking in the imprints and the push-up mound indicate that the sand was wet and did not dry for some time after the footprint maker walked up the dune (Roberts 2008: 205). Therefore, it is likely that they were made during a period of rain lasting several days. Whilst this information is useful for understanding the conditions that led to the preservation of the trackway, it does not provide any information on the climate of the area at the time.

All of the authors who have considered the context of the Nahoon Point footprints based on geological evidence have done so using a fairly coarse stratigraphic approach, based predominantly on the lithology of the aeolianite and marine deposits. Therefore, whilst there is a general environmental model into which the footprints can be placed, this model is at a relatively low temporal resolution and provides only a limited understanding of the environmental context of the footprints.

The dominant orientation of cross-bedding structures (northward) in the aeolianites indicates that the prevailing winds blew predominantly from the southwest and southeast during the period in which they were forming (Le Roux 1989b; Roberts 2008). However, neither Le Roux (1989b) nor Roberts (2008) indicate whether there is any variation in this pattern through the vertical extent of the aeolianites.

Roberts (2008) and Jacobs & Roberts (2009) argue that the footprint-bearing aeolianite was formed during a sea-level regression or lowstand between two MIS 5e sea-level highstands. A deposit of beachrock, with a maximum elevation of 1 m

above present sea level, has been recorded at Nahoon Point (Mountain 1966; Roberts 2008). In one location, a stack within the intertidal zone, it is overlain by an aeolianite deposit. Although the beachrock does not directly underlie the aeolianite at the footprint site and there is no stratigraphic link between the aeolianite at the footprint site and that which overlies the beachrock, Roberts (2008) argues that the beachrock directly pre-dates the formation of the footprint site aeolianite. Therefore, it has been attributed to an early MIS 5e highstand which is estimated to have been roughly 2 m above present sea level (Roberts 2008; Jacobs & Roberts 2009).

The human footprints were made on an active dune which became stabilised and vegetated and (at some point during or after this process) lithified (Roberts 2008). The formation of dunes at Nahoon Point after the deposition of beachrock has been argued to indicate a period of sea-level regression following the early MIS 5e highstand (Roberts 2008; Jacobs & Roberts 2009). Based on comparing the median age for the footprints (124 ka) with global sea level curves for MIS 5e, sea level was estimated at +1 m at the time the footprints were made (Jacobs & Roberts 2009). Sea level is believed to have continued falling to an unknown level during the formation of the dune (Roberts 2008; Jacobs & Roberts 2009).

The aeolianite at the footprint site was planed off at roughly 6 m above present sea level (Roberts 2008). Raised marine benches and notches are reported at between 4 and 6 m above present sea level from various locations around East London (Davies 1971; Roberts 2008; Jacobs & Roberts 2009). At East Beach, marine sediments have been deposited into or onto erosional features in aeolianite up to 6.1 m above present sea level (Jacobs & Roberts 2009). The deposition of aeolian deposits on top of these marine deposits suggests regression after this highstand (Jacobs & Roberts 2009). These features have been interpreted as the result of a sea-level highstand of at least +6 m after the deposition of the dune in which the footprints were found (Roberts 2008; Jacobs & Roberts 2009).

The calcrete that overlies the aeolianite at the footprint site has not been analysed or interpreted (Mountain 1966; Roberts 2008; Jacobs & Roberts 2009) as it significantly

postdates the formation of the aeolianites and thus, can reveal nothing about palaeoenvironmental conditions during this period.

2.5.2. Critique of existing model

A number of studies have provided evidence for two global sea-level highstands separated by a regression during MIS 5e (Chen *et al*. 1991; Neumann & Hearty 1996; Wilson *et al*. 1998; Zazo 1999; Dumas *et al*. 2006; Hearty *et al*. 2007; Kopp *et al.* 2009, 2013; Thompson *et al*. 2011; O'Leary *et al*. 2013; Gischler 2014; Cawthra *et al*. 2018). (The timing and levels of these events will be discussed in detail in Chapters 3 and 6.) However, the data on which the local sequence developed by Roberts (2008) and Jacobs and Roberts (2009) is based can be interpreted in several different ways. Unresolved stratigraphic problems mean that it is possible that only one highstand is represented at Nahoon Point and East Beach (Table 2.1).

Table 2.1. A summary of ages and sea level estimates for the phases identified in the MIS 5e palaeoenvironmental model developed by Roberts (2008) and Jacobs & Roberts (2009).

Phase	**Age**	**Sea Level Estimate**	**Comments**
First Highstand	>124 ± 4 ka**?**	+2 m	• Evidence at Nahoon Point • Under-estimate? • Could represent an earlier (MIS 7) highstand or the second MIS 5e highstand
First Regression	124 ± 4 ka	<0 m	• Evidence at Nahoon Point and East Beach • No correlation between the two locations
Second Highstand	117.3 ± 6.2 ka	+6 m	• Evidence at Nahoon Point and East Beach • No correlation between the two locations
Second Regression	115.8 ± 7.5 ka	<0 m	• Evidence at East Beach • No correlation to Nahoon Point

The beachrock at Nahoon Point is suggested by Roberts (2008) to indicate a sea level of +2 m because its maximum elevation is 1 m above present sea level. He

does not provide any indication of why he believed the beachrock would have formed a metre below mean sea level. However, beachrock can form in different parts of the intertidal zone, at varying depths below sea level (Cooper 2001; Knight 2007; Mauz *et al*. 2015). It is possible that the +2 m estimate is a significant under-estimate. Therefore, it is perhaps more accurate to consider the beachrock as indicating a highstand at a minimum of +2 m.

No reasoning (other than a similarity in lithology) is given for the temporal correlation of the aeolianite at the footprint site and the aeolianite overlying the beachrock (Roberts 2008; Jacobs & Roberts 2009). Due to the general similarity in the lithology of Nahoon Formation aeolianites (Le Roux 1989a, b), this correlation is problematic. Therefore, while the aeolianite in the stack could be contemporaneous with the footprint-bearing aeolianite, they could also have vastly different ages. This makes it difficult to determine the stratigraphic relationship between the dated dune deposit and the (undated) Nahoon Point beachrock. Therefore, the beachrock could potentially date to the second MIS 5e highstand or to a pre-MIS 5e highstand.

The base of the exposed portion of the footprint-bearing dune is only 1 m above mean sea level (Figure 2.6). Therefore, its formation could only have occurred during a period where sea level was lower than at present. Thus, while their attribution of the dune's formation to a regression appears to be accurate, Jacobs & Roberts' (2009) estimate of a sea level 1 m above present when the footprints were made seems improbable.

The combination of the stratigraphic evidence and dates at both Nahoon Point and East Beach indicate that a late MIS 5e highstand did occur in the area. The aeolianite overlying the East Beach conglomerate indicates regression after this highstand.

The stratigraphic relationship between Nahoon Point and East Beach is currently poorly understood. This hampers nuanced understandings of palaeoenvironmental conditions throughout the sequence pieced together from the locations by Jacobs & Roberts (2009). There are extensive exposures of aeolianite along the coast

between the two locations (Figure 2.3). These could provide a means to link the two dated locations across the landscape in a single stratigraphic model. However, none of the previous researchers who have published on the aeolianite in the area have attempted to do this.

Analysis of these exposures, along with more detailed palaeoenvironmental analysis of the palaeodune at the footprint site, could help to place Nahoon Point and East Beach into a more nuanced palaeoenvironmental model. Of particular importance is determining how many (and which) MIS 5e sea-level highstands are recorded in the sequence in the area. This is due to the uncertainty surrounding the relationships between the beachrock and aeolianite deposits in Roberts' (2008) and Jacobs and Roberts' (2009) stratigraphic model. The approach utilised to achieve the palaeoenvironmental reconstruction is presented in Chapter 4.

3. LITERATURE REVIEW

The aeolianite and marine deposits at Nahoon Point, Blind River, and East Beach (discussed in detail in Chapter 2) have been dated to Marine Isotope Sub-Stages (MIS) 5e and MIS 5d. Therefore, the focus of this review is on both of these periods. MIS 5e was an interglacial while MIS 5d was a notably cooler stadial period (Shackleton 1969; Shackleton *et al*. 2003; Govin *et al*. 2015; Railsback *et al*. 2015). This combined period, which spans 130 – 105 ka, is referred to as 'Early MIS 5' throughout the rest of this dissertation.

This chapter is divided into four sections. The first and second sections are devoted to reviewing information relevant to the palaeoenvironmental interpretation of coastal aeolianite and beachrock. This includes sub-sections on the formation of aeolian and shallow marine deposits, and the cementation of these sediments. A review of the research into coastal aeolianite and beachrock deposits in South Africa is presented in the third section. Finally, the fourth section is intended to place the Nahoon Point footprints (and nearby archaeological deposits) within the current knowledge about the South African archaeological record of Early MIS 5.

3.1. COASTAL AEOLIANITE

Coastal aeolianites can preserve considerable evidence for past environmental conditions. Reconstructing these conditions requires analysis of a range of aeolianite properties which provide information on depositional and post-depositional processes. In order to understand the information these can provide, and how to attain them, it is necessary to review what is known about the formation of aeolian deposits (particularly dunes), and the processes through which these deposits are cemented to form aeolianite.

3.1.1. Aeolian processes

Aeolian sediments form as a result of the transport and deposition of particles by wind. A wide variety of aeolian landforms and sediment types are recognised in modern and ancient sediments (Pettijohn *et al*. 1973; Bridge & Demicco 2008; Boggs 2014) but the focus of this review is on the formation of dunes and related (inter-dune) deposits.

The development of aeolian depositional landforms requires a supply of sediment and winds strong and frequent enough to entrain and transport the sediment (Bagnold 1941; Livingstone & Warren 1996; McLaren 2007). Aeolian deposits are common in coastal areas because suitable sediment (such as beach sand) is readily available and strong winds are very common (Fairbridge & Johnson 1978; McKee & Ward 1983; Goldsmith 1985; Tinley 1985; Brooke 2001).

The formation of a dune follows a set of fairly well-understood sedimentological processes that are controlled by the existing morphology of the dune, with different depositional and erosional processes taking place on different parts of the dune and surrounding deposits (Bagnold 1941; Pettijohn *et al*. 1973; Hunter 1977a, b; Kocurek 1981, 1988, 1991; Kocurek & Dott 1981; Pye 1983; Boggs 2014). Sediment is transported by saltation up the windward stoss slope (Figure 3.1), with some erosion of grains from this slope taking place. Sediment may also be deposited on the windward slope by the process of grain creep. Upon passing the crest of the dune and reaching the point of flow separation (Figure 3.1), the effects of gravity and the reduction in wind strength on the leeward side of the dune result in the size-selective deposition of grains. This process, known as grainfall, can cause deposition on both the steep leeward slope (slipface) and on the flat interdune surface behind the dune. Grains are also deposited by flows (or avalanches) of sediment down the slipface when the sediment at the crest becomes unstable – a process termed grainflow.

Three major types of bedform are recognised within aeolian deposits (Hunter 1977 a, b; Fryberger *et al*. 1979; Kocurek 1991; Boggs 2014). The first is the topset bed, which corresponds to the deposits on the stoss (windward) slope of a dune. The second is the foreset bed, which is formed on the leeward slope of the dune and is relatively steeply inclined. These beds prograde in the direction of wind transport. Due to the steep angle of foreset beds relative to the underlying surface, they are also referred to as cross-beds. The third bedform type is the bottomset, which is applied to low-angle and horizontal beds which may occur in interdune areas or as sand sheets in flatter areas where dunes have not formed.

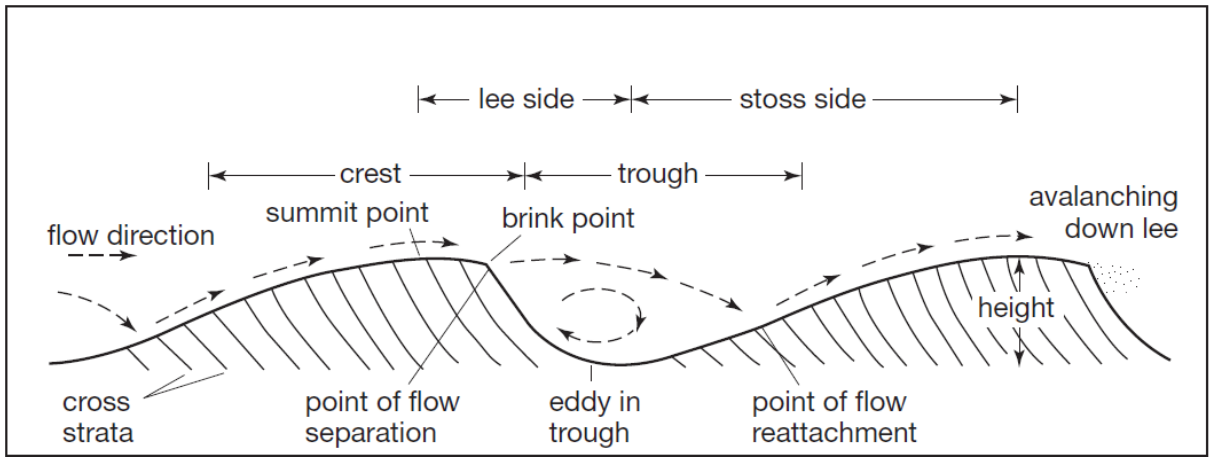


Figure 3.1. A cross section schematic of idealised dunes which depicts the different features of a dune and the processes that occur around these features (after Boggs 2014).

The morphology of coastal aeolian deposits is influenced by numerous different variables including climate (wind and rainfall regimes), sediment supply (which is controlled by many factors), shoreline configuration, the geology and geomorphology of the area, and vegetation growth (Pye 1983; Goldsmith 1985; Tinley 1985; Jackson *et al*. 2014). Unsurprisingly, a variety of different dune morphological types have been described in coastal environments (Pye 1983; Goldsmith 1985; Tinley 1985; Illenberger 1996; Tsoar 2001; Jackson *et al*. 2014). Many dunes form as the result of the coalescence, overlap or superimposition of smaller individual dunes; the component landforms may be of the same type or of different types (Tinley 1985; Illenberger 1996; Bateman *et al*. 2011). Determining the types of dunes preserved in aeolianites or palaeo-dune deposits can provide information on a range of past climatic and environmental factors, although this is not always straightforward (Klappa 1980; Kocurek & Dott 1981; Kocurek 1991; Illenberger 1996; Roberts *et al*. 2008, 2009, 2014; Bateman *et al*. 2011; Rowe & Bristow 2015).

Due to the manner in which dunes form, they regularly migrate as sediment is eroded from the windward slope and deposited on the leeward slope. Therefore, even in modern dunes, bedding structures are commonly destroyed or truncated (Rubin & Hunter 1982; Kocurek 1981, 1988, 1991). Truncated cross-bedded foresets are the most likely bedforms to be preserved, and therefore, they are often used in the study of palaeodunes (Pettijohn *et al*. 1973; Kocurek 1981, 1991). The orientation of these beds is strongly controlled by the palaeocurrent at the time of

their deposition, which allows for the determination of palaeowind directions if conditions are suitable (Pettijohn *et al*. 1973; Potter & Pettijohn 1977; Kocurek 1991; Boggs 2014).

Bounding surfaces, or the contacts between distinct sets of cross-bedded foresets, are also important for understanding the formation of sequences of dune deposits. A set of three categories have been defined for these features (Brookfield 1977; Kocurek 1981, 1991). First-order surfaces are the result of a dune migrating over the truncated surface of a dune of similar size. Second-order surfaces form when a smaller dune migrates over a larger one. Third-order surfaces occur when a major change in conditions take place (i.e. when the upper dune migrates in a different direction to the lower dune). Kocurek (1991) also defined the 'supersurface' – the upper contact of an aeolian deposit which has properties indicative of a significant break in aeolian deposition (Lancaster 1993).

3.1.2. Aeolianite cementation

An aeolian deposit becomes aeolianite when the sediment in the deposit is cemented by calcium carbonate ($CaCO_3$) (Fairbridge & Johnson 1978; Brooke 2001; McLaren 2007). The diagenesis of aeolianite is controlled by a wide range of variables, ranging from large-scale climatic processes to small-scale features within a deposit (Gardner & McLaren 1994; McLaren 2001; McLaren & Gardner 2004). However, the general process – as summarised in the following paragraph – is reasonably well understood (Reeckman & Gill 1981; Moore 1989; McLaren 1993, 2007; Gardner & McLaren 1994; McLaren & Gardner 2004).

Water enters the deposit from the surface, as rain or run-off, and percolates down through the vadose zone. As the water moves through the sediment, it dissolves bioclasts (composed of calcite or aragonite), and takes in $CaCO_3$. The water becomes supersaturated with $CaCO_3$ and re-precipitates it around the grains in the deposit, cementing them together. A number of processes can cause $CaCO_3$ supersaturation and precipitation within a deposit. Examples are: a reduction of CO_2 as a result of degassing (due to the circulation of groundwater, often in response to tidal pumping), increasing dissolution of bioclasts due to heating of the land surface

(and sub-surface), the introduction of highly saline sea water into groundwater in spray zones, and a decrease in water volume due to evapotranspiration. As the process continues the deposit becomes more heavily cemented, the bioclasts are slowly dissolved entirely, and available pore space is gradually filled by precipitated $CaCO_3$.

The initial cementation of aeolianite can occur very rapidly – in some cases less than a century (Reeckmann & Gill 1981; Gardner & McLaren 1994; Dravis 1996; Kindler & Mazzolini 2001; McLaren 2007). The speed at which diagenesis continues after initial cementation is less well understood, and studied aeolianite deposits display differing degrees of diagenesis, suggesting that the process is often 'incomplete' (Reeckman & Gill 1981; McLaren 1993; Gardner & McLaren 1994; McLaren & Gardner 2004; Frebourg *et al*. 2008).

Like the degree of diagenesis, the style of diagenesis also varies. A range of different cement types are known to occur within aeolianite, and a number of climatic geological, and environmental factors have been argued to control the occurrence of these types (Reeckman & Gill 1981; McLaren 1993; Frebourg *et al*. 2008). The composition of the sediment determines how much $CaCO_3$ is available, and the size, shape and packing of the grains controls how easily water moves through the deposit (Gardner & McLaren 1994; McLaren & Gardner 2004; McLaren 2007). The rainfall and temperature of a location can have an effect on the diagenetic process, as can the presence of sea water – either covering the deposit or in the form of spray (Reeckman & Gill 1981; McLaren 1993, 2001; Gardner & McLaren 1994; McLaren & Gardner 2004).

The determination of the cement type/s within an aeolianite deposit can provide information on the climatic and/or environmental conditions that were present at the time of cementation (Ward 1973, 1975; Tucker & Wright 1990; McLaren & Gardner 2004). However, due to the complex mix of factors described above, it is seldom possible to attribute a particular set of diagenetic features to a specific climate or environment (McLaren & Gardner 2004).

3.2. BEACHROCK

Beachrock deposits have been used in the estimation of past sea levels through two methods. The first is through the environmental associations of depositional facies, and the second is through the use of the cements which lithified the deposits (Vousdoukas *et al*. 2007; Caron 2011; Cooper 2013; Kelly *et al*. 2014; Mauz *et al*. 2015). These are discussed in turn here.

3.2.1. Coastal marine deposition

Deposition and erosion in coastal marine environments occurs through the movement of sediment by waves, swash and backwash (Reading & Collinson 1996; Anthony 2009; Davidson-Arnott 2010). Different combinations of these processes take place in different parts of the coastal zone (Figure 3.2), resulting in the formation of distinct landforms and sedimentary facies in these zones (Clifton *et al*. 1971; Davidson-Arnott & Greenwood 1976; Clifton 1976; Hunter *et al*. 1979; Moslow 1984; Shipp 1984; Roep 1986; Reading & Collinson 1996; Doucette 2000; Swales *et al*. 2006). The facies are distinctive enough to be used, when found in ancient deposits, to reconstruct palaeoenvironments, especially past sea levels (e.g. Carr *et al*. 2010; Roberts *et al*. 2012; Cooper 2013; Kelly *et al*. 2014; Mauz *et al*. 2015; Cawthra *et al*. 2018).

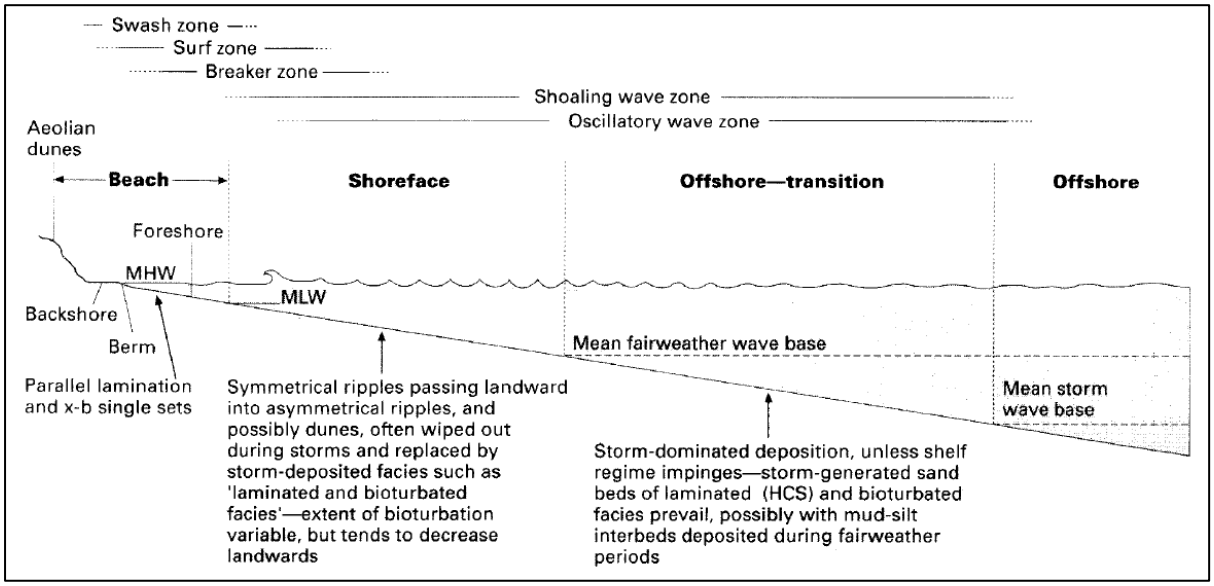


Figure 3.2. A cross-section through a generalised shoreline profile with the various zones indicated (Reading & Collinson 1996).

The morphology and depositional properties of gravel and boulder beaches differ from sandy beaches due to the influence of textural differences on the effectiveness of waves and swash and backwash processes (Oak 1984; Orford *et al*. 1991; Reading & Collinson 1996; Bluck 1999; Anthony 2009; Cooper 2013). However, despite a relative paucity of research when compared to sandy beaches, gravel and boulder facies have been identified and associated with specific modern coastal environments, and then utilised in sea level reconstructions from ancient deposits (Bluck 1967, 1999, 2011; Oak 1984; Williams & Caldwell 1988; Postma & Nemec 1990; Bluck *et al*. 2001; Haslett & Curr 2001; Bezerra *et al*. 2003).

3.2.2. Beachrock cementation

Beachrock is formed through the precipitation of calcium carbonate cements between and around the grains and clasts in beach sediments (Bricker 1971; Hanor 1978; Hopley 1986; Vousdoukas *et al*. 2007; Mauz *et al*. 2015). Water in the sediment becomes supersaturated with carbonate, which results in the precipitation of calcium carbonate through the deposit (Vousdoukas *et al*. 2007; Mauz *et al*. 2015).

Mechanisms of calcium carbonate supersaturation and cement precipitation include direct precipitation by marine or meteoric waters, the mixing of groundwater and seawater, tidal pumping (resulting in CO_2 degassing), evaporation of water due to heating by the sun, and even microbial activity (Schmalz 1971; Moore 1973; Plummer 1975; Hanor 1978; Hopley 1986; Meyers 1987; Kindler & Bain 1993; Gischler & Lomando 1997; Neumeier 1999; Calvet *et al*. 2003; Omoto 2004; Kelletat 2006; Vieira & De Ros 2006; Gischler 2007; Knight 2007; Vousdoukas *et al*. 2007; Mauz *et al*. 2015). These processes are most pronounced in the intertidal zone where the water table and seawater meet and, as a result, almost all beachrock cementation takes place within the intertidal zone beneath un-cemented beach deposits (Hopley 1986; Ramsay 1991, 1995; Gischler 2007; Vousdoukas *et al*. 2007; Mauz *et al*. 2015; Wiles *et al*. 2018). Field observations indicate that this process can occur very rapidly, on a timescale of decades or less (Frankel 1968; Kelletat 2006; Vousdoukas *et al*. 2007; Cawthra & Uken 2012; Wiles *et al*. 2018).

Three different forms of calcium carbonate are known from beachrock cements: low magnesian calcite (LMC), high magnesian calcite (HMC) and aragonite (Russell 1963; Bricker 1971; Milliman 1974; Tucker & Bathurst 1990a, b; Neumeier 1998, 1999; Calvet *et al*. 2003; Vousdoukas *et al*. 2007; Mauz *et al*. 2015). LMC cements are associated with meteoric water and form within the upper beach (Figure 3.3). HMC cements form between the lower beach and the lower shoreface (and very rarely in the upper beach), while aragonite cements precipitate between the lower foreshore and the edge of the subtidal zone (Figure 3.3).

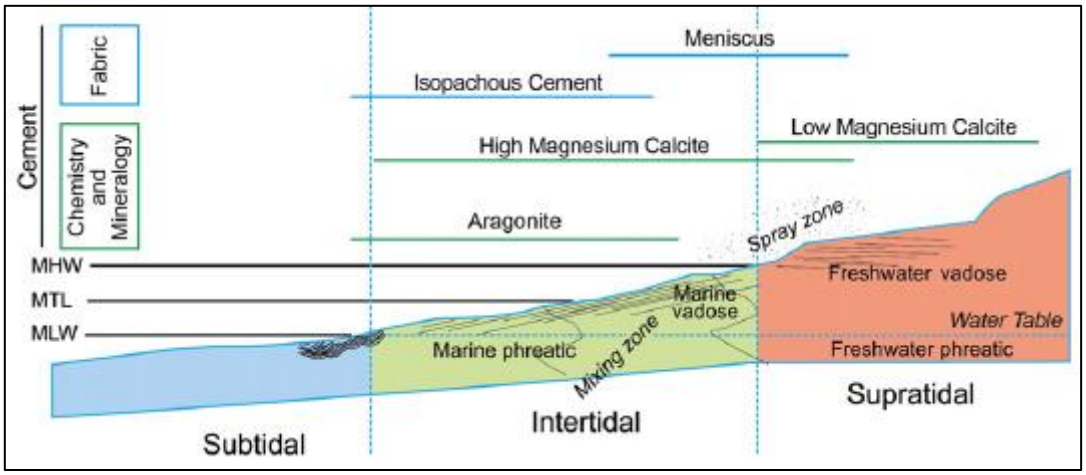


Figure 3.3. The distributions of different calcium carbonate cement types and their fabrics within the coastal zone (after Mauz *et al*. 2015).

Different combinations of cement properties – including the shape and size of crystals, their distribution around grains and in pore spaces, and their fabric – occur in different parts of the intertidal and supratidal zones (Bricker 1971; Dunham 1971; Longman 1980; Meyers 1987; James & Ginsburg 1990; Tucker & Bathurst 1990a, b; Whittle *et al*. 1993; Gischler & Lomando 1997; Adams & MacKenzie 1998; Neumeier 1998; Webb *et al*. 1999; Flügel 2004; Vousdoukas *et al*. 2007; Mauz *et al*. 2015). Identifying the type and properties of calcium carbonate cements in a beachrock deposit allows the determination of where in relation to mean sea level (in which part of the coastal zone) the deposit was cemented (Gischler 2007; Vousdoukas *et al*. 2007; Desreulles *et al*. 2009; Mauz *et al*. 2015; Wiles *et al*. 2018). This means that beachrock cement can be a useful proxy for past sea levels (Vousdoukas *et al*. 2007; Cawthra & Uken 2012; Mauz *et al*. 2015; Cooper *et al*. 2018; Wiles *et al*. 2018).

Multiple generations of cement may be precipitated into a single deposit, and these may form under different conditions as sea levels change, producing a “mixed” signal within the deposit (Whittle *et al*. 1993; Vousdoukas *et al*. 2007; Mauz *et al*. 2015; Wiles *et al*. 2018). However, careful analysis and interpretation of the cements allows their use in sea level reconstructions despite this complication (e.g. Wiles *et al*. 2018).

3.3. SOUTH AFRICAN COASTAL AEOLANITES AND BEACHROCK

The study of aeolianite and beachrock deposits has provided information on a range of palaeoenvironmental factors along South Africa’s coasts. This section is a review of this past research which is aimed at placing the deposits at Nahoon Point into a broader context of Middle and Late Pleistocene coastal depositional and sea level history.

3.3.1. Coastal aeolianites and dunes in South Africa

Coastal dunes and aeolianite are common along South Africa’s coastline, occurring regularly on sandy and mixed shores (Davies 1971, 1972, 1973; Roberts *et al*. 2014; Cawthra & Bateman 2016). In this dissertation, following Roberts *et al*. (2014), these deposits are considered within a tripartite division of South Africa’s coast into the west coast (from Saldanha to Cape Agulhas), southern coast (from Cape Agulhas to just north of East London), and east coast (from north of East London to the Mozambique border). The only major break in the distribution of coastal aeolian deposits is along the southern part of the east coast, from a little north of East London to central Kwa-Zulu Natal (Roberts *et al*. 2014; Cawthra & Bateman 2016). This is due to the dominance of a steep, rocky shoreline in this area (Roberts *et al*. 2014; Knight & Grab 2015; Cawthra & Bateman 2016).

Reported ages for these aeolian deposits range from the Miocene (~23 – 5 Ma) to the Late Pleistocene (~130 – 12 ka) and Holocene (~12 ka to present) (Bateman *et al*. 2004, 2011; Carr *et al*. 2007, 2010; Porat & Botha 2008; Roberts *et al*. 2008, 2012, 2014; Jacobs *et al*. 2011; Cawthra & Bateman 2016). The primary focus of this section is on Middle and Late Pleistocene (~780 – 12 ka). Onshore coastal aeolian deposits formed during this period date to between MIS 11 and MIS 2 (~410 ka –

~12 ka) (Roberts *et al*. 2014). A peak in aeolian deposition on the southern coast occurred during MIS 6 and MIS 5 (Roberts *et al*. 2014). Offshore aeolianite deposits have been reported and studied on the coastal plains off the southern and east coasts (Martin & Flemming 1987, 1988; Porat & Botha 2008; Bateman *et al*. 2011; Cawthra 2012; Cawthra *et al*. 2012a, b, 2014, 2016, 2018; Salzmann *et al*. 2013; Cooper & Green 2016; Botha 2018). These deposits indicate the continuation of aeolian deposition when shorelines regressed during periods of significantly lower sea level (Porat & Botha 2008; Bateman *et al*. 2011; Cawthra *et al*. 2014, 2016, 2018; Roberts *et al*. 2014; Botha 2018).

Published sequences in all three regions (the west, southern and east coasts) indicate phases of aeolian deposition punctuated by periods of palaeosol and calcrete development indicative of reduced deposition and increased landscape stability, predominantly during glacial periods (Barwis & Tankard 1983; Bateman *et al*. 2004, 2011; Butzer 2004; Porat & Botha 2008; Roberts *et al*. 2008, 2009, 2014; Botha 2018).

Late Pleistocene aeolianites on the west coast preserve evidence for large landward-advancing dune plumes which were formed by strong southerly winds, suggesting similar conditions to the present day (Barwis & Tankard 1983; Butzer 2004; Roberts *et al*. 2009, 2014). Aeolian deposits dating to the Middle and Late Pleistocene on the southern coast primarily formed as part of shore-parallel vertically-accreting cordons which are notably more vertically extensive than the west coast dunes (Illenberger 1996; Bateman *et al*. 2004, 2011; Roberts *et al*. 2008, 2014). The orientation of bedding structures and parabolic dunes indicates that wind direction was predominantly from the west and southwest, as it is today (Roberts *et al*. 2008, 2014). East coast Late Pleistocene dunes generally represent shore-parallel vertically-accreting cordons, although these are sometimes more complex in composition than the cordons on the southern coast (Martin & Flemming 1987, 1988; Porat & Botha 2008; Cawthra 2012; Roberts *et al*. 2014; Botha 2018). Unlike the west and southern coasts, there is evidence for variation in dominant wind directions over time (Cawthra 2012; Porat & Botha 2008; Roberts *et al*. 2014; Botha 2018).

The differences in the dune systems (both ancient and modern) along these different parts of the coast have been linked to climatic and ecological factors (Roberts *et al*. 2014). On the arid west coast, strong winds during the dry summers resulted in the dominance of relatively sparsely vegetated landward-advancing dune systems (Roberts *et al*. 2014). Weaker winds and wetter conditions along the southern and eastern coasts meant that dune formation was heavily influenced by vegetation growth, leading to the development of vertically-accreting systems and a rarity of landward-advancing dunes (Illenberger 1996; Porat & Botha 2008; Bateman *et al*. 2011; Roberts *et al*. 2014).

Trace fossils in aeolianite deposits spanning MIS 6 and MIS 5 have given insight into the palaeoenvironments and palaeo-ecology of the southern Cape during these periods (Roberts *et al*. 2008; Helm *et al*. 2018a, b, 2019). Recent work has led to the discovery of a large number of trace fossils representing a wide range of vertebrate species in aeolianite deposits (Roberts *et al*. 2008; Helm *et al*. 2017, 2018a, b, c, 2019). These include trackways made by elephant, giraffe, rhino, the giant Cape horse (extinct), long-horned buffalo (also extinct) and humans (Roberts *et al*. 2008; Helm *et al*. 2018a, c, 2019).

The aeolianites at Nahoon Point have yet to be analysed in the detail which has allowed such nuanced palaeoenvironmental interpretations of other aeolian deposits along South Africa's coastlines. However, there is considerable potential for this study to provide similar context to Nahoon Point and its surrounds.

3.3.2. Early MIS 5 sea levels

For most of MIS 5e, global air and sea surface temperatures were similar to, or higher than, that of the recent pre-industrial past (Shackleton *et al*. 2003; NEEM Community Members 2013; Govin *et al*. 2015). Between 135 – 129 ka (Terminal MIS 6 and early MIS 5e), they began to increase markedly (Govin *et al*. 2015). From 129 to 120 ka, different regions gradually reached their respective MIS 5e temperature maxima (Jouzel *et al*. 2007; NEEM Community Members 2013; Govin *et al*. 2015). Temperatures decreased significantly from ~118 ka onward, dropping to well below modern levels by mid-MIS 5d (NEEM Community Members 2013; Govin *et al*. 2015;

Railsback *et al*. 2015). This led to a reduction, and later growth, in the polar ice caps which resulted in significant changes in eustatic sea level (Lambeck *et al*. 2002, 2012; Siddall *et al*. 2007; Dutton & Lambeck 2012; Murray-Wallace & Woodroffe 2014).

There is considerable geological evidence for two distinct highstands (Figure 1.1) at or above present sea level, and a relative lowstand between them, within MIS 5e (Chen *et al*. 1991; Neumann & Hearty 1996; Wilson *et al*. 1998; Zazo 1999; Dumas *et al*. 2006; Hearty *et al*. 2007; Kopp *et al.* 2009, 2013; Thompson *et al*. 2011; O'Leary *et al*. 2013; Gischler 2014). The timing of these events is debated, but it seems that the first highstand occurred during early MIS 5e (~132 ka and ~126 ka), followed by the lowstand in mid-MIS 5e (~126 ka to ~122 ka), and the second highstand in later MIS 5e (~122 ka to ~118 ka) (Neumann & Hearty 1996; Hearty et al. 2007; Blanchon *et al*. 2009; Kopp *et al.* 2009, 2013; Thompson *et al*. 2011). The changes within MIS 5e appear to have occurred fairly quickly, and the highstands may have lasted as little as ~2 kyr (Dumas *et al*. 2006; Hearty *et al*. 2007; Kopp *et al.* 2009, 2013; Rohling *et al*. 2009; Lambeck *et al*. 2012). It is also generally agreed that sea level rise from the MIS 6 lowstand, and the decrease during late MIS 5e/MIS 5d (from ~118 ka) both took place relatively rapidly (Hearty & Neumann 2001; Hearty *et al*. 2007; Kopp *et al.* 2009, 2013; Rohling *et al*. 2009; Lambeck *et al*. 2012).

Despite the general trends, there was considerable regional variation in relative sea levels during these periods (Hearty *et al*. 2007; Kopp *et al.* 2009, 2013; Lambeck *et al*. 2012). Therefore, global data cannot be applied uncritically to any specific location. In South Africa, erosional and depositional features in aeolianite and beachrock have been major sources of evidence in Quaternary sea level studies (Cooper & Flores 1991; Ramsay 1995; Ramsay & Cooper 2002; Carr *et al*. 2010; Roberts *et al*. 2012; Cawthra & Bateman 2016; Cawthra *et al*. 2018; Cooper *et al*. 2018).

Raised marine benches ranging between 6 m and 8 m above present sea level have long been reported along South Africa's coastlines (Maud 1968; Davies 1970, 1971, 1972, 1973, 1980; Tankard 1976; Marker 1984, 1987; van Andel 1989). These were

assumed to have been associated with the Last Interglacial (or MIS 5e) despite the lack of dates for the features (Davies 1970, 1971, 1972, 1973, 1980; Barwis & Tankard 1983; van Andel 1989).

Deposits near Durban, on the KwaZulu Natal (KZN) coast indicate the occurrence of two highstands (5 m and 7 m above present sea level) within a relatively short period of time (Cooper & Flores 1991). Unfortunately, these deposits have not been dated. Ramsay and Cooper (2002) recognise two sea-level highstands in data collected from various dated sites in KZN. The dates for the sites generally have large error margins that include several marine isotope stages. They argue that the average sea level for both highstands was approximately 4 m above present levels. A single dated beachrock deposit 44 m below sea level is suggested to indicate sea level dropped this low between the two highstands. While they attribute the second highstand to MIS 5c, there is no local or global evidence to support a highstand of this level during this period (Carr *et al*. 2010: 361 – 362).

It is most likely that the two highstands identified on the KZN coast by Cooper and Flores (1991) and Ramsay and Cooper (2002) both date to MIS 5e. However, due to the lack of, or apparent inaccuracy of dates, it is impossible to determine when precisely in MIS 5e these highstands occurred. Due to the lack of direct stratigraphic correlation between the dated deposits and the dating issues (Ramsay & Cooper 2002), the estimate of a -44 m sea level between the highstands may be incorrect.

Barwis & Tankard (1983) identified evidence for two highstands separated by a relative lowstand at Swartklip, near Cape Town, in the form of beachrock and estuarine deposits. The second highstand is argued to have reached between 5.1 m and 8 m above present sea level. This sequence has not been dated, but is argued to date to between 135 ka and 120 ka based on comparison with marine isotope records (Barwis & Tankard 1983).

The most securely dated evidence for South African sea levels during Early MIS 5 comes from several locations on the southern coast between Cape Town and Plettenberg Bay. At the Swartvlei Estuary, facies indicating sea levels ranging up to

~+8.5 m have been dated to between 138 ± 7.3 ka and 127 ± 5.7 ka, while overlying aeolian deposits date between 113 ± 5.6 ka and 95 ± 4.1 ka (Carr *et al*. 2010). At Cape Agulhas, a beach deposit which formed when the local sea level was ~+5.6 m yielded a date of 118 ± 7.2 ka, while an aeolianite deposit lying above it was dated to 104 ± 7 ka (Carr *et al*. 2010). Beachrock indicative of a sea level around +6.2 m at Dana Bay was found to date between 125 ± 9 ka and 116 ± 9 ka (Roberts *et al*. 2012).

A beachrock deposit at the Great Brak Estuary, which was argued to indicate a sea level of ~+7 m, has been dated to 125 ± 6.7 ka; it is overlain by aeolianite dated to 122 ± 6.9 ka (Carr *et al*. 2010). Cawthra *et al*. (2018) interpret the same feature as evidence for a sea level of ~+6.3 m. Younger beachrock units, suggesting a sea level of +6.8 m, were dated to between 121 ± 7 ka and 118 ± 7 ka in the same area (Cawthra *et al*. 2018). Deposits of aeolianite and beachrock that are currently below sea level indicate a drop in sea level to below -20 m by 115 ± 7 ka (Cawthra *et al*. 2018).

Despite the lack of dates in some cases, and the large error margins on those that have been reported, it seems that the evidence for Early MIS 5 highstands in South Africa is broadly referable to the global patterns both temporally and in terms of the sea levels reached. The first highstand, with ages ranging from 130 ± 8.3 ka to 125 ± 6.7 ka, reached +6.2 m to +8.5 m, while the second highstand, dated to between 121 ± 7 ka and 118 ± 7 ka, peaked between +5.6 m and +6.8 m. Considerably less is known about sea levels in the region during the apparent mid-MIS 5e lowstand and the MIS 5d regression.

3.4. EARLY MIS 5 ARCHAEOLOGY OF SOUTH AFRICA

The Nahoon Point Footprints and the artefactual material from Blind River and East Beach fall within the period known as the Middle Stone Age (MSA). Generally, the South African MSA is considered to have begun ~280 ka and ended between 40 ka and 20 ka (Thackeray 1992; Wadley 1993, 2015; Barham & Mitchell 2008; Lombard *et al*. 2012; Wurz 2013).

Research into MSA sites in South Africa has yielded considerable evidence for behaviours which may be indicative of advanced cognitive abilities in human populations (McBrearty & Brooks 2000; Henshilwood & Marean 2003; Wurz 2013; Wadley 2015). Cultural material that may be indicative of symbolic behaviour, and the complexity of techniques utilised in the production of various tools and weapons have both received considerable attention as ways to gauge cognitive abilities (Wurz 1999, 2013, 2016; McBrearty & Brooks 2000; Henshilwood *et al*. 2001, 2002, 2004, 2009, 2011, 2018; Wadley 2001, 2010; Klein & Edgar 2002; Wadley *et al*. 2004, 2009; Lombard 2005, 2007a, b; d'Errico & Henshilwood 2007; Henshilwood 2007; d'Errico *et al*. 2008; Mackay & Welz 2008; Villa *et al*. 2009; Watts 2009, 2010; Lombard & Phillipson 2010; Mourre *et al*. 2010; Texier *et al*. 2010; Wilkins *et al*. 2012; Henshilwood & Lombard 2013). Subsistence behaviour and the ability of human populations to adapt to different environmental conditions have also featured in this debate (e.g. Klein 1979, 2001, 2008; Klein & Cruz-Uribe 1996; Milo 1998; Parkington 2003; Faith 2008, 2011; Steele & Klein 2008, 2009; Wadley 2010, 2015; Clark 2011; Weaver *et al*. 2011; Dusseldorp 2012; Clark & Kandel 2013; Marean 2014, 2016).

The Greater Cape Floristic Region (GCFR), an area of the western and southern cape that is dominated by Fynbos vegetation (and was for much of the MSA although with some variation in the degree to which it dominated [Marean et al. 2014]), has been at the centre of research into human-environmental interactions, particularly subsistence behaviours, partly because it was occupied continuously through the changing conditions associated with several glacial and interglacial cycles (Compton 2011, 2016; Marean 2014, 2016; Marean *et al*. 2014; Carr *et al*. 2016). The GCFR has come to be seen as a vital area in the emergence of behaviours indicative of modern cognitive abilities in human populations (Marean 2014, 2016; Marean *et al*. 2014; Carr *et al*. 2016). The longevity of human occupation has been linked to the availability of a variety of plant and animal species in the highly diverse ecosystems in the GCFR and to human populations having access to marine food resources at many of the sites (Marean 2010, 2014, 2016; Marean *et al*. 2014; Carr *et al*. 2016).

Apart from Nahoon Point and Blind River, only eight archaeological or palaeoanthropological sites in South Africa (including two sites just 300 m apart) preserve dated evidence for human presence/occupation during Early MIS 5 (Table 3.1).

These sites are located within a wide range of modern environments (Figure 3.4), and the available palaeoenvironmental data suggest that the situation was similar during Early MIS 5 (Table 3.2). However, all of the coastal sites fall within the GCFR (Marean *et al*. 2014; Carr *et al*. 2016). Therefore, the East London sites represent the only known South African evidence for human occupation of coastal areas outside of the GCFR during Early MIS 5. Archaeological surveys along the coast of Pondoland (roughly 200 km northeast of East London) have resulted in the discovery of a number of MSA sites (Fisher *et al*. 2013). These sites indicate coastal or near-coastal occupation, but those which have been dated are all significantly younger than MIS 5, apart from one which was occupied before 130 ka and contains a mixed (post-depositionally) assemblage of MSA and Acheulean artefacts (Fisher *et al*. 2013, 2019).

Almost all of what is known about human subsistence behaviour during Early MIS 5 is based on assemblages from coastal sites located within the GCFR (Dusseldorp 2010; Clark & Kandel 2013; Marean 2014, 2016; Marean *et al*. 2014; Carr *et al*. 2016). Research on these sites has shown the widespread exploitation of marine food resources within this period of time (Klein 1976; Thackeray 1988; Klein & Cruz-Uribe 1996; Stynder 1997; van Pletzen 2000; Henshilwood *et al*. 2001; Halkett *et al*. 2003; Parkington 2003; Klein *et al*. 2004; von den Driesch 2004; Marean *et al*. 2007; Avery *et al*. 2008; Steele & Klein 2008; Jerardino & Marean 2010; Thompson 2010; Thompson & Henshilwood 2011; Van Niekerk 2011; Langejans *et al*. 2012, 2017; Clark & Kandel 2013; Marean 2014, 2016; Kyriacou *et al*. 2015; Jerardino 2016; Klein & Bird 2016; Will *et al*. 2016). This was part of a general increase in human diet breadth (the range of species humans exploit for subsistence) between MIS 6 and early MIS 4 (Dusseldorp 2010; Clark & Kandel 2013; Marean 2014, 2016).

Table 3.1. Published dates/date ranges and Marine Isotope Stage (MIS) attributions for South African archaeological and palaeoanthropological sites with deposits argued to provide evidence for human presence or occupation during Early MIS 5 (130 – 105 ka). Note that the MIS attributions are those of this author, and may not always correspond precisely to those presented by the researchers who dated them. Nahoon Point and Blind River are excluded as they are discussed in Chapter 2. Dating techniques: amino acid racemisation (AAR), electron spin resonance (ESR), optically stimulated luminescence (OSL), infrared stimulated luminescence (IRSL), and Uranium-Thorium (U/Th).

Site	**Deposit/ Unit**	**Technique (Author)**	**Dates**	**MIS Attribution**
Border Cave	4WA	AAR (Miller *et al*. 1999)	>100 ka	MIS 6 – early MIS 5d
		ESR (Grun *et al*. 2003)	168 ± 5 ka – 113 ± 5 ka	
Florisbad	Unit F	ESR (Grun *et al*. 1996)	121 ± 6 ka	MIS 5e
		OSL (Grun *et al*. 1996)	133 ± 31 ka	
Hoedjiespunt	AH II	IRSL, ESR, U/Th (Will *et al*. 2013)	130 – 100 ka	MIS 5e
Klasies River Main	LBS	AAR (Bada and Deems 1975)	~110 ka	Late MIS 5e/early MIS 5d
		Oxygen Isotopes (Shackleton 1982)	~120 ka	
		U/Th (Vogel 2001)	>108.6 ± 3.4 ka	
		OSL (Feathers 2002)	106.8 ± 12.8 ka	
Langebaan		Corrected IRSL and U/Th (Roberts & Berger 1997)	~117 ka	Late MIS 5e/MIS 5d
Pinnacle Point 9C	RTE -OYCS	OSL (Matthews *et al*. 2011)	120 ± 7 ka	MIS 5e
	RTE -BYDS		126 ± 9 ka	
Pinnacle Point 13B	LC-MSA Middle	OSL (Jacobs 2010)	125.4 ± 6.9 ka	MIS 5e
	LC-MSA Upper		126 ± 5 ka	
	LBG 1		122 ± 6 ka 127 ± 8 ka	MIS 5e
	LRS		110 ± 4 ka	MIS 5d
Wonderwerk Cave	Stratum 2	U/Th (Beaumont & Vogel 2006)	220 ± 14 ka – 73 ± 5 ka	MIS 7 – MIS 5a

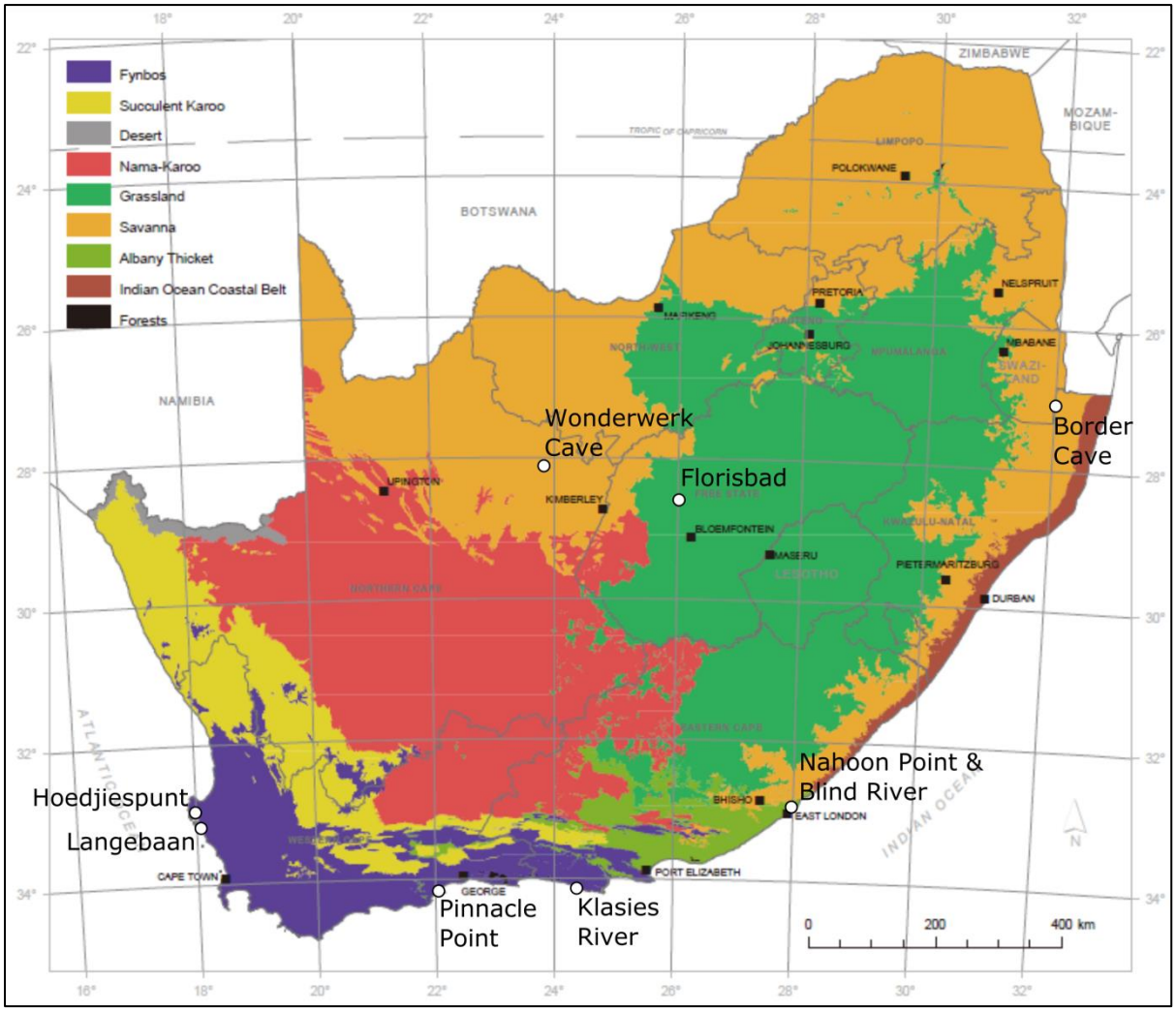


Figure 3.4. The locations of South African MIS 5e/5d (130 – 105 ka) archaeological and palaeoanthropological sites and the current extent of the major biomes within South Africa (after Rutherford *et al*. 2006). Note that the Fynbos biome and GCFR are broadly comparable geographically.

As the modern environments and ecology at East London differ considerably from that of the GCFR (Figure 3.4), one cannot use the palaeoenvironmental and palaeo-ecological data from that better-researched area to understand past conditions at Nahoon Point and the associated sites. At present, there is no evidence for the nature of human subsistence behaviour at the East London sites during Early MIS 5. Given the likely differences between their environments at this time, known patterns of subsistence behaviour at sites in the coastal GCFR and the interior can provide only rough indications of potential human subsistence patterns around East London. Only location-specific data obtained from the East London sites and their surrounds can give any real context to human occupation of this area during Early MIS 5.

Table 3.2. A summary of the known palaeoenvironmental conditions at South African Early MIS 5 archaeological and palaeoanthropological sites.

Site	Conditions	References
Border Cave	Sub-humid tropical climate; precipitation higher than present; mean temperature similar to present; shift from woodland vegetation (MIS 5e) to Miombo savanna (MIS 5d)	Avery 1992, 1993
Florisbad	MIS 5e: site was on shoreline of palaeo-lake considerably larger than current pan; climate likely wetter than present; grassland vegetation dominant	Brink 1987; Butzer 1988; Kuman *et al*. 1999; Toffolo *et al*. 2017
Hoedjiespunt	MIS 5e: site within 1 km of shoreline (similar to present); Fynbos vegetation dominant	Stynder 1997
Klasies River Main	MIS 5e/5d transition: vegetation a mix of different types (thicket, Fynbos, grassland, forest) but relatively open compared to present; climate warmer and drier than present; rainfall likely more seasonal than present; sea-surface temperatures and sea level comparable to those of today	Klein 1976; Butzer 1978; Avery 1987; Deacon & Geleijnse 1988; Hillestad-Nel *et al*. 2018; Langejans *et al*. 2017; Reynard *et al*. 2017
Langebaan	Late MIS 5e: wind regime similar to present; sea level ~1.3 m above present	Roberts & Berger 1997; Roberts 2008
Pinnacle Point	MIS 5e climate was relatively warm and wet; vegetation dominated by Fynbos species; MIS 5e: shoreline ~0.08 km from the site; end MIS 5d: shoreline reaches 0.5 km away	Fisher *et al*. 2010; Matthews *et al*. 2011
Wonderwerk Cave	No available information	-

4. METHODOLOGY

The data required to address the aims of the project (Section 1.2) were collected using a variety of field-based and laboratory techniques. The field methods, which form the base of the study, are described in Section 4.1. The laboratory methods, which provide complementary data for the field results, are considered in Section 4.2. Finally, the approach used in interpreting the data acquired in the field and in the laboratory is outlined in Section 4.3.

4.1. FIELD METHODS

The fieldwork component of this study comprises three stages. First, a foot survey was carried out to constrain the study area and identify suitable locations for logging sedimentary profiles. Second, profiles were logged to collect stratigraphic and sedimentary data across the study area. Third, samples for various laboratory analyses were collected from the profiles.

4.1.1. Survey and Mapping

Previous work on the aeolianite deposits around East London indicates that they are predominantly found between Blind River and the Quenera River in an area centred on Nahoon Point (Mountain 1945; Le Roux 1989a, b; Roberts 2008; Jacobs & Roberts 2009). However, exposures are only present between Blind River and the Nahoon River; the deposits between the Nahoon and Quenera Rivers are covered by modern dunes. Exposed aeolianite is found almost exclusively within the Reserve. Therefore, the fieldwork was restricted to this area. The known extent of aeolianite in the area around Nahoon Point is indicated in Figure 2.2.

The Nahoon Point Nature Reserve was surveyed on foot to determine the extent of the exposed aeolianite and related sedimentary deposits within the reserve. This, along with the sedimentary logging described below, helped to address Aim 1. The locations of any relevant exposures were recorded using a handheld GPS unit (with accuracy ranging between 4 m and 15 m). Exposures of aeolianite and beachrock were found to be present along most of the coastline within the reserve. No exposures were identified within the inland part of the reserve. It is likely that

aeolianite is present within this area, but is covered by younger aeolian deposits and vegetation and therefore could not be analysed.

Based on the foot survey, the study area was delimited to several kilometres of coastline along which there is fairly continuous exposure of aeolianite and/or beachrock deposits (Figure 4.1). The northeastern limit of the study area is Lookout Point; the southwestern limit is a stack ~500 m to the west of Bats Cave.



Figure 4.1. The study area (as defined after surveying) within the Nahoon Point Nature Reserve (Imagery: Google Earth, 23 July 2017).

The study area thus includes Nahoon Point in its entirety, Coves 1 – 4, and Bats Cave. The archaeological site near Bats Cave (Section 2.4.1) and the Nahoon Point Footprint site both fall within the study area. Some aeolianite and beachrock is present to the west beyond the study area. However, these exposures [with the exception of the East Beach sample site (Jacobs & Roberts 2009)] are heavily

weathered and are not suitable for detailed analysis. The profile at East Beach was not analysed in detail due to serious security risks. However, a short visit was conducted to confirm the stratigraphy observed by Jacobs & Roberts (2009) (see Figure 2.6). The nearby archaeological site of Blind River (Section 2.4.2) also falls outside of the study area.

4.1.2. Logging

The stratigraphy at Nahoon Point was clarified, in order to address Aim 1 of the project, by recording exposed aeolianite strata, and marine deposits stratigraphically associated with the aeolianite, along the coastline within the study area. These exposures are predominantly seaward-facing cliffs, with two stacks within the current inter-tidal zone also being logged. In total, 20 profiles were logged for this study. The locations of the profiles are described in detail in Chapter 5.

Logging involves creating a detailed diagram that records the stratigraphy of a profile and an accompanying written description of the sedimentological properties of each sedimentary unit visible within the profile (Miall 1977, 1996; Tucker 1986; Nichols 2009). Logging, whether from cores or *in situ* exposures, is the fundamental basis for the study of sedimentary sequences as it provides an understanding of the macroscopic physical properties of the sediment within a stratigraphic framework (Miall 1977, 1996; Tucker 1986; Nichols 2009).

A number of lithological properties were recorded based on *in situ* analysis of each unit. These include (but are not limited to): sedimentary structures (including bedding type if relevant), bedding thickness, orientation and inclination of bedding, the nature of the contacts between the unit and other units, sediment texture, colour, degree of cementation, unit thickness, the lateral extent of the unit, the presence of disturbance by various means, and the presence of rhizoliths. These properties provide information on the processes involved in the deposition of the sedimentary units, the environment into/onto which the sediment was deposited, and post-depositional processes which may have affected the deposit (Potter & Pettijohn 1962; Pettijohn *et al*. 1973; Hunter 1977a, d; Klappa 1980; Kocureck & Dott 1981; Kocurek 1996; Brooke 2001; McLaren 2007; Frébourg *et al*. 2008).

The logged stratigraphy was used to determine whether features at Nahoon Point pre-date, post-date, or are contemporaneous with the formation of the human footprints. This was achieved by comparing the stratigraphy of the different logged profiles across the landscape and identifying marker events or deposits which could be used to create a model of relative chronology that includes all the logged sedimentary units. This allowed the identification of which units should be considered to be products of which environmental phase in the sequence of the study area and, ultimately, which units could be used to reconstruct the MIS 5e palaeoenvironment/s of Nahoon Point and its surrounds.

4.1.3. Sampling

Sediment samples for different laboratory analyses were taken from suitable locations within the aeolianite in the logged profiles. The location from which each sample was taken is indicated on the logs presented in Section 5.1.2. The samples varied in volume, but were generally between 150 g and 200 g in mass. A total of 68 bulk samples were collected from a variety of sedimentary units across the logged profiles. The samples were taken far enough from unit boundaries to ensure that there was no contamination from mixing between units.

The collection of bulk samples was not conducted systematically. Instead, units were selected for sampling based on field observation of their stratigraphic position and their macroscopic sedimentary properties. The number of samples taken for each sampled unit varied based on the observed variation in macroscopic properties and the thickness of the unit. Each sample was given a code to allow easy contextualisation of the sample within the stratigraphy. The codes followed this format: P1U1.1. In this example, the sample was the stratigraphically-lowest sample taken from Unit 1 (U1) of Profile 1 (P1).

Two oriented block samples were also collected from the aeolianite for the production of thin sections. As with the bulk samples, these were given sample codes and the sampling locations are presented in the relevant logs in Section 5.1.2. These samples were taken from two facies directly or closely associated with the

stratum in which the footprints were found. Each block sample included the full vertical thickness of a bed (~2 cm to 4 cm) and was 10 – 15 cm wide.

4.2. LABORATORY ANALYSIS

Laboratory-based analyses of sediment properties can provide a great deal of data which either cannot be collected in the field, or can be collected with greater accuracy and sensitivity in the laboratory. A number of laboratory analyses were conducted on bulk samples and oriented block samples collected from the study area. The various pre-treatments and analyses are described in the sub-sections below.

4.2.1. Treatment of Samples

All of the aeolianite bulk samples were removed from the bags into which they were placed in the field. They were dried in an oven for 50°C for 48 hours and then placed into new bags to prevent the reabsorption of any moisture that may have been in the original bags. Each sample was split into four sub-samples of 20 g to 30 g and a larger reserve sample. The oriented block samples did not undergo any pre-treatment.

4.2.2. Density and Porosity

Determining the grain density and the porosity of each aeolianite bulk sample required measuring the dry and saturated mass and volume of a solid (still cemented) sub-sample. Sub-samples (with volumes ranging from 1.5 ml to 9.5 ml) from all 68 samples were analysed. Each sub-sample was weighed on a scale to determine its dry mass (see Sub-section 4.2.1. for drying procedure). It was then placed into a container of distilled water for 48 hours. The saturated sub-sample was re-weighed and placed into a container of water to determine its saturated volume through displacement. As 1 ml of distilled water weighs 1 g, it was possible to determine the proportion of the saturated volume that was made up of water-filled pore space (pore volume) and the proportion of the saturated volume that was the volume of the sediment itself. The pore volume was determined by subtracting the initial dry mass from the saturated mass of the sample, thus indicating how much water mass (and therefore, volume) was present due to the saturation of the pores.

The grain density of each sample was calculated using the formula (Manger 1963):

$$Density = Dry\ mass \div Total\ unsaturated\ volume$$

The porosity of each sub-sample was calculated using the following formula (Manger 1963):

$$Porosity = (Pore\ volume \div Total\ saturated\ volume) \times 100$$

The density and porosity of aeolianite are controlled by both the original depositional structure of the sediment and by subsequent cementation of the sediment particles by calcium carbonate cement during the process of lithification (McLaren 1993; McLaren & Gardner 2004). Therefore, determining the density and porosity of the aeolianite can provide information on the conditions under which deposition and post-depositional cementation took place (McLaren 1993, 2007; McLaren & Gardner 2004).

4.2.3. Carbonate Content

The calcium carbonate ($CaCO_3$) content of aeolianite is controlled by both the original composition of the aeolian sediment and the nature (and degree) of post-depositional chemical processes (McLaren 1993, 2007; Gardner & McLaren 1994; McLaren & Gardner 2004; Frebourg *et al*. 2008). $CaCO_3$, which can occur as either calcite or aragonite, is mainly present in aeolianites as bioclasts (such as shell fragments) or in the form of cement which binds grains together (Brooke 2001; McLaren 2007; Frebourg *et al*. 2008).

The carbonate (CO_3) content of the aeolianite was determined from bulk samples using the Loss on Ignition (LOI) method, following the technique of Heiri *et al*. (2001). Determining the carbonate content of the sampled aeolianite units allowed a rough estimate of how much $CaCO_3$ is present within these units. Sub-samples of 67 of the 68 samples were analysed. A single sub-sample could not be analysed as it was too small. The following procedure was repeated for sub-samples taken from each bulk sample (see Table 4.1): a porcelain crucible was heated to 50°C and then weighed. The mass (to the nearest 0.0001 g) was recorded. The sub-sample was placed into the crucible, and the crucible and sediment were weighed using the same balance. The crucible was put into a furnace and the sediment was burnt at 900°C for one

hour. After burning, the crucible was allowed to cool and then re-weighed in the same balance. The final mass was subtracted from the initial combined mass (crucible and sediment) to find the mass of the carbonate contained within the sub-sample. This was then converted to a percentage of the initial sub-sample mass to allow comparison between samples.

Table 4.1. Example of the table used to record the relevant data during the analysis of carbonate content through Loss on Ignition.

Sample name	**Crucible mass (g)**	**Crucible plus sediment mass (g)**	**Sample mass (g)**	**Post-ignition mass (g)**	**Mass lost (g)**	**%CO_3**
Example	20.0000	31.5214	11.5214	27.6421	3.8793	33.6704

The analysis of thin sections (Section 4.2.5.) and the use of Fourier transform infrared (FTIR) analysis (Section 4.2.6.) will provide the means to determine the relationship between the carbonate content results and the amount and form (calcite or aragonite) of calcium carbonate within the samples.

4.2.4. Particle Size

Sediment particle size distributions were determined using a Malvern Mastersizer 3000. Laser granulometers, such as the Mastersizer, measure the diffraction angles of light striking particles within a sediment sample (Loizeau *et al*. 1994). As the size of an object determines the angle of diffraction of the light that strikes it, particle size can be assessed from the angle of diffraction (Loizeau *et al*. 1994). Comparison of the results produced by laser granulometers with those of traditional methods for the determination of sediment particle size, such as sieving, has revealed that laser granulometry is acceptably accurate and is appropriate for windblown sand (Konert & Vandenberghe 1997).

The sub-samples (from all 68 samples) used for the analysis of particle size were treated with an acid solution to dissolve the calcium carbonate ($CaCO_3$) cement which holds the sand grains together in aeolianite (McLaren 1993, 2007; McLaren &

Gardner 2004; Roberts 2008). The $CaCO_3$ was removed to free the sand grains from the matrix and allow their measurement with the Mastersizer 3000. This stage required some experimentation in order to determine what concentration of acid would dissolve the $CaCO_3$ satisfactorily without causing any chemical etching of the grains in the samples. The final procedure was as follows: Each sub-sample (20 – 30 g) was placed into a container. A 20% solution of acetic acid (CH_3COOH) was added to the sediment. The sub-sample was left overnight to allow the acid to dissolve the $CaCO_3$. The sediment was then rinsed with distilled water in a sieve with a 34 µm aperture size and placed into an oven at 50°C until it was dry. The 34 µm sieve was chosen to ensure that no sand-sized or large silt-sized grains were lost. The sediment was checked under a microscope to determine visually whether or not all of the $CaCO_3$ had been removed or not. If it had, then the sample was bagged and stored for analysis; if there was any trace of remaining $CaCO_3$ in the sample, then the cycle was repeated. This continued until each sub-sample was visually clean of $CaCO_3$.

Although the Mastersizer 3000 is designed to measure particles up to ~2000 µm in diameter, grains larger than 1000 µm can cause blockages. Therefore, the decalcified sand was put through a 1000 µm aperture sieve before being analysed in the Mastersizer. None of the 68 aeolianite samples contained grains large enough to be caught in the 1000 µm sieve.

Experimental work has shown that the properties of the Standard Operating Procedure (SOP) used to control the settings on a laser granulometer strongly control the accuracy of analysis (Sperazza *et al*. 2004; Dias 2014). Furthermore, it has been demonstrated that different SOP properties are required for finer (silts and clays) sediments and coarser (sands) sediments (Sperazza *et al*. 2004; Dias 2014).

The SOP used on the Mastersizer 3000 during analysis was based on that developed by Dias (2014) for sand-sized sediments. Minor adaptations were made to the SOP to account for differences in the version of the machine and software used in this study. The properties of the SOP are listed below in Table 4.2.

Table 4.2. The standard operating procedure (SOP) settings used on the Mastersizer 3000 for particle size analysis.

Property	**Setting**
Particle Name	Silica (RI 1.544, AI 1.0)
Particle Refractive Index	1.544
Particle Absorption Index	1.000
Dispersant Name	Water
Dispersant Refractive Index	1.330
Scattering Model	Mie
Analysis Model	General Purpose
Weighted Residual	0.61 %
Laser Obscuration	10 – 20%

The distribution data yielded from the Mastersizer analysis were categorised into Wentworth's (1922) size classes to allow the textural classification of the sediment. The various moment measures (Folk 1966) relevant to the analysis of grain size – such as sorting, skewness, and kurtosis – were calculated using the programme Gradistat, which was developed by Blott and Pye (2001). The particle size data provide information on the depositional processes that formed the various sampled features at Nahoon (Folk 1971; Bagnold & Barndorff-Nielsen 1980).

4.2.5. Thin Section Analysis

The two oriented block samples collected from the footprint site were impregnated with resin before having thin sections cut from them by the technicians of the Thin Section Preparation Labs at the School of Geosciences, University of the Witwatersrand. The thin sections were cut through the sampled beds, parallel to their slopes. The analysis of the thin sections was carried out with an Olympus BX41 microscope using both bright field illumination and cross-polarised light following Stoops (2003). The identification and description of minerals and structures within the thin sections was made using mineralogical reference texts and the literature on

the cements typically found within aeolianites (Reeckman & Gill 1981; Bullock *et al*. 1985; Moore 1989; McLaren 1993, 2007; Gardner & McLaren 1994; McLaren & Gardner 2004; Melgarejo and Martin 2011).

The use of the petrographic microscope to analyse the mineralogical composition of the thin sections aided the identification of both primary and secondary materials within the sediment. The primary materials in aeolianite generally include silicates (predominantly quartz) and calcium carbonate ($CaCO_3$), which is most often present in the form of marine shell fragments composed of the mineral aragonite or its polymorph, calcite (Brooke 2001; McLaren 2007). The most common, and most important, secondary mineral in aeolianites is calcite (Brooke 2001; McLaren 2007). The aragonite in shell fragments can be altered into calcite without losing the form of the fragment (McLaren 2007; Shillito *et al*. 2009). Calcite is also precipitated as a cement after the dissolution of shell fragments (either aragonite or calcite) and/or the introduction of calcite in solution from the landscape surface (McLaren 1993, 2007; Brooke 2001; McLaren & Gardner 2004).

Analysis of the thin sections provided data on the original composition of the sediment and its cementation, particularly the structure of the cement. These data also improved the interpretation of the carbonate content of the bulk samples in terms of how they relate to the proportion of calcium carbonate present within the samples. These analyses allow insight into the source of the cement and may provide information on diagenetic processes. The structure and composition of the carbonate cement in the aeolianite can be useful proxies for environmental conditions at the time of lithification if they are analysed and interpreted carefully (McLaren 1993; McLaren & Gardner 2004). This is particularly important for understanding the influence of post-depositional processes on the aeolianite deposits. Calcite and aragonite (both of which can contribute to the total calcium carbonate in the form of bioclasts and cement) were distinguished using Fourier Transform Infrared (see below) and not through microscopic analysis of the thin sections.

4.2.6. Fourier Transform Infrared Analysis

Fourier Transform Infrared (FTIR) spectroscopy relies on the measurement of the absorption of different wavelengths of infrared light by a sample (Smith 2011). As different elements absorb different proportions of each wavelength, it is possible to determine the molecular composition of the sample based on these measurements (Smith 2011). FTIR is a qualitative and semi-quantitative analysis; therefore, while it can be used to detect the presence of particular elements or compounds, it can provide only limited data on their proportions within a sample (Smith 2011).

Sub-samples of four aeolianite bulk samples taken from the footprint site were analysed by Marine Wojcieszak of the Evolutionary Studies Institute at the University of the Witwatersrand. These samples were taken from the two units from which the thin sectioned samples were collected. The samples underwent all of the other laboratory analyses conducted on bulk samples (density and porosity, carbonate content and particle size). Therefore, the FTIR results could be compared (and used to complement) the results of the other laboratory analyses.

The analysis was conducted on finely ground sub-samples with a Bruker Alpha spectrometer using an attenuated total reflection (ATR) module (M. Wojcieszak pers. comm. 2017). Multiple measurements were carried out, and the acquired spectra were corrected for the influence of atmospheric spectra (M. Wojcieszak pers. comm. 2017).

A number of primary and secondary minerals can be present within aeolianite. Carbonate content analysis (Section 4.2.3.) and thin section analysis (Section 4.2.5.) both provide information on the chemical and mineralogical composition of the aeolianite. However, FTIR can complement the data collected through these techniques and allow more nuanced interpretations of the results. For example, FTIR analysis can be used to distinguish aragonite from calcite in bioclasts within a bulk sample (Weiner *et al*. 2002; Shillito *et al*. 2009). This allows a determination of the intensity of some diagenetic processes within the deposit that thin section analysis does not.

4.3. INTERPRETATION OF RESULTS

The recorded properties (both field and laboratory data) of the aeolianite (and any other geological features of interest) were used to determine what processes led to the formation of these features. This was achieved through comparison of these features and properties with the existing sedimentological and geomorphological literature on the formation of modern and ancient dune systems and marginal marine deposits (see Sections 3.1 and 3.2 for a summary of the relevant sources), and by placing them into the context of regional palaeoenvironmental evolution during the Late Pleistocene.

The use of modern analogues to interpret ancient deposits relies on the assumption that sedimentary and geomorphic processes operating in the past followed the same set of 'laws' as those operating today (Baker 2014; Knight & Harrison 2014). This study follows the principle of 'weak' uniformitarianism, which holds that modern analogues are the best means for extrapolating environmental conditions from the geological record (Baker 2014; Knight & Harrison 2014; Romano 2015). However, care must be taken to account for the fact that many processes occurred at different rates during various periods in the past, and that processes which operate at under present conditions may not have taken place under past conditions, and *vice versa* (Baker 2014; Knight & Harrison 2014; Miall 2014; Romano 2015). Therefore, it was important to use the literature critically, with an awareness of the potential downfalls of this approach.

It was vital to differentiate the products of post-depositional processes from the original depositional features in order to ensure that only the features produced during the period of interest are considered. The existing literature on aeolianite formation clearly distinguishes depositional from post-depositional features at both macroscopic and microscopic scales (Reeckman & Gill 1981; Moore 1989; McLaren 1993, 2007; Gardner & McLaren 1994; McLaren & Gardner 2004). The identification of specific processes allows for the inference of the environmental conditions at the time the processes were in operation. This will address Aims 2 and 3 of the project.

The environmental information gained from the analysis of the sedimentology and geomorphology was combined to create a reconstruction of the regional environment during MIS 5e at Nahoon Point when the human footprints were produced. This addresses Aim 3 of the project.

5. RESULTS

The results of the various field-based and laboratory analyses utilised for this research (described in Chapter 4) are presented in this chapter. The chapter is split into two sections. The first section (with a single exception) contains results of the work carried out in the study area itself. The second details results of the different laboratory analyses conducted on samples collected from the study area. The results will be discussed in the following chapter (Chapter 6).

5.1. FIELD RESULTS

The results of the fieldwork conducted for this project are presented in this section. They are divided into three distinct sub-sections. The first sub-section details the locations of the 20 logged profiles within the study area. The second includes the sedimentary logs and descriptions for each profile as well as the grain size properties of the samples taken from the various sampled sedimentary units. Finally, in the third sub-section, information on the sedimentary context and archaeological properties of artefactual deposits found within the study area are presented.

5.1.1. Profile location description

As stated in Chapter 3, a total of 20 profiles was logged for this study (see Figure 5.1 and Table 5.1). Nine were logged from exposures of aeolianite on, or in the immediate vicinity of, Nahoon Point. The remaining 11 were recorded from exposures along the coast to the southwest of Nahoon Point.

Profiles 1 and 2 were logged from an aeolianite exposure roughly 50 m long which is located on the southern edge of Nahoon Point (Figure 5.1). This low, flat outcrop is the site which preserved the human footprints. It disappears below the current dune system roughly 20 m to the northeast of the footprint location.

The next exposure of the aeolianite rises out of the sand around 60 m to the East. This outcrop is higher and longer, continuing around Nahoon Point for several hundred metres (Figure 5.1). Profiles 3 and 4 were recorded from different ‘faces’ of this outcrop. Profile 5 was logged from a stack in the current intertidal zone ~50 m to the southeast of this outcrop (Figure 5.1). The outcrop is eventually obscured by

vegetated dunes on the northeastern corner of Nahoon Point. Around 100 m north-eastward up the coastline, on the edge of the parking lot, a small (30 m long) exposure appears out of the modern dunes (Figure 5.1). Profile 6 was recorded from this exposure. Profile 7 was logged from a small (~2.5 m wide) and low outcrop of conglomerate and aeolianite on the edge of the intertidal zone to the northeast of the parking lot (Figure 5.1).

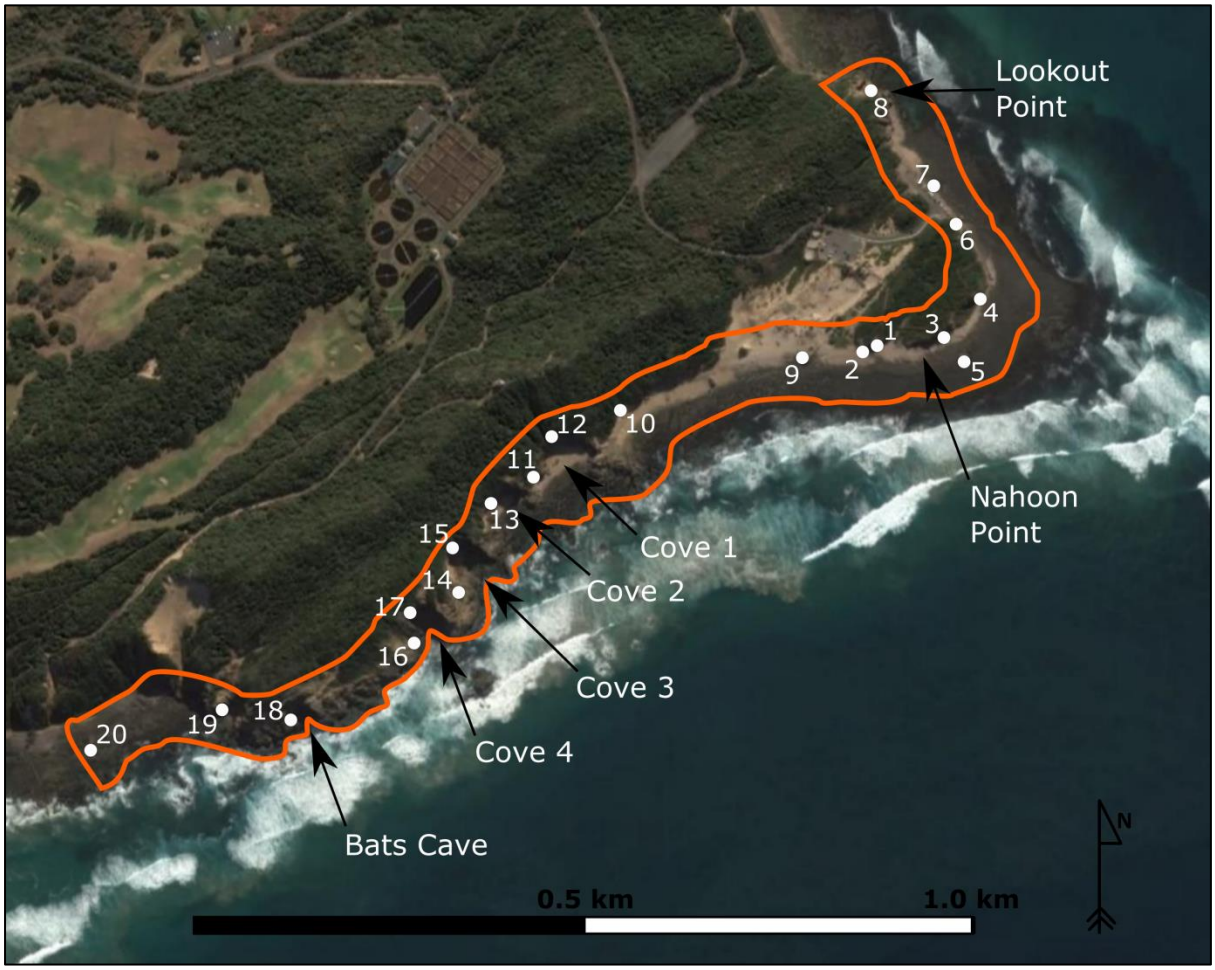


Figure 5.1. The locations within the study area of the 20 profiles (see Table 5.1) logged for this project (Imagery: Google Earth, 23 July 2017).

To the North of Nahoon Point, there is a smaller point known locally as Lookout Point (Figure 5.1). It is dominated by an aeolianite outcrop (and overlying sands) that rises up to 35 m above the surrounding terrain. Profile 8 was recorded in a small cove, the Mermaid's Pool, located on the northeastern edge of Lookout Point.

Table 5.1. The co-ordinates of each logged profile, the elevations relative to high tide level for the bases of the profiles, and the logged height of each profile.

Log	Location	Co-ordinates	Base (relative to high tide level)	Height of logged profile
1	Footprint Site, Nahoon Point	32°59’51”S, 27°57’01”E	1.5 m	5.0 m
2	Footprint Site, Nahoon Point	32°59’51”S, 27°57’00”E	1 m	5.7 m
3	Nahoon Point	32°59’51”S, 27°57’05”E	1 m	13.8 m
4	Nahoon Point	32°59’49”S, 27°57’06”E	1 m	8.3 m
5	Nahoon Point Stack	32°59’52”S, 27°57’05”E	-1 m	6.6 m
6	Nahoon Point North	32°59’46”S, 27°57’05”E	0.5 m	6.4 m
7	Parking Lot	32°59’44”S, 27°57’04”E	0 m	3.4 m
8	Lookout Point	32°59’40”S, 27°57’01”E	-0.5 m	8.6 m
9	West of Nahoon Point	32°59’52”S, 27°56’57”E	1.5 m	2.3 m
10	East of Cove 1	32°59’53”S, 27°56’50”E	1 m	5.0 m
11	Cove 1	32°59’56”S, 27°56’43”E	1 m	11.5 m
12	Cove 1	32°59’55”S, 27°56’44”E	1.5 m	8.3 m
13	Cove 2	32°59’58”S, 27°56’41”E	0 m	25.0 m
14	Cove 3	33°00’01”S, 27°56’40”E	-0.5 m	10.6 m
15	Cove 3	33°00’00”S, 27°56’39”E	1 m	17.0 m
16	Cove 4	33°00’03”S, 27°56’37”E	-1.2 m	11.0 m
17	Cove 4	33°00’02”S, 27°56’37”E	1.5 m	23.0 m
18	Bats Cave	33°00’07”S, 27°56’31”E	-1.5 m	30.0 m
19	Small Cove	33°00’07”S, 27°56’27”E	-0.5 m	8.2 m
20	Bats Cave Stack	33°00’08”S, 27°56’21”E	-1.4 m	4.9 m

Profile 9 was logged from a small, isolated outcrop on the westernmost edge of Nahoon Point (Figure 5.1). This outcrop is ~3 m high and is only exposed on the edge of the intertidal zone before disappearing under modern sand deposits.

A prominent unconformity/disconformity in the aeolianite is present on several parts of Nahoon Point. It is associated with a well-developed, but discontinuous, raised marine bench that has an elevation ranging from 4 m to 6.5 m above high tide level.

Profiles 10 to 19 are within an extensive outcrop of aeolianite to the southwest of Nahoon Point (Figure 5.1). This outcrop is present along more than a kilometre of coastline and rises up to 50 m above high tide level. Profile 10 was recorded from a small outcrop that is partially buried by the modern dune system but is clearly associated with the major outcrop mentioned above. Profiles 11 to 17 were logged in a series of four coves that have been eroded into the aeolianite. Moving south-westward, away from Nahoon Point, Profiles 11 and 12 were recorded from Cove 1; Profile 13 was logged in Cove 2; Profiles 14 and 15 were recorded in Cove 3; and Profiles 16 and 17 were logged from Cove 4. Profile 18 was recorded in the vicinity of Bats Cave. This is a large sea cave eroded into the aeolianite on the southwestern edge of the exposure. Profile 19 was logged in a small cove on the western end of the exposure. Profile 20 was recorded from a stack located within the intertidal zone to the west of the major aeolianite exposure (Figure 5.1). As stated in the previous chapter, the East Beach location logged by Jacobs and Roberts (2009) was also visited and briefly examined. This visit confirmed their description of the sediments and stratigraphy except that no direct stratigraphic relationship between their basal marine unit and the lowermost aeolianite unit could be observed.

A prominent unconformity/disconformity in the aeolianite could be traced along the length of the large exposure. This is associated with a well-developed, but often discontinuous, raised marine bench that has an elevation ranging from 3.8 m to 7 m above high tide level.

5.1.2. Sedimentary Logs

Descriptions of the sedimentary properties of the logged profiles, and the associated logs, are presented below. No attempt is made here to correlate the profiles in relation to facies as, due to the manner in which dunes and interdunes form, deposits of the same facies may be deposited at different times on different parts of the landscape. Stratigraphic correlation between profiles will be discussed in Chapter 6. High tide level was used as an approximate calibration for the elevation of the base of each logged profile. The results of grain size analysis (conducted with the Mastersizer 3000) are also presented in this section. The mean grain size and the degree of sorting are given for each of the 68 bulk samples that were analysed. All of

the samples have grain size distributions that are symmetrical and mesokurtic. All of the samples were composed almost exclusively of sand-sized grains. However, silt and clay-sized particles were present in very small quantities in many of the samples.

Profile 1:

Eight distinct units were identified within Profile 1 (Figures 5.2 & 5.3). The base of the profile is 1.5 m above high tide level. This profile contained the human footprints and associated faunal trackways within Unit 5 (Roberts 2008). The aeolianite is composed of moderately well sorted to well sorted medium sand, and is well-cemented and a light creamy yellowish brown colour (Munsell: 2.5Y8/3) when freshly exposed. The contacts between adjacent aeolianite units are conformable and sharp. Relatively small deformed bedding features are common throughout the lower units (Figure 5.4). These features all have a similar basic form. A ‘basin’ with (relatively) vertical sides is visible in the centre of each feature. The base of the ‘basin’ is either fairly flat or has two lobes. The laminae beneath the ‘basin’ of the feature are often compressed and sometimes truncated by its curved bottom. Laminated and/or massive sand fills the ‘basin’ and the overlying bedding is affected to some degree for a few centimetres above the top of the ‘basin’, as the laminae gradually return to a horizontal disposition. There is a great deal of variation in the dimensions and shapes of the features (both the central ’basin’ and the surrounding disturbance) and the thickness and surface texture of the sediment within them. Some have sharp, clearly visible outlines and others are harder to distinguish from the surrounding sediment. As these disturbances are visible only in profile, perpendicular to the dip of the beds, their lateral extent down the slope is not known.

Unit 1 (0 – 25 cm) comprises a single set of low-angle cross-bedded toesets 2 – 3 cm thick which dip 5° towards 010° N. Some disturbance to bedding (deformation features) is visible. The lower contact is not visible due to the deposition of beach sand against the profile. The visible thickness of the unit ranges from a few centimetres to 35 cm. Unit 2 (25 – 30 cm) is a set of low-angle cross-laminated toesets 3 – 5 mm thick which dip 5° towards 010° N. The unit thickens towards the east of the profile to 12 cm thick. Unit 3 (30 – 220 cm) is a set of low-angle cross-

bedded toesets up to 3 cm thick which initially dip 5° towards 010° N. The dip gradually increases to 10° towards 010° N as the beds grade into low-angle foresets. Grain size decreases around halfway up the unit from medium sand to relatively fine medium sand. Deformation features are common, particularly in the upper parts of the unit. The unit thickens slightly towards the east of the profile, but is of fairly uniform thickness. Unit 4 (220 – 257 cm) comprises a set of low-angle cross-laminated foresets 3 – 9 mm thick which dip 10° towards 010° N. The unit becomes thinner to the west of the profile, eventually disappearing.

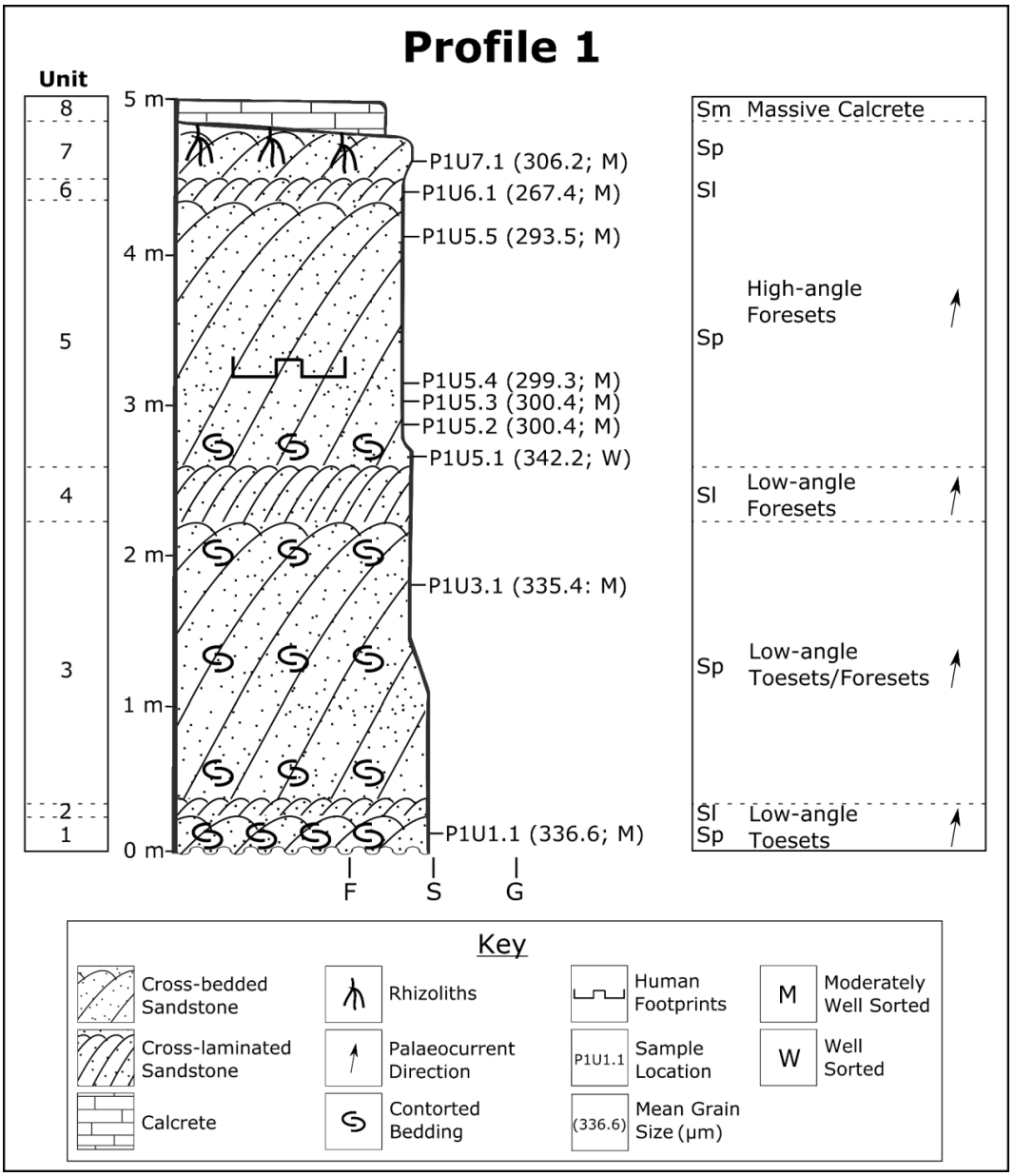


Figure 5.2. The logged sequence of Profile 1. The base of the exposure is 1.5 m above high tide level.

Unit 5 (257 – 435 cm) is composed of high-angle cross-bedded foresets 4 – 15 cm thick which dip 15° towards 010° at the base of the unit and steepen to 20° towards 010° N near the top of the unit. A marked reduction in grain size (from relatively fine medium sand to medium/fine sand) occurs approximately 10 cm above the base of the unit. Average bed thickness increases up through the unit. There is some disturbance to the bedding (deformation features) in the lower 20 cm of the unit. The unit is of fairly uniform thickness, but thins considerably to the west of the profile. Unit 6 (435 – 445 cm) is a thin set of high-angle cross-laminated foresets 1 – 5 mm thick which dip 20° towards 010° N. The laminae are relatively poorly cemented brittle in comparison to the other units. The sediment has a distinct pale brownish colour (Munsell: 10YR8/2). This unit ranges in thickness from 5 to 15 cm.

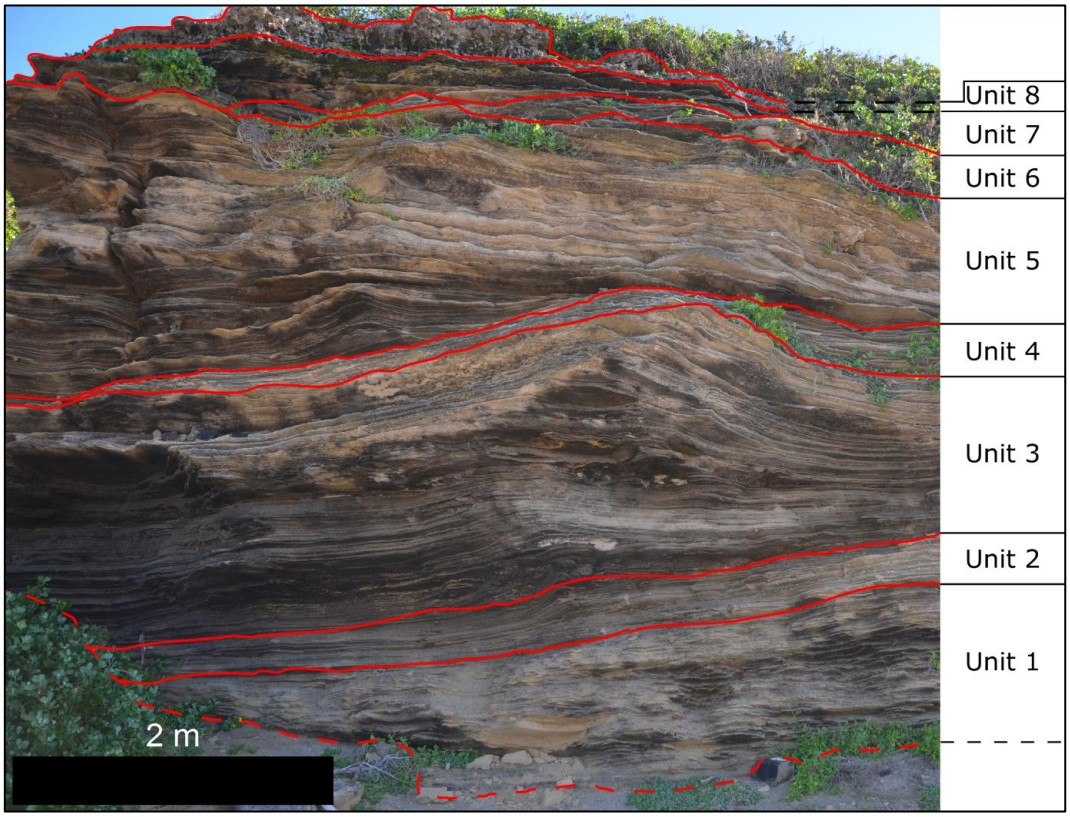


Figure 5.3. A photograph of Profile 1 with the units marked. Note that the dip is away from the camera.

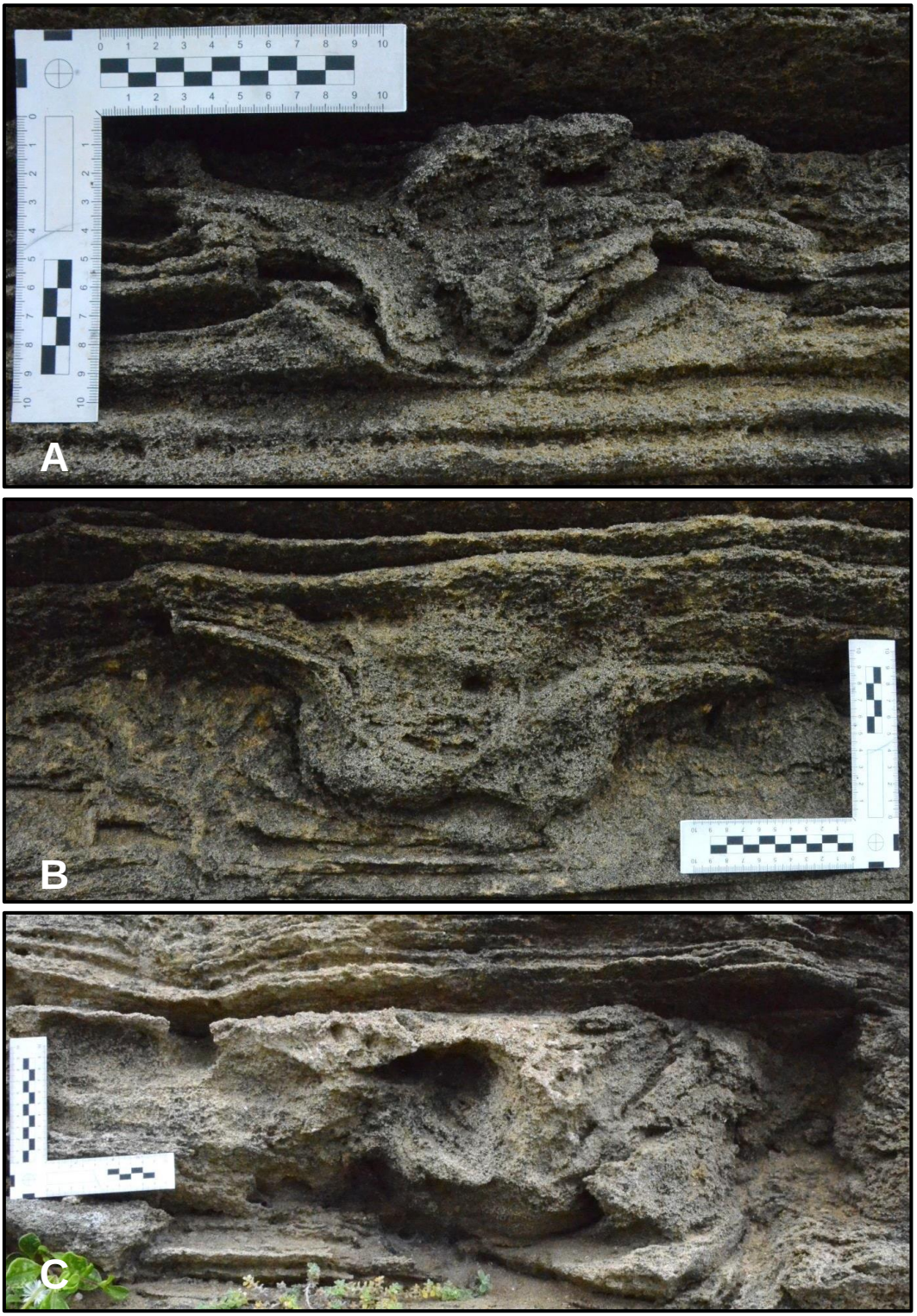


Figure 5.4. Several examples of disturbed bedding Unit 3 of Profile 1. These “types” are found throughout the units where disturbances occur (P1: U1, U3 and U5; P2: U1, U2 and U3) with no indication of lateral or stratigraphic patterns in the distribution of different forms. These features range from 5 cm to 50 cm in overall width.

Unit 7 (445 – 485 cm) comprises high-angle cross-bedded foresets ~4 cm thick which dip between 20° and 25° towards 010°. Some small rhizoliths (up to 10 mm thick and up to 5 cm long) are present in the upper 10 cm of the unit. Grain size increases slightly from the base of the unit relative to Unit 6 to become medium sand. Unit thickness is fairly consistent across the profile, but thins towards the west. The upper contact with Unit 8 is a sharp unconformity which dips 10° towards 190° S. This truncation correlates with the +6 m raised marine bench or platform on this part of Nahoon Point and can be considered a supersurface as it marks a hiatus in aeolian deposition. Unit 8 (485 – 500 cm) is a massive calcrete composed of well-sorted medium/fine sand with no visible internal structure. The sediment is light grey in colour (Munsell: 2.5Y7/2), highly cemented and (macroscopically, based on visual inspection) appears considerably less porous than the aeolianite. The unit ranges in thickness from 10 cm to 30 cm.

Single bulk samples for laboratory analysis were collected from Units 1, 3, 6 and 7. Five bulk samples were collected from Unit 5, as this was the unit associated with the footprints. A single block sample for thin sectioning was collected from Unit 5, from the same position as bulk sample P1U5.4. These samples were both taken from the aeolianite bed in which the footprints were found. The results of the analysis of these samples are presented in Section 5.2.

Profile 2:

Profile 2 is located 10 m to the west of Profile 1, within the same exposure. The base of this profile is 1 m above high tide level. Six distinct units were identified within Profile 2 (Figures 5.5 & 5.6). The aeolianite in Units 1 to 4 is composed of moderately well-sorted medium sand, and is well-cemented and a light creamy yellowish brown colour (Munsell: 2.5Y8/3) when freshly exposed. Deformation features identical to those in Profile 1 were observed. Unit 5 is aeolianite, but differs from the underlying deposit.

Unit 1 (0 – 84 cm) is a set of low-angle cross-laminated toesets 1 – 4 mm thick which dip 5° towards 010° N. The lower contact is not visible due to the deposition of beach sand against the profile. The laminae are often heavily disturbed (deformation

features), especially higher up in the unit. The unit disappears below the beach surface to the west and thickens slightly to the east. Unit 1 is overlain conformably by Unit 2.

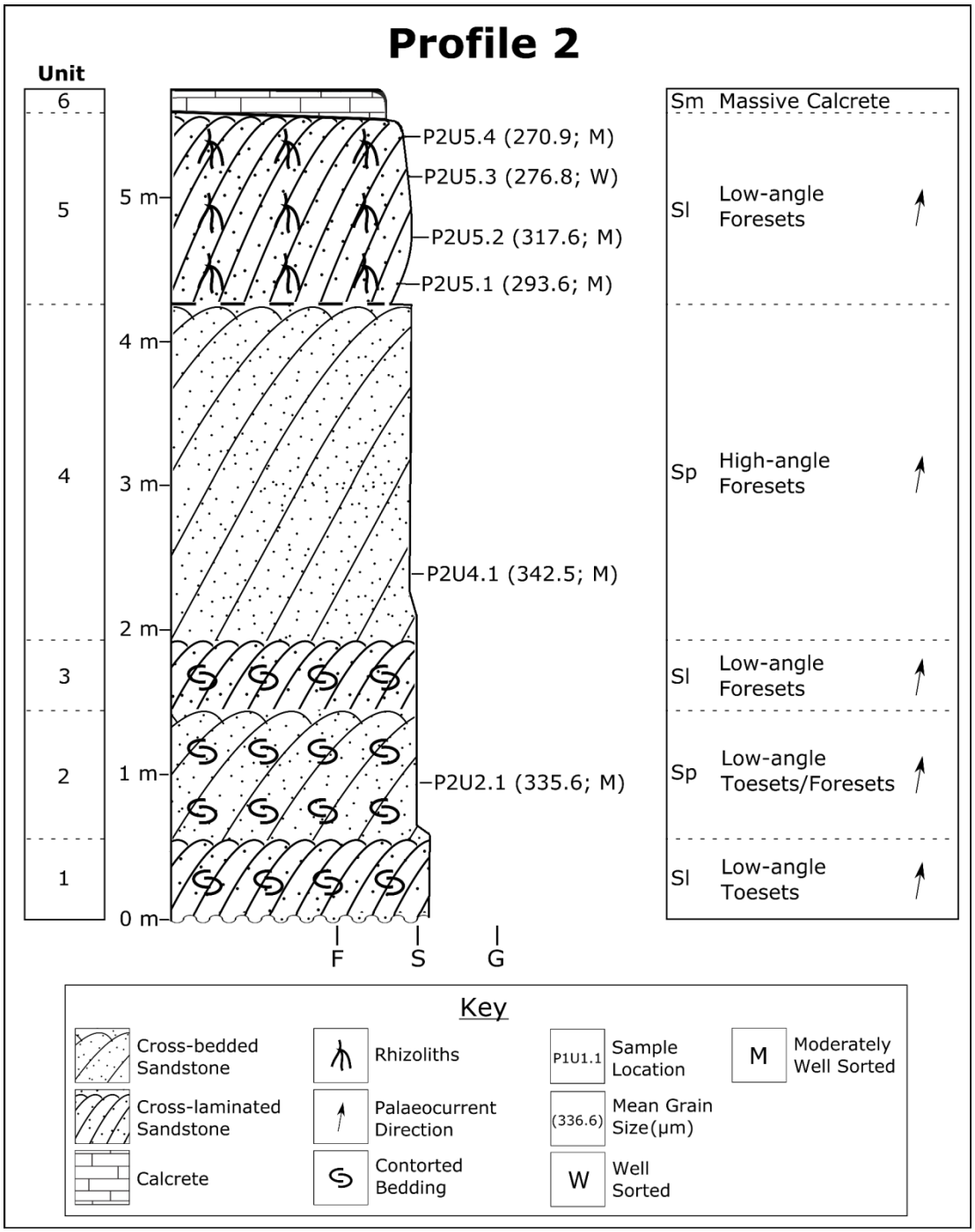


Figure 5.5. The logged sequence of Profile 2. The base of the exposure is 1 m above high tide level.

Unit 2 (84 – 147 cm) is a set of low-angle cross-bedded toesets several cm thick which dip 5° towards 010° N. The dip increases to 10° towards 010° N as the beds

steepen into low-angle foresets. From just above the base of the unit, the grain size decreases from relatively coarse medium sand to medium sand. Deformation features are very common. The unit thins to the west of the profile, eventually pinching out, and thickens to around 2 m towards the west. The contact with Unit 3 is conformable. Unit 3 (147 – 195 cm) comprises a set of low-angle cross-laminated foresets 2 – 6 mm thick which dip 10° towards 010° N. Very few deformation features were observed. The unit thins considerably to the west of the profile, pinching out within a few metres but is of fairly uniform thickness to the east. It is overlain conformably by Unit 4. Unit 4 (195 – 422 cm) comprises high-angle cross-bedded foresets several cm thick which dip 15° - 20° towards 010° N. The sediment is slightly coarse medium sand but decreases in size to medium sand a little above the base of the unit. It remains fairly constant throughout the rest of the unit. The sediment is far more highly cemented than in stratigraphically lower units. The unit thickens to about 2.5 m to the east, and thins rapidly to the west. The contact with Unit 5 is diffuse with some irregularity and localised erosion evidenced by truncation of bedding. It is a first-order bounding surface. The contact dips landward (010° N). Unit 5 (422 - 561 cm) is comprised of low-angle cross-laminae 2 – 6 mm thick, which dip 10° towards 010° N. The sediment is moderately well-sorted to well-sorted slightly fine medium sand which initially coarsens up to medium sand before returning to a similar texture near the top of the unit. The unit is slightly darker in colour (Munsell: 2.5Y7/3) and druzy (the sediment having a relatively ‘rough’ and lumpy surface due to crystal growth) and less cleanly cemented than stratigraphically lower units. Rhizoliths up to 10 cm in length are very common, and range in thickness from 5 mm to 40 mm. The unit thickens to the west of the profile to 2.5 m thick, but thins to the east where it lies against the partially eroded surface of the older dune (Unit 4). The upper contact with Unit 6 is a sharp unconformity which dips 10° towards 190° S. As in Profile 1 (the contact between Units 7 and 8), this unconformity appears to be part of a raised bench or platform. It is a supersurface, indicative of a break in aeolian deposition. Unit 6 (561 – 574 cm) is a massive calcrete composed of well-sorted medium/fine sand with no visible internal structure. The sediment is light grey in colour (Munsell: 2.5Y7/2), highly cemented and (based on visual inspection) appears considerably less porous than the aeolianite. The unit ranges in thickness from 10 cm to 30 cm.

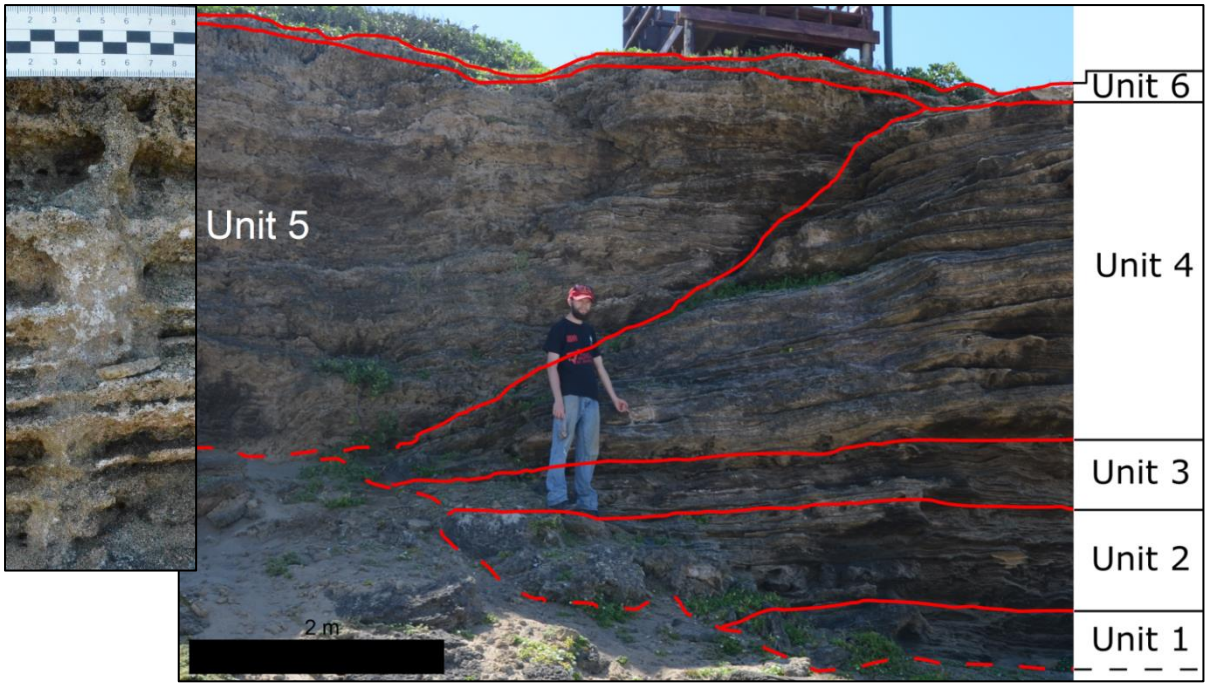


Figure 5.6. A photograph of Profile 2 with the units marked. Inset: close-up photograph of a rhizolith in Unit 5 (scale is in centimetres).

Single bulk samples were taken from Unit 2 and Unit 4 and four samples were collected from within Unit 5. An oriented block sample for thin sectioning was taken from the same position as the bulk sample P2U5.2. This was taken in order to compare Unit 5 to the underlying aeolianite in Profile 1 (Units 1 – 7) and Profile 2 (Units 1 to 4) in as much detail as possible. The laboratory results for these samples are presented in Section 5.2.

Profile 3:

Profile 3 comprises six units in a sequence almost 14 m in height (Figures 5.7 & 5.8). The base of the profile is 1 m above high tide level. Unit 1 (0 – 116 cm) is a set of cross-laminated toesets (dipping 5° towards 090° E) which steepen rapidly into high-angle foresets (dipping up to 30° towards 090° E). The laminae are 2 – 8 mm thick and are composed of highly cemented well-sorted relatively fine medium sand that fines upward and is pale yellow (Munsell: 2.5Y8/4) in colour. The lower contact of the unit is not visible due to the deposition of beach sand against the profile. There is little variation in the thickness of the unit across the profile. The upper contact with Unit 2 is conformable and sharp.

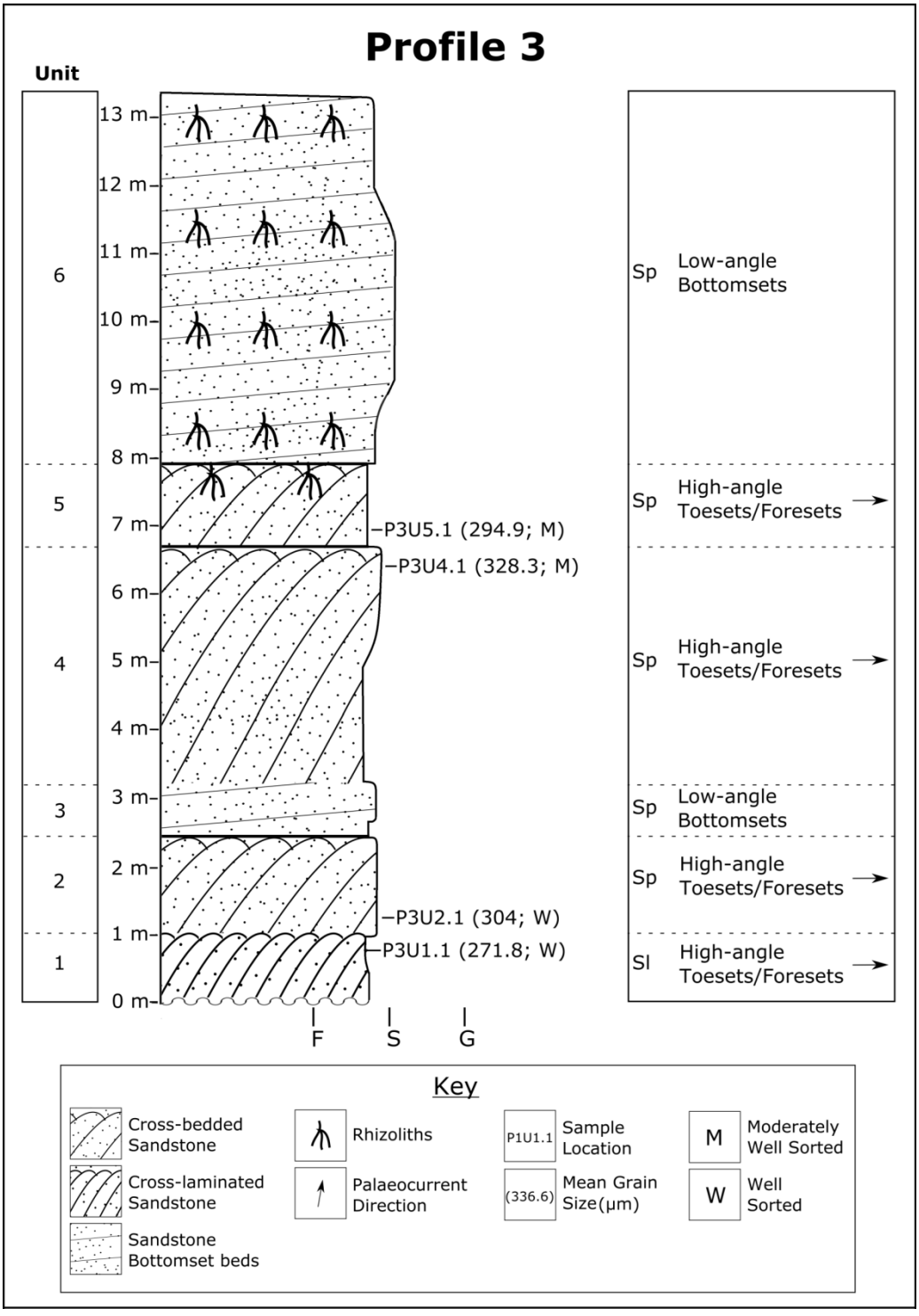


Figure 5.7. The logged sequence of Profile 3. The base of the exposure is 1 m above high tide level.

Unit 2 (116 – 243 cm) contains two sets of cross-bedded toesets which dip 5° towards 090° E that steepen into high-angle foresets with a dip of up to 30° towards 090° E. The beds are 2 – 3 cm thick and composed of highly cemented pale yellow (Munsell: 2.5Y8/4) well-sorted medium sand. The upper contact with Unit 3 is

unconformable and dips 5° towards 090° E, truncating the cross-beds of Unit 2. This feature is a first-order bounding surface. Unit 3 (243 – 318 cm) is a single set of low-angle bottomset beds several centimetres in thickness which dip 5° towards 090° E. The beds are highly cemented and composed of relatively fine medium sand that is pale yellow (Munsell: 2.5Y8/4) in colour. The sediment coarsens upward somewhat. No obvious change in the thickness of the unit occurs across the exposure. The upper contact with Unit 4 is conformable and fairly sharp, dipping 5° towards 090° E. Unit 4 (318 – 670 cm) comprises three sets of cross-bedded toesets (separated by first-order bounding surfaces) which dip 5° towards 090° E and steepen into high-angle foresets with a maximum dip of 30° towards 090° E. The beds are highly cemented and pale yellow (Munsell: 2.5Y8/4) in colour. The sediment is moderately well-sorted relatively fine medium sand that coarsens up notably. There is little change in the thickness of Unit 4 across the exposure. The contact with Unit 5 is an unconformity, a first-order bounding surface, that truncates the cross-beds in Unit 4 at an angle of 10° towards 090° E.



Figure 5.8. A photograph of Profile 3 with the units marked.

Unit 5 (670 – 795 cm) contains two sets of cross-bedded toesets with a dip of 10° towards 090° E which steepen into high-angle foresets dipping 20° towards 090° E. The beds are up to 8 cm thick and are composed of highly cemented moderately well-sorted relatively fine medium sand that is pale yellow (Munsell: 2.5Y8/4) in colour. Some small rhizoliths (up to 10 mm thick and a few centimetres long) are

present within the top 10 cm of the unit. The unit thins very slightly eastward. The upper contact with Unit 6 is unconformable and dips 10° towards 090° E. This contact is a first-order bounding surface. Unit 6 (795 – 1380 cm) contains low-angle bottomset beds 2 cm to 5 cm thick which dip 10° towards 090° E. The beds in the unit are fairly druzy and not as highly cemented as in the underlying units. The druziness becomes more pronounced towards the top of the unit. The sediment is medium to medium/fine sand that is pale yellow (Munsell: 2.5Y8/4) in colour. At the base of the unit, it is fine medium sand. It coarsens up, reaching a peak of medium sand about halfway up the unit, before fining up to become medium/fine sand near the top of the unit. Rhizoliths are common and they increase in size (up to 50 mm wide) and frequency up through the unit. Unit 6 varies in thickness across the exposure, largely due to erosion of the upper surface.

Single bulk sediment samples were collected from Units 1, 2, 4 and 5. The laboratory results for these samples are presented in Section 5.2.

Profile 4:
The exposure from which Profile 4 was logged is a little less than 8.5 m high, and has its base 1 m above high tide level. Seven distinct sedimentary units were identified (Figures 5.9 & 5.10).

Unit 1 (0 – 98 cm) is made up of low-angle bottomset beds up to 7 cm thick which dip 4° towards 060° ENE. The beds are composed of highly cemented pale yellow (Munsell: 2.5Y7/3) coloured moderately well-sorted medium sand that fines slightly upward through the unit. The lower contact of the unit is not visible due to the deposition of sand and gravel against the base of the profile. The upper contact with Unit 2 is conformable and sharp, dipping 4° towards 060° ENE. Unit 2 (98 – 270 cm) comprises two sets of cross-bedded toesets dipping 5° towards 060° ENE which steepen rapidly into high-angle foresets with a maximum dip of 20° towards 060° ENE. The reactivation surface between the sets is a first-order surface. The beds range in thickness from 2.5 to 6 cm and contain highly cemented well-sorted medium sand that is pale yellow (Munsell: 2.5Y8/3) in colour. At the base of the unit, the grain size is similar to Unit 1, but it steadily fines up within the first metre to become fine

medium sand. Within the top 50 cm, the sediment coarsens up again. The upper contact with Unit 3 is unconformable and relatively diffuse due to localised disturbance by erosion. It is a first-order surface. The contact dips 5° towards 240° WSW despite the localised disturbance. Unit 3 (270 – 362 cm) is a set of low-angle bottomset beds up to 5 cm thick, that dip 10° towards 060° ENE. The beds contain highly cemented medium sand that is pale yellow (Munsell: 2.5Y8/4) in colour. The upper contact with Unit 4 is conformable and sharp.

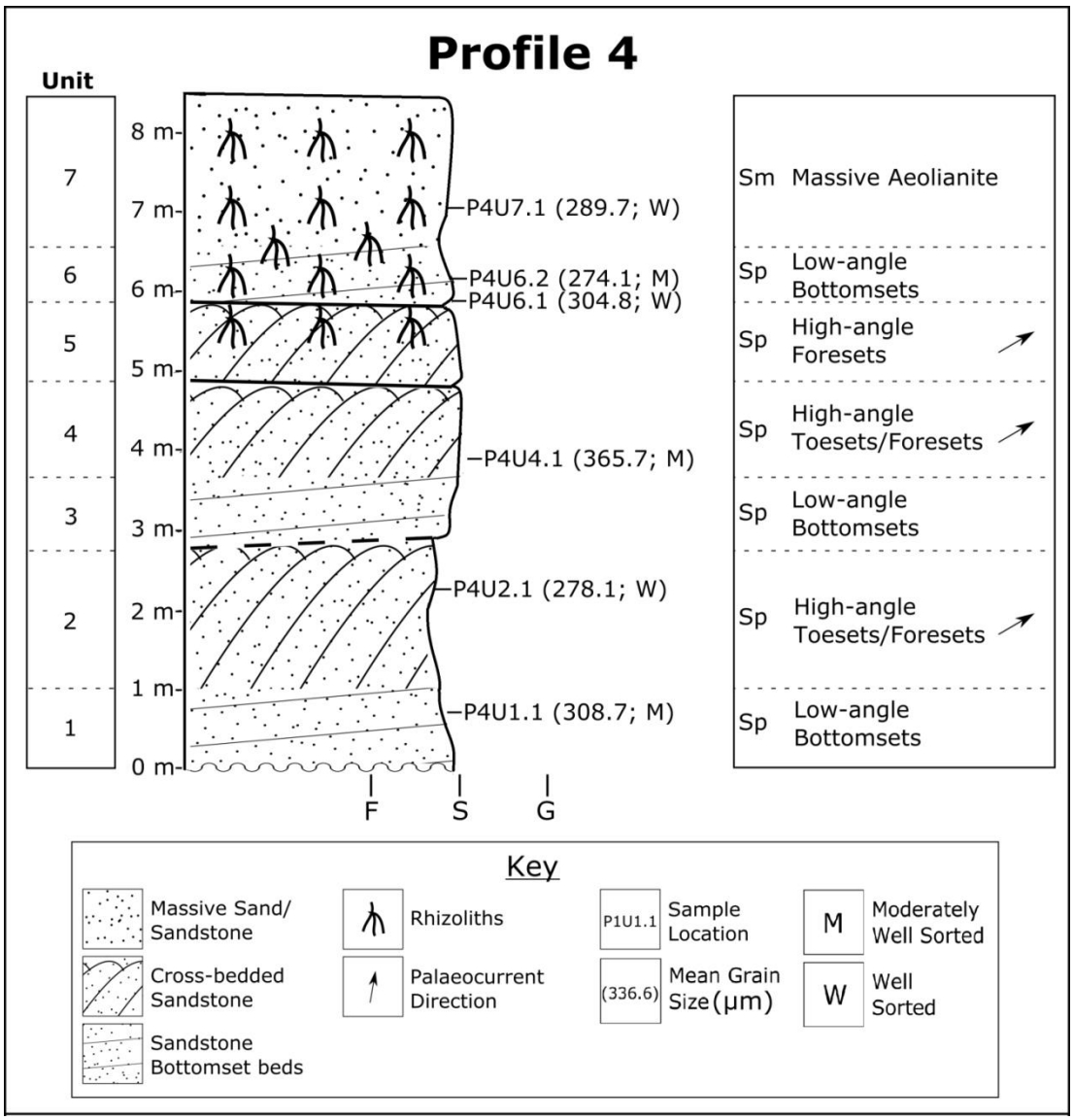


Figure 5.9. The logged sequence of Profile 4. The base of the exposure is 1 m above high tide level.

Unit 4 (362 – 482 cm) is a set of cross-bedded toesets with a dip of 4° towards 060° ENE, which steepen into high-angle foresets that dip 25° towards 060° ENE. The

beds are 2 – 5 cm thick. They are composed of pale yellow (Munsell: 2.5Y8/4) moderately well-sorted medium sand that is highly cemented, but is notably less so than the sediment in lower units. The upper contact with Unit 5 is an unconformable and sharp first-order bounding surface, dipping 20° towards 060° ENE to the West of profile, and flattening to 5° towards 060° ENE on the eastern end.

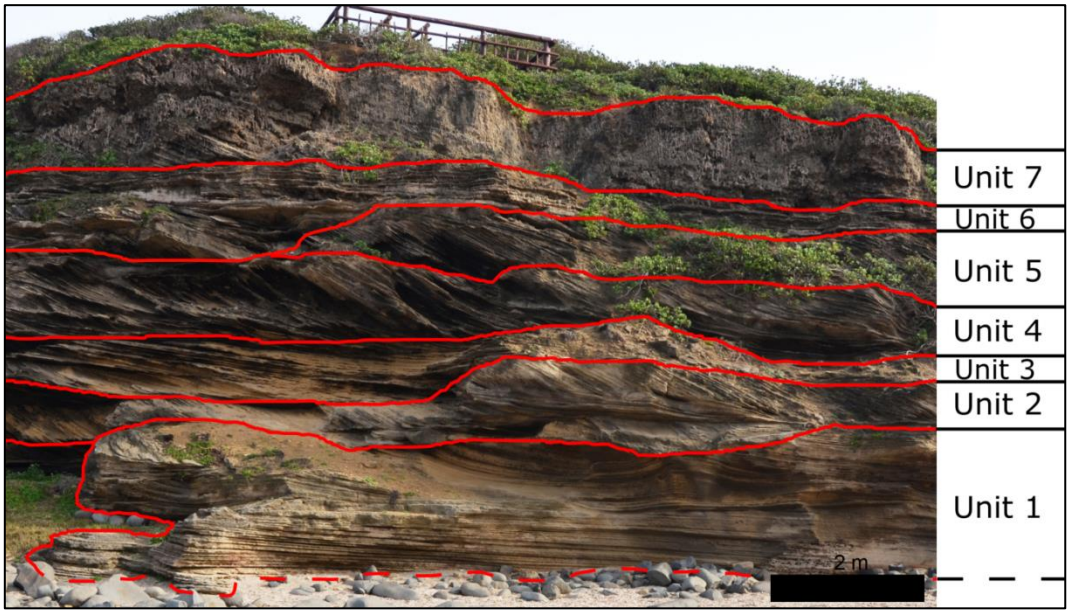


Figure 5.10. A photograph of Profile 4 with the units marked.

Unit 5 (482 – 582 cm) is a set of high-angle concave-up cross-bedded foresets 2 – 3 cm thick which dip 30° towards 060° ENE at the base of the unit, and flatten to 20° towards 060° ENE at the top. The beds are made up of pale yellow (Munsell: 2.5Y8/4) coloured fine medium sand. The sediment becomes slightly druzy near the top of the unit. Some rhizoliths are visible in the unit. The largest are 20 mm wide and 10 cm long, but the majority are much smaller. The upper contact with Unit 6 is unconformable and sharp, and dips 2° towards 060° ENE. This contact is a first-order bounding surface. Unit 6 (582 – 654 cm) is a set of low-angle bottomset beds ~12 cm thick which dip 2° towards 060° ENE. The beds are highly cemented pale yellow (Munsell: 2.5Y8/3) coloured moderately well-sorted to well-sorted medium sand, which fines up to a fine medium sand. Rhizoliths up to 50 mm thick and 10 cm long are present at low frequency throughout the unit. The upper contact with Unit 7 is conformable but disturbed by bioturbation by plant roots (rhizoliths). Unit 7 (654 – 834 cm) is a massive aeolianite deposit with no visible internal structure. The sediment is well-sorted medium/fine sand that is pale yellow (Munsell: 2.5Y8/2) in

colour. The deposit is very highly cemented and gradually becomes very druzy up through the unit. Rhizoliths up to 50 mm in width and 15 cm in length are extremely common, and increase in frequency upward. At the top of the unit, the majority of the visible deposit is composed of rhizoliths.

Single bulk samples for laboratory analysis were taken from Units 1, 2, 4 and 7. Two bulk samples were collected from Unit 6. The results of the analyses conducted on these samples are presented in Section 5.2.

Profile 5:

Profile 5 is ~6.5 m high, and the base is 1 m below high tide level. Five units were identified (Figures 5.11 & 5.12).

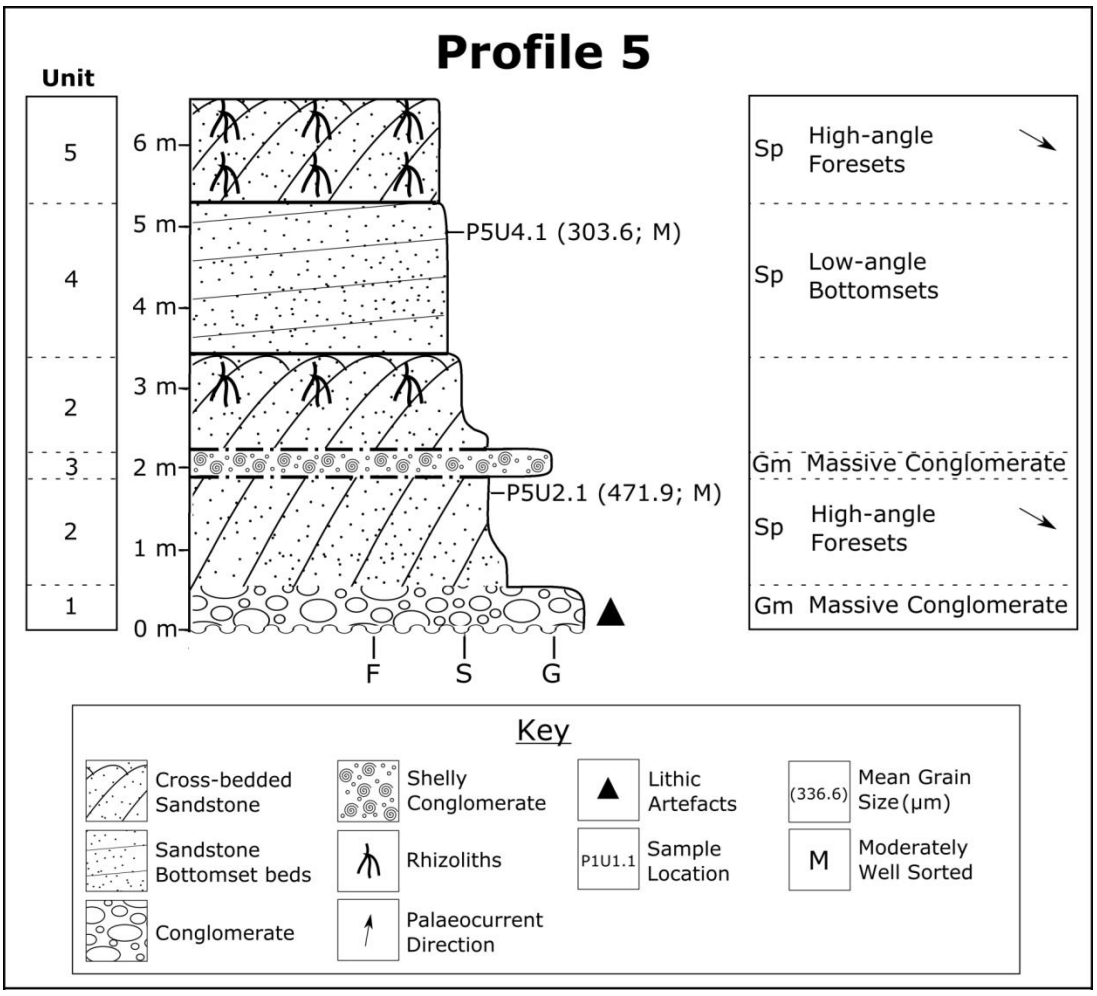


Figure 5.11. The logged sequence of Profile 5. The base of the exposure is 1 m below high tide level.

Unit 1 (0 – 50 cm) is a conglomeratic beachrock containing moderately sorted well-rounded dolerite clasts 30 cm to 140 cm long. Spherical and elongated clasts are equally common. The clasts coarsen upward somewhat through the unit but remain poorly sorted. The matrix is very highly consolidated and cemented pale brown (Munsell: 10YR8/2) medium sand. The deposit is massive, with no visible internal structures. As the unit falls within the intertidal zone, it is highly weathered. The deposit is widespread with remnants found all the way around Nahoon Point. Rare re-worked aeolianite blocks were found at some locations (Figure 5.13). Lithic artefacts, including blades, are fairly common (see sub-section 5.1.4. for a more detailed description). The lower contact of the deposit is not visible at Profile 5 due to the presence of beachrock and loose boulders around the base of the stack. However, to the west of Profile 5, the conglomerate was found to lie unconformably on highly eroded remnants of aeolianite deposits (Figure 5.13). The deposit ranges in thickness, from a minimum of 35 cm to a maximum of 60 cm. The upper contact with Unit 2 is conformable and undulates according to the clasts in the upper surface of Unit 1. The contact dips very slightly (~2°) towards 210° SSW.

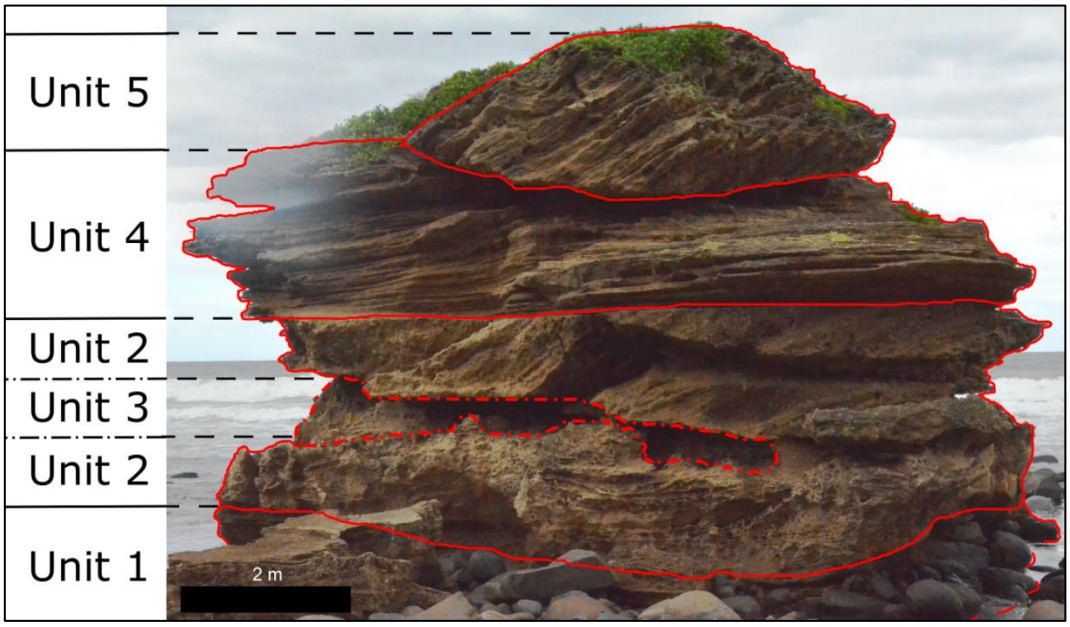


Figure 5.12. A photograph of Profile 5 with the units marked.

Unit 2 (50 – 335 cm) comprises two sets of toesets, dipping 10° towards 120° ESE, which steepen into high-angle foresets with a maximum dip of 20° towards 120° ESE. The sets are separated by a first-order bounding surface. The beds are ~1 cm thick at the base, and gradually thicken to around 7 cm thick. They are highly

cemented and composed of light grey (Munsell: 2.5Y7/2) coloured moderately well-sorted medium/coarse sand that gradually fines up to medium sand. Small rhizoliths (up to 15 mm thick and a few centimetres long) are present in low numbers across the unit within the top 1.5 m. The unit is of fairly uniform thickness across the profile. The upper contact with Unit 4 is unconformable and sharp and approximately flat. It represents a first-order bounding surface.

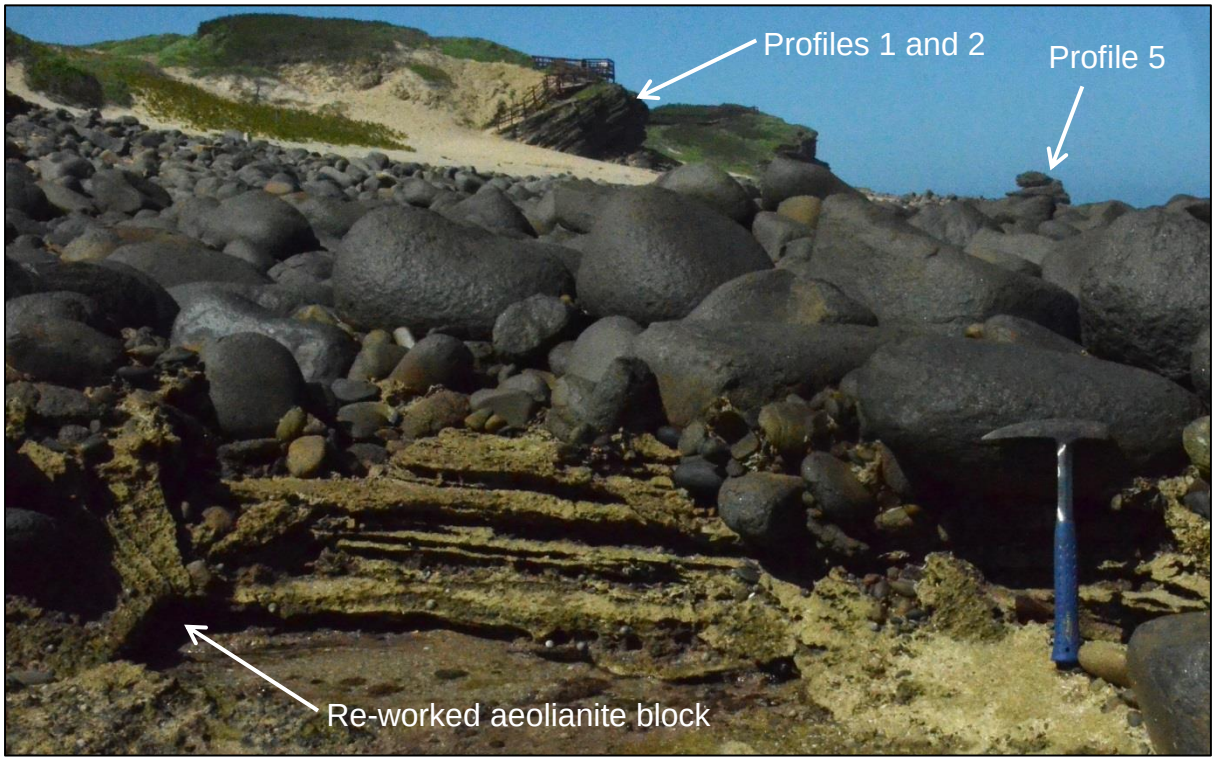


Figure 5.13. Beachrock conglomerate lying unconformably on an eroded aeolianite deposit on Nahoon Point. Note the re-worked aeolianite block that has been incorporated into the conglomerate.

Unit 3 (185 – 215 cm) is a deposit of coquinite containing poorly sorted clasts up to 50 cm long and large quantities of marine shell fragments. This unit was deposited into a long erosional hollow up to 40 cm deep within Unit 2. The hollow cuts horizontally through most of Unit 2, and is only absent on the extreme northern edge of the exposure. The upper and lower surfaces of the hollow are irregular, but both dip 5° towards 210° SSW. The matrix is composed of very highly consolidated and cemented pale brown (Munsell: 10YR8/2) coloured medium/fine sand. The coquinite has been eroded, and there are many gaps in its distribution within the hollow. Unit 4 (335 – 525 cm), which overlies Unit 2, is a set of low-angle bottomset beds which dip

5° towards 120° ESE. The beds are ~1 cm thick at the base of the unit but thicken up to ~10 cm thick at the top. The beds are composed of light grey (Munsell: 2.5Y7/2) moderately well-sorted fine medium sand and are highly cemented at the base, but become less cemented and relatively druzy higher up. The unit thins landward (030° NNE) due to the unconformable upper contact (a first-order bounding surface) with Unit 5 that dips 30° towards 030° NNE. It is thickest (~2 m) on the seaward end of the profile. Unit 5 (525 – 655 cm) is a single set of cross-bedded high-angle foresets 2 – 5 cm thick which dip 30° towards 120° ESE. The beds are made up of relatively poorly cemented very fine medium sand that is light grey (Munsell: 2.5Y7/2) in colour. The sediment is fairly druzy across much of the unit. Rhizoliths are common and present in a range of sizes up to 40 mm thick and 15 cm long. The upper surface of Unit 5 is eroded.

Single bulk samples were taken from Unit 2 and Unit 4 for analysis in the laboratory. The results for these samples are presented in Section 5.2.

Profile 6:

Two units were identified within the small exposure from which Profile 6 was recorded (Figures 5.14 & 5.15). The base of the profile is 0.5 m above high tide level. Unit 1 (0 – 585 cm) is a single set of cross-bedded toesets which steepen up-dip into high-angle foresets. The beds range in thickness from 1.5 cm to 10 cm; they are thickest at the base and generally thin upslope. The bedding dips towards 020° NNE with a maximum inclination of 30°. Some slumping of bedding is visible about halfway up the unit and at its base. This affects the bedding angles locally, creating a “hump” of shallower beds on the slope. The visible extent of the unit thickens to the west to around 8 m thick, and thins to the east to around 2.5 m. The sediment is composed of light creamy yellowish brown (Munsell: 2.5Y8/3) coloured moderately well-sorted to well-sorted medium sand and is relatively poorly cemented and quite druzy. It is most highly cemented at the base of the unit. Some rhizoliths up to 50 mm thick and 10 cm long are present within the upper 30 cm of the unit. The lower contact of the unit is not visible due to undercutting of the cliff and subsequent deposition of sand into the erosional gap. The contact with Unit 2 is sharply

unconformable and roughly flat; it is a supersurface, indicative of a hiatus in deposition.

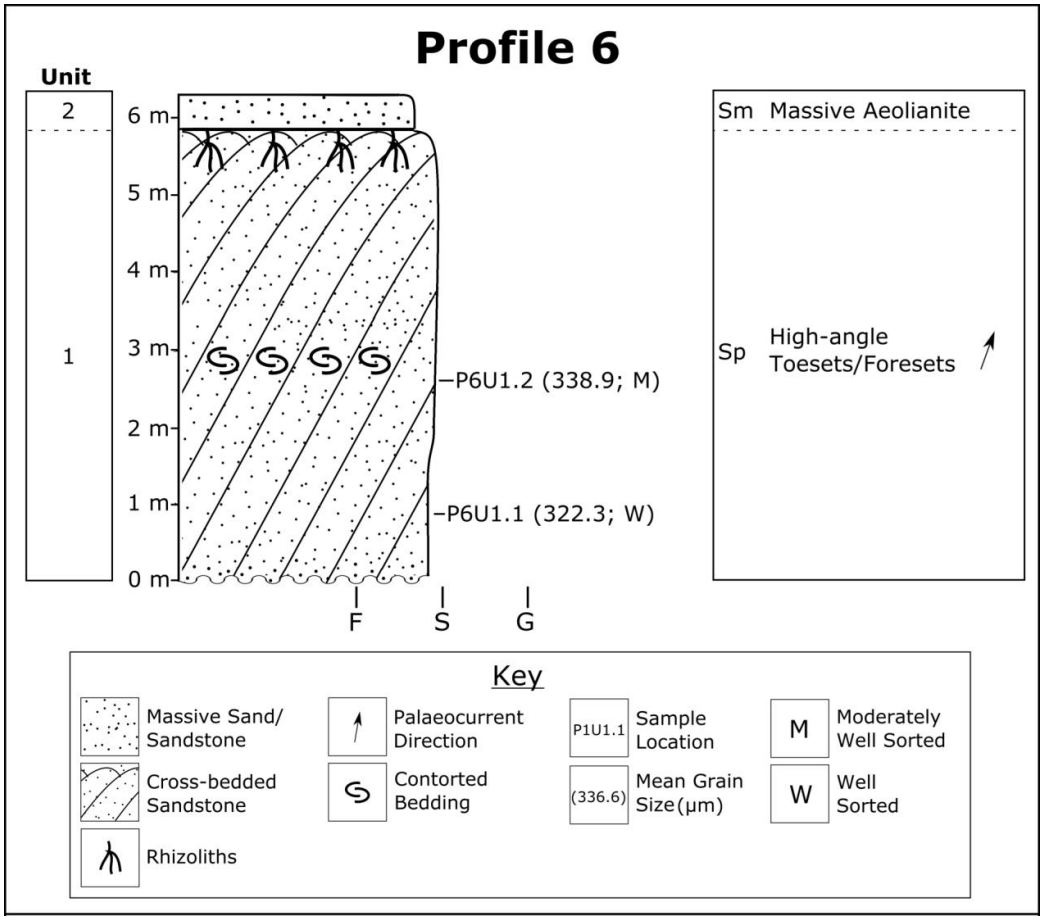


Figure 5.14. The logged sequence of Profile 6. The base of the exposure is 0.5 m above high tide level.

Unit 2 (585 – 635 cm) is light grey (Munsell: 2.5Y7/2) coloured massive aeolianite composed of well-sorted medium/fine sand with no visible internal structure. The sediment is highly cemented and (macroscopically) appears to be considerably less porous than the underlying aeolianite. Rhizoliths are common, and reach up to 60 mm in width and 20 cm in length.

Two bulk sediment samples for laboratory analysis were collected from Unit 1. The results for these samples are presented in Section 5.2.

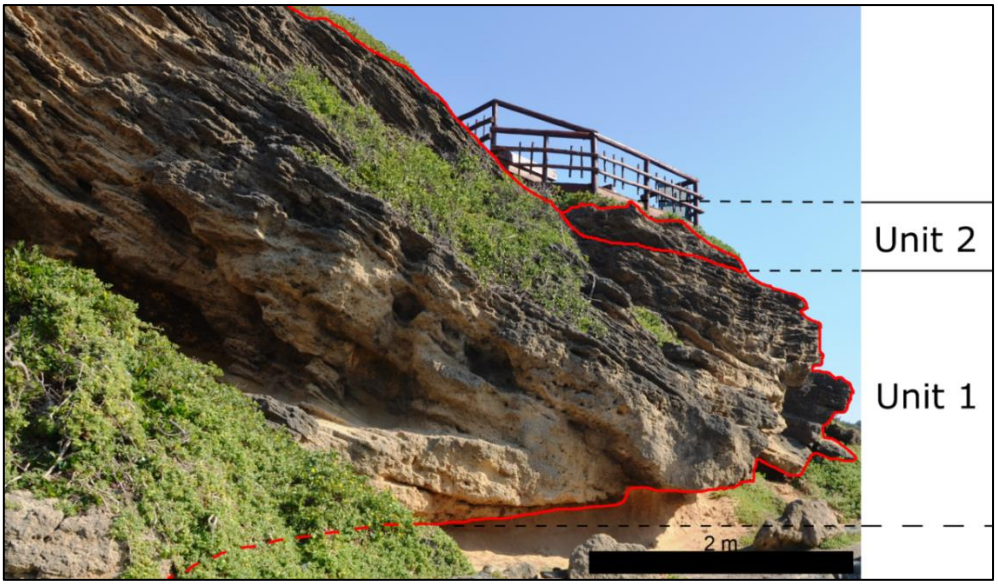


Figure 5.15. A photograph of Profile 6. Only a limited part of Unit 2 is visible due to the vegetation at the top of the profile and the angle from which the photograph was taken.

Profile 7:

The outcrop from which Profile 7 was logged is ~3.5 m high and has its base at high tide level. Five units were identified (Figures 5.16 & 5.17). Unit 1 (0 – 150 cm) is a massive conglomerate with rounded to well-rounded dolerite clasts up to 112 cm in length. Spherical forms are more common than elongated ones. The clasts are inversely graded, although moderately well sorted throughout. The matrix is very pale brown in colour (Munsell: 10YR8/2) and is composed of very highly cemented and compacted medium sand with rare coarse sand grains and granules. Lithic artefacts are commonly found within this deposit (see sub-section 5.1.4. for a more detailed description). The lower contact of the unit is not visible due to the deposition of sand. The upper contact is conformable and undulating. Unit 2 fills gaps in the relief of the upper surface of Unit 1 created by the presence of large boulders and apparent erosion of some of the matrix from this surface. Unit 3 lies on top of both Unit 2 and Unit 1.

Unit 2 (140 – 155 cm) is a thin deposit of structureless conglomerate. It is very pale brown in colour (Munsell: 10YR8/2) and is composed of very highly cemented medium sand, a high density of marine shell fragments, and rare moderately sorted dolerite pebbles. The thickness of Unit 2 ranges from 2 cm to 20 cm. The upper

contact with Unit 3 is conformable to the undulating surface of Unit 2. Unit 3 (155 – 217 cm) is a set of cross-bedded toesets which steepen rapidly into high-angle foresets. The beds are composed of relatively coarse medium sand, are 2 – 4 cm thick, and have a maximum inclination of 25° towards 040° NE. The sediment is pale yellow (Munsell: 2.5Y8/3) in colour when freshly exposed and is very highly cemented and weathered. Coquina has been deposited into some erosional hollows, and honeycomb weathering is widespread. The upper contact with Unit 4 is unconformable and flat, truncating the beds of Unit 3. It is a first-order bounding surface.

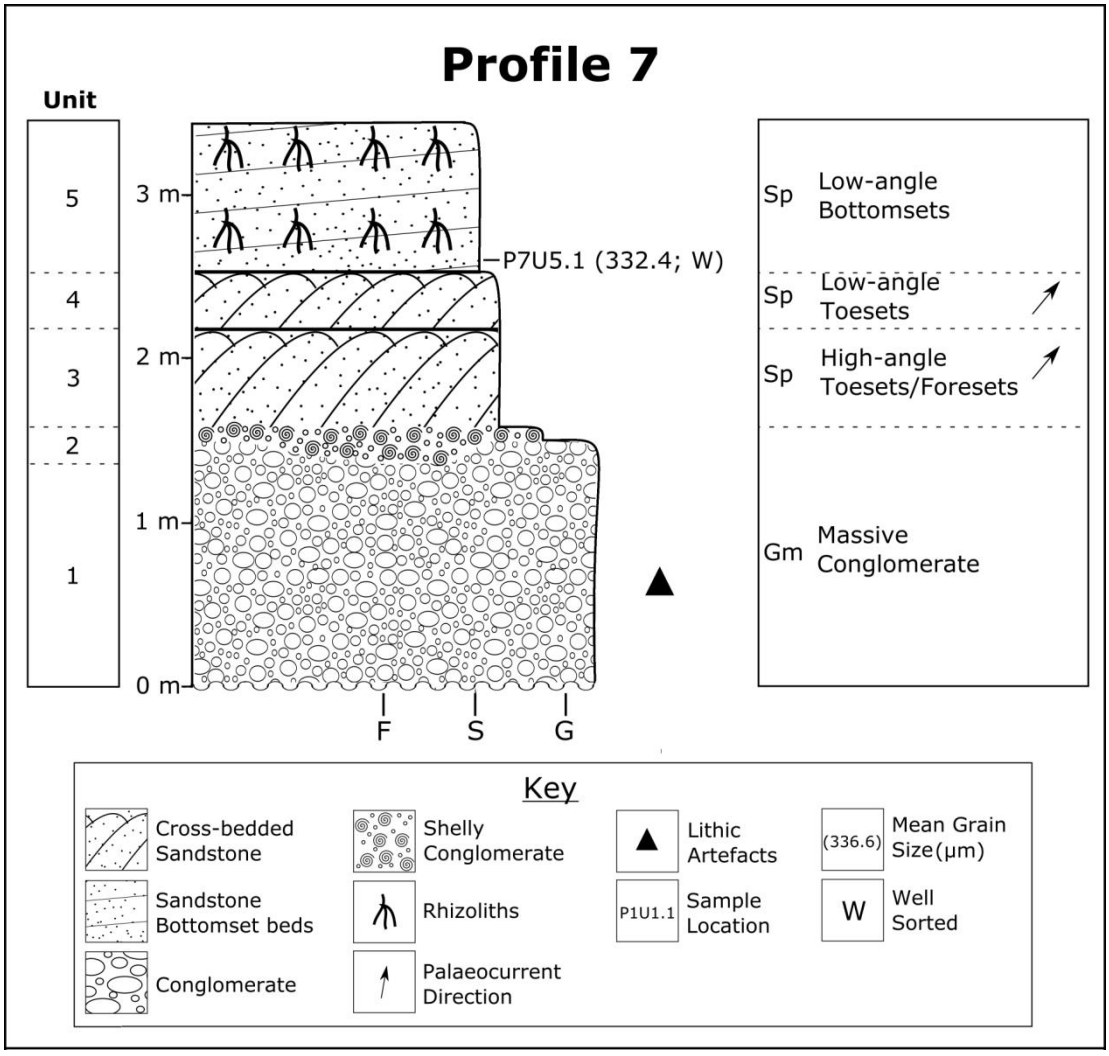


Figure 5.16. The logged sequence of Profile 7. The base of the exposure is at high tide level.

Unit 4 (217 – 250 cm) comprises a single set of low-angle toesets 0.5 – 1.5 cm thick which dip 10° towards 040° NE. The sediment is relatively coarse medium sand that is pale yellow (Munsell: 2.5Y8/3) in colour. It is generally highly cemented and is

weathered, with notable honeycomb weathering. It is, however, druzy in places, and loses structure upwards, particularly to the west. The upper contact with Unit 5 is unconformable and flat and represents a first-order bounding surface. Unit 5 (250 – 342 cm) is a set of low-angle bottomsets 0.5 – 4 cm thick which dip 5° towards 210° SSW. The sediment is pale yellow (Munsell: 2.5Y8/3) highly cemented well-sorted medium sand, which is slightly finer than that in Units 3 and 4. Although the bedding is generally clear, there is some loss of structure near the top of the unit. Much of the sediment is druzy, and rhizoliths up to 5 cm thick and 12 cm long are common.

A single bulk sample was collected from the aeolianite of Unit 5 for laboratory analysis. The results for this sample are presented in Section 5.2.



Figure 5.17. A photograph of Profile 7 with the units marked.

Profile 8:

Four sedimentary units were identified within Profile 8 (Figures 5.18 & 5.19). The base of the exposure is 0.5 m below high tide level. Unit 1 (0 – 700 cm) is a set of high-angle foresets which dip at angles between 15° and 20° towards 340° NNW. The beds are 2 – 6 cm thick at the base of the visible deposit but thicken to ~30 cm up-dip. The sediment is pale yellow (2.5Y8/3 or 2.5Y7/3) in colour. It is moderately well-sorted to well-sorted relatively coarse medium sand which fines upward through the unit. The lower 200 cm of the deposit has been highly weathered by wave-action and splash. Whilst fairly massively and cleanly cemented throughout, the sediment becomes increasingly druzy within the top 100 cm. From about 200 cm above the base of the visible exposure, rhizoliths are present. These increase in size (up to 6 cm thick and 15 cm long) and frequency higher up in the unit. They are most

common on the landward end (West) of the profile and gradually peter out seaward (East). The lower contact is not visible due to the deposition of beach sand. The unit thickens considerably to the South (up-dip) and to the West. The maximum thickness of the unit is approximately 25 m. The upper contact with Unit 3 is highly variable: in more seaward locations, it is a gently (~2°) eastward-dipping unconformity; on the landward side of the exposure, it is an irregular unconformity where the upper surface of the dune has been eroded to varying degrees. A raised marine bench with an elevation of up to 4 m above high tide level is associated with the unconformity on the seaward end of the exposure. This contact is a supersurface, indicating a break in deposition.

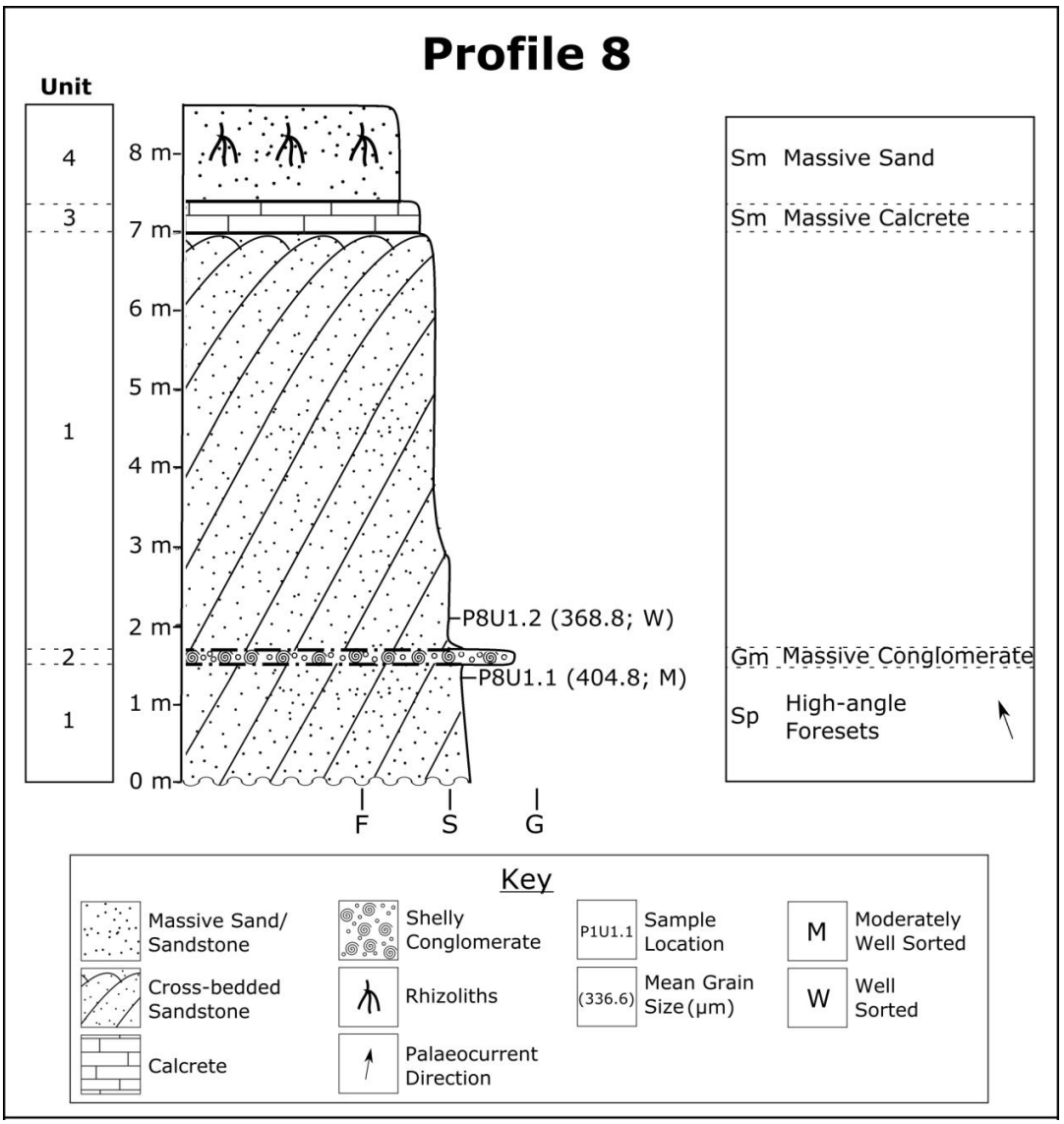


Figure 5.18. The logged sequence of Profile 8. The base of the exposure is 0.5 m below high tide level.

Unit 2 (150 – 162 cm) is coquinite deposited into an erosional pocket within Unit 1. This deposit is composed of a highly cemented and compacted medium/fine sand matrix, rare clasts up to pebble-size, and a high concentration of shell fragments. A single unidentifiable bone fragment was present within this deposit. The coquinite is highly weathered and there are many gaps within the deposit. The erosional gap (and the associated coquinite) extends from several metres from the seaward end of the exposure to approximately 6 m inland of the high-tide mark. Beyond this point, the aeolianite is weathered, but no erosional notches are visible. Unit 3 (700 – 730 cm) is a highly cemented massive calcrete with no internal structure. The sediment is medium/fine sand that is light grey in colour (Munsell: 2.5Y7/2) when freshly exposed. The unit varies in thickness around the exposure, but can be as thick as 1 m. Unit 4 lies unconformably on the weathered surface of Unit 3.



Figure 5.19. A photograph of Profile 8 with the units marked. A concrete wall extends from the profile towards the viewer.

Unit 4 (730 – 860 cm) is a massive structure-less fine sand deposit that is pale yellow (Munsell: 2.5Y8/4) in colour. The sediment is relatively highly consolidated and partially calcified, particularly in the lowermost part of the deposit. Highly calcified rhizoliths up to 5 cm thick and 20 cm long are present throughout the unit. The sediment is currently vegetated and modern roots are common in the upper

parts of the deposit. The thickness of the unit is variable, with a maximum observed thickness of 2 m.

Two bulk samples for laboratory analysis were taken from Unit 1. The results for these samples are presented in Section 5.2.

Profile 9:

Profile 9 was recorded from a low outcrop less than 2.5 m high. The base of the exposure is 1.5 m above high tide level. Beachrock conglomerate (correlating with that described in Unit 1 of Profile 5) was deposited around and against the seaward end of the outcrop. Four sedimentary units were identified in the profile (Figures 5.20 & 5.21).

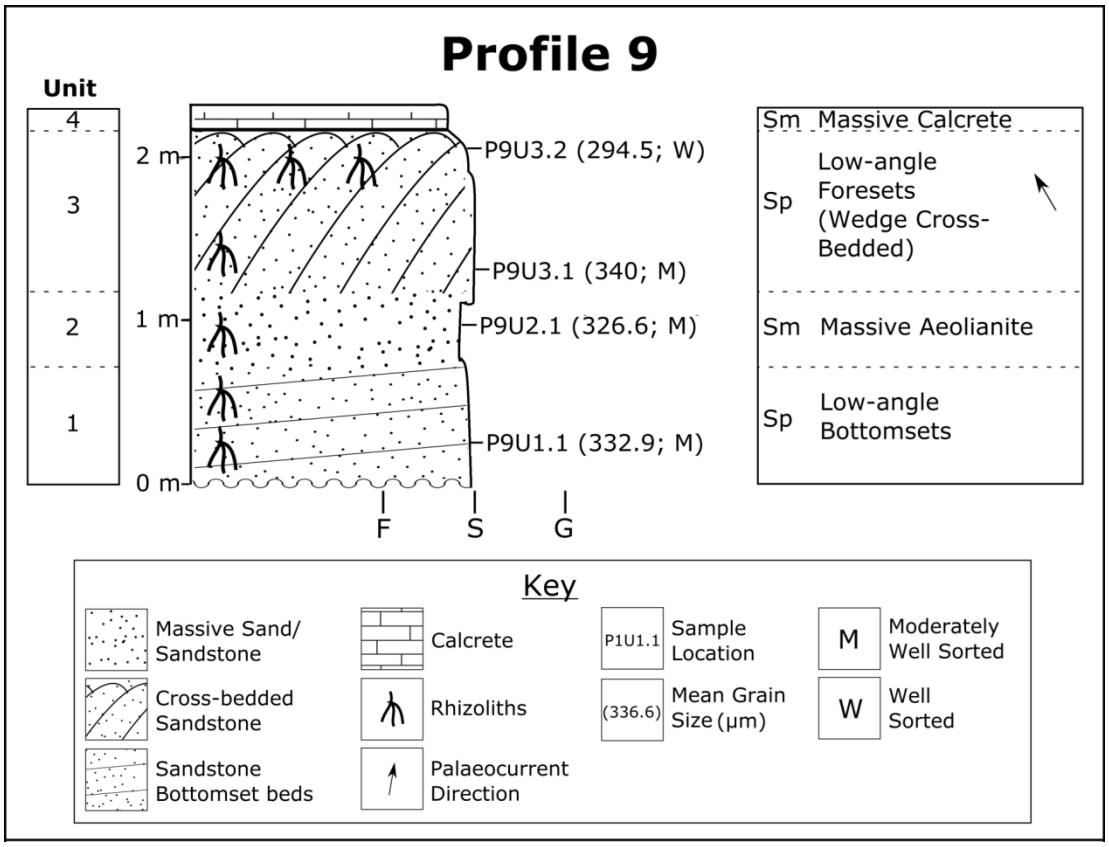


Figure 5.20. The logged sequence of Profile 9. The base of the exposure is 1.5 m above high tide level.

Unit 1 (0 – 80 cm) is a set of low-angle bottomsets which dip 10° towards 150° SSE, flattening to 5° up-dip. The beds are 5 – 6 cm thick at the base, and thin to ~3 cm near the top. The beds are composed of highly cemented pale yellow (Munsell:

2.5Y8/2) coloured moderately well-sorted medium sand. Some small rhizoliths (up to 10 mm thick and 5 cm long) are present on the landward (North) end of the profile. The lower contact is not visible due to the deposition of sand and boulders around the base of the profile. The unit thins notably (to ~30 cm) seaward across the profile. The upper contact with Unit 2 is conformable and fairly sharp, dipping 10° towards 150° SSE, flattening to 5° up-dip. Unit 2 (80 – 125 cm) is a single massive aeolianite bed with no visible internal structure. It is composed of very highly cemented pale yellow (Munsell: 2.5Y8/3) moderately well-sorted medium sand. Some rhizoliths (up to 15 mm thick and 5 cm long) are visible, and are most common on the landward end of the profile. The unit thins considerably seaward, reaching a visible thickness of only 5 cm. The upper contact with Unit 3 is conformable and sharp. It dips 10° towards 150° SSE, flattening to 5° up-dip, roughly parallel to the upper surface of Unit 1.

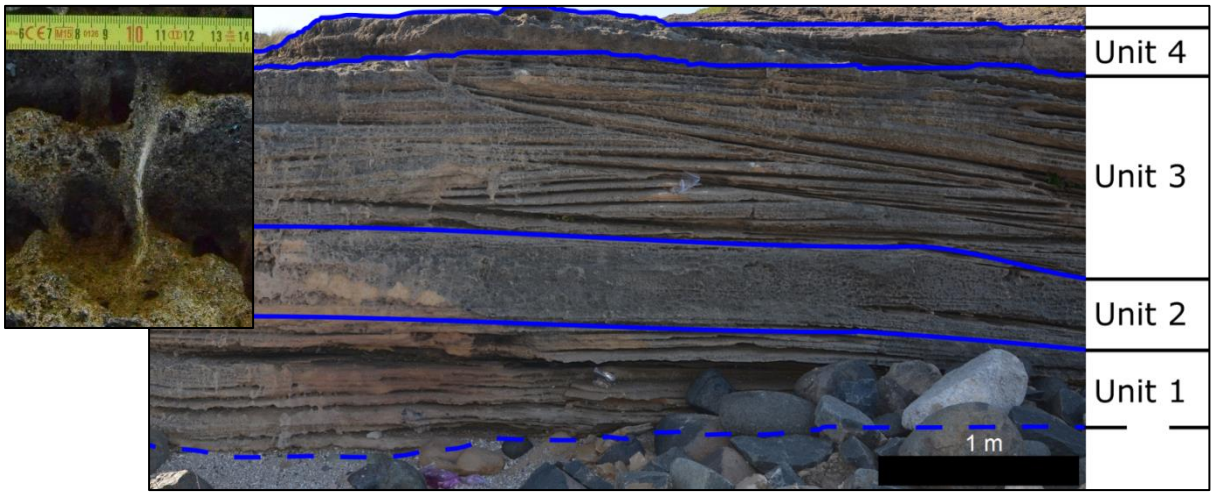


Figure 5.21. A photograph of Profile 9 with the units marked. Inset: close-up photograph of a rhizolith in Unit 1(the scale is in centimetres).

Unit 3 (125 – 218 cm) comprises several sets of wedge cross-bedded formsets which comprise low-angle topsets and low-angle foresets. The topsets cross the width of the profile, while the foresets are only present towards the landward end. The topsets are 1 – 3 cm thick and dip 10° towards 150° SSE, shallowing to 5° towards 150° SSE up-dip (landward). The foresets range in thickness from 1 to 2.5 cm, and dip at angles ranging between 2° and 4° towards 330° NNW. The beds are composed of pale yellow (Munsell: 2.5Y8/3 or 2.5Y8/2) moderately well-sorted to well-sorted medium sand that fines up through the unit. The sediment is highly

cemented, but notably less so than in Unit 2. Some rhizoliths (up to 20 mm thick and 8 cm long) are present within the unit, particularly on the landward end of the profile. The unit is fairly uniform in thickness across the profile, with a maximum of ~1.5 m. The upper contact with Unit 4 is a sharp unconformity with an inclination of ~2° towards 150° SSE. This surface is a raised marine bench with an elevation of 4 m above high tide level. The contact is a supersurface, indicating a break in deposition. Unit 4 (218 – 230 cm) is a massive calcrete with no internal structure. The sediment is light grey (Munsell: 2.5Y7/2) medium/fine sand that is very highly cemented and has considerably fewer pore spaces than the aeolianite. It ranges in thickness from 8 cm to 20 cm.

Single bulk sediment samples for laboratory analysis were taken from Units 1 and 2. Two were collected from within Unit 3. The results for these samples are presented in Section 5.2.

Profile 10:

Profile 10 contains three distinct units in an exposure with its base 1 m above high tide level (Figures 5.22 & 5.23). Unfortunately, the slope of a modern dune obscures the profile above the top of Unit 3. Therefore, the nature of the sequence above this point is not known. Unit 1 (0 – 43 cm) is a set of low-angle laminated topsets 3 – 6 mm thick which dip 10° towards 260° W, steepening to 12° up-dip. The laminae are composed of highly cemented pale yellow (Munsell: 2.5Y8/2) coarse medium sand. The lower contact of the unit is not visible due to the deposition of beach sand against the profile. Unit 1 thins rapidly to the West, eventually disappearing below the beach. It thickens to ~60 cm thick on the eastern edge of the profile. The upper contact with Unit 2 is conformable and fairly sharp. Unit 2 (43 – 175 cm) is a set of low-angle topsets 1.5 – 4 cm thick which dip 10° towards 260° W, steepening to 12° up-dip. The beds are highly cemented and contain pale yellow (Munsell: 2.5Y8/2) well-sorted slightly coarse medium sand which fines up to medium sand. Small rhizoliths (up to 5 mm wide and a few centimetres long) are present in low numbers in the upper part of the unit. Unit 2 thins gradually to the West, eventually ‘pinching out’ at the edge of the exposure. The upper contact with Unit 3 is conformable but

slightly disturbed by bioturbation by the many rhizoliths which penetrate from Unit 3 into the top of Unit 2.

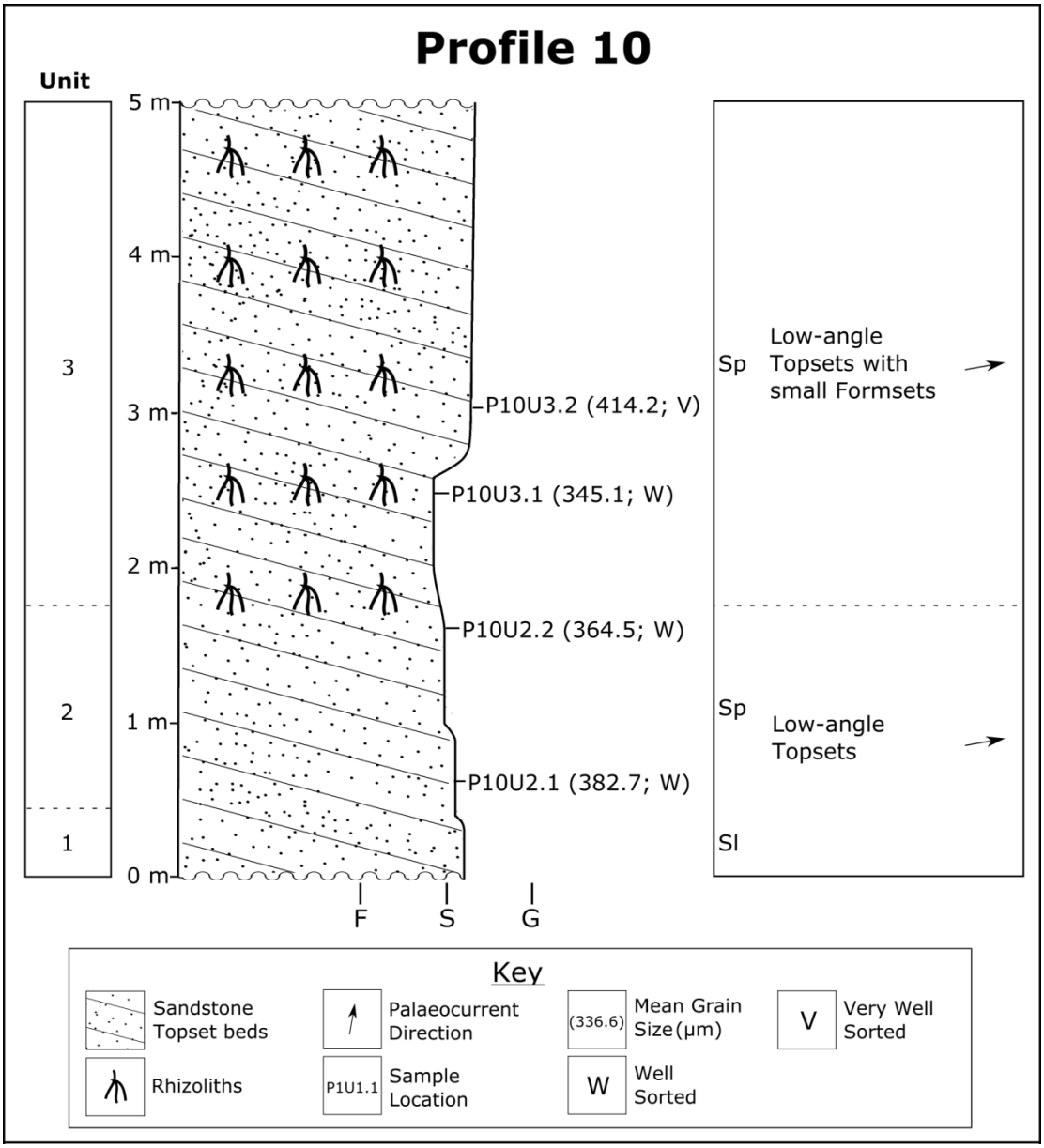


Figure 5.22. The logged sequence of Profile 10. The base of the exposure is 1 m above high tide level.

Unit 3 (175 – 500 cm) comprises a set of low-angle topsets and multiple small formsets which represent miniature dunes up to 45 cm in height which rise up from the slope. Second-order bounding surfaces separate the topsets and smaller formsets. The topsets dip 10° towards 260° W. The beds are 2 – 4 cm thick and are composed of pale yellow (Munsell: 2.5Y8/3) well-sorted to very well-sorted medium sand which coarsens up to relatively coarse medium sand. The sediment is highly

cemented, but is very druzy, especially in the upper beds. Rhizoliths up to 50 mm thick and 10 cm long are common but decrease in numbers near the top of the unit. Unit 3 thins westward across the exposure, eventually disappearing. The upper surface of Unit 3 is not visible due to the deposition of modern dunes.

Two bulk sediment samples were taken from Unit 2 and from Unit 3 to be analysed in the laboratory. The results for these samples are presented in Section 5.2.

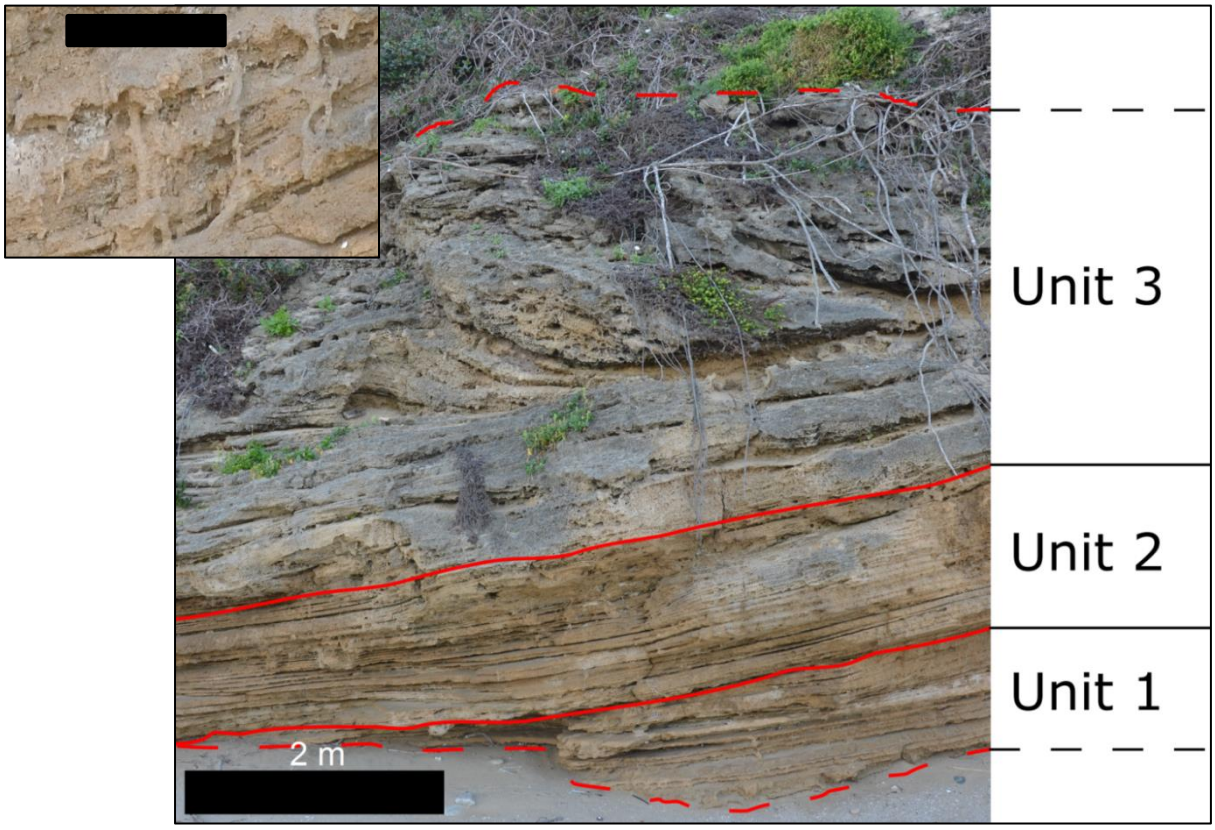


Figure 5.23. A photograph of Profile 10 with the units marked. Inset: a close-up photograph of several rhizoliths in Unit 3 (scale bar is 10 cm).

Profile 11:

Profile 11 is ~12 m high and its base is 1 m above high tide level. Three units were identified, all of which are aeolian (Figures 5.24 & 5.25). Unit 1 (0 – 610 cm) is a single set of arched formset beds 10 cm to 20 cm thick. The beds first appear on the western edge of the profile as cross-bedded foresets which dip 10° towards 070° ENE. These very rapidly become low-angle topsets dipping 10° towards 260° W. The beds are composed of very highly cemented pale yellow (Munsell: 2.5Y8/4) well-sorted medium sand that fines up slightly through the unit. Some rhizoliths, up to 20

mm in thickness and 8 cm in length, are visible from roughly halfway up the unit. The lower contact of the unit is not visible due to the deposition of beach sand against the profile. The unit varies in thickness from 2.5 m to 8 m due to the undulating nature of the deposit. The upper contact with Unit 2 is sharply conformable.

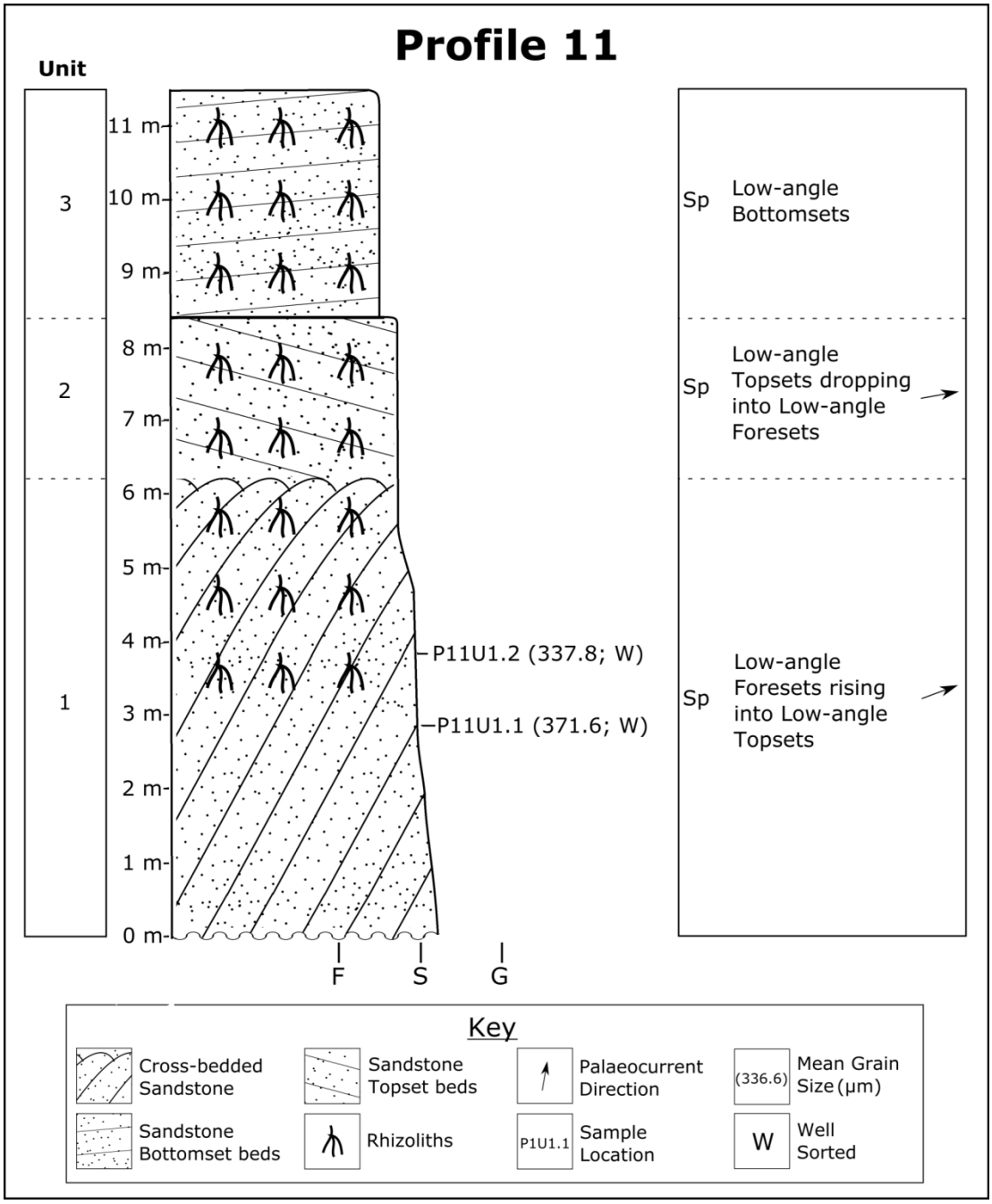


Figure 5.24. The logged sequence of Profile 11.The base of the exposure is 1 m above high tide level.

Unit 2 (610 – 850 cm) is a single set of domed formset beds ~20 cm thick. The beds first appear to the West of the profile as topsets which dip 10° towards 260° W; they

gradually become low-angle foresets dipping 12° towards 080° E. The beds contain slightly fine medium sand that is pale yellow (Munsell: 2.5Y8/4) in colour. Rhizoliths up to 20 mm in width and 10 cm in length occur more commonly than in Unit 1. Unit 2 thickens to the West of the profile, to a maximum observed thickness of ~6 m. To the East, the foresets lie against the slope of Unit 1. Therefore, the unit becomes thinner and eventually 'pinches out' between Unit 1 and Unit 3. The upper contact with Unit 3 is unconformable and fairly sharp, although some localised irregularities occur. Overall, the contact dips 10° towards 080° E. This contact is a supersurface, indicating a depositional hiatus.

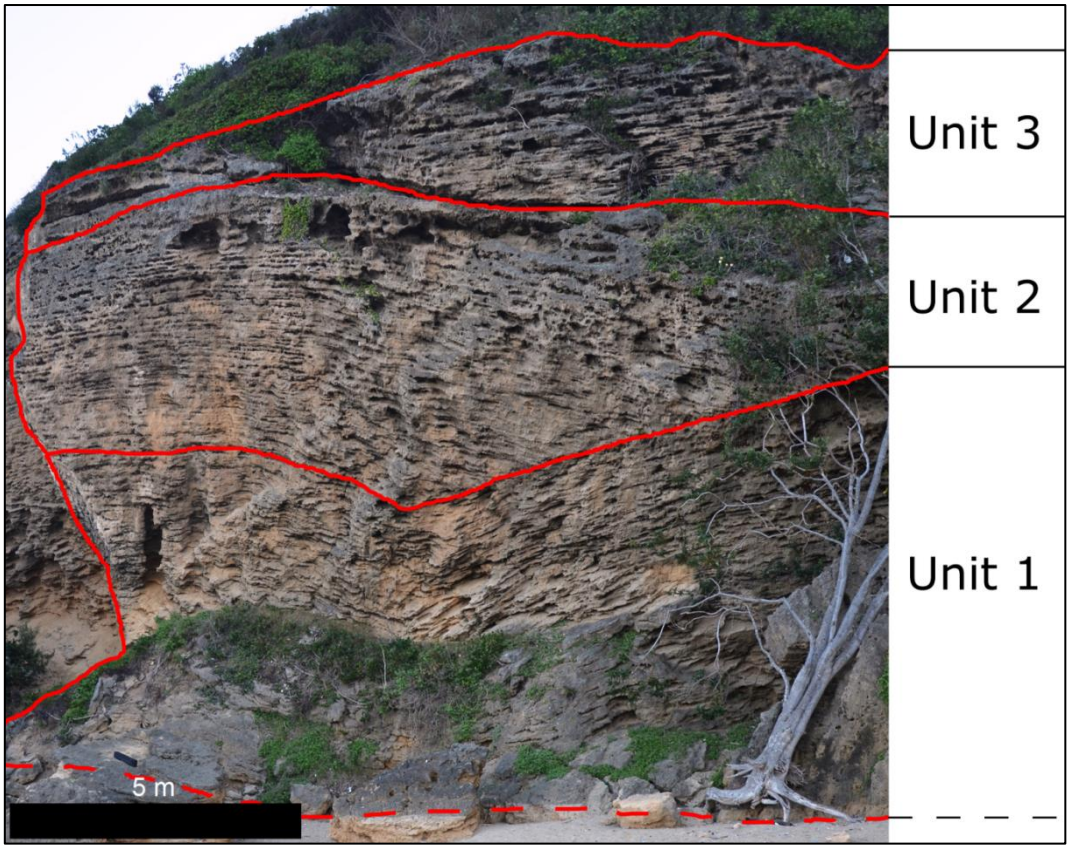


Figure 5.25. A photograph of Profile 11 with the units marked.

Unit 3 (850 – 1150 cm) is a single set of bottomset beds 5 – 10 cm thick which initially dip 5° towards 080° E, but steepen to 10° towards 080° E further East, before flattening to 5° towards 080° E once again. The beds are made up of relatively fine medium sand that is pale yellow (Munsell: 2.5Y7/4) in colour. The sediment is relatively poorly cemented and fairly druzy. Rhizoliths up to 50 mm in width and 15 cm in length are very common. Unit 3 thins considerably to both the East and West

of the profile to a minimum observed thickness of 80 cm. It is thickest (maximum 3 m) when it fills hollows in the upper surface of Unit 2.

Two bulk sediment samples for laboratory analysis were collected from Unit 1. The results for these samples are presented in Section 5.2.

Profile 12:

Profile 12 is a little less than 8.5 m high and its base is 1.5 m above high tide level. Five sedimentary units are recognised (Figures 5.26 & 5.27). Unit 1 (0 – 200 cm) is a set of low-angle arched formset beds ~15 cm thick. The beds first appear to the West of the profile as topsets dipping 10° towards 280° W; they become shallower toward the arched peak, and then develop into foresets which dip 12° towards 100° E. The foreset beds gradually lose structure down dip. The beds are composed of highly cemented pale yellow (Munsell: 2.5Y8/3) relatively coarse medium sand. The lower contact of the unit is not visible due to the deposition of beach sand against the profile. The visible thickness of the unit varies, as it thins eastward, eventually pinching out. Unit 1 is overlain by both Unit 2 and Unit 3. Unit 2, to the East (100°), lies conformably on the surface of Unit 1. The contact with Unit 3, to the West (280°), is also conformable. Unit 2 (200 – 350 cm) is a deposit of aeolianite that first appears at the crest of Unit 1 and then continues down the eastern (~100°) slope to the base of the exposed profile. The deposit is a single massive bed, with no internal structure. At the top of the slope, it is a just a few centimetres thick; it thickens downslope to a maximum of ~2 m. The bed is composed of very pervasively cemented relatively fine medium sand that is pale yellow (Munsell: 2.5Y8/3) in colour. Rare and isolated rhizoliths are present within the unit. The upper surface of Unit 2 is roughly parallel to that of the underlying Unit 1. The contact with Unit 3 at this surface is conformable and sharp. Unit 3 (350 – 450 cm) is a single massive bed that appears at the western end of the profile, where it overlies Unit 1 conformably. It is relatively thin (20 – 30 cm thick) and dips at a low angle towards 100° E. However, to the East of the profile, where Unit 3 lies conformably on the surface of Unit 2, it becomes considerably thicker (up to 1.5 m) and dips at ~10° towards 100° E. No internal structure is visible within the unit. The sediment is very highly cemented pale yellow (Munsell: 2.5Y8/3) moderately well-sorted relatively fine medium sand that is

somewhat finer than that in Unit 2. Small (~10 mm thick and up to 5 cm long) rhizoliths are occasionally visible. The upper surface of the unit undulates, but overall, dips towards 100° E. The contact with Unit 4 is largely sharply unconformable with rare localised erosion. This contact is a third-order bounding surface.

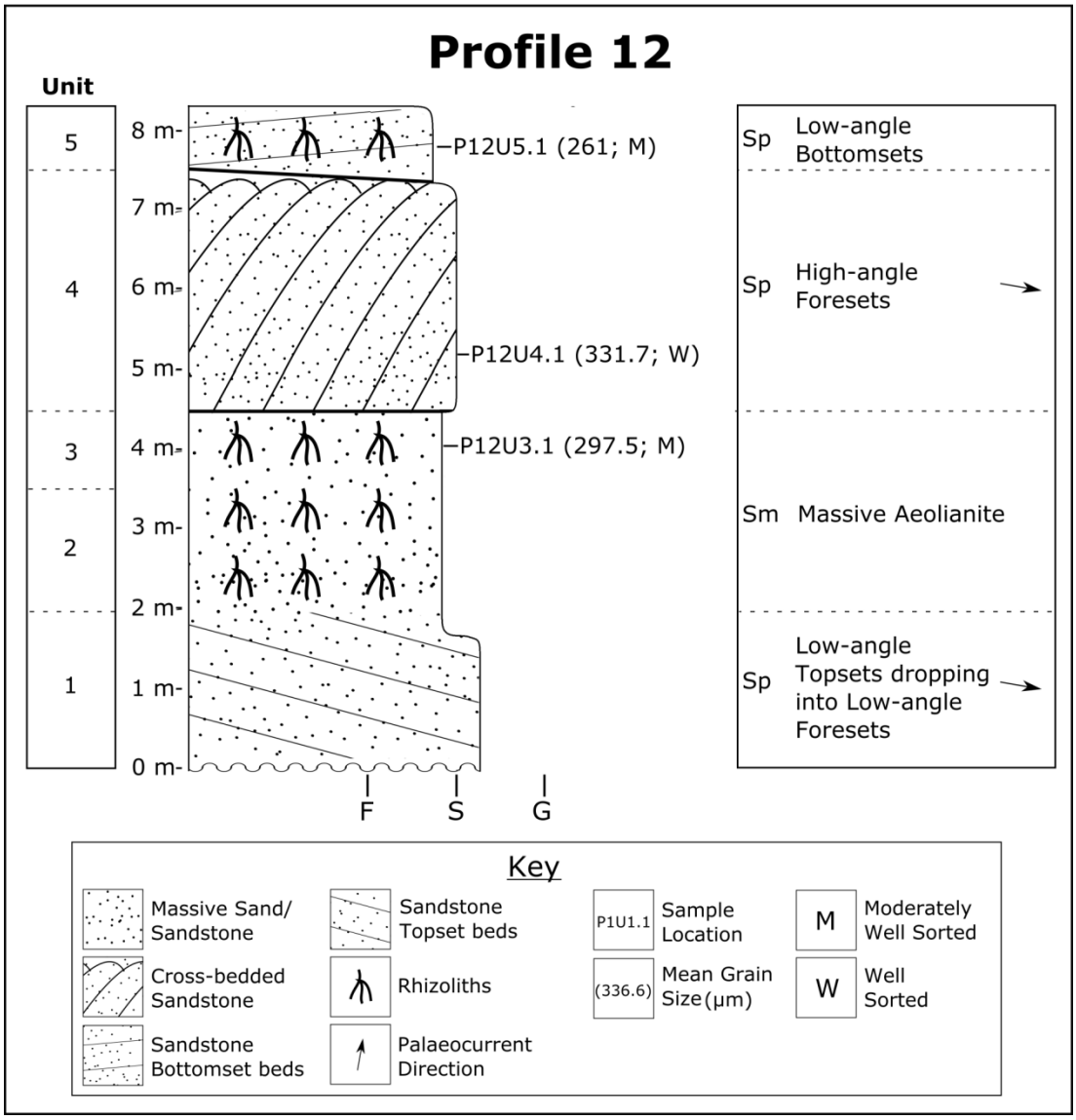


Figure 5.26. The logged sequence of Profile 12. The base of the exposure is 1.5 m above high tide level.

Unit 4 (450 – 750 cm) is a single set of high-angle cross-bedded foresets between 8 and 17 cm thick that dip 25° towards 100° E. The beds are composed of pale yellow (Munsell: 2.5Y8/3) well-sorted medium sand that is highly cemented, but not as highly as the underlying units. The sediment is fairly druzy. The unit thins to the West, eventually pinching out between the slope of Unit 3 and the base of Unit 5. It

thickens to the East, reaching a maximum of 4.5 m thick. The upper contact with Unit 5 is unconformable and sharp, truncating the cross-beds. The dip of the contact ranges between 5° and 10° towards 100° E. In more seaward locations, there is a well-developed raised marine bench with a mean elevation of 4.5 m above high tide level. This contact is a supersurface, indicating a depositional hiatus. Unit 5 (750 – 830 cm) is a set of low-angle bottomset beds ~5 cm thick which dip 5° towards 100° E. The beds comprise relatively poorly cemented, druzy pale yellow (Munsell: 2.5Y7/4) moderately well-sorted relatively fine medium sand. Rhizoliths of a range of sizes, up to 50 mm thick and 15 cm long, are extremely common within the unit. The unit ranges in thickness largely due to erosion; the maximum observed thickness is ~1.5 m.

Single bulk sediment samples were taken from Units 3, 4 and 5 for laboratory analysis. The results for these samples are presented in Section 5.2.

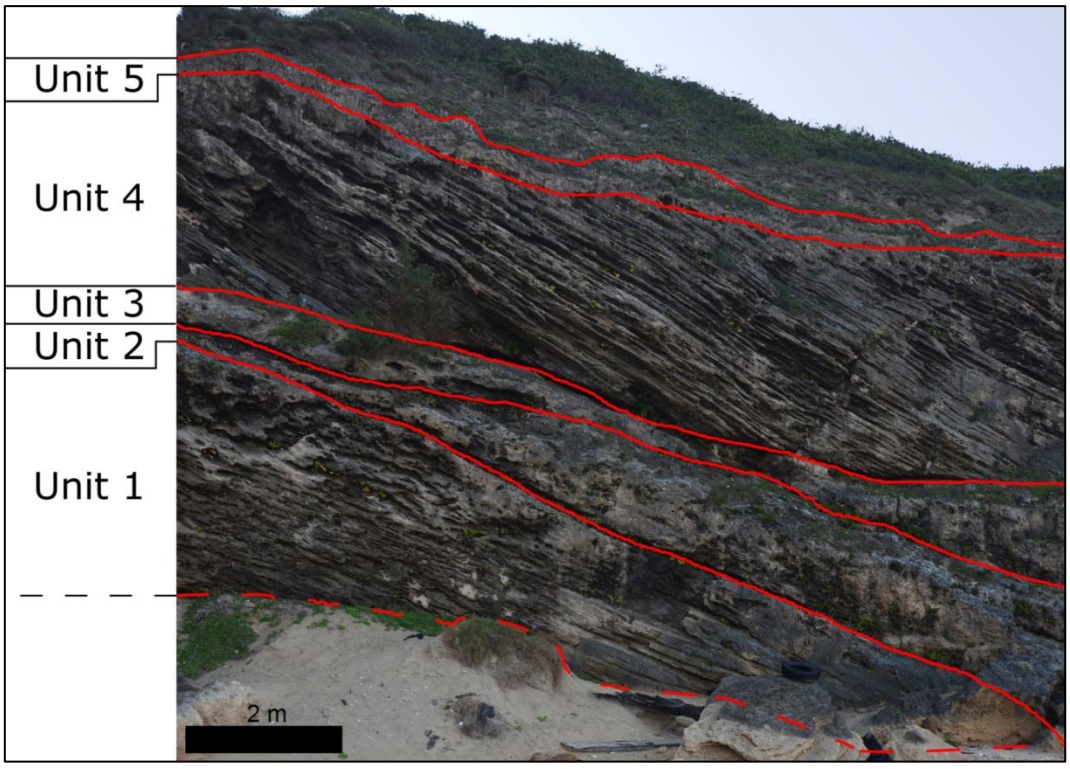


Figure 5.27. A photograph of Profile 12 with the units marked. Note that the contact between Units 1 and 3 (where Unit 2 pinches out) is to the left (280° W) of the part of the exposure shown in the photograph.

Profile 13:

Profile 13 is a sequence 25 m in height with its base at high tide level. Four units were identified within the sequence (Figures 5.28 & 5.29). Unit 1 (0 – 150 cm) is a set of domed foresets which dip at varying inclinations towards 070° ENE. The beds are highly cemented relatively coarse medium sand, and are pale yellow (Munsell: 2.5Y8/3) in colour. Rhizoliths are common, but are generally small, with a maximum thickness of 20 mm and a length of up to 10 cm. The lower contact of the unit is not visible due to the collapse of aeolianite blocks from the exposure and the deposition of beach sand. The visible unit thins landward, eventually disappearing beneath Unit 2. Seaward, it thickens to a maximum of ~3.5 m, before thinning again and disappearing below sea level. The upper contact with Unit 2 is conformable and sharp. It dips landward (300° WNW) at an inclination of ~10°. Unit 2 (150 – 1300 cm) comprises seven sets of toesets which steepen up-dip into high-angle foresets, which dip towards 030° NNE with a maximum inclination of 25°. The sets are separated by first-order bounding surfaces. The beds thicken up within each set from <1 cm thick at the reactivation surface, to a maximum of 15 cm thick. The beds are composed of pale yellow (Munsell: 2.5Y8/3) medium sand that fines up very slightly through the unit. The sand in the basal laminae of each set is notably finer than that in the beds higher up in the sets. There is little visible variation in the thickness of Unit 2 across the exposure. The upper contact with Unit 3 is variable; it is conformable in places, but is largely an erosional unconformity. The contact is associated with a raised bench with an elevation of 4 m to 5 m above high tide level. It constitutes a supersurface created by a hiatus in deposition. Unit 3 (1300 – 2250 cm) is a single set of high-angle topsets 10 – 15 cm thick which dip 15 - 20° towards 210° SSW. The sediment is highly cemented, but is quite druzy in texture. The beds contain well-sorted to moderately well-sorted relatively coarse medium sand that fines upward to medium sand. Some rhizoliths are present, especially near the top of the unit, but they are rare. The unit thickens inland, and thins considerably seaward. The upper contact with Unit 4 is unconformable and diffuse, with some localised erosion and disturbance by bioturbation due to root growth (rhizoliths). Unit 4 (2250 – 2500 cm) is a massive deposit of pale yellow (Munsell: 2.5Y8/3) medium/fine sand with no visible internal structure. The sediment is very druzy and contains many

rhizoliths in a range of sizes up to 50 mm wide and 20 cm long. The thickness of the unit varies between 1 m and 2.5 m.

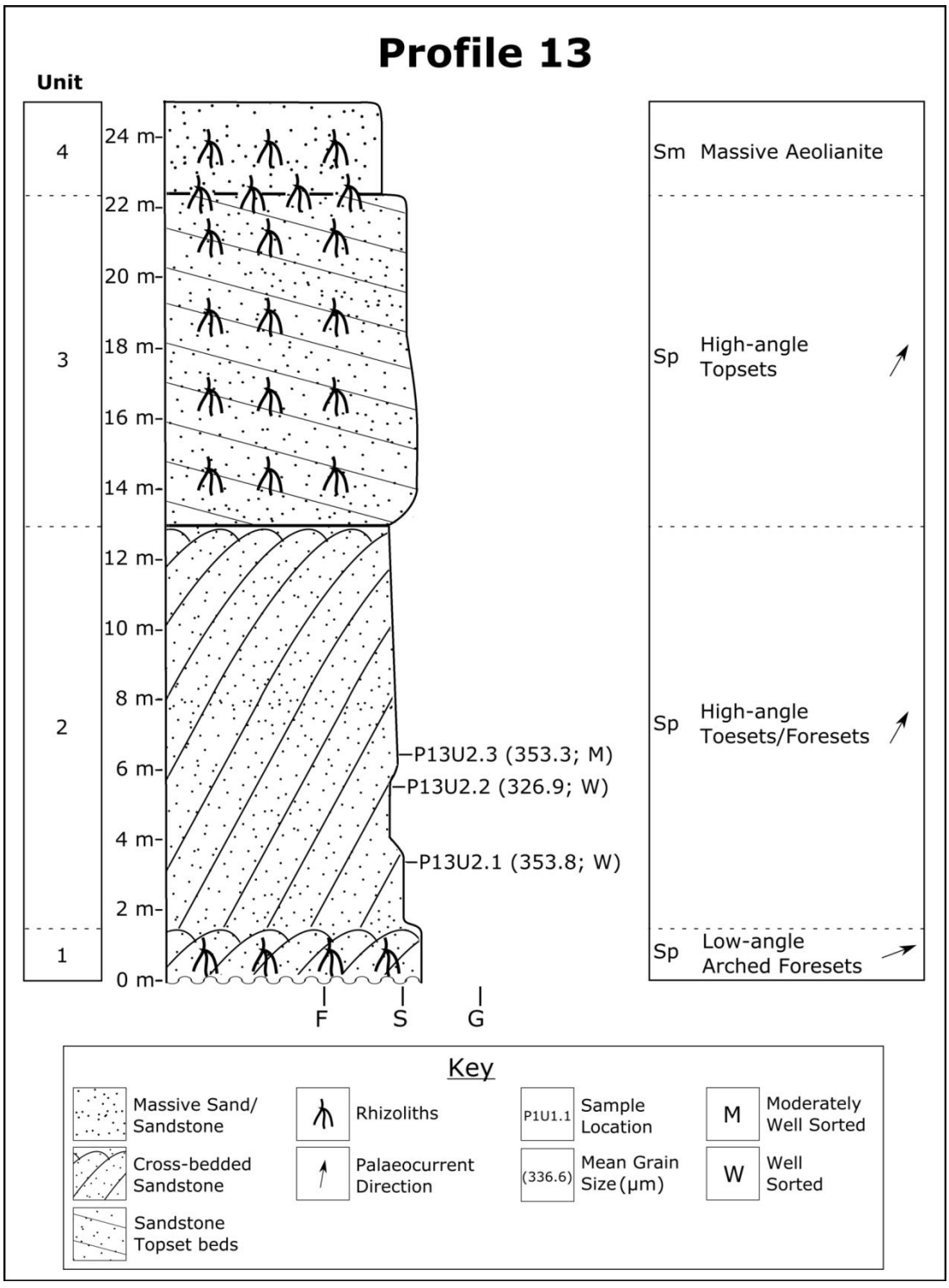


Figure 5.28. The logged sequence of Profile 13. The base of the profile is at high tide level.

Three bulk sediment samples were collected from within Unit 2 for analysis in the laboratory. The results for these samples are presented in Section 5.2.

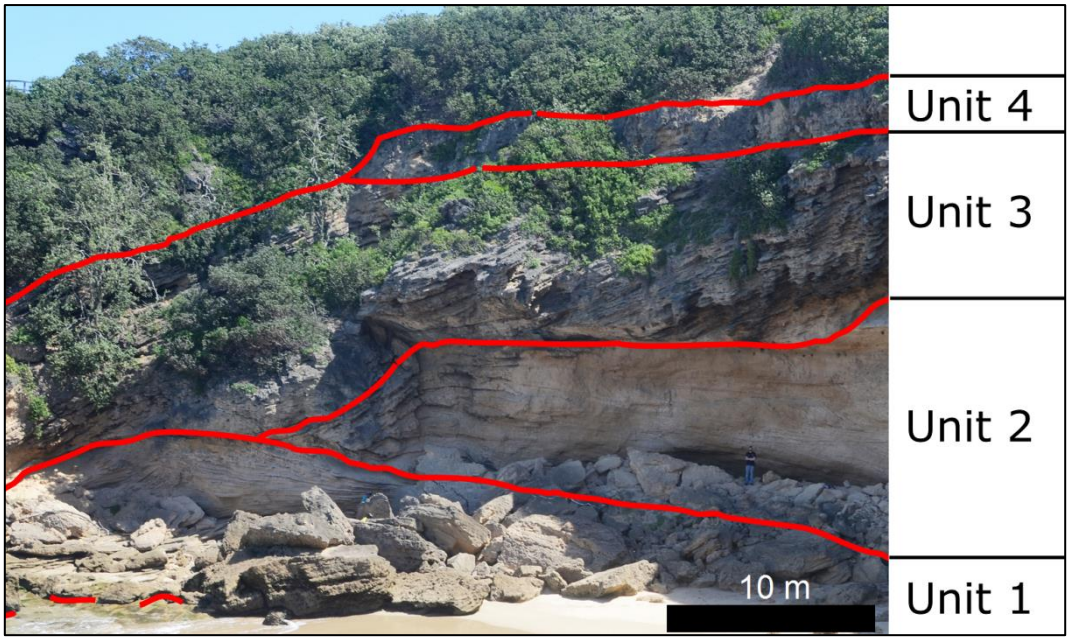


Figure 5.29. A photograph of Profile 13 with the units marked. The sediment above Unit 4 is an unconsolidated aeolian deposit of Holocene age.

Profile 14:

A sequence ~10.5 m high was logged for Profile 14. The base of the sequence is 0.5 m below high tide level. Four sedimentary units were identified (Figures 5.30 & 5.31). Unit 1 (0 – 240 cm) comprises three sets of high-angle topset beds separated by first-order bounding surfaces. The beds become shallower up through the sets: in the lowest, they dip 30° towards 100° E; beds in the middle set dip 20° towards 100° E; those in the top set dip 15° towards 100° E. The beds are 2 – 5 cm thick in all three sets. The beds are composed of very highly cemented pale yellow (Munsell: 2.5Y8/2) well-sorted relatively coarse medium sand that fines up to medium sand. As much of the unit falls within the intertidal zone, many erosional features are present. Some parts of the unit are coated in a thin layer of calcrete. The lower contact of the unit is not visible as the deposit continues below low tide level. The visible unit is of fairly uniform thickness across the profile but does thicken slightly landward (280° W). The upper contact with Unit 2 is a sharp unconformity that truncates the beds at an angle of 5° towards 100° E. This contact is a first-order surface.

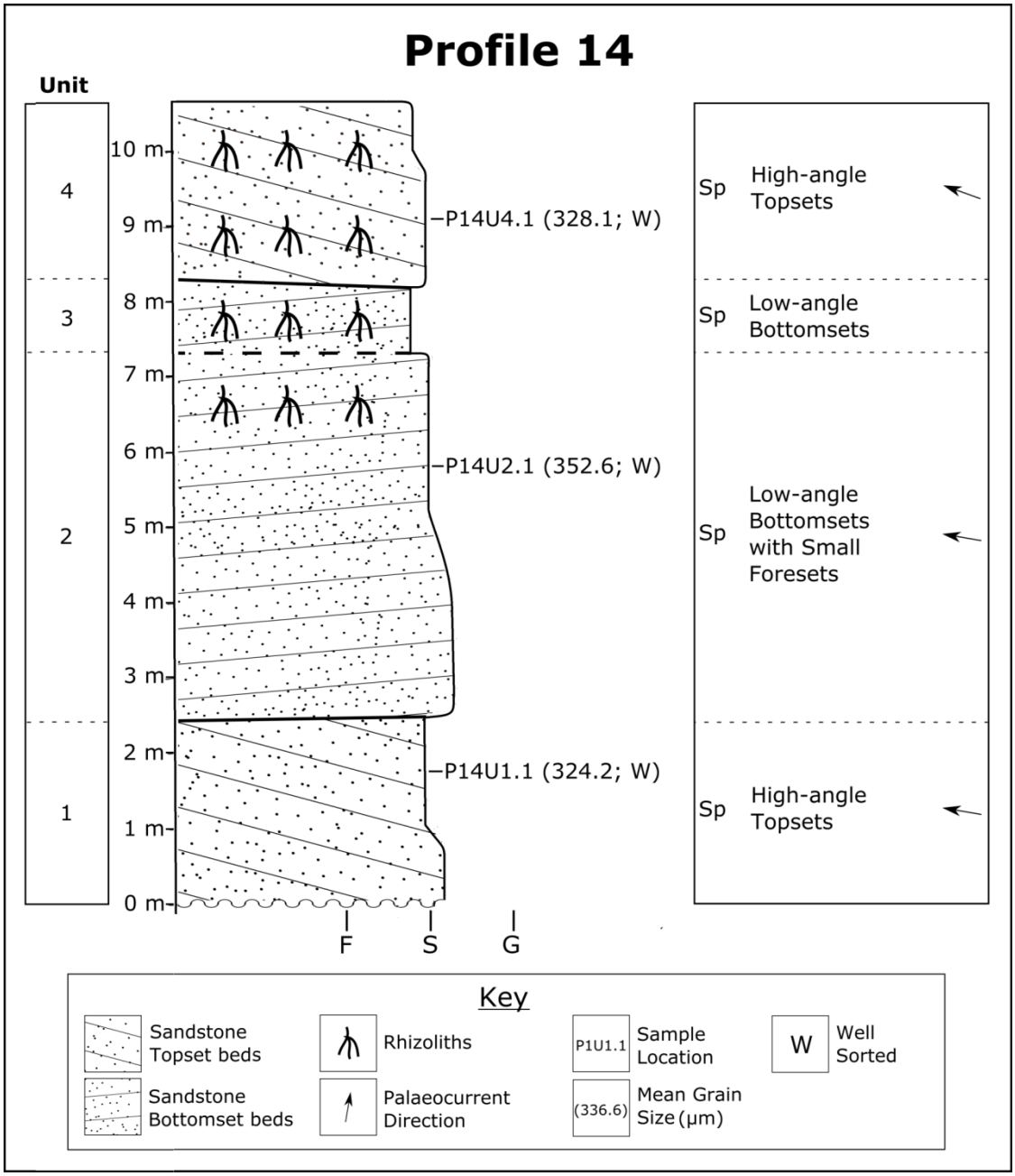


Figure 5.30. The logged sequence of Profile 14. The base of the exposure is 0.5 m below high tide level.

Unit 2 (240 – 730 cm) is composed primarily of low-angle bottomset beds several centimetres thick which dip 5° towards 100° E. A number of formsets (small dunes ranging in height from 30 cm to 1.8 m) are present within this unit. Topsets, dipping towards 100° E, rise from the bottomsets and then curve into foresets which dip towards 280° W. The beds are composed of pale yellow (Munsell: 2.5Y8/4) well-sorted slightly coarse medium sand that fines up to medium sand. The sediment is highly cemented but becomes slightly druzy near the top of the unit. Small rhizoliths

(up to 20 mm thick and 7 cm long) are present, predominantly on the landward end of the profile. They increase in frequency upward. The unit thins notably on the western end of the profile, to ~80 cm thick, as the beds dip down landward (280° W). The upper contact with Unit 3 is diffuse and unconformable on the seaward end of the profile. It is conformable on the landward slope of Unit 2. This is a first-order bounding surface.

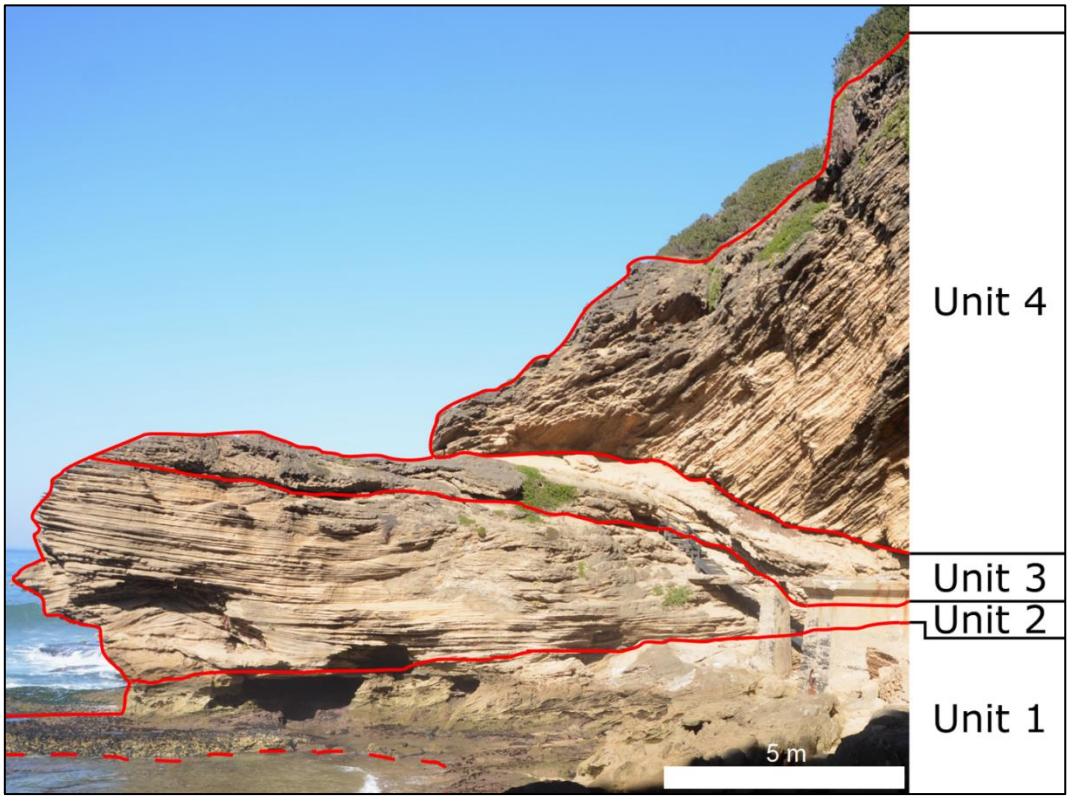


Figure 5.31. A photograph of Profile 14 with the units marked.

Unit 3 (730 – 830 cm) is a single set of low-angle bottomset beds which dip 5° towards 280° W, steepening to 10° up-dip. On the landward side, the beds dip more steeply (up to 25° towards 280° W) as they lie on top of the natural slope of the underlying Unit 2. The beds range in thickness from 10 cm to 20 cm. The sediment is highly cemented, but fairly druzy, pale yellow (Munsell: 2.5Y8/4) relatively fine medium sand. The beds, and the unit as a whole, thicken notably seaward (100° E). Rhizoliths are fairly common across the exposed extent of Unit 3. The upper surface of Unit 3 is somewhat weathered, and the contact with Unit 4 is unconformable. It dips 10° towards 280° W on the landward end of the profile, steepening to 25° on the landward end. It is directly associated with a raised bench 3.8 m above high tide

level. This contact is a supersurface which indicates a break in deposition at this location. Unit 4 (830 – 1060 cm) is a single set of high-angle topsets up to 12 cm thick that initially dip 20° towards 110° ESE, but steepen up-dip to 30° towards 110° ESE. The beds contain pale yellow (Munsell: 2.5Y8/3) well-sorted medium sand that fines upward to medium/fine sand. The rock is druzy, and becomes more so up through the unit. Rhizoliths up to 50 mm wide and 20 cm long are very common. The unit thins seaward, with the natural edge of the dune being roughly halfway along the profile. It thickens considerably landward, with a maximum observed thickness of 15 m.

Single bulk sediment samples for laboratory analysis were taken from Units 1, 2 and 4. The results for these samples are presented in Section 5.2.

Profile 15:

Profile 15 is 17 m high, and its base is 1 m above high tide level. Six distinct sedimentary units were identified within the sequence (Figures 5.32 & 5.33). Unit 1 (0 – 97 cm) is a single set of high-angle foresets 3 – 5 cm thick which dip 25° towards 020° NNE. The beds are composed of very highly cemented pale yellow (Munsell: 2.5Y8/4) moderately well-sorted medium sand. The lower contact of the unit is not visible due to the deposition of beach sand. Across the extent of the profile, the visible thickness of Unit 1 varies very little. The upper contact with Unit 2 is unconformable and flat and represents a first-order bounding surface. Unit 2 (97 – 288 cm) comprises several sets of low-angle bottomsets 2 – 4 cm thick which dip 10° towards 020° NNE. The beds are highly cemented well-sorted medium sand that is pale yellow (Munsell: 2.5Y8/2) in colour. The unit is of fairly uniform thickness across the profile. The upper contact with Unit 3 is a sharp unconformity that truncates the beds at an angle of 10° towards 200° SSW. This contact is a first-order bounding surface. Unit 3 (288 – 435 cm) is a set of low-angle bottomset beds 2 – 4 cm thick which dip 10° towards 200° SSW, flattening to 5° higher up in the unit. The beds are composed of pale yellow (Munsell: 2.5Y8/2) medium sand that is highly cemented but fairly druzy. Rhizoliths are present in low numbers and are generally small (up to 15 mm thick and 6 cm long). The unit thins to the North, eventually pinching out between Unit 2 and Unit 4. However, it thickens markedly to the South, reaching a

maximum observed thickness of ~3 m. The upper contact with Unit 4 is conformable and fairly sharp, dipping 5° towards 200° SSW.

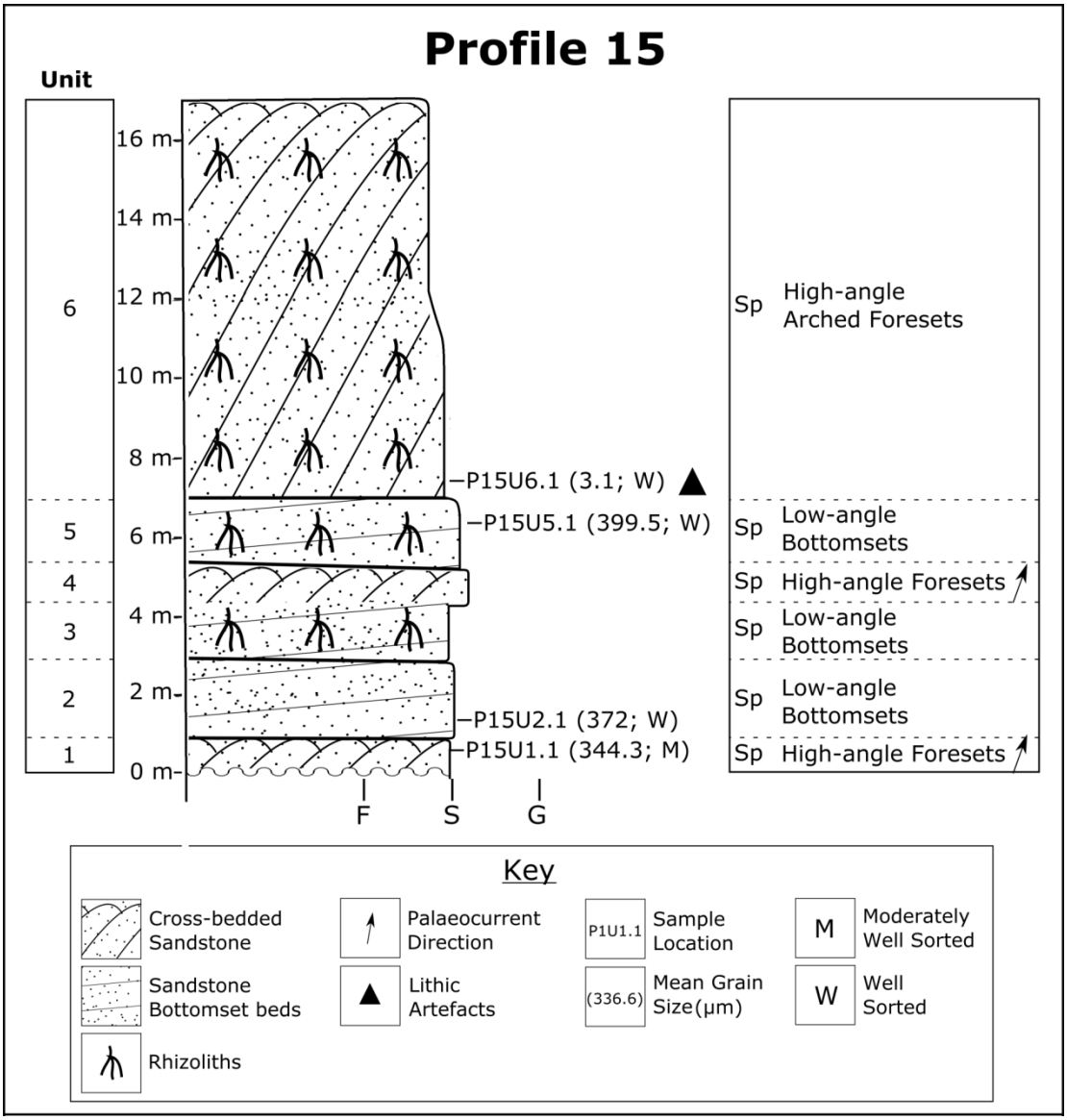


Figure 5.32. The logged sequence of Profile 15. The base of the exposure is 1 m above high tide level.

Unit 4 (435 – 530 cm) comprises four sets of high-angle foreset beds 2 – 5 cm thick which dip 15° towards 020° NNE. The sets are separated by first-order bounding surfaces. The sediment is fairly highly cemented, but is slightly druzy. The beds are composed of relatively coarse medium sand that is pale yellow (Munsell: 2.5Y8/2) in colour. The unit thins to the South, eventually pinching out; it is of fairly uniform thickness across the rest of the profile. The upper contact with Unit 5 is a fairly sharp unconformity that dips 10° towards 200° SSW. It is a first-order bounding surface.

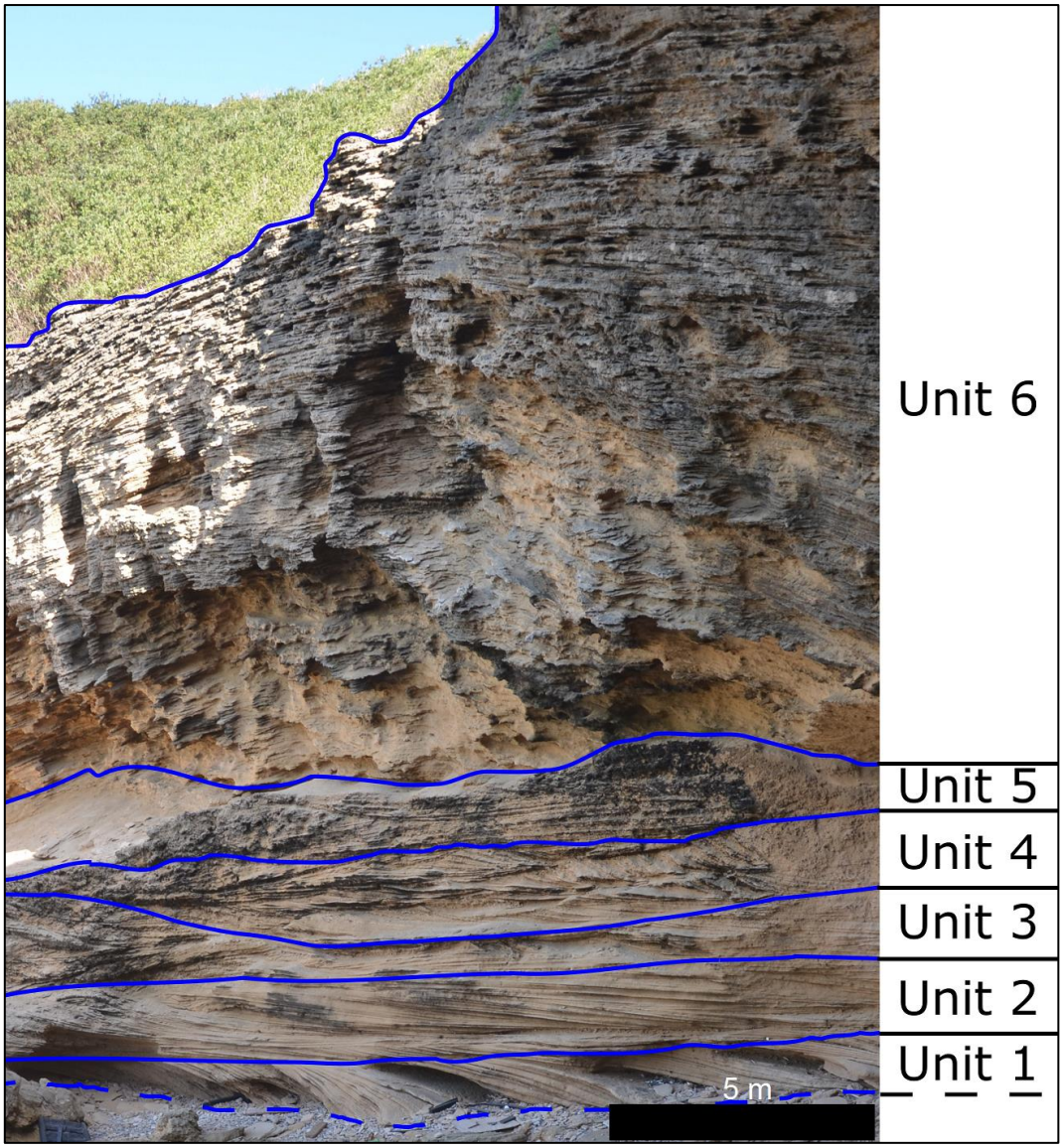


Figure 5.33. A photograph of Profile 15 with the units marked.

Unit 5 (530 – 693 cm) is a set of low-angle bottomset beds 2 – 4 cm thick which dip 10° towards 200° SSW. The beds are relatively poorly cemented pale yellow (Munsell: 2.5Y8/2) well-sorted medium sand. The rock is very druzy and rhizoliths are very common across the unit. Unit 5 thins to both the North and South, eventually 'pinching out' in both directions. The upper contact with Unit 6 is unconformable and irregular. This contact is associated with the raised marine bench in seaward locations. It is a supersurface, indicative of a hiatus in deposition. Unit 6 (693 – 1700 cm) is a single set of arched foresets which dip steeply in varying directions. The beds are 12 – 15 cm thick and composed of pale yellow (Munsell: 2.5Y8/4) well-sorted medium sand that fines up to a relatively fine medium sand. The

sediment is not as highly cemented as in underlying units and is fairly druzy. Rhizoliths up to 50 mm wide and 20 cm long are present throughout the unit but increase in frequency upwards. Several lithic artefacts were discovered within the aeolianite, roughly 1 m above the contact with Unit 5 (see sub-section 5.1.4. for a more detailed description). The unit thickens considerably landward, reaching up to 15 m thick. The current top of Unit 6 has been highly eroded, and some of the upper portion of it appears to have been removed.

Single bulk sediment samples were taken from Units 1, 2, 5 and 6 for laboratory analysis. The results for these samples are presented in Section 5.2.

Profile 16:

The sequence logged for Profile 16 is a little over 11 m high. Its base is 1.2 m below sea level. Two sedimentary units were identified (Figures 5.34 & 5.35). Unit 1 (0 – 400 cm) is composed of low-angle bottomset beds up to 50 cm thick, which dip 5° towards 180° S. The beds thin markedly up-dip to around 30 cm thick. The beds are composed of moderately well-sorted to well-sorted medium sand throughout, but fine upwards notably. The sediment is light grey in colour (Munsell: 2.5Y7/2) and very highly cemented. A single lithic artefact was found within this unit (see sub-section 5.1.4. for a more detailed description). The lower boundary of the unit is not visible as it is below low-tide level. As much of the unit is within the intertidal zone, it is highly weathered. The bedding is most visible in areas protected from waves and spray. Pockets of weathered coquina are present within erosional gaps in the aeolianite. The upper contact with Unit 2 largely follows the slightly hummocky upper surface of the topmost bed of Unit 1. However, it is highly weathered and represents an unconformity. The contact can be directly correlated with the well-developed raised bench in the area, which is 3.8 m above high tide level at this location. This contact is a supersurface, which indicates a break in deposition. A small deposit of lithic artefacts was found at this interface (see sub-section 5.1.4. for a more detailed description). Unit 2 (400 – 1100 cm) is a single set of high-angle topset beds 10 to 12 cm thick which dip 20° towards 180° S. The sediment is pale yellow (Munsell: 2.5Y8/3) medium sand that is initially coarser than at the top of Unit 1, but fines slightly upward. The beds are not as highly cemented as those in Unit 1 and are

considerably less weathered. The unit thickens considerably to the north, reaching up to 14 m in thickness. Rhizoliths are present, but are relatively low in frequency and generally fairly small. They become larger (up to 50 mm in thickness and 20 cm in length) and more common higher up in the unit and nearer the peak of the dune.

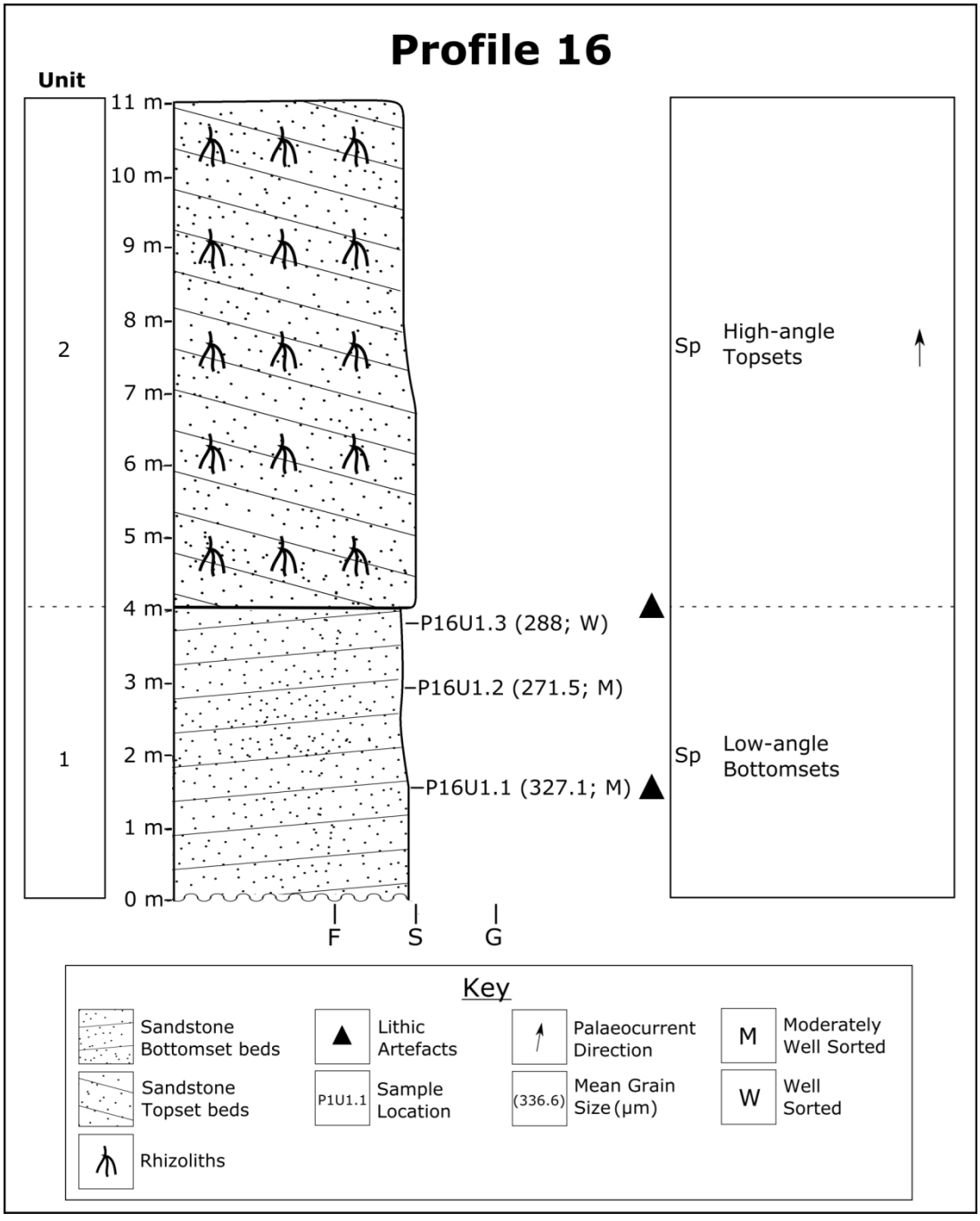


Figure 5.34. The logged sequence of Profile 16. The base of the exposure is 1.2 m below high tide level.

Three bulk sediment samples for laboratory analysis were collected from within Unit 1. The results for these samples are presented in Section 5.2.

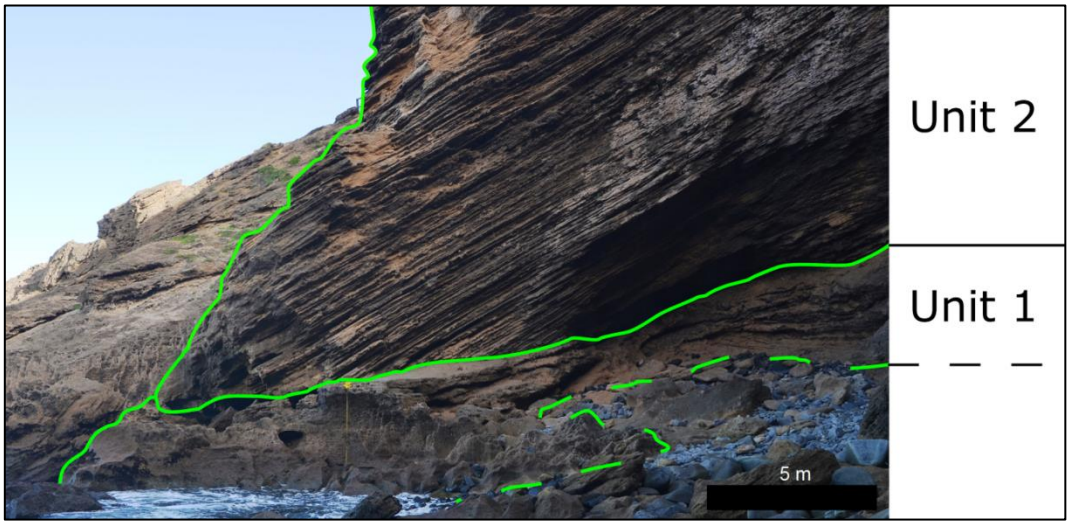


Figure 5.35. A photograph of Profile 16 with the units marked. The units continue to the left of the profile.

Profile 17:

Three units were identified within Profile 17 (Figures 5.36 & 5.37). The logged sequence is 23 m high, and its base is 1.5 m above high tide level. Unit 1 (0 – 600 cm) comprises a set of high-angle topsets between 5 cm and 20 cm thick which dip 15° toward 180° S. The sediment is fairly highly cemented but very druzy. The beds are composed of light grey (Munsell: 2.5Y7/2) medium/fine sand. The lower contact of the unit is not visible due the deposition of sand against the profile. The visible extent of the unit thins considerably to the East and West with the natural slope of the dune. It eventually disappears from view at both ends of the profile. The upper contact with Unit 2 appears to follow the surface of Unit 1. However, there is significant weathering to this surface that occurred before its burial by Unit 2 and the contact appears to be an unconformity. It is also associated with the raised marine bench. This contact is a supersurface and indicates a hiatus in deposition. Unit 2 (600 – 2000 cm) is a single set of domed foresets up to 15 cm thick which dip in varying directions. The sediment is pale yellow (Munsell: 2.5Y8/3) medium sand that is coarser than at the top of Unit 1, but fines upward to medium/fine sand. The sediment is highly cemented but gradually becomes more druzy upwards through the unit. Rhizoliths start to appear from roughly midway up the unit and become

steadily more common toward the top. The unit thins markedly seaward. The upper contact with Unit 3 is unconformable and heavily disturbed by bioturbation.

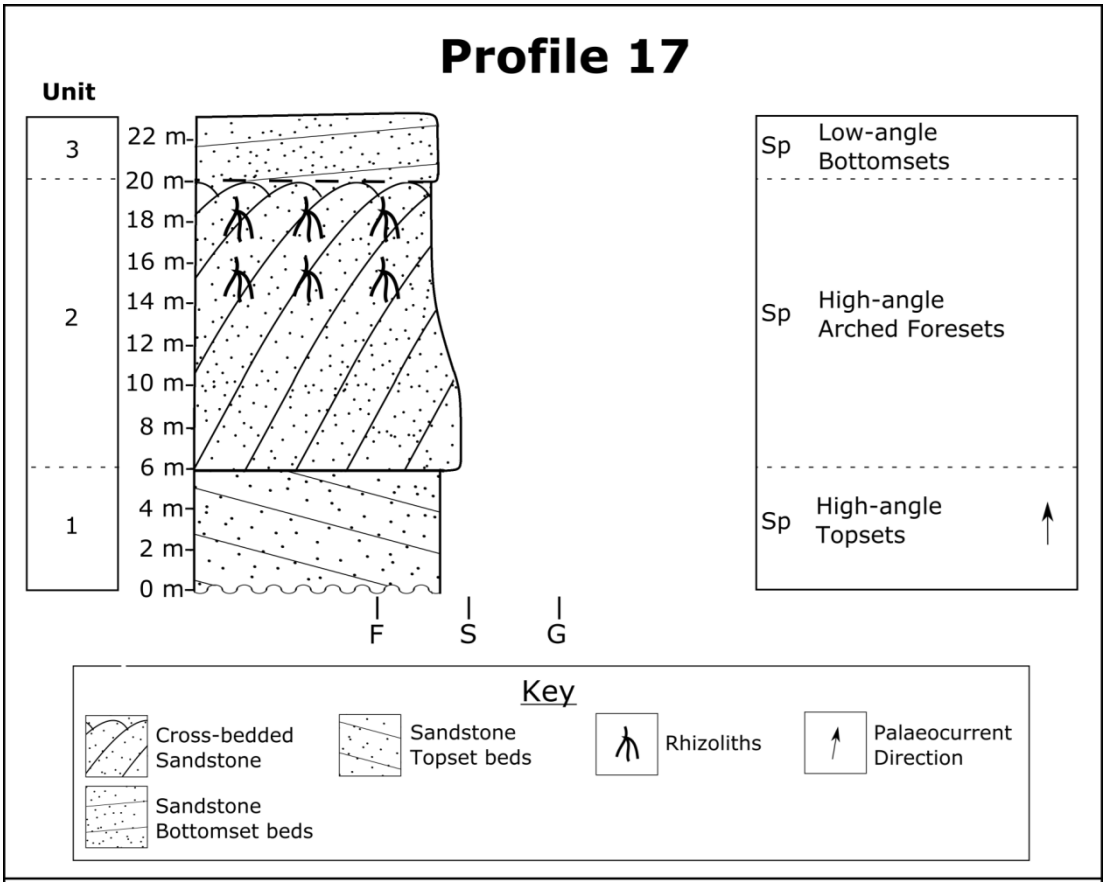


Figure 5.36. The logged sequence of Profile 17. The base of the exposure is 1.5 m above high tide level.

Unit 3 (2000 – 2300 cm) is a set of low-angle bottomset beds up to 10 cm thick which dip 5° towards 270° W. The sediment is relatively poorly cemented and very druzy. The beds are composed of pale yellow (Munsell: 2.5Y8/2) relatively fine medium sand. Rhizoliths up to 50 mm wide and 20 cm long are very common throughout the unit. Unit 3 ranges in thickness from 1 m to 3.5 m.

No sediment samples were collected from Profile 17.

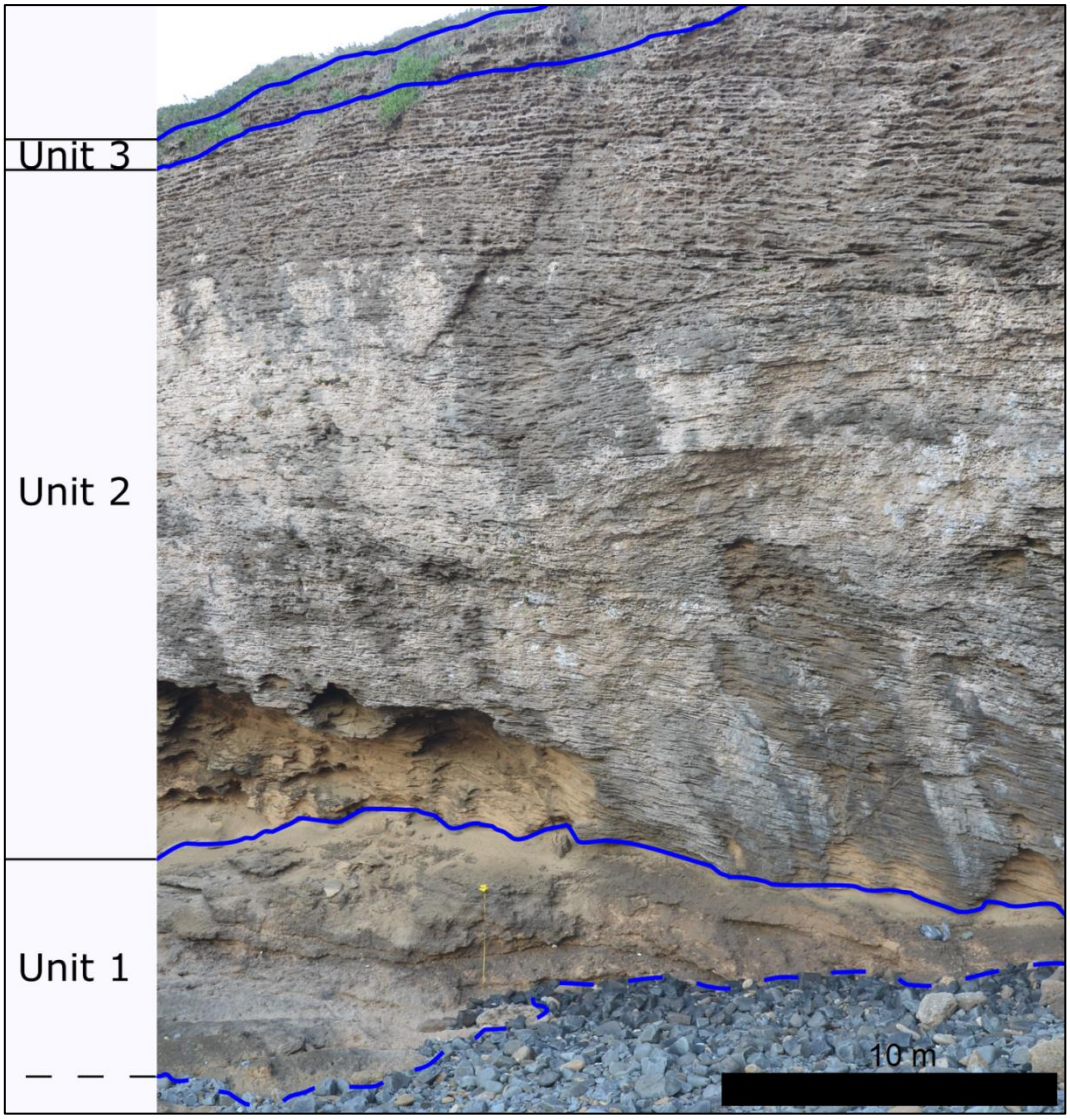


Figure 5.37. A photograph of Profile 17 with the units marked.

Profile 18:

The sequence from which Profile 18 was logged is 30 m high and has its base 1.5 m below high tide level. Four distinct aeolianite units were identified (Figures 5.38 & 5.39). Unit 1 (0 – 750 cm) is a set of high-angle foresets 6 cm to 8 cm thick with a maximum dip of 20° towards 080° E. The beds are highly cemented and composed of pale yellow (Munsell: 2.5Y8/3) medium sand that fines up to relatively fine medium sand. As much of the unit is within the intertidal zone, the rock is highly weathered. The lower contact of Unit 1 is not visible as the unit disappears below the low tide level. This unit is of fairly uniform thickness across the exposed profile, but does thin slightly to the West. The upper contact with Unit 2 is a sharp unconformity that dips 5° towards 080° E. This is a third-order bounding surface. Unit 2 (750 – 960 cm) is a

set of low-angle foresets ~8 cm thick which dip 10° towards 350° N. The beds are pale yellow (Munsell: 2.5Y8/3) relatively coarse medium sand that fines upward to medium sand. The sediment is relatively poorly cemented, and becomes increasingly druzy up through the unit. The deposit thins gradually to both the West and the East. The upper contact with Unit 3 is unconformable, dipping 10° towards 260° W. This unconformity is associated with the well-developed raised marine bench between Profile 16 and Profile 18. This feature has an elevation of 6 m – 7 m above high tide level around Profile 18. It is a supersurface, and indicates a depositional hiatus.

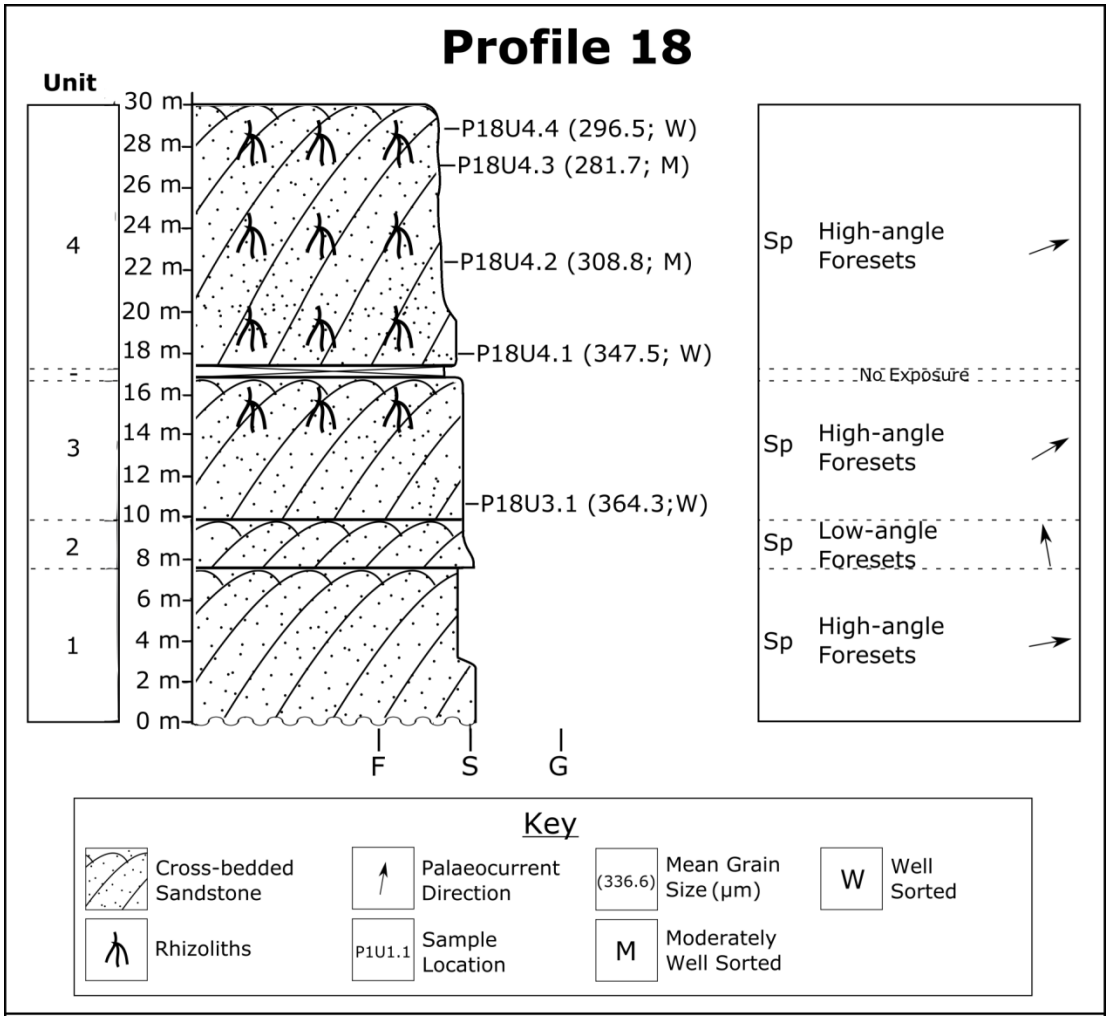


Figure 5.38. The logged sequence of Profile 18. The base of the exposure is 1.5 m below high tide level.

Unit 3 (960 – 1660 cm) is a single set of high-angle foresets 9 – 12 cm thick, which dip 20° towards 060° ENE. The beds are pale yellow (Munsell: 2.5Y8/3) well-sorted medium sand and are highly cemented. In some places, particularly in the lower

reaches of the unit, the beds lose some of their structure. Some rhizoliths are present within the upper 1 m of the unit. These are generally small, with a maximum width of 20 mm and lengths of up to 8 cm. The upper contact with Unit 4 is obscured due to the deposition of sand against the profile. However, it appears to be a fairly sharp unconformity that can be classified as a first-order bounding surface.

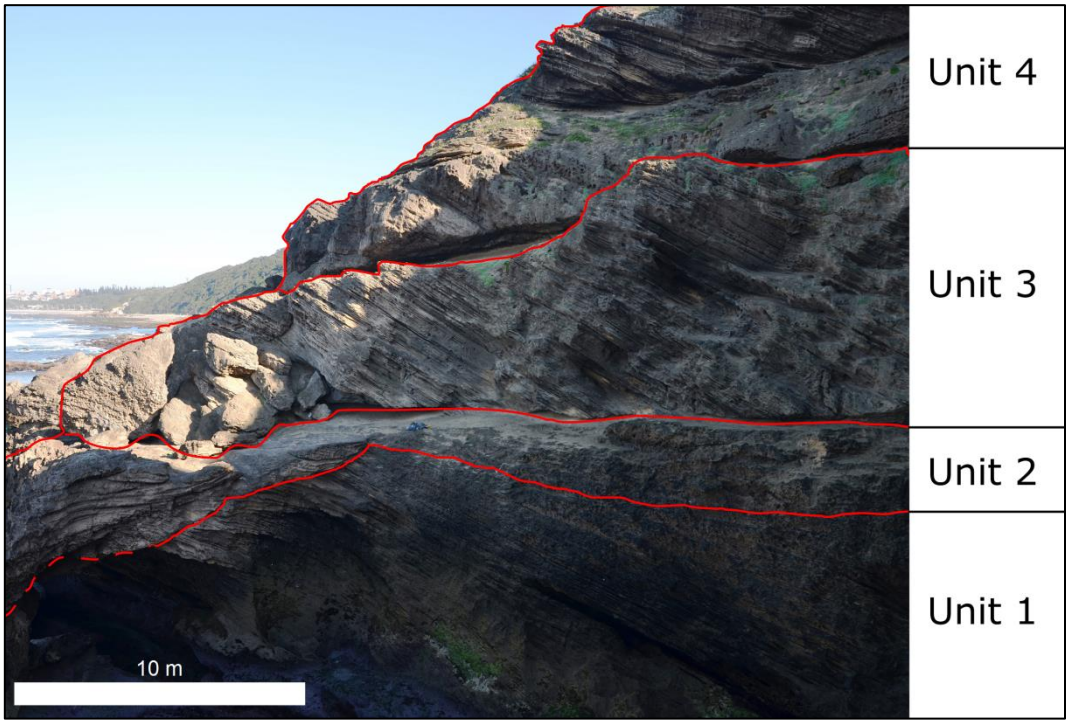


Figure 5.39. A photograph of Profile 18 with the units marked.

Unit 4 (1700 – 3000 cm) comprises two sets of large-scale high-angle foresets separated by a first-order bounding surface. The foresets are 6 – 10 cm thick, and dip 20° towards 070° ENE. These beds contain pale yellow (Munsell: 2.5Y7/3) moderately-well sorted to well-sorted medium sand that fines upward to medium/fine sand. The sediment is very highly cemented, but is very druzy in texture. Rhizoliths are fairly common throughout the unit. They increase in size (maximum 80 mm thick and 26 cm long) and frequency upward. Unit 4 thins markedly to the East, thinning to less than 1.5 m; it thickens to the West up to ~20 m. The upper surface is eroded and irregular. In some places, a thin layer of calcrete coats the upper surface of Unit 4.

A single bulk sediment sample for laboratory analysis was taken from Unit 3. Another four bulk samples were collected from within Unit 4. The results for these samples are presented in Section 5.2.

Profile 19:

Three sedimentary units were identified within Profile 19 (Figures 5.40 & 5.41). The logged profile is just over 8 m in height, and its base is 0.5 m below high tide level.

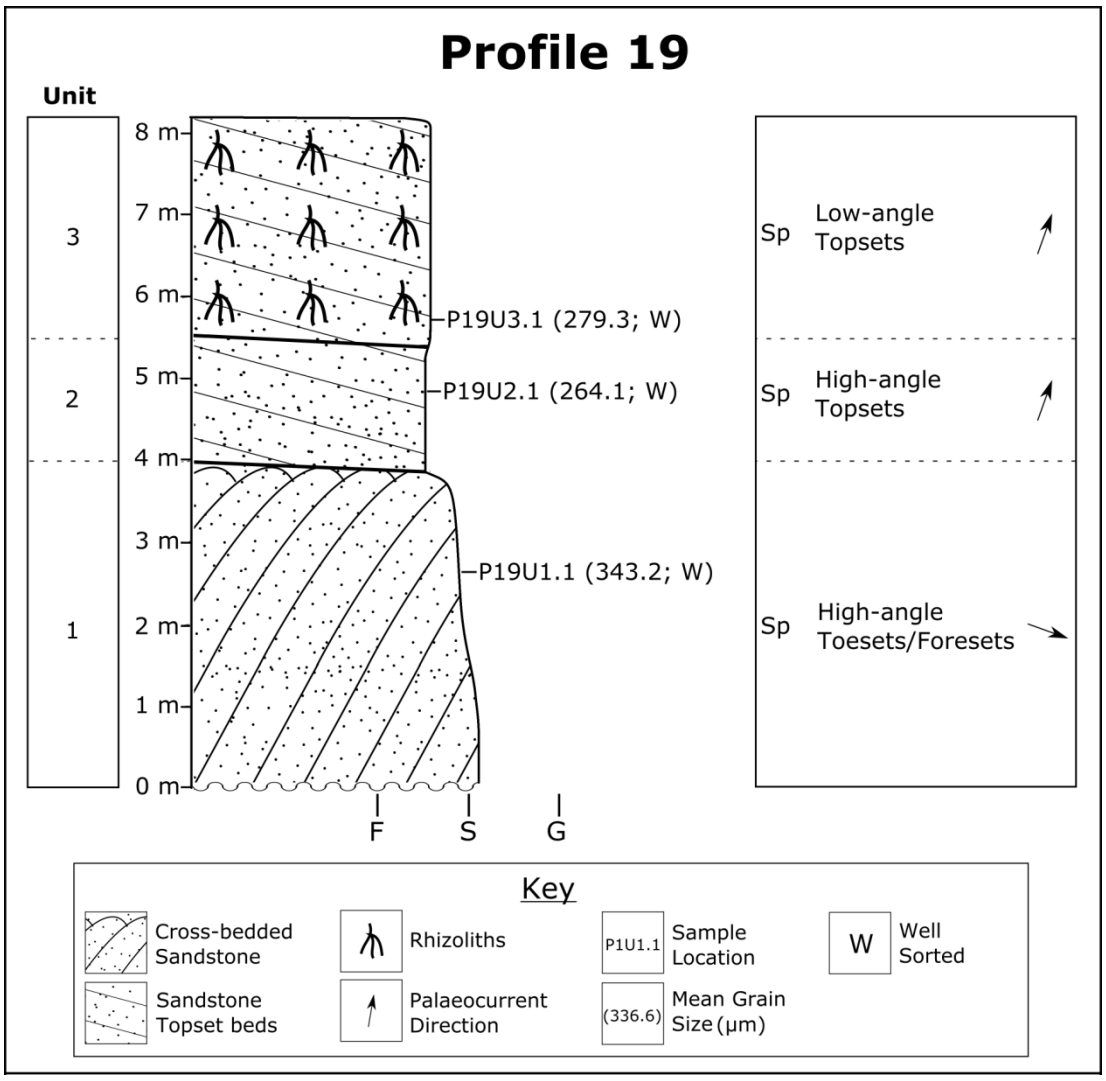


Figure 5.40. The logged sequence of Profile 19. The base of the exposure is 0.5 m below high tide level.

Unit 1 (0 – 394 cm) comprises five sets of toesets dipping 5° towards 110° ESE, which steepen up into high-angle foresets. The sets are separated by first-order bounding surfaces. In the lower sets, the foresets reach a maximum of inclination of 15° towards 110° ESE. In the upper sets, the foresets have a maximum dip of 30°

towards 110° ESE. The beds are 1.5 – 5 cm thick and are composed of very highly cemented pale yellow (Munsell: 2.5Y8/3) well-sorted medium/coarse sand that fines up to medium sand. The beds thicken upward through the sets. As most of the unit is within the current intertidal zone or the splash zone, it is highly weathered and many erosional features are present. The lower contact of Unit 1 is not visible due to the deposition of sand against the profile. The unit thickens somewhat towards the seaward edge of the profile and thins landward. The upper contact with Unit 2 is a fairly sharp unconformity that dips 5° towards 110° ESE. This contact is a supersurface, indicating a hiatus in deposition.

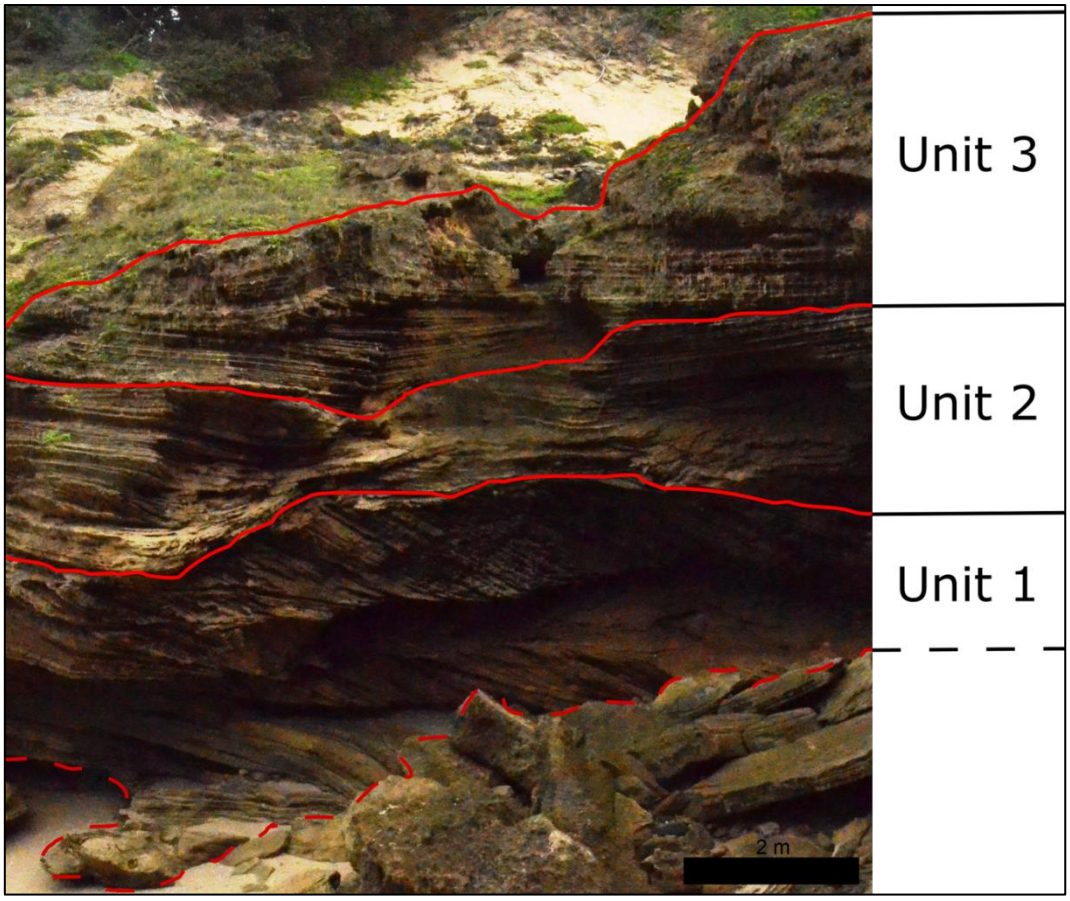


Figure 5.41. A photograph of Profile 19 with the units marked.

Unit 2 (394 – 535 cm) is a set of high-angle topset beds 2 – 4 cm thick which dip 15° towards 200° SSW. The beds are very highly cemented pale yellow (Munsell: 2.5Y8/4) well-sorted medium/fine sand. The unit thickens seaward to a maximum of 2.5 m, and thins slightly towards the landward end of the profile. The upper contact with Unit 3 is sharp and slightly truncates the beds of Unit 2. It is a first-order bounding surface.Unit 3 (535 – 815 cm) comprises several sets of low-angle topsets

4 – 5 cm thick which dip 5° towards 200° SSW, steepening up-dip to 10° towards 200° SSW. The beds are very highly cemented pale brown (Munsell: 10YR8/3) well-sorted medium/fine sand. Rhizoliths are very common throughout the unit, but they increase notably in size (to a maximum of 40 mm wide and 16 cm long) upward. The unit thickens towards the seaward end of the profile, and thins markedly landward.

Single bulk sediment samples were taken from Units 1, 2 and 3 for analysis in the laboratory. The results for these samples are presented in Section 5.2.

Profile 20:

Profile 20 contains six distinct units in a sequence almost 5 m high (Figures 5.42 & 5.43). These units include dolerite bedrock and both conglomerate and aeolianite sedimentary units. The base of the profile is 1.4 m below high tide level. The conglomerate units have a large lateral extent in all directions beyond the stack. Unit 1 (0 – 30 cm) is highly weathered and faulted dolerite bedrock which is exposed in varying thicknesses across a stretch of coastline on the western edge of the study area. Unit 2 rests unconformably on Unit 1. The weathered upper surface of the dolerite dips gently seaward (~160° SSE). Unit 2 (30 – 145 cm) is a set of low-angle bottomsets several centimetres in thickness which dip 10° towards 160° SSE. The beds are composed of well-sorted relatively fine medium sand which is pale white (Munsell: 2.5Y8/1). The unit thins rapidly seaward across the profile, eventually disappearing from view below sea level. The upper contact with Unit 3 is unconformable and sharp. It dips 10° towards 160° SSE, steepening rapidly to 20° towards 160° SSE on the landward end of the profile. Unit 3 (145 – 195 cm) is a bedded conglomeratic beachrock with well-rounded, moderately sorted sandstone and dolerite clasts ranging between 5 cm and 40 cm in length. The beds dip ~12° towards 160° SSE. The clasts are predominantly elongated and relatively flat and most are imbricated seaward (160° SSE). The matrix is very highly compacted and highly cemented light yellowish brown (Munsell: 2.5Y6/3) medium sand with rare coarse sand grains and granules. Lithic artefacts are commonly found within this deposit. The unit thickens seaward along the profile, reaching a maximum of 1.5 m. The upper contact with Unit 4 is a disconformity which truncates the beds at roughly 0° inclination.

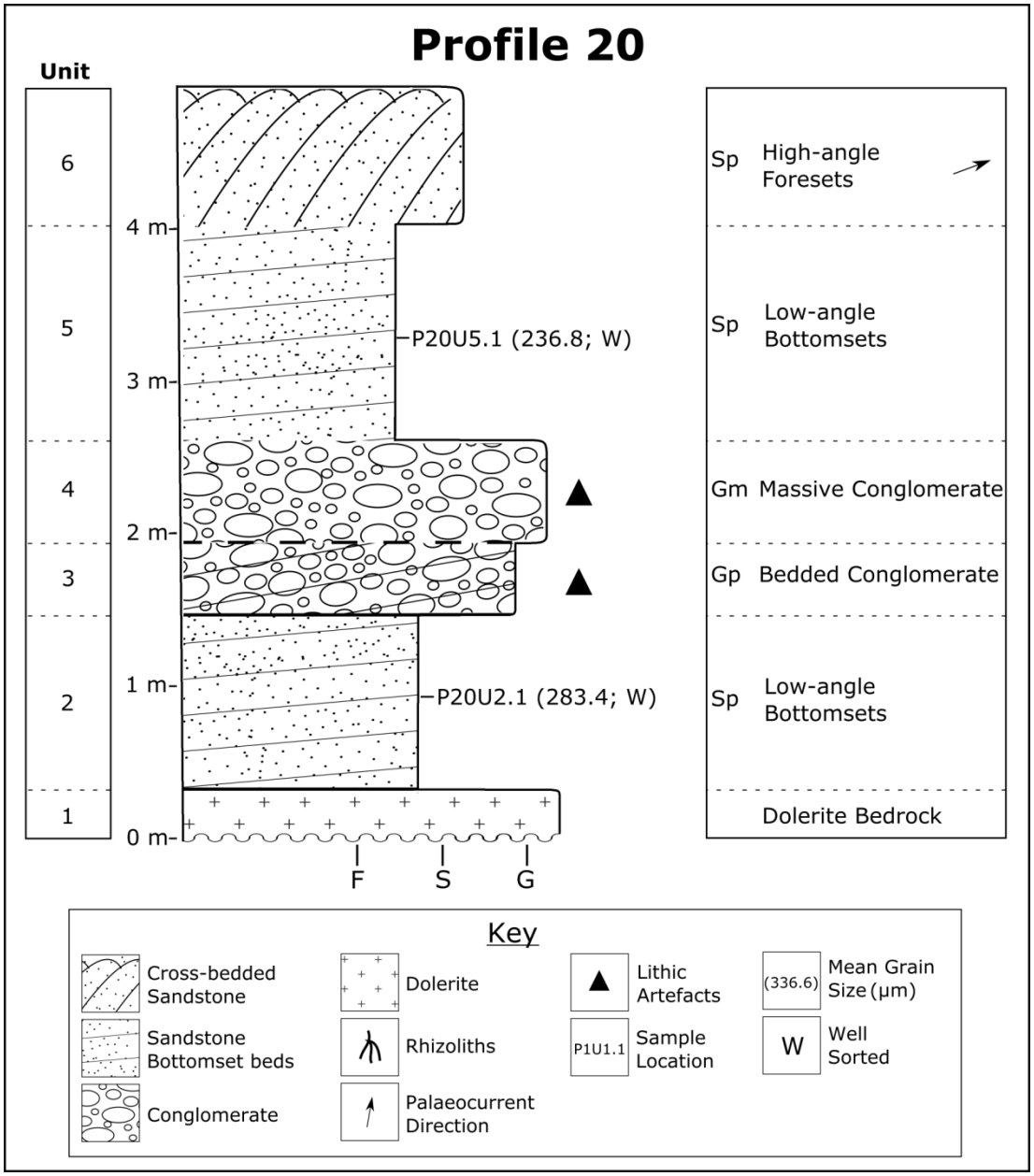


Figure 5.42. The logged sequence of Profile 20. The base of the exposure is 1.4 m below high tide level.

Unit 4 (195 – 260 cm) is massive shelly conglomerate with well sorted and well-rounded sandstone and dolerite clasts. The clasts range in maximum length from 20 cm to 90 cm. Both elongated and spherical forms are common. The matrix is very highly compacted and cemented pale brown (Munsell: 10YR8/2) medium sand with some coarse sand grains and granules. A number of lithic artefacts are present in the unit (see sub-section 5.1.4. for a more detailed description). The unit thins seaward, to a minimum of ~10 cm; it is 80 cm at its thickest point, on the landward

end of the profile. The upper contact with Unit 5 is conformable and fairly sharp, although there is some undulation due to the nature of the surface of Unit 4. Unit 5 (260 – 400 cm) is a set of low-angle bottomsets several centimetres thick which dip 10° towards 160° SSE. They steepen to around 15° towards 160° SSE on the seaward end of the profile. The beds are composed of highly cemented pale white (Munsell: 10YR8/1) well-sorted fine sand. Rhizoliths of a wide range of sizes (up to 3.5 cm in thickness and 17 cm in length) are common across the extent of the unit. The deposit is coated with a thick layer of calcrete across much of the profile. The unit is of fairly uniform thickness across the profile, with a maximum of 1.5 m. The upper contact with Unit 6 is conformable and quite sharp. Unit 6 (400 – 490 cm) is a single set of high-angle foresets 8 to 10 cm thick which dip 25° towards 070° ENE. The sediment is very highly cemented relatively coarse medium sand that is pale white (Munsell: 10YR8/1) in colour. The top of the unit is eroded and so the current thickness varies considerably. Unit 6 is only present across ~1.5 m at the landward end of the profile.

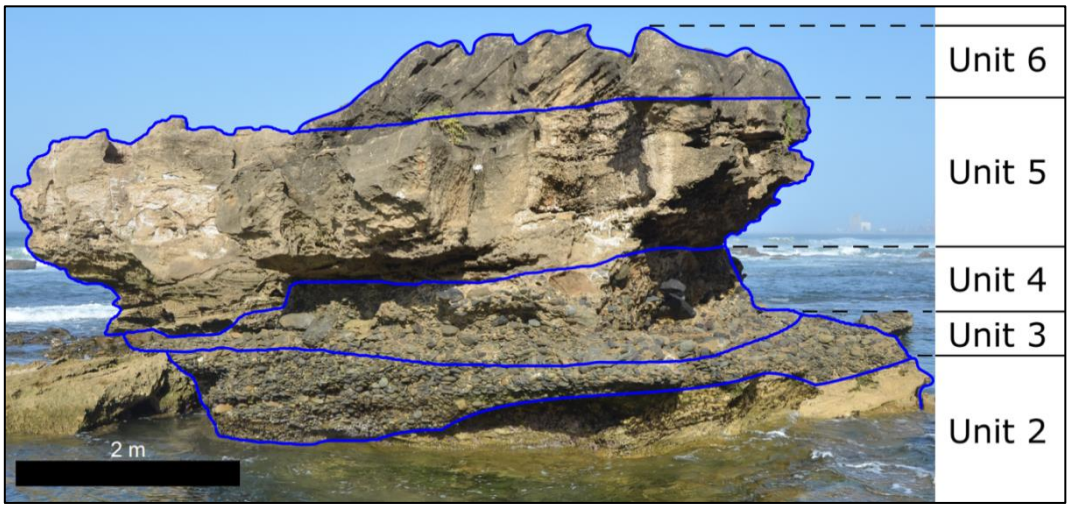


Figure 5.43. A photograph of Profile 20 with the units marked. Unit 1, the dolerite, is not visible as it is underwater.

Single bulk sediment samples for laboratory analysis were taken from Unit 2 and Unit 5. The results for these samples are presented in Section 5.2.

5.1.3. Artefact deposits

Lithic artefacts were found in a number of deposits across the study area during the foot survey (Figure 5.44; Table 5.2). The assemblages in these deposits are

generally either very small or distributed across large areas at very low densities. However, they supplement the previously reported occurrences of evidence for human presence in the area (Figure 5.44; Table 5.2). The artefacts in these deposits are all produced on dark grey/black fine-grained quartzite or on a darker hornfels. No quartzite or hornfels outcrops were identified within the study area during the foot survey. The archaeology and geomorphic and sedimentary context of each analysed artefactual deposit is described in turn below. The locations that have been reported before, with the exception of 'Bats Cave', are not discussed here.

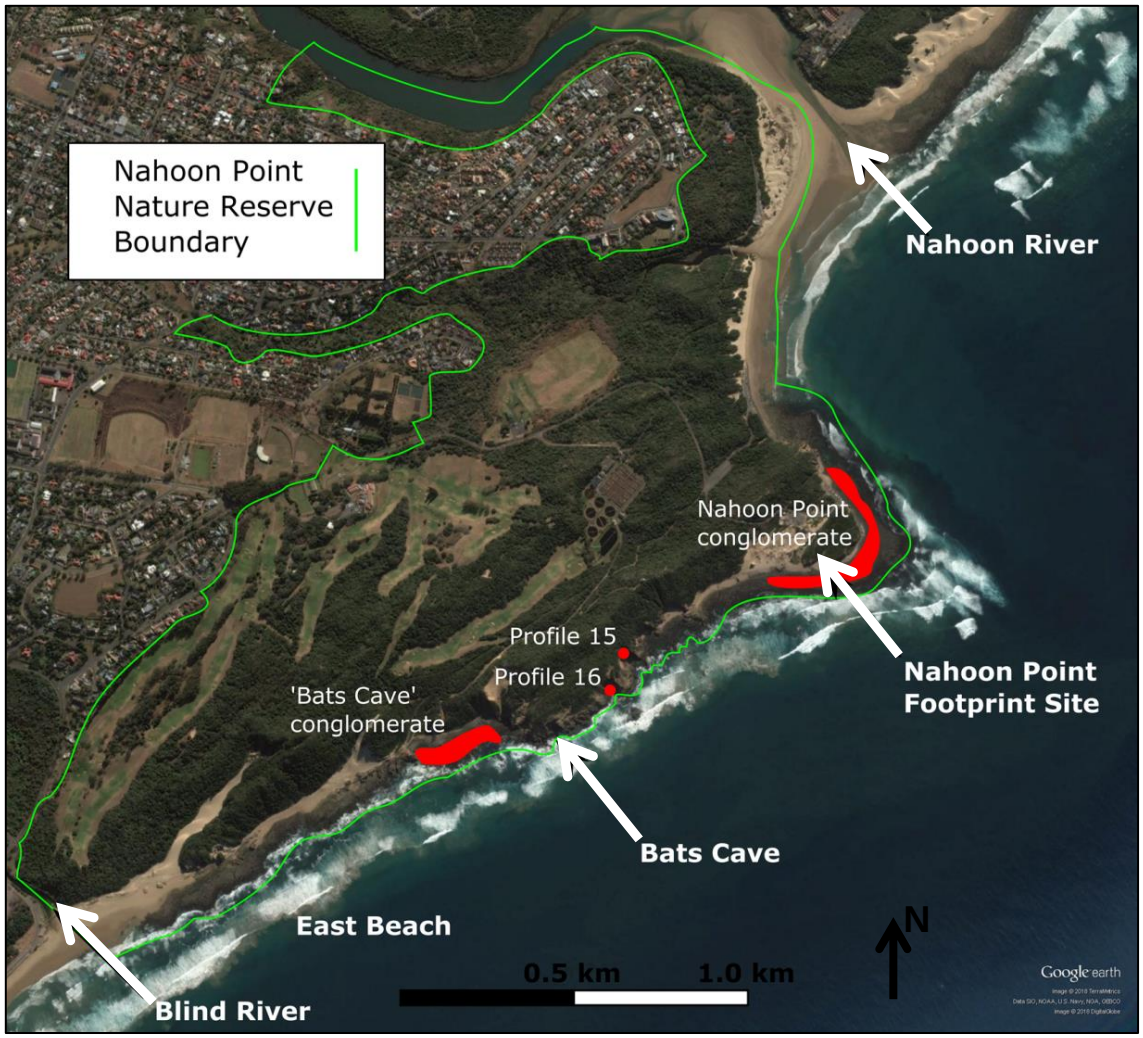


Figure 5.44. Map of the Nahoon Point Nature Reserve indicating the locations of artefact-bearing deposits discovered and/or recorded during the survey of the study area (in red) and several previously reported sites (white arrows) (Imagery: Google Earth, 23 July 2017). As discussed in the text, the artefacts from Profiles 5 and 7 are within the Nahoon Point conglomerate, while those from Profile 20 are within the 'Bats Cave' conglomerate.

Table 5.2. A summary of the stratigraphic position and sedimentary/geomorphic context of the previously-reported (marked with asterisks) and newly-discovered evidence for human presence within the study area during the Late Pleistocene.

Location	Profile; Unit	Context
*Nahoon Point Footprint Site	P1; U5	Aeolianite (Mountain 1966; Roberts 2008)
Nahoon Point	P5; U1 P7; U1	Conglomerate beachrock
Profile 15	P15; U6	Aeolianite
Profile 16	P16; U1	Aeolianite
Profile 16	P16; U2	Aeolianite – on raised marine bench at base of deposit
*'Bats Cave'	P20; U3 & 4	Conglomerate beachrock (Deacon 1966)
*East Beach	N/A	Shelly conglomerate beachrock (Jacobs & Roberts 2009)
*Blind River	N/A	Estuarine calcarenite and storm beach gravel (Wang *et al*. 2008)

Isolated lithic artefacts are relatively common, albeit at a low density, in the extensive conglomerate deposits around Nahoon Point (Figure 5.45). This conglomerate is present within Profile 5 and Profile 7 (Figures 5.11 & 5.17). The observed artefacts are cemented into or onto the sandstone matrix of the conglomerate. They are notably smaller (between 6 cm and 10 cm in length) than the natural clasts in the conglomerate (20 – 140 cm long) and are considerably less rounded. Surficial weathering of the artefacts is fairly limited given their exposure in the current intertidal zone. The artefacts observed in this deposit were all flakes and blades.

Two hornfels artefacts (a flake and a core) were found in an aeolianite block that had fallen from the near the base of Unit 6, Profile 15 (Figure 5.46). No other clasts were visible within the sandstone. The lithics were closely associated within the block. The block's original position was ~40 cm above the contact with Unit 5. The lithics are very fresh and display little sign of weathering. The flake is 6.5 cm long and the core has a maximum dimension of 8.1 cm.



Figure 5.45. A relatively well preserved blade photographed *in situ*, cemented to the conglomerate around Nahoon Point. This conglomerate was recorded in the lowermost units of Profiles 5 and 7. The scale is in centimetres.



Figure 5.46. The two artefacts discovered at Profile 15. The scale bar is 5 cm long.

Two small artefactual deposits were found within the aeolianite deposits of Profile 16. The first is a single hornfels lithic artefact which was found protruding from the

profile of Unit 1 (Figure 5.47A). As it is within the splash-zone, this artefact is highly weathered. The length of the artefact could not be measured.

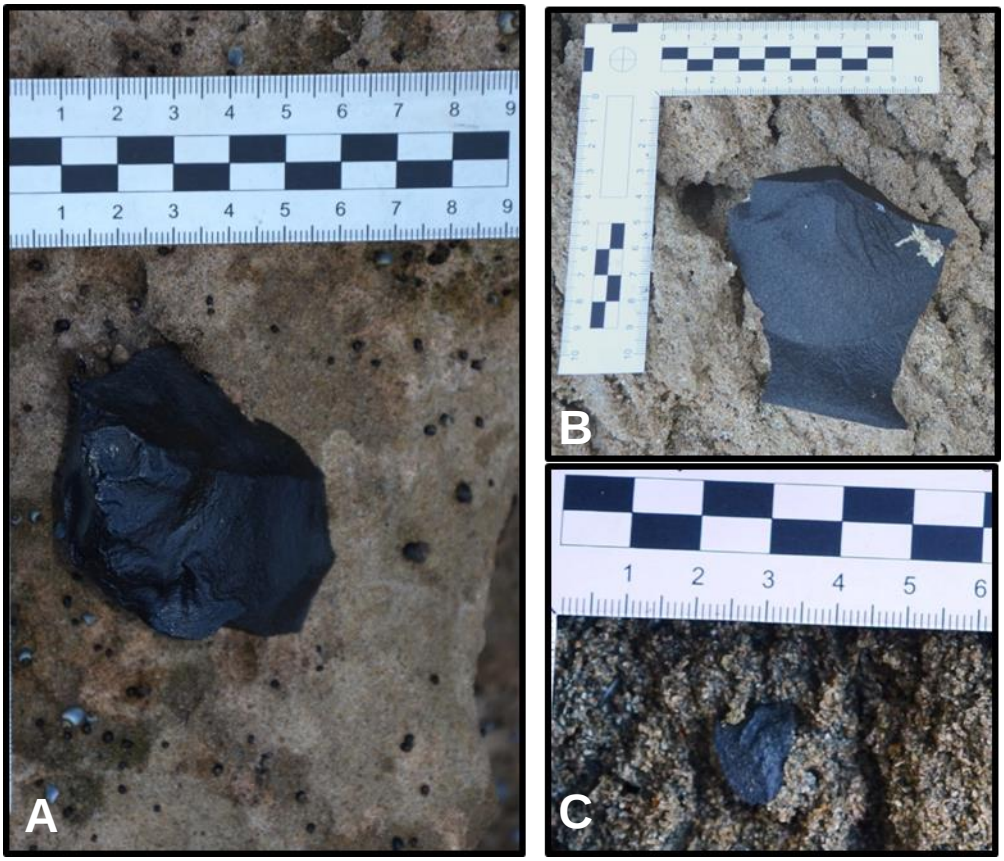


Figure 5.47. Examples of artefacts discovered in aeolianite units in Profile 16. A) the single lithic in Unit 1. B) relatively large overshot flake found at the contact between Unit 1 and Unit 2. C) small flake found at the contact between Unit 1 and Unit 2. All artefacts were photographed *in situ* within the aeolianite.

The second deposit within Profile 16 is a small assemblage (six artefacts) which was discovered at the contact between Unit 1 and Unit 2 (Figure 5.47B and C). The artefacts are all hornfels flakes, mostly ranging in size between <1 cm and 2 cm in length. The only one outside this size range is an overshot flake ~6 cm in maximum dimension (Figure 5.47B). This is a flake which, instead of terminating with a sharp edge, takes some of the bottom of the core with it when it is struck (Andrefsky 2005). The smaller flakes also appear to be knapping debris. All the artefacts are in fresh (un-weathered) condition. They are in close horizontal association (within an area of less than 1 m^2) and all appear to have been discarded on the same surface. The deposit lies between the raised bench that truncates Unit 1 and the base of the Unit 2 deposit

The richest artefact-bearing deposits in the study area are the conglomerates to the west of Bats Cave (Figure 5.48) that were previously reported by Hilary Deacon (1966). The artefact-bearing conglomerate deposits at Profile 20 are within this relatively large expanse of beachrock. Lithics are cemented into the sandstone matrix throughout the visible horizontal extent of the deposits in far greater concentrations than in the conglomerate around Nahoon Point. As at Nahoon Point, the lithics are considerably less weathered and generally smaller (measured range: 3 cm to 10 cm) than the natural clasts in the conglomerate (5 cm to 130 cm in length). The typologically-identifiable artefacts are all flakes and blades made on hornfels and (less commonly) quartzite. Artefacts are occasionally found in association with one another, unlike at Nahoon Point.

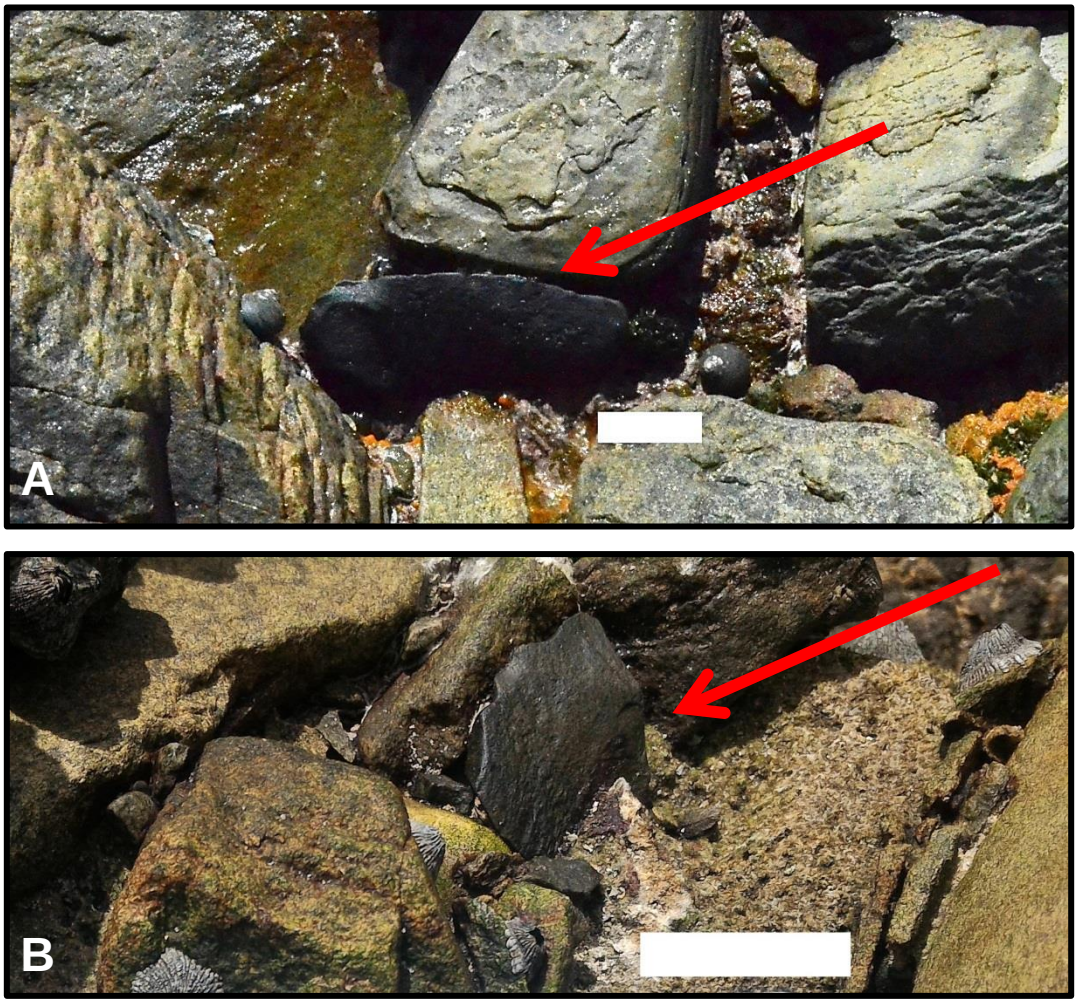


Figure 5.48. A blade (A) and a flake (B) (arrowed) photographed *in situ* within the conglomerate deposit near Bats Cave. The scale bars are 2 cm long in both photographs.

5.2. LABORATORY RESULTS

The data presented in this section are the results of the laboratory analysis of bulk samples and thin section samples. The various methods and techniques utilised for the analyses are detailed in Chapter 4: Section 4.2. The only laboratory results not presented here are those produced by the grain size analysis carried out on the 68 bulk samples with the Mastersizer 3000. These results were included in the sedimentary descriptions of the profiles (Section 5.1.2).

5.2.1. Density and Porosity

The density of the 68 bulk samples analysed ranged between 1.40 and 2.38 (Table 5.3). The mean density was 1.76 and the standard deviation was 0.22. The majority of samples (51) have densities between 1.5 and 2.0. The results show variation not only between units, but within units as well. There is no discernible correlation between the density values and the properties of the units that were recorded in the field such as the texture of the sediment, depositional structures, and the presence or absence of rhizoliths (Section 5.1.2.).

The measured porosity of the 68 bulk samples ranged widely from 4.2% to 46.8% (Table 5.3). Mean porosity was 28.6% and the standard deviation was 8.52%. The majority of the samples (57) had porosity ranging between 20.0% and 40.0%; a fairly broad range for the majority of samples. The variation both within and between units is even more noticeable than in the density values. As with the density, there is no indication of a predictable relationship between the properties of a unit recorded in the field and the porosity of the rock from that unit (Section 5.1.2.).

5.2.2. Carbonate content

Of the 68 bulk samples, carbonate (CO_3) content was determined for 67 samples (Table 5.3). Sample P1U5.3 was not analysed as not enough sediment was available to allow the completion of all laboratory analyses. Carbonate content ranged from 18.5% to 34.3% of the mass of the analysed samples. The mean carbonate content was 27.1%; the standard deviation of the results was 3.5%. One of the samples contained less than 20% carbonate, and only 16 samples had carbonate content of 30% or higher. Therefore, fifty of the samples had carbonate

content falling between 20% and 30%. The variability in carbonate values is fairly high both between units and within units.

Table 5.3. The porosity, density and carbonate content of the 68 bulk samples collected from the study area along with the means, standard deviations, and maximum and minimum values for each variable.

Sample	Porosity (%)	Relative Density	Carbonate (% Mass)
P1U1.1	42.8	1.50	31.0
P1U3.1	35.5	1.88	31.4
P1U5.1	24.2	1.56	25.5
P1U5.2	30.2	1.61	30.6
P1U5.3	28.8	1.70	NO DATA
P1U5.4	37.1	1.72	25.5
P1U5.5	28.4	1.65	26.0
P1U6.1	36.0	1.63	26.3
P1U7.1	37.8	1.64	29.4
P2U2.1	27.6	1.70	31.1
P2U4.1	24.3	1.73	30.2
P2U5.1	21.4	1.75	28.3
P2U5.2	25.5	1.87	28.8
P2U5.3	30.0	1.48	25.9
P2U5.4	30.8	2.14	26.0
P3U1.1	28.9	1.66	20.9
P3U2.1	37.1	1.83	23.1
P3U4.1	37.3	1.68	27.4
P3U5.1	30.9	1.66	29.8
P4U1.1	34.3	1.60	24.2
P4U2.1	25.8	1.46	25.0
P4U4.1	34.0	1.43	30.7
P4U6.1	8.7	2.20	29.9
P4U6.2	19.1	1.98	26.6
P4U7.1	14.0	2.07	23.3
P5U2.1	24.0	2.05	30.3
P5U4.1	39.0	1.94	28.0
P6U1.1	46.8	1.45	28.3
P6U1.2	32.5	1.57	33.2
P7U5.1	17.1	1.97	30.9
P8U1.1	26.3	1.77	33.6
P8U1.2	24.7	2.09	29.5
P9U1.1	25.4	1.89	31.5
P9U2.1	27.5	1.49	24.9
P9U3.1	32.8	1.83	32.0
P9U3.2	25.8	1.83	26.5

Table 5.3. continued

Sample	Porosity (%)	Relative Density	Carbonate (% Mass)
P10U2.1	15.6	2.16	24.1
P10U2.2	29.2	1.83	21.2
P10U3.1	21.6	1.82	18.5
P10U3.2	40.0	1.74	23.1
P11U1.1	39.1	1.56	25.0
P11U1.2	30.0	1.52	30.5
P12U3.1	42.0	1.67	24.2
P12U4.1	34.5	1.72	24.7
P12U5.1	25.4	2.01	25.3
P13U2.1	27.0	1.47	25.0
P13U2.2	38.8	1.52	31.8
P13U2.3	37.8	1.73	26.3
P14U1.1	8.6	2.31	25.8
P14U2.1	28.3	1.72	24.8
P14U4.1	28.2	1.70	27.0
P15U1.1	37.5	1.66	33.9
P15U2.1	18.2	1.82	27.8
P15U5.1	31.4	1.83	26.1
P15U6.1	33.0	1.40	24.0
P16U1.1	21.2	2.14	30.8
P16U1.2	26.8	1.95	25.8
P16U1.2	27.3	1.54	24.4
P18U3.1	38.0	1.74	34.3
P18U4.1	28.5	1.48	21.2
P18U4.2	33.0	1.58	28.0
P18U4.3	28.7	1.64	26.6
P18U4.4	28.6	1.64	26.5
P19U1.1	32.2	1.59	24.6
P19U2.1	30.0	1.68	23.5
P19U3.1	21.0	1.87	26.5
P20U2.1	9.3	1.95	23.6
P20U5.1	4.2	2.38	22.7
Mean	28.6%	1.76	27.1%
SD	8.5%	0.22	3.5%
Maximum	46.8%	2.38	34.3%
Minimum	4.2%	1.40	18.5%

There is no discernible relationship between the carbonate content and the density or the porosity of the samples (Table 5.3). Likewise, there is no indication of a

correlation between the macroscopic properties of the units that were noted in the field and the carbonate content of the samples from those units (Section 5.1.2.).

5.2.3. Thin section analysis

Oriented block samples were collected from Unit 5 of Profile 1 (P1U5.4) and Unit 5 of Profile 2 (P2U5.2). Sample P1U5.4 was taken from the bed in which the footprints were found. These units have almost identical lithologies and most of the differences between them are in terms of their depositional structures and degree of bioturbation by roots (Figures 5.2 & 5.5).

A single thin section was cut from each of these samples. The thin sections were cut parallel to the slopes of the respective sampled beds, rather than across the beds. Sample P1U5.4 included the entire vertical thickness of the thin bed that was sampled. Sample P2U5.2 sampled the lower three-quarters of the bed from which it was taken. As the thin section analysis (see Section 4.2.5) was largely comparative, the results for the samples are presented below in terms of the properties of both samples and the similarities and differences between them.

The sediment in both samples is composed of quartz grains, bioclasts, calcite, and clay minerals (Figures 5.49 & 5.50). The bioclasts are predominantly shell fragments, but some fairly complete foraminifera are present. The quartz and bioclastic grains are well-sorted and range in size from very fine sand to coarse sand. They are predominantly well rounded to very well rounded, although some more angular grains are also visible. The bioclasts are more commonly elongated in form than the quartz grains. There is no obvious organisation in the fabric of either sample.

Calcite is present in both samples in the form of crystals that were precipitated around and between quartz and bioclastic grains (Figures 5.49 & 5.50). It is found in three different morphological forms within these samples, namely: meniscus, rim, and pore-filling cements. Meniscus cement was not observed in P1U5.4, and is very rarely visible in P2U5.2. Rim cements are well developed in both samples, but especially so in P1U5.4. The grains are almost always fully coated (in this cross-

sectional view) with calcite. The thickness of the rim cement varies considerably within the samples.

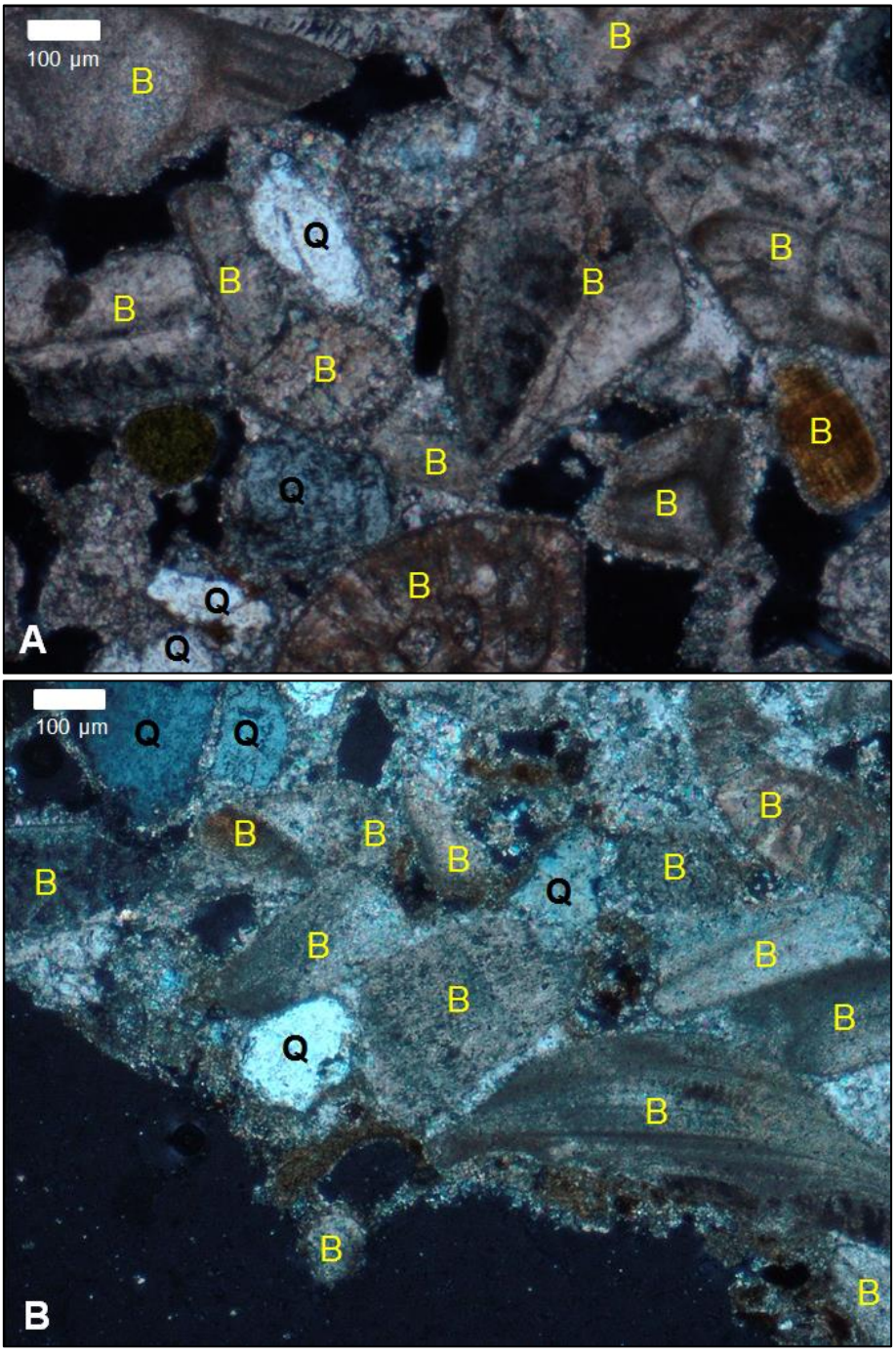


Figure 5.49. Photomicrographs of sample P1U5.4 taken under cross-polarised light. Bioclasts (B) and quartz grains (Q) are marked.

The occurrence and distribution of pore-filling cement is highly variable within the samples (Figures 5.49 & 5.50). Some pores are filled completely (or nearly completely) while others of similar size are entirely free of cement. Although this mix

of filled and unfilled pores is present in both samples, pore-filling cement is generally better developed in P1U5.4 than in P2U5.2.

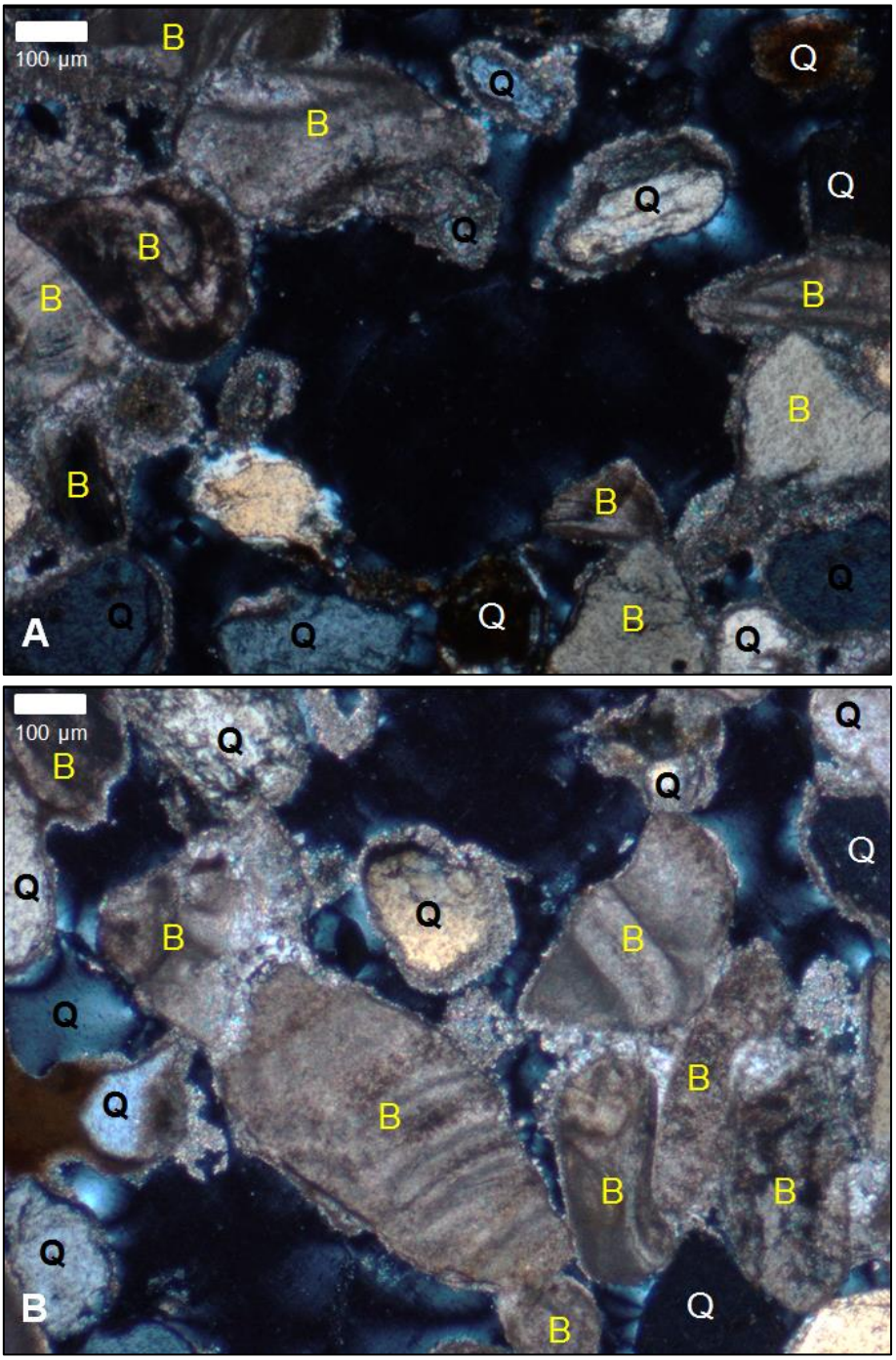


Figure 5.50. Photomicrographs of sample P2U5.2 taken under cross-polarised light. Bioclasts (B) and quartz grains (Q) are marked.

The cemented grains are either weakly or strongly cemented (Figures 5.49 & 5.50). Weakly cemented grains are connected by very little cement, often only a single ‘strand’. Strongly cemented grains are stuck together with considerably more

cement. Multiple grains may be connected together by this thick calcite matrix. Some grains are seemingly not cemented to any other grains. In all three cases, the rim cement on the grains is well developed. P1U5.4 is dominated by strongly cemented grains, while weakly cemented and non-cemented grains are very rare. P2U5.2 contains notably more weakly cemented and non-cemented grains than P1U5.4. However, strongly cemented grains are still very common The rim cements were precipitated in the form of elongated micro-sparite crystals. Away from the grains and into the filled pore space, the crystals become more equant in form and increase in size. The crystals generally have either an equigranular xenotopic fabric or an equigranular hypidiotipic fabric. With both fabrics, articulation between the crystals is fairly regular in form.

Both of the samples had carbonate content very near the mean of all the analysed samples (Table 5.3). Sample P1U5.4 was 25.5% carbonate, while sample P2U5.2 contained 28.8% carbonate. The only identified source of carbonate in the samples is calcium carbonate, which is present in the form of bioclasts and calcite cement.

Clay mineral particles are found in both samples within calcite cement. Both rim cement and pore-filling cement were found to contain clay (Figure 5.51). The clay was most often associated with rim cements. However, when it was found in filled pores, it was present in higher quantities than in the rim cements. Clay (in both of these cement types) was more common in P2U5.2 than in P1U5.4. In a number of cases, the clay minerals are present in the form of sand-sized grains which appear to have undergone significant alteration (Figure 5.51A).

5.2.4. Fourier Transform Infrared Analysis

The results of the Fourier Transform Infrared (FTIR) analysis were interpreted by Marine Wojcieszak of the Evolutionary Studies Institute at the University of the Witwatersrand. Of the multiple spectra obtained for each sample, the spectrum with the best signal to noise ratio was chosen for interpretation (M. Wojcieszak pers. comm. 2017). The spectra for the four analysed samples are very similar, indicating very limited mineralogical variation (Figure 5.52). Only calcite, quartz and a small amount of clay minerals were identified within the samples. Aragonite was not

detected. The dominant constituent of all four samples is calcite. This confirms the composition determined through the analysis of the thin section samples (Section 5.2.3). Based on the lack of aragonite in the FTIR spectra, the bioclasts identified in the thin section samples (Figures 5.49 & 5.50) must have undergone chemical alteration from aragonite to calcite without losing their physical form.

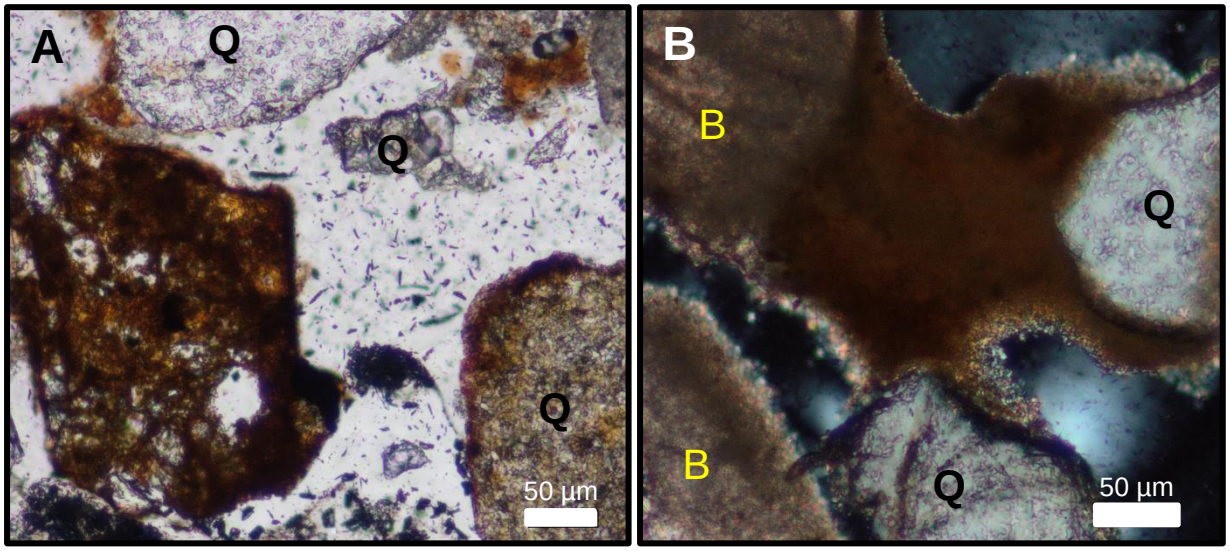


Figure 5.51. Concentrations of clay (the brown to reddish-brown in these images) within both rim cements and pore-filling cements and in the form of obviously altered sand-sized grains: A) sample P1U5.4. B) sample P2U5.2 under cross-polarised light. Bioclasts (B) and quartz grains (Q) are marked. Note the altered sand-sized grain to the left of image A.

The FTIR results indicate that all of the carbonate within the samples is in the form of calcite (one of the forms of calcium carbonate). The carbonate content of the four samples - P1U3.1 (31.4%), P1U5.5 (26.0%), P1U6.1 (26.3%) and P2U5.3 (25.9%) - was fairly similar. The units from which these samples were taken differ in terms of depositional structures and bioturbation; P1U3 is a deposit of low-angle toesets/foresets, P1U5 is a deposit of high-angle foresets, P1U6 comprises high-angle laminated foresets, and P2U5 is a deposit of heavily-bioturbated (rhizoliths) low-angle foresets (Figures 5.2 & 5.5). However, they are very similar in lithology. Therefore, it is not surprising that the FTIR results are so consistent between the samples.

Although only four of the 68 bulk samples were analysed with FTIR, the considerable similarity in the lithology of the aeolianite across the study area (see Section 5.1.2.)

suggests that the FTIR results can be applied (with due caution) to understanding the composition of all the recorded aeolianite deposits. The variation in carbonate content (Table 5.3) - and the inferred variation in calcium carbonate content - across the 68 samples indicates differences in the proportions of mineral components between samples. However, based on the similarities observed in the field, it is most likely that there is little to no difference in what components are present despite variation in their proportions.

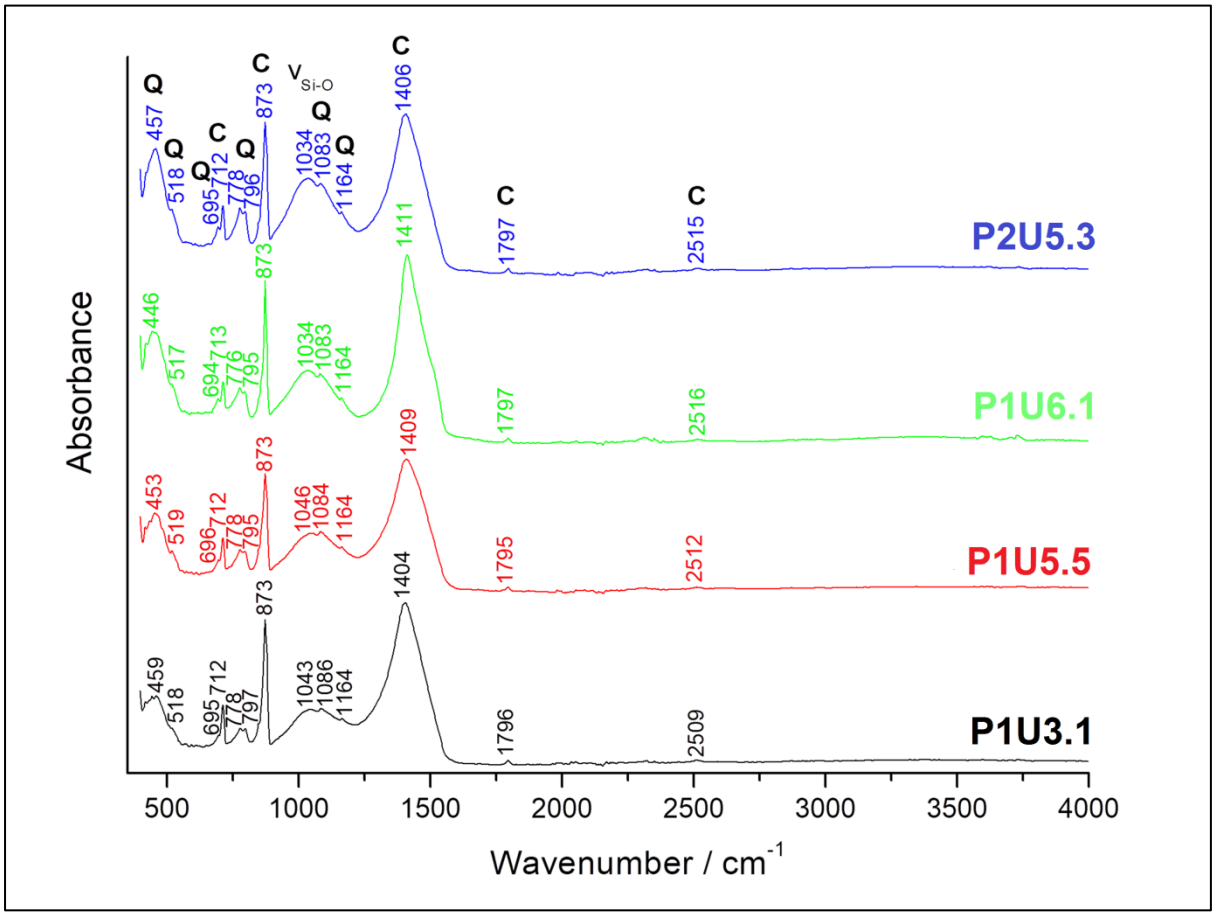


Figure 5.52. The ATR-FTIR spectra for the four analysed samples (figure courtesy of M. Wojcieszak). On the spectra, the letter 'C' indicates peaks associated with calcite, the letter 'Q' denotes peaks attributed to quartz, and 'V_{Si-O}' marks the stretching vibrations of Si-O bonds, interpreted as showing the presence of clay.

6. DISCUSSION

The ultimate goal of this project was to reconstruct the physical environmental conditions at Nahoon Point during Early Marine Isotope Stage 5. The results of field and laboratory analyses (presented in Chapter 5) are discussed here in order to achieve this goal. The chapter is divided into six sections. The stratigraphic sequence developed for the study area will be considered in Section 6.1. In Section 6.2, the aeolian sedimentary and geomorphic data collected for this study are interpreted to reconstruct the landscape in the study area during the phases of aeolian deposition. The direction of palaeo-winds is considered in Section 6.3. Section 6.4 will be a discussion of the processes by which the various deposits in the study area were cemented. The evidence for past sea levels is discussed in Section 6.5. Finally, in Section 6.6, the evidence for human occupation of the study area is considered in the context of the reconstructed palaeoenvironments and the archaeological record of Early MIS 5.

6.1. STRATIGRAPHY

In this section, a stratigraphic sequence for the logged profiles is developed based on the field results. The sedimentary facies in the sequence are discussed in the second sub-section. Finally, the sequence is compared to the stratigraphic model previously developed for the area in the third sub-section.

6.1.1. Stratigraphic sequence

Stratigraphic correlation between logged profiles was largely achieved by tracking unconformities between the profiles across exposures. Bounding surfaces separating distinct aeolian deposits were present within almost all of the profiles in the study area. First, second and third order bounding surfaces and supersurfaces were all identified (Brookfield 1977; Kocurek 1988, 1991).

Most of the bounding surfaces appear to be the result of relatively localised processes. However, a major unconformity/disconformity in the aeolianite deposits could be followed from Profile 19 through to Profile 12 (Figure 6.1). This feature is a supersurface, indicative of a significant break in aeolian deposition (Kocurek 1991). In some parts of this area, this feature truncates the bedding of underlying aeolian

deposits. It is often part of, or directly associated with, a raised marine bench that has an elevation ranging between 3.8 m and 7 m above high tide level.

Similar unconformities/disconformities were visible in all of the logged profiles around Nahoon Point except for Profiles 5 and 7. These are also supersurfaces, representing a significant hiatus in aeolian deposition at these locations. Due to the relatively discontinuous nature of the aeolianite deposits in this part of the study area, it was not possible to directly track these unconformities between all the logged profiles in which they appear (Figure 6.1). However, it was possible to track them across individual exposures (e.g. between Profiles 1 and 2, and around the Lookout Point).

As the supersurfaces within the aeolianite exposures around Nahoon Point and Lookout Point and within the large exposure between Profile 12 and Profile 19 could be tracked within each of the exposures and are the only unconformities of this nature in the profiles, it is reasonable to argue that they represent the same event despite the lack of continuous exposure. This interpretation is supported by the fact that these surfaces are all part of or clearly associated with raised marine benches with elevations between 4 m and 6.5 m above high tide level. Therefore, it seems that this can be viewed as a single feature, representative of one event. Thus, it can be used as a stratigraphic marker within the profiles where it is present (Figure 6.1).

Marine benches cut into aeolianite are also present within Profile 20 (in a small bay to the west of Bats Cave) and the profile logged from cliff exposures at East Beach by Jacobs & Roberts (2009). These features are overlain by marine conglomerates in both locations. These are, in turn, covered by younger aeolianite deposits (Figures 2.6, 5.41 & 5.42). The contacts between the conglomerates and the overlying aeolianites are conformable, suggesting fairly rapid burial of the marine deposits. No benches or other intertidal erosional features (other than obviously recent ones), or any unconformities of any kind are present in the younger aeolianite at these locations. Therefore, Profile 20 and the East Beach profile each record a single sea-level highstand event.

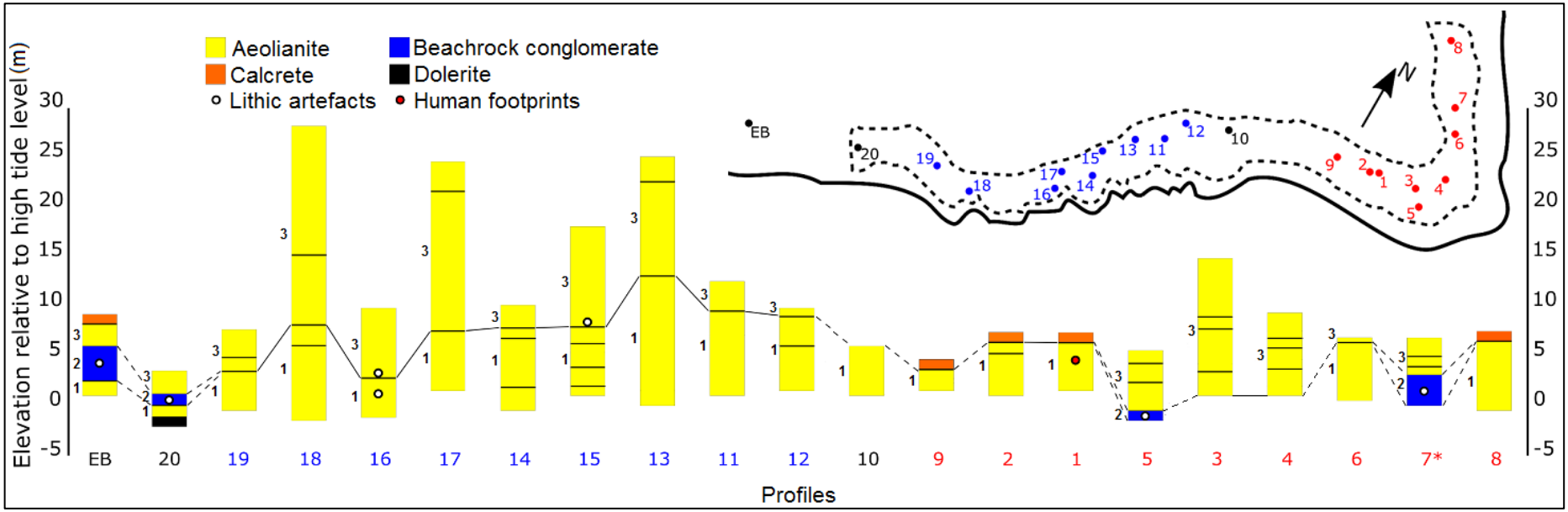


Figure 6.1. Stratigraphic correlation of the logged profiles (which have been simplified in this diagram) across the study area. Profiles marked in red are on Nahoon Point and those indicated in blue are within the continuous exposure. Note that the published profile for the East Beach (EB) sample site, recorded by Jacobs & Roberts (2009), has been included. The major unconformity/disconformity is indicated with solid lines where it could be tracked directly and with dashed lines where the correlation was inferred (see the text for discussion). Phase 1 includes the aeolianite below the major unconformity/disconformity, while the aeolianites of Phase 3 lie on top of the unconformity. The beachrock conglomerates of Phase 2 are correlated with the hiatus between Phase 1 and Phase 3, which is marked by the major unconformity. The younger marine and aeolian deposits (of Holocene age) are not included in this diagram. Note that the calcrete and dolerite units and the beachrock in Profile 5 have been thickened to make them visible in the diagram. Profile 7 (indicated with an asterisk) has been doubled in height for the same reason. The locations of the profiles within the reserve (solid line) and within the study area (dashed line) are indicated in the inset map.

In Profile 5 and Profile 7, both at Nahoon Point, marine conglomerate deposits are overlain by aeolianites (Figures 5.11, 5.12, 5.16 & 5.17). This conglomerate, although somewhat discontinuous due to erosion, is found all the way around Nahoon Point. At neither Profile 5 nor Profile 7 is it possible to determine what material the conglomerates were deposited onto. However, in some locations within the intertidal zone at Nahoon Point the beachrock was found to lie unconformably on highly eroded remnants of aeolianite deposits, and some blocks of aeolianite were incorporated into the beachrock (Figure 5.13). Conglomerate was deposited against the exposure from which Profile 9 was logged. This evidence indicates that the beachrock conglomerate on Nahoon Point was deposited between two periods of aeolianite formation. However, it is unclear how long the period between the formation of the older aeolianite and the deposition of the beachrock was. Therefore, this cannot be used uncritically as an age or environmental constraint.

The aeolianites at Profiles 3, 4, 5 and 7 contain a number of unconformities (Figures 5.11, 5.12, 5.16 & 5.17). However, these all constitute first order bounding surfaces and are not indicative of a significant hiatus in aeolian deposition (Kocurek 1988, 1991). Raised benches and other evidence of erosion in the intertidal zone are absent from these profiles, except for a notch and associated coquinite deposit in Profile 5 which is of fairly recent (Holocene) age. Therefore, the sequences on Nahoon Point, like those of Profile 20 and East Beach, indicate a single sea-level highstand bracketed by the formation of aeolianite deposits which could therefore be either transgressive or regressive.

The stratigraphy of the sequences where marine and aeolian deposits are preserved, and the marine origin of both the conglomerate deposits and the raised benches, indicate that the formation of the conglomerates around Nahoon Point and to the west of Bats Cave can be correlated stratigraphically with the hiatus in aeolian deposition evidenced by the major unconformity/disconformity in the aeolianites. Therefore, the deposits in the logged profiles can be placed into three stratigraphic groupings (Figures 6.1, 6.2 & 6.3).

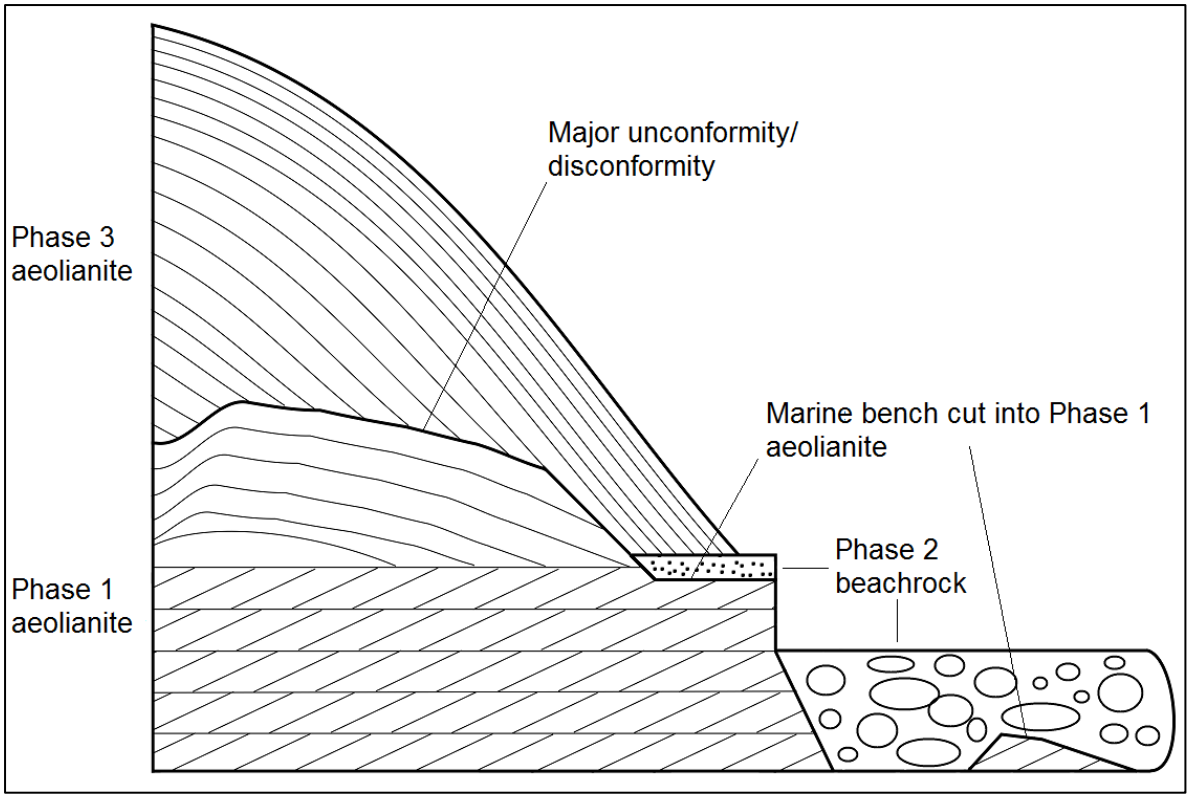


Figure 6.2. A generalised stratigraphic cross-section of the aeolianite and beachrock deposits in the study area. The sea is to the right and the land to the left of the diagram. Note the position of the major unconformity/disconformity between the Phase 1 and 3 aeolianites and the marine benches cut into the Phase 1 deposits.

The first grouping, Phase 1, includes all aeolianite deposits which stratigraphically underlie the major unconformity/disconformity (Figure 6.2). It is present in all the logged profiles except Profiles 3, 4, 5 and 7. Three facies, all indicative of aeolian depositional environments, were recognised (Figure 6.3). The marine conglomerate deposits within Profiles 5, 7 and 20 and the East Beach profile of Jacobs & Roberts (2009) are placed into Phase 2, which also encompasses the formation of the raised benches across the study area (Figure 6.2). Three beachrock facies were identified within these deposits (Figure 6.3). Finally, the aeolianite deposits that stratigraphically overlie the major unconformity/disconformity and the marine deposits are grouped into Phase 3 (Figure 6.2). Deposits from this phase are found within all the logged profiles except for Profiles 1, 2, 8, 9 and 10. Four aeolian facies (including the three identified within Phase 1) were recognised in this phase (Figure 6.3).

The unconsolidated sands of the Schelm Hoek Formation that unconformably overlie the aeolianite are excluded from this study as they date to the Holocene (Tinley 1985; Le Roux 1989 a, b; Illenberger 1992; Roberts *et al*. 2006). The shelly marine conglomerate in erosional notches in the aeolianite of Profiles 5 and 8 is also excluded (Figures 5.11, 5.12, 5.18 and 5.19). As these deposits post-date Phase 3 and were formed during a sea level higher than the present, they most likely date to the mid-Holocene highstand (Miller *et al*. 1993; Bateman *et al*. 2004).

As described in Section 5.1.2, calcretes cap the aeolianite in a number of locations in the study area (see Figure 6.1 for their distribution). Calcretes form during periods of limited deposition and landscape stability, and generally date to relatively cool periods along South Africa's coastline (Goudie 1973; Watts 1980; Butzer 2004; Wright 2007; Roberts *et al*. 2009, 2014). Therefore, the calcrete in the study area records conditions during a period some time after the formation of the aeolianites. As these rocks clearly postdate Early MIS 5 (the focus of this project) they will not be considered in this chapter. Future work on the area may include them if they can be dated to an acceptable degree of accuracy.

6.1.2. Sedimentary facies

The sediment in the deposits of all the aeolianite facies (in both Phase 1 and Phase 3) in the study area is composed predominantly of shell fragments (and other bioclasts) and rounded to well-rounded quartz grains (Figures 5.49 – 5.51). Therefore, beach sand is the most likely source of sediment for the aeolianite deposits. Similar composition has been reported previously for Nahoon Formation aeolianites in the study area and across the wider known range of the formation (Mountain 1966; Le Roux 1989a, b; Roberts 2008; Jacobs & Roberts 2009; Roberts *et al*. 2014). Some clay minerals were observed in thin section (Section 5.2.3) and detected using FTIR (Section 5.2.4) and clay-sized grains were present in many of the particle size distributions. These are most likely the product of the alteration of proportionally rare grains of dolerite within the sediments during the diagenesis of the deposits.

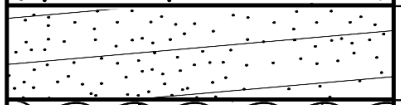
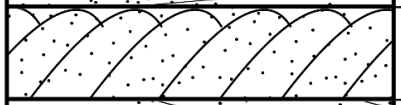
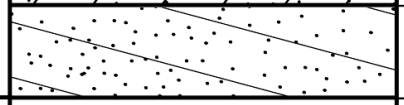
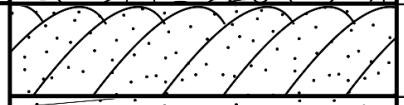
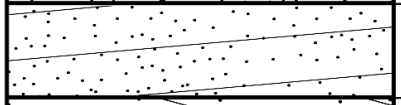
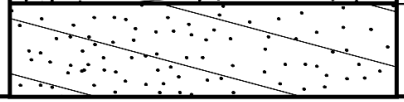
Phase		Facies	Environment and Process of Deposition
3		VII: Massive bioturbated aeolianite	Environment and specific aeolian depositional process unknown
		III: Low-angle bedding	Grainfall and wind-ripple deposition on interdunes and toes of dune slopes, and as sand sheets
		I: High-angle foresets	Grainflow, grainfall and wind-ripple deposition on leeward dune slopes
		II: Topsets	Grain creep deposition on windward dune slopes
2		VI: Massive shelly conglomerate	Combination of swash and backwash in intertidal zone
		V: Massive conglomerate	Deposition of larger clasts in intertidal zone by strong waves;landward transport of smaller clasts by weaker waves
		IV: Low-angle bedded conglomerate	Deposition by high energy waves in supratidal zone or uppermost intertidal zone; selective downslope removal of large and spherical clasts by gravity and backwash
1		I: High-angle foresets	Grainflow, grainfall and wind-ripple deposition on leeward dune slopes
		III: Low-angle bedding	Grainfall and wind-ripple deposition on interdunes and toes of dune slopes, and as sand sheets
		II: Topsets	Grain creep deposition on windward dune slopes

Figure 6.3. The facies identified in the three depositional phases within the profiles at the study area. Note that the stratigraphic ordering of the Phase 1 and 3 deposits varies between profiles. Each facies is described and discussed in detail in the text.

Phase 1:

Three aeolian facies were identified within the Phase 1 deposits, and named as follows: Facies I High-angle foresets; Facies II Topsets; Facies III Low-angle bedding. The properties of these facies are described below and summarised in Figure 6.3.

Facies I (High-angle foresets) deposits within Phase 1 were found in 11 of the 20 logged profiles, namely Profiles 1, 2, 6, 8, 9, 11, 12, 13, 15, 18 and 19. Steeply-dipping cross-bedded foresets dominate, but lower-angle toesets, which steepen into the foresets, are also common. Deposits range in thickness from 0.95 m to 12 m. The beds are mainly planar and concave-up, although rare convex-up bedding was observed. There is considerable variation in the thickness of lamination and bedding within and between deposits. This facies is the product of deposition on leeward dune slopes by the processes of grainflow, grainfall and wind-ripple deposition (Hunter 1977, 1981; Fryberger *et al*. 1979; Kocurek & Dott 1981; Kocurek 1991; Roberts *et al*. 2008, 2009, 2014; Bateman *et al*. 2011). The occurrence of reactivation surfaces and the density of rhizoliths vary considerably between and within deposits.

Deformed bedding is common within Facies I deposits at the Footprint Site on Nahoon Point (Profiles 1 and 2). These features have previously been attributed to slumping caused by foreset avalanching (Mountain 1966; Le Roux 1989a, b; Roberts 2008). However, the specific form of these features (see Figure 5.4) is not consistent with published descriptions or illustrations of the deformations or disturbances typically produced by avalanching, or by any non-biological deformational process common in aeolian sands (McKee *et al*. 1971; McKee & Bigarella 1972; Doe & Dott 1980; Allen 1982; Horowitz 1982; Pye 1983; Rossetti 1999). Instead, these features share many similarities with published examples of vertebrate tracks exposed in cross-section (Figure 6.4). These include the presence of an imprint with fairly straight sides, deformation of laminae beneath the imprint (the undertracks), curved laminae above and filling the imprint (overtracks), and deformed and/or truncated laminae around the imprint (Loope 1986; Allen 1989, 1997; Lockley 1991; Lea 1996;

Fornos *et al*. 2002; Milan & Bromley 2006; Milan *et al*. 2007, 2015; Roberts *et al*. 2008; Helm *et al*. 2018b, 2019).

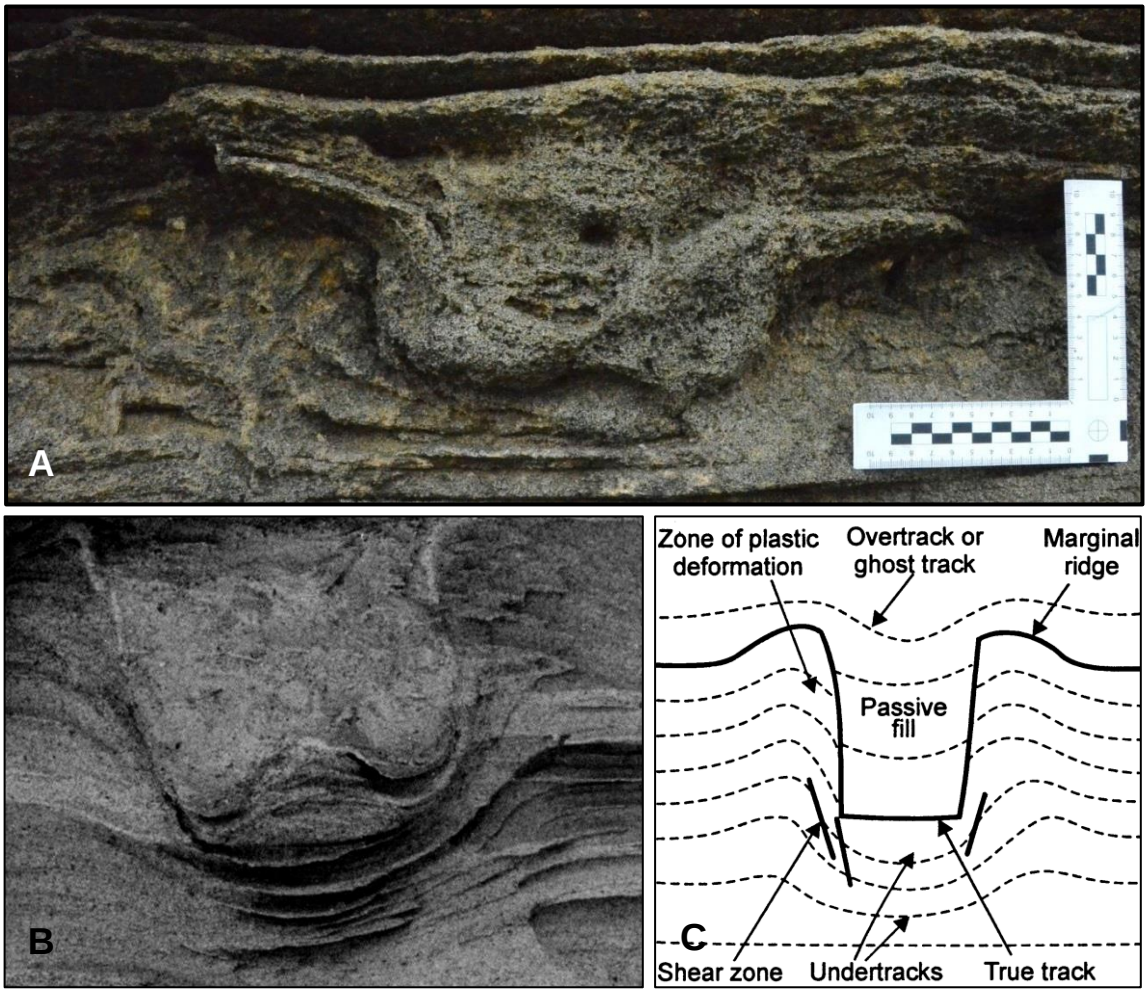


Figure 6.4. Comparison between a track observed at Nahoon Point and published real-world and theoretical examples of similar tracks. A: cross-section of a track preserved in the aeolianite at the Footprint Site. B: photograph of a naturally-produced cross-section through an ungulate track preserved in Holocene aeolian deposits in the Nebraska Sand Hills (Loope 1986). C: theoretical cross-section of an animal track and associated sediment deformation in a stratified deposit (Fornos *et al*. 2002).

The range of sizes and forms suggest that these features were made by a number of different vertebrate species. Without more research, it is difficult to make meaningful taxonomic assessments. However, a number of imprints have two lobes (see Figure 6.4) which are consistent with hoofprints, thus indicating that some of the tracks were produced by ungulates (Loope 1986; Lea 1996; Fornos *et al*. 2002; Milan *et al*. 2007). Future research can provide a better indication of the taxa that are represented.

Facies II (Topsets) deposits dating to Phase 1 were found within Profiles 9, 10, 11, 12, 14 and 17. They range in thickness between 1.5 m and 6 m. In all cases, except at Profile 9, they are the basal unit/s in the exposed local sequences. This facies is characterised by low-angle topset beds and a minority of steeper topsets. The beds are predominantly planar but convex-up tangential beds were also observed. These topsets, which represent the windward slopes of palaeo-dunes, are supercritically-climbing translatent strata formed through grain creep deposition (Hunter 1977, 1981; Kocurek 1991). No reactivation surfaces were observed within the deposits, although they are often truncated by unconformities and overlain by other aeolianite facies. However, smaller formsets are present on the surfaces of some topsets in one case (Profile 10). In some cases, where dune crests are preserved, the topsets are observed to dip down into foresets of Facies I (Profiles 9, 11 and 12).

Facies III (Low-angle bedding) deposits within Phase 1 were observed in Profiles 9, 14, 15, 16 and 20. The facies is characterised by low-angle bedding which is predominantly planar, but often convex-up. The deposits range between 0.45 m and 4.90 m in thickness. Bedding thickness varies considerably, up to a maximum of 50 cm. This facies was formed through the processes of grainfall and wind-ripple deposition; the low bedding angles rule out grainflow as a contributing depositional process (Hunter 1977, 1981; Kocurek 1991; Caputo 1995; Roberts *et al*. 2008, 2009, 2014; Bateman *et al*. 2011). These beds were deposited in several different environments. Some (e.g. Profiles 9 and 20) formed as sand sheets with no known relationship to contemporary dune deposits (Figures 5.21 & 5.43). The other deposits formed in relatively flat interdune areas and on the toes of both windward (Facies II) and leeward (Facies I) dune slope deposits (Figures 5.31, 5.33 & 5.35). In Profile 15, the Facies III deposits alternate vertically with dune deposits that periodically over-ran the interdune area (Figure 5.33).

Phase 2:

Beachrock conglomerate deposits attributed to Phase 2 are divided into three facies which are indicative of different depositional environments and processes. They are named as follows: Facies IV Low-angle bedded conglomerate; Facies V Massive

conglomerate; Facies VI Massive shelly conglomerate. The properties of these facies are described below and summarised in Figure 6.3.

Facies IV (Low-angle bedded conglomerate) was recorded within Unit 3 of Profile 20 (Figures 5.42 & 5.43). As it was only found in one location, the lateral extent of its deposition is unknown, as is any lateral variation in its properties that may have existed. The tabular bedding, which dips seaward at a low angle, is indicative of deposition either in the upper intertidal zone or in the supratidal zone (Bezerra *et al*., 2003; Mauz *et al*. 2015). Modern gravel beach sediments with similar properties (dominated by relatively small, flat, elongated and imbricated clasts) are generally found a little above mean high water (Bluck 1967, 1999, 2011; Oak 1984; Williams & Caldwell 1988; Postma & Nemec 1990; Haslett & Curr 2001). Therefore, this facies was deposited within the supratidal zone or within the uppermost intertidal zone. Gravel deposits in this part of the tidal frame form through deposition of clasts by high energy waves during storms and then subsequent selective downslope removal of large and spherical clasts by gravity and backwash (Bluck 1967, 1999, 2011; Postma & Nemec 1990; Haslett & Curr 2001).

Facies V (Massive conglomerate) was recorded in Unit 1 of Profile 5, Unit 1 of Profile 7 and Unit 4 of Profile 20 (Figures 5.11, 5.12, 5.16, 5.17, 5.42 & 5.43). Clast size varies across the lateral extent of the clast-supported deposits, suggesting some spatial variation in depositional energy. The very large size (more than a metre in length) of some of the boulders suggests that storm waves likely played a role in the formation of some parts of the deposits. The properties of the clasts in the deposit – large (most of boulder size), moderately to well-sorted, rounded to well-rounded and both spherical and elongated – are most similar to beachface deposits of modern boulder and cobble beaches (Bluck 1967, 1999, 2011; Oak 1984; Williams & Caldwell 1988; Postma & Nemec 1990; Haslett & Curr 2001). Thus, these deposits were formed within the intertidal zone by the deposition of larger clasts by strong waves (particularly storm waves) and the selective landward transport of smaller clasts by weaker waves (Bluck 1967, 1999, 2011; Oak 1984; Williams & Caldwell 1988; Postma & Nemec 1990; Cooper & Flores 1991; Mauz *et al*. 2015). As a result, beachface deposits like these have coarser texture seaward (further down the

intertidal zone) and finer texture landward (further up the intertidal zone) (Bluck 1967, 1999, 2011; Oak 1984; Williams & Caldwell 1988; Postma & Nemec 1990; Haslett & Curr 2001; Cooper *et al*. 2017). Therefore, inverse grading of clasts at Profiles 5 and 7 may suggest landward migration of the intertidal zone (likely due to sea level rise) during the formation of these deposits (Postma & Nemec 1990; Haslett & Curr 2001). The notably smaller clasts in the deposit at Profile 20 may indicate either a lower energy system than that on Nahoon Point, or deposition higher up on the beachface.

Facies VI (massive shelly conglomerate) was recorded in Unit 2 of Profile 7 (Figures 5.16 & 5.17), and reported at East Beach by Jacobs & Roberts (2009). The sediment is relatively fine-grained (up to pebble-sized) and matrix-supported. The thickness of these deposits is extremely variable, from 20 cm thick at Profile 7 to ~3.5 m thick at East Beach. The texture of the deposits (sandy with rare pebbles) indicates that this facies formed under a significantly lower energy regime than Facies IV and V. The properties of these deposits are broadly similar to several beachrock deposits on the KwaZulu Natal coast which have been interpreted as forming within the intertidal zone through a combination of the effects of swash and backwash (Cooper & Flores 1991; Cawthra & Uken 2012; Kelly *et al*. 2014). The lack of bedding structures rules out a more precise determination of where within the intertidal zone these deposits formed, but it is clear that they did form within this zone.

Phase 3:

Phase 3 aeolianite deposits are not as widespread as those from Phase 1 (Figure 6.1). Four distinct aeolian facies were identified, including one not observed in Phase 1. The facies are named as follows: Facies I High-angle foresets; Facies II Topsets; Facies III Low-angle bedding; Facies VII Massive bioturbated aeolianite. The properties of these facies are described below and summarised in Figure 6.3.

Facies I (High-angle foresets) deposits are considerably rarer in Phase 3 than in Phase 1. They were found in Profiles 3, 4, 5, 7, 15, 17, 18 and 20. This facies is characterised by steeply-dipping cross-bedded foresets and occasionally, lower-angle toesets. Deposits range in thickness from 1.25 m to 20 m. The beds are mainly

planar but some concave-up beds were observed. There is considerable variation in the thickness of lamination and bedding within and between deposits. The facies is the product of deposition on leeward dune slopes by the processes of grainflow, grainfall and wind-ripple deposition (Hunter 1977, 1981; Fryberger *et al*. 1979; Kocurek & Dott 1981; Kocurek 1991; Roberts *et al*. 2008, 2009, 2014; Bateman *et al*. 2011).

Facies II (Topsets) is characterised by high-angle planar topset beds. Phase 3 deposits of this type were found within Profiles 13, 14, 16 and 19; none were observed on Nahoon Point. Deposit thickness ranged from 2.5 m to 15 m. No reactivation surfaces were observed within the deposits, except in Profile 19. These topsets, which formed on the windward slopes of palaeo-dunes, are supercritically-climbing translatent strata formed through grain creep deposition (Hunter 1977, 1981; Kocurek 1991). No dune crests (where the transition from Facies I to II would occur) were observed in this phase. This is largely due to the relatively un-eroded state of the upper Phase 3 aeolianites compared to the lower Phase 1 deposits.

Facies III (Low-angle bedding) deposits dating to Phase 3, which are between 0.72 m and 5.85 m thick, were observed in Profiles 3, 4, 5, 7, 11, 12, 17 and 20. This facies is characterised by low-angle bedding which is almost exclusively planar. Concave-up bedding was observed in a single instance (Profile 11). Bedding thickness ranged between 0.5 and 10 cm. This facies was formed through the processes of grainfall and wind-ripple deposition; the low bedding angles rule out grainflow as a contributing depositional process (Hunter 1977, 1981; Kocurek 1991; Caputo 1995; Roberts *et al*. 2008, 2009, 2014; Bateman *et al*. 2011). These beds were deposited in several different environments. Some (e.g. Profiles 5, 7 and 20) formed as sand sheets with no known relationship to contemporary dune deposits (Figures 5.12, 5.17 & 5.43). The other deposits formed in relatively flat interdune areas and on the toes of leeward (Facies I) dune slope deposits, some of which formed during Phase 1 (Figures 5.8, 5.10, 5.25, 5.27 & 5.37). In Profiles 3 and 4, the Facies III deposits alternate vertically with dune deposits that periodically over-ran the interdune area (Figures 5.8 & 5.10).

Facies VII (Massive bioturbated aeolianite) deposits are present in Profiles 3, 6 and 13. The deposits comprise massive aeolianite with a very high density of large rhizoliths. In all three cases, the Facies VII deposits are the uppermost units in the local sequences. They range between 0.5 m and 2.5 m in thickness. No depositional structures are visible within the aeolianite. Any original bedding would have been destroyed by bioturbation during root growth (Klappa 1980). Therefore, it is not possible to determine the environment of deposition or to identify the specific aeolian depositional process that formed them.

6.1.3. Comparison to previous model

The stratigraphic sequence developed for this study (Figure 6.2) is similar to the one presented by Roberts (2008) and Jacobs & Roberts (2009) but differs in one significant aspect. The aforementioned authors recognised four stratigraphic phases within a model that was developed from the footprint site on Nahoon Point and a profile logged at East Beach (Figure 2.6). The lowermost unit in this model is the coarse beachrock conglomerate found around Nahoon Point and in the bay to the west of Bats Cave (just to the east of East Beach). This unit is suggested to be evidence for a sea-level highstand up to several metres above the present level. It is overlain by the footprint-bearing aeolianite at Nahoon Point and a contemporary aeolianite deposit at East Beach. The truncation of the aeolianite at both locations by raised benches, and the deposition of a relatively fine shelly conglomerate at East Beach are argued to indicate a second sea-level highstand of at least 6 m above present level. The East Beach conglomerate is overlain by a younger aeolianite deposit, indicating a second period of the deposition and cementation of wind-blown sand.

Both the previously published stratigraphic sequence and the one developed from this study include two periods of aeolian deposition and aeolianite formation (this study's Phases 1 and 3) separated by a hiatus resulting from a sea-level highstand (this study's Phase 2). In both cases, the formation of marine benches and the deposition of the conglomerate at East Beach are attributed to this highstand. The only disagreement between the two models is the stratigraphic position of the coarse beachrock.

This study argues that a three-phase model better explains the stratigraphy than the four-phase one previously proposed for the area, for the following reasons:

1. Roberts (2008) and Jacobs & Roberts (2009) assert that the coarse beachrock underlies the oldest aeolianite phase. However, at both Nahoon Point and East Beach, the stratigraphic relationship between the beachrock and the aeolianite could not be directly observed (Deacon 1966; Mountain 1966; Roberts 2008; Jacobs & Roberts 2009). Instead, this relationship was assumed based on the fact that the beachrock is exposed at a lower elevation than the visible base of the aeolianite at both locations (Roberts 2008; Jacobs & Roberts 2009). Likewise, it seems that the main reason they viewed the East Beach conglomerate and the coarse beachrock as representing different highstand events is the difference between their elevations. This is a problematic assumption, as the lack of any recorded direct stratigraphic relationship means that these features could have formed during different parts of the same event or during different events. This concern is especially relevant because the coarse beachrock deposits lie further seaward than the exposures at the footprint site and East Beach.

2. The presence of aeolianite deposits beneath the coarse beachrock on Nahoon Point and at Profile 20, and blocks of re-worked aeolianite at Nahoon Point indicate the formation of the beachrock subsequent to a period of aeolianite formation. The deposition of the coarse beachrock against the aeolianites at the base of Profile 9 (which have been found to date to Phase 1) means that the formation of the beachrock deposits could only have occurred after this phase.

3. Finally, the lack of marine benches above the coarse beachrock deposits in Profiles 5, 7 and 20 means that there is no evidence for more than one sea-level highstand in these sequences. As these profiles are relatively seaward compared to the locations where raised benches were identified, it seems unlikely that there would be no evidence for a later pre-Holocene highstand if one had occurred after the deposition of the coarse beachrock. This suggests

that the beachrock and the raised benches are more likely to represent different stages in a single highstand event, rather than two distinct highstands.

Based on the evidence discussed above, the three-phase stratigraphic sequence described in the first part of this section will be used throughout the rest of this dissertation. The three phases, various aspects of palaeoenvironmental conditions during them, their ages and evidence for human occupation will be discussed in the following sections.

6.2. AEOLIAN LANDFORMS

The stratigraphic sequence in the study area (described in the previous section) records the interplay between, and changes in the relative dominance of, aeolian and marine depositional processes and their respective environments of deposition. In this section, the sedimentology and geomorphology of the aeolianite deposits in Phases 1 and 3 are used to identify the aeolian landforms that were present within the study area. As no Phase 2 aeolian deposits were identified in the study area, this phase is not discussed here.

6.2.1. Phase 1

The Phase 1 aeolianite deposits represent the remains of several different dune and interdune types. The morphological histories of these deposits are described here, moving landward through the study area (see Figure 5.1 for profile locations). The non-vegetated northward-dipping toesets and foresets (Facies I) in Profiles 1, 2 and 6 (Figures 5.2, 5.5 & 5.14) represent shore-parallel dunes which initially advanced landward (north and north-west) (Roberts *et al*. 2009; Jackson *et al*. 2014; Rowe & Bristow 2015). A high density of rhizoliths higher up in these profiles indicates the eventual stabilisation of these dunes (Klappa 1980; Hesp 2002, 2004). The Facies II deposits in Profiles 9 and 20 (Figures 5.21 & 5.43) suggest the formation of sand sheets in these parts of the study area, while the overlying Facies I and III deposit at the former location indicates the subsequent development of a small lightly vegetated foredune (Fryberger *et al*. 1979; Hesp 1988, 2002; Jackson *et al*. 2014; Rowe & Bristow 2015).

The continuous aeolianite exposure between Profile 19 and Profile 10 represents the remains of a dune cordon or barrier with a complex formation history (Tinley 1985; Illenberger 1996; Roberts *et al*. 2009, 2014, Bateman *et al*. 2011; Cawthra *et al*. 2012a, 2014). The deposits at Profile 8 seem to be part of the same feature, although there is a lack of inland exposures to confirm this (Figure 5.1). The cordon is the result of the coalescence of several different types of aeolian deposits assigned to Facies I, II and III (see Figures 5.22 – 5.41). These include lightly vegetated coast-parallel foredunes, transverse dunes with foresets which prograded landward or perpendicular to the coastline, and sand sheets (Facies III) which formed in interdune areas or at the windward base of dunes (Hunter 1977 a, b; Fryberger *et al*. 1979; Kocurek 1981; Rubin & Hunter 1982; Hesp 1988, 2002; Illenberger 1996; Porat & Botha 2008; Roberts *et al*. 2008, 2009, 2014; Jackson *et al*. 2014; Rowe & Bristow 2015). Parabolic dunes formed from blow-outs in the vegetated transverse dunes as a result of onshore winds (Pye 1983; Illenberger 1996; Hesp 2002; Roberts 2008; Roberts *et al*. 2008, 2009, 2014). All of these deposits coalesced over time and became fixed and heavily vegetated (as evidenced by a high density of rhizoliths), forming a roughly coast-parallel cordon (Figure 5.1). Although there appears to have been some landward growth of the cordon, vertical accretion was dominant at this time. The cordon deposits were cemented before the sea-level highstand of Phase 2, as except for where they were truncated by the raised marine bench, the upper surfaces of the deposits are fairly well preserved.

6.2.2. Phase 3

The Phase 3 aeolianites, like the older deposits, represent a number of different types of aeolian deposit. The morphological histories of these deposits are described here, moving landward through the study area (see Figure 5.1 for profile locations). The interbedded dune (Facies I) and interdune/sand sheet (Facies II) deposits at Profiles 3, 4, 5 and 7 (Figures 5.8, 5.10, 5.12 & 5.17), in which reactivation surfaces are common and rhizoliths are rare except in the uppermost beds, indicate the migration of transverse dune deposits perpendicular to the coast (Profile 3, 4 and 5) and landward (Profile 7) (Kocurek 1981; Roberts *et al*. 2009; Jackson *et al*. 2014; Rowe & Bristow 2015). The highly-vegetated Facies III and VII deposits at the tops of Profiles 3, 4 and 6 suggest the stabilisation of land surfaces above the dune

deposits (Klappa 1980; Hesp 2002, 2004). The sequence at Profile 20, in the west of the study area, records the development of a thick sand sheet deposit (Facies III), which is overlain by a transverse dune, evidenced by high-angle foresets of Facies I, that prograded perpendicular to the shoreline (Hunter 1977a, b; Fryberger *et al*. 1979; Jackson *et al*. 2014; Rowe & Bristow 2015).

The deposits between Profile 19 and Profile 12 (see Figures 5.24 – 5.41) indicate resumption of the development of the coast-parallel dune cordon above the cemented Phase 1 aeolianites. Except at Profile 18, all of the Facies I and II deposits were formed by dunes which initially prograded landward but soon became fixed and highly vegetated (Rubin & Hunter 1982; Pye 1983; Illenberger 1996; Hesp 2002, 2004; Roberts *et al*. 2009, 2014; Jackson *et al*. 2014; Rowe & Bristow 2015). A lack of accommodation space due to the existing Phase 1 deposits prevented further inland transgression. This resulted in the promotion of vertical accretion and the formation of parabolic dunes from blowouts (Pye 1983; Tinley 1985; Illenberger 1996; Hesp 2002, 2004; Roberts *et al*. 2008, 2009, 2014). At Profile 18 (Figures 5.38 & 5.39), the Facies I deposits are the product of transverse dunes prograding perpendicular to the coast and coalescing with the other dunes in the cordon (Illenberger 1996; Jackson *et al*. 2014; Roberts *et al*. 2009, 2014; Rowe & Bristow 2015). A number of generally highly-vegetated Facies III and VII deposits (Figures 5.25, 5.27, 5.29 & 5.37) fill topographic (due to dune morphology) or erosional hollows in the upper parts of the cordon, suggesting a decrease in aeolian deposition and increasing land surface stability (Klappa 1980; Hesp 2002, 2004).

6.3. PALAEO-WIND

The orientation of bedding structures in aeolian deposits is a good proxy for the direction of the winds which formed them (Pettijohn *et al*. 1973; Potter & Pettijohn 1977; Kocurek 1991; Boggs 2014). In this section, the evidence for palaeo-wind conditions during Phase 1 and Phase 3 is discussed. Unfortunately, the lack of aeolian deposits during Phase 2 means that wind patterns during this time cannot be reconstructed.

Based on the orientation of dune bedding within all Phase 1 deposits in the logged profiles, the wind was predominantly from between south and west-north-west (with major peaks in wind from the southwest and northwest) during this period of time, but winds from the south-east also contributed to dune formation (Figure 6.5). The available evidence indicates that the wind was predominantly from between south and west-north-west during Phase 3 (Figure 6.5). Winds from the southeast also contributed significantly to dune formation. The wind patterns during Phase 1 and Phase 3 appear to have been broadly similar although there are some differences in the apparent contribution of winds from different directions (Figure 6.5). South-westerly winds were most common during Phase 1, while winds from between the west and west-south-west were far more common during Phase 3. Onshore winds (from the south-east) played a greater role in dune formation during Phase 3 than in Phase 1.

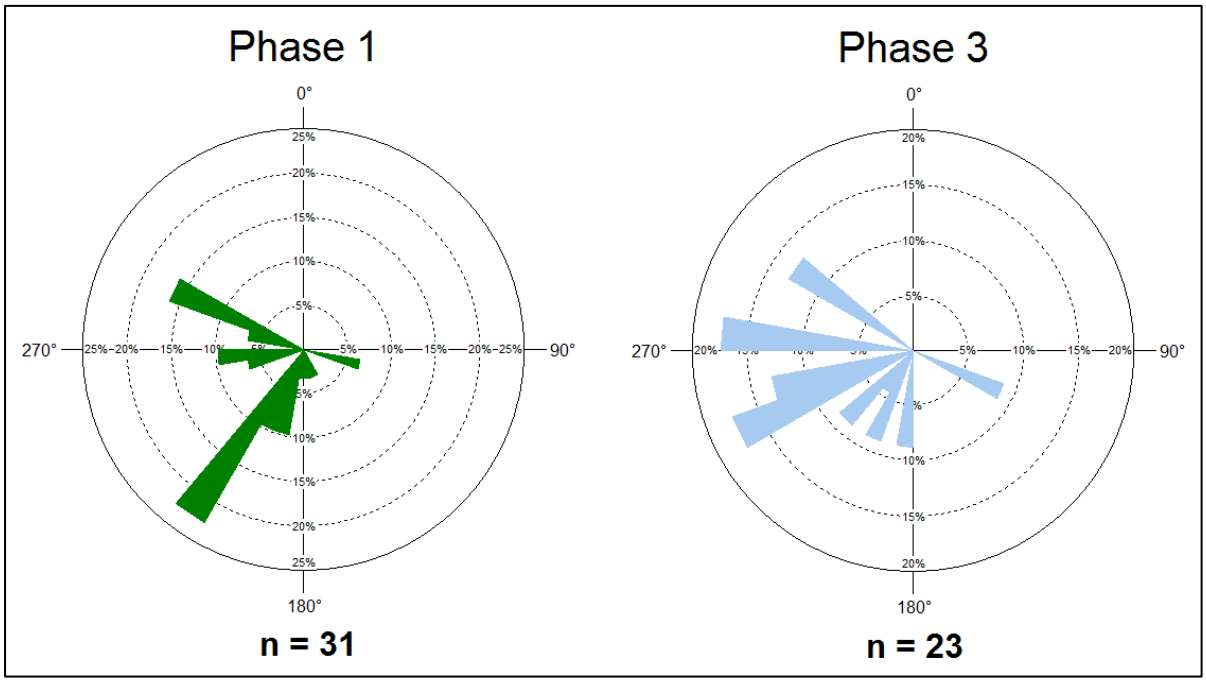


Figure 6.5. Wind roses for Phase 1 and Phase 3 based on dune bedding dip orientation measurements collected from the 20 logged profiles.

The modern wind patterns in the area were described in Section 2.1.1 (see Figure 2.2). There are some clear similarities between the modern wind regime and the winds that formed dunes during Phases 1 and 3 (Figures 2.2 and 6.5). The first major similarity is the dominance of winds from the west and south-west (alongshore) over other winds. The second is the relatively high frequency of north-

westerlies (offshore winds) compared to southerlies and south-westerlies (onshore winds). However, north-easterly winds, which are dominant in summer at East London today, appear to have played no role in dune-building during either Phase 1 or Phase 3. The palaeo-wind data are most similar to the modern winter wind regime in the area.

It is possible that a bimodal wind regime, similar to that of today, existed in the study area during these phases. If the south-westerlies were stronger and/or more common than the north-easterlies, then any landforms produced by the latter winds would very likely have been deleted by the former winds. Many non-vegetated (based on the absence of rhizoliths) dune deposits with bedding orientations indicative of formation by winds from between the south-south-west and the west (with crests perpendicular to the coastline) have numerous reactivation surfaces and occasional thin interbedded interdune deposits. This may reflect alternation between the weaker north-easterlies and stronger south-westerlies.

Rainfall patterns may also have influenced the geomorphic potential of winds from different directions as wet sand is too cohesive to allow significant activation by aeolian processes (Namikas & Sherman 1995; Cornelis & Gabriels 2003; Davidson-Arnott *et al*. 2005; Bauer *et al*. 2009). If, as today, rain was markedly less common in winter than during the rest of the year, then the influence of the south-westerlies on dune formation would have been amplified whilst that of the north-easterlies would have been retarded.

Given the similarities between the geomorphic data and the modern wind data, it seems likely that, during both Phase 1 and Phase 3, a wind regime broadly comparable to modern conditions existed. This would have entailed a strongly bimodal shore-parallel wind regime, with more frequent south-westerly winds contributing to dune-building and the less common north-easterlies producing no preserved bedforms. Offshore and onshore winds were markedly less common although they made significant contributions to dune-building. It is also likely that rainfall seasonality was fairly similar to present patterns, with relatively dry winters and wetter summers.

6.4. CEMENTATION OF DEPOSITS

The processes by which the deposits of the three stratigraphic phases were cemented are considered in this section. The cementation of aeolianite (Phases 1 and 3) and the cementation of beachrock (Phase 2), while similar in some ways, are also fairly different. Therefore, their cementation is considered in separate sub-sections below.

6.4.1. Aeolianite

Aeolian sands become aeolianite when they are cemented through the precipitation of calcium carbonate (mainly calcite) cements around and between the grains in the sediment (Fairbridge & Johnson 1978; Brooke 2001; McLaren 2007). This process mainly takes place in the vadose zone but can also occur in the phreatic zone if the water table rises and the sediment becomes waterlogged (Muller 1971; Reeckman & Gill 1981; Moore 1989; McLaren 1993, 2007; Gardner & McLaren 1994; McLaren & Gardner 2004). The initial cementation of aeolianite can occur very rapidly – in some cases less than a century (Reeckmann & Gill 1981; Gardner & McLaren 1994; Dravis 1996; Kindler & Mazzolini 2001; McLaren 2007).

The results of the petrographic and FTIR analyses of samples from the Footprint Site (Profiles 1 and 2) indicate that these sediments are composed of marine shell fragments and other bioclasts, calcite cement, quartz and clay minerals. The bioclasts are all composed of calcite, indicating that the aragonite within them underwent diagenesis without affecting their physical form. The cement properties in the analysed thin sections (Figures 5.49 – 5.51) are fairly typical of vadose diagenesis in aeolianites (McLaren 1993, 2007; Gardner & McLaren 1994; McLaren & Gardner 2004). Clay minerals within the sediments are the product of the alteration of very rare dolerite grains during diagenesis.

Macroscopic analysis indicates that the lithology of all the aeolianite deposits in the study area is very similar to the sampled units. This similarity in composition is confirmed by previous work on aeolianites in and near the study area (Mountain 1966; Le Roux 1989a, b; Jacobs & Roberts 2009). Despite the similarity in lithology, a great deal of variation in the style and degree of aeolianite cementation (e.g. how

well or poorly cemented the sediment was or whether it was druzy or not) could be observed in the field, often even within a single deposit (see Section 5.1.2).

As there is no source of carbonate (CO_3) other than calcite ($CaCO_3$) within the sampled aeolianite, the carbonate content of the 68 bulk aeolianite samples (Table 5.3) can be used as a rough proxy for relative calcite content in these samples. Carbonate content (and thus, the proportion of calcite in the samples), along with the density and porosity of the samples, vary considerably both within and between different aeolianite deposits. All three of these properties are initially controlled by the original source material (how much calcite and aragonite is available in the sediments) and formation processes (how tightly grains are packed during deposition), and later affected by diagenetic processes (Reeckman & Gill 1981; McLaren 1993, 2001, 2007; Gardner & McLaren 1994; McLaren & Gardner 2004). As the source material seems broadly similar across the deposits, and because there is so much variation in these properties even within single deposits, it seems that these properties are largely a result of diagenetic processes.

The considerable variability in field and laboratory results indicates that there has been a great deal of variation in the diagenetic processes acting on the aeolianites in the study area. This is common in aeolianite deposits globally (Friedman 1964; Schroeder 1988; McLaren 1995, 2001, 2007; McLaren & Gardner 2004). It is likely that the diagenesis of any particular part of a given deposit has been affected by a number of environmental factors (such as the presence or absence of roots, or heat and moisture availability in the sediment) at any time since the original deposition of the aeolian deposits (Reeckman & Gill 1981; Moore 1989; McLaren 1993, 2007; Gardner & McLaren 1994; Dravis 1996; Kindler & Mazzolini 2001; McLaren & Gardner 2004). Therefore, beyond it being clear that the majority of cementation occurred in the vadose zone, it is difficult to make any palaeoenvironmental interpretations based on the diagenesis of the aeolianite deposits in the study area.

6.4.2. Beachrock

The cementation of beach sediments to form beachrock considerably reduces the likelihood of their destruction by erosional processes and thus preserves evidence

for past sea levels (e.g. Cooper 1991; Ramsay 1995; Ramsay & Cooper 2002; Vousdoukas *et al*. 2007; Cawthra & Uken 2012; Mauz *et al*. 2015). Understanding the process by which beachrock becomes cemented, and where and under what conditions this takes place, provides important information for making sea level determinations from these deposits (Hopley 1986; Kelletat 2006; Knight 2007; Vousdoukas *et al*. 2007; Cooper 2013; Mauz *et al*. 2015).

Beachrock is formed through the precipitation of calcite and aragonite cements (in a variety of forms and proportions) between and around the grains and clasts in beach sediments (Bricker 1971; Hanor 1978; Hopley 1986; Vousdoukas *et al*. 2007; Mauz *et al*. 2015). This occurs most often in the intertidal zone where the water table and seawater meet and, as a result, almost all beachrock cementation takes place within the intertidal zone beneath un-cemented beach deposits (Ramsay 1991, 1995; Gischler 2007; Vousdoukas *et al*. 2007; Mauz *et al*. 2015).

The identification of the types and structures of cement, and their proportions within a beachrock deposit can allow the identification of where specifically within the intertidal zone cementation occurred (Gischler 2007; Vousdoukas *et al*. 2007; Desreulles *et al*. 2009; Mauz *et al*. 2015). As the cements within the beachrocks identified in the study area have not been analysed, this approach cannot be used for this study. However, studies of both modern and ancient beachrocks along the KwaZulu-Natal (KZN) coast, to the north of East London, provide some help in this regard. These studies all conclude that, at these microtidal locations, beachrock cementation occurred between mean low water and mean sea level (Cooper & Flores 1991; Ramsay 1991, 1995; Ramsay & Cooper 2002; Cawthra & Uken 2012; Cawthra *et al*. 2012a; Wiles *et al*. 2018).

Whilst it is not possible to determine where precisely within the tidal frame the cementation of the East London beachrocks took place, it is clear that this must have occurred somewhere in the intertidal zone. The results from KZN suggest that the lower intertidal zone is a likely location for this process to have taken place, but this cannot be assumed to have been the case. Future analysis of the cements in the beachrocks in the study area may provide greater resolution.

6.5. SEA LEVEL

In this section, the evidence for Early MIS 5 sea levels in the study area will be discussed, along with the chronology of the three phases. Throughout this dissertation, high tide level has been used as a marker for elevation within the study area. For the purposes of this section, a conversion to mean sea level is required. The average tidal range along this part of East London's coast is 1.63 m (Bursey & Wooldridge 2002). Therefore, the mean sea level for the study area is approximately 0.82 m below high tide level. This rough measure is used in the estimates presented below.

The Phase 1 and 3 aeolian deposits formed up to, and further seaward than, the current high tide mark. This indicates that (at least some of) these landforms must have been deposited during periods when sea level was lower than present. However, the formation of coastal dunes means that the shoreline cannot have been too distant from its current position (Brooke 2001; Murray-Wallace & Woodroffe 2014: 123-124). Unfortunately, there is no available evidence on which to base any more precise estimate of sea level during these phases.

There is considerably more, and far more useful, evidence for sea levels during Phase 2 than for the two aeolian phases. This evidence is in the form of depositional features: the beachrock recorded in several locations, and erosional features: the raised benches that are found across the study area. These features, their locations and elevations, and the sea level estimates made from them are presented in Table 6.1.

Sea level estimates were made based on the environmental associations of the different beachrock facies. In each case, the relationship of the particular facies to mean sea level was used to determine whether the deposit was indicative of deposition at, above, or below mean sea level. The current tidal range was used to create error margins for the estimates.

Marine benches and platforms form within the intertidal zone, but there is little certainty as to precisely where in relation to mean sea level they form (Stephenson

2000; Murray-Wallace & Woodroffe 2014: 115 – 116). Therefore, the sea level when these features formed could have been anywhere within the height of the tidal range at the time. Sea level estimates were made for the different recorded elevations of the raised benches/platforms assuming the same mean tidal range as the present (see Table 6.1).

Table 6.1. A summary of the evidence for local sea level during Phase 2 collected from the study area and the estimates made from this evidence. The roman numerals indicate the facies to which a particular beachrock deposits was classified. Elevations and estimates relative to mean sea level are given for each location. These were determined using the elevations relative to high tide level (presented in Section 5.1), the beachrock facies properties, and the mean tidal range of 1.63 m. *The elevation for the East Beach beachrock deposit is that presented by Jacobs & Roberts (2009). Note that the estimates for the beachrock are for sea level at the time of deposition, not lithification.

Location	Evidence Type	Elevation	Sea Level Estimate
Profile 5	Beachrock (V)	+0.32 m	> -0.50 to +0.32 m
Profile 7	Beachrock (V)	+2.32 m	> +1.50 to +2.32 m
Profile 20	Marine bench	+0.87 m	+0.05 to +1.69 m
Profile 20	Beachrock (IV)	+1.37 m	< +1.37 to +2.19 m
Profile 20	Beachrock (V)	+2.02 m	> +1.20 to +2.02 m
East Beach*	Beachrock (VI)	+6.10 m	+5.28 to +6.92 m
Profile 1	Marine platform	+6.82 m	+6.00 to +7.64 m
Profile 2	Marine platform	+7.32 m	+6.52 to +8.14 m
Profile 8	Marine bench	+4.82 m	+4.00 to +5.64 m
Profile 9	Marine bench	+4.82 m	+4.00 to +5.64 m
Profile 12	Marine bench	+5.32 m	+4.50 to +6.14 m
Profile 13	Marine bench	+5.82 m	+5.00 to +6.64 m
Profile 14	Marine bench	+4.62 m	+3.80 to +5.44 m
Profile 16	Marine bench	+4.62 m	+3.80 to +5.44 m
Profile 18	Marine bench	+7.82 m	+7.00 to +8.64 m

The beachrock deposit at Profile 5 formed when mean sea level was a minimum of -0.50 to +0.32 m. The small marine bench at Profile 20 was formed when mean sea level was +0.05 to +1.69 m. The Facies IV beachrock at Profile 20 indicates mean sea level at a maximum of +1.37 to +2.19 m, while the Facies V deposit at this

location formed when mean sea level was a minimum of +1.20 to +2.02 m. The beachrock in Profile 7 was deposited when mean sea level was a minimum of +1.50 to +2.32 m. The fine beachrock (Facies VI) at East Beach was deposited when the sea level was +5.28 to +6.92 m.

The raised benches and platforms associated with the major unconformity across the study area range in elevation from 4.62 m to 7.82 m above mean sea level (Table 6.1). Therefore, the sea level estimates based on these features vary quite widely. The lowest estimate is +3.80 to +5.44 m (at Profiles 14 and 16). The maximum possible sea level reached appears to have been between 7.00 m and 8.64 m above mean sea level (around Profile 18).

The estimates suggest that the Phase 2 sea-level highstand was stepped, with apparent still-stands of unknown duration between periods of rising levels. The coarse beachrock indicates a rise from a sea level similar to today's to one that was a minimum of 1.50 to 2.32 m above present mean sea level. The raised marine benches and the shelly beachrock at East Beach indicate a subsequent rise from a minimum of +3.80 m to an absolute maximum of +8.64 m. The wide error margins on the estimates mean that it is possible that smaller sea level changes within these ranges could have occurred without any evidence being preserved.

Stepped sea level increases have been reported for various parts of the Quaternary, including MIS 5e (Blanchon & Shaw 1995; Bard *et al*. 1996; Hearty *et al*. 1999, 2007; Hearty & Neumann 2001; Hearty 2002; Blanchon *et al*. 2009; Camoin *et al*. 2012; Gischler 2014). These events have been attributed to pulses in the collapse of polar ice sheets and the release of meltwater from glaciers, both of which resulted in the sudden introduction of large quantities of fresh water into the oceans (Blanchon & Shaw 1995; Bard *et al*. 1996; Hearty *et al*. 1999, 2007; Hearty 2002; Camoin *et al*. 2012; Nicholl *et al*. 2012; O'Leary *et al*. 2013; Gischler 2014; Long *et al*. 2015).

The only relatively well-dated evidence for MIS 5e sea levels in South Africa is from several sites along the southern coast (Carr *et al*. 2010; Roberts *et al*. 2012; Cawthra *et al*. 2018). Various deposits at these sites indicate the occurrence of two

highstands during MIS 5e, followed by a significant drop in sea level during MIS 5d. Estimates of peak sea levels range from ~+5.6 m to ~+8.5 m. Undated deposits near Durban, on the east coast, which have been argued to date to MIS 5e suggest the occurrence of two highstands at +5 m and +7 m within a relatively short period of time (Cooper & Flores 1991; Ramsay & Cooper 2002).

There is considerable global evidence for two distinct highstands, and a relative lowstand between them, within MIS 5e (Chen *et al*. 1991; Neumann & Hearty 1996; Wilson *et al*. 1998; Zazo 1999; Dumas *et al*. 2006; Hearty *et al*. 2007; Kopp *et al*. 2009, 2013; Thompson *et al*. 2011; O'Leary *et al*. 2013; Gischler 2014; Skrivanek *et al*. 2018). The precise timing of these events is debated, but it seems that the first highstand occurred during early MIS 5e, followed by the lowstand in mid-MIS 5e, and the second highstand in later MIS 5e (Neumann & Hearty 1996; Hearty *et al*. 2007; Blanchon *et al*. 2009; Kopp *et al*. 2009, 2013; Thompson *et al*. 2011; O'Leary *et al*. 2013).

No evidence for the first MIS 5e highstand was observed in the study area. However, this event has been identified in the sedimentary record at some locations along the southern coast, with maximum sea levels between +6.2 m and +8.5 m with ages ranging from 130 ± 8.3 ka to 125 ± 6.7 ka (Carr *et al*. 2010; Roberts *et al*. 2012; Cawthra *et al*. 2018), The Phase 1 deposits appear to correlate broadly with the mid-MIS 5e lowstand (see Figure 6.6). Global sea level estimates for this event range from several metres above, to several metres below the present level (Hearty *et al*. 2007; Siddall *et al*. 2007; Kopp *et al*. 2009, 2013).

Estimates of peak global sea level during the second MIS 5e highstand (equivalent to Phase 2 in the study area – see Figure 6.6) generally range between +6 m and +9 m (Hearty *et al*. 2007; Siddall *et al*. 2007; Kopp *et al*. 2009, 2013; Murray-Wallace & Woodroffe 2014). Deposits at several locations along the southern coast dating between 121 ± 7 ka and 118 ± 7 ka suggest that this highstand reached a peak of +5.6 m to +6.8 m in the region (Carr *et al*. 2010; Cawthra *et al*. 2018). The maximum inferred highstand level in the study area – +7.00 to +8.64 m – is somewhat higher than these estimates, but not significantly so.

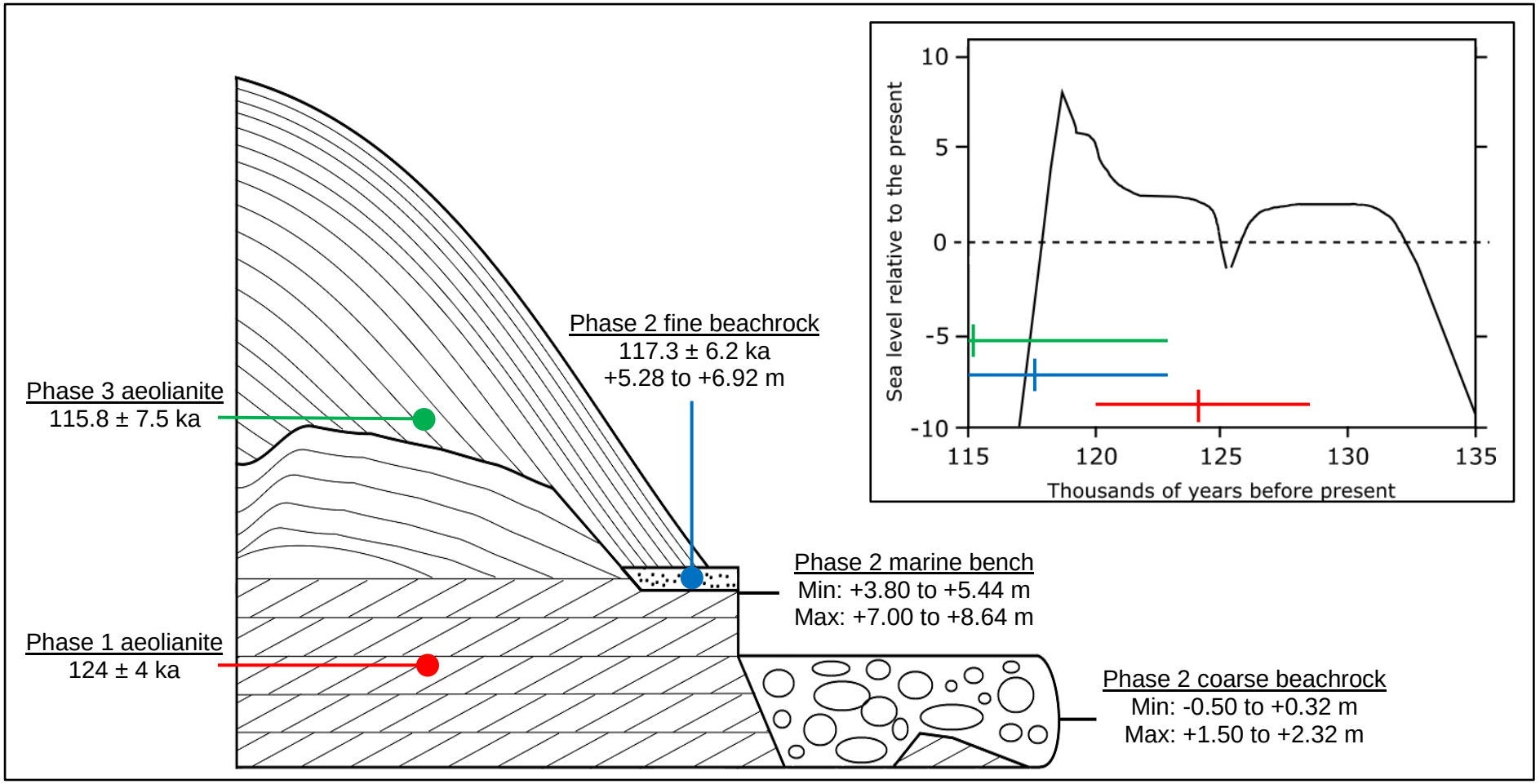


Figure 6.6. A generalised geological cross-section of the deposits in the study area with the sea level estimates for various features indicated. Dates obtained by Jacobs & Roberts (2009) are presented for the dated deposits. Inset: An MIS 5e global sea level graph (after Hearty *et al*. 2007). The date ranges (horizontal lines) and mean ages (vertical lines) for the three dated deposits are superimposed over the graph. Note that the date ranges for the Phase 2 fine beachrock and the Phase 3 aeolianite continue beyond the edge of the graph, past 115 ka.

In terminal MIS 5e and MIS 5d (during the period when Phase 3 deposits were forming – see Figure 6.6) a rapid and significant reduction in global sea level resulted in a drop to as low as 50 m below present (Hearty *et al*. 2007; Siddall *et al*. 2007; Kopp *et al*. 2013; Murray-Wallace & Woodroffe 2014). Evidence from the southern coast indicates a drop in sea level to below -20 m by 115 ± 7 ka (Cawthra *et al*. 2018), which is roughly contemporaneous with the dated basal Phase 3 aeolianite at East Beach (Jacobs & Roberts 2009). There is no direct evidence for sea levels in the study area at this time, but it is likely that they were broadly similar to the rest of the southern coast.

The large error margins on both the dates from the study area and the dates obtained from the southern coast make nuanced comparisons between them and to the global data difficult. However, the global and South African dates and sea level estimates (including those from the study area) are broadly comparable.

6.6. HUMAN OCCUPATION

This section is devoted to discussing the Early MIS 5 archaeological evidence found within and near the study area. In the first part of this section, the evidence for human presence is discussed to determine whether or not it can provide any information on human behaviour around the Nahoon Point Nature Reserve. The resources that may have been available to past human populations within the area are considered in the second part of the section.

6.6.1. Human presence and behaviour

There is evidence for human presence in the study area during all three of the identified stratigraphic phases (Figure 6.1 & Table 5.2). The Nahoon Point footprints and the single lithic artefact that was found in Profile 16, which were preserved within aeolian deposits of Facies I and III, indicate human presence during Phase 1. The footprints were made by an individual walking up the leeward slope of a dune (Roberts 2008), while the lithic artefact was discarded on a sand sheet deposit. Artefactual material from Phase 2, which can be broadly referred to the Middle Stone Age (MSA) on the basis of typology, was found within deposits of Facies IV, V and VI. These sediments were deposited either within the intertidal zone or the lower supratidal zone. Small assemblages of MSA lithic artefacts from Profile 15 and

Profile 16 indicate human presence during Phase 3. These artefacts are in very fresh condition and were found within aeolian deposits of Facies I and II. Therefore, they were discarded on the windward and leeward slopes of dunes.

Despite the limited sample sizes, there is a difference between the types of lithic artefacts found in the Phase 1 and 3 deposits and those discovered in the Phase 2 deposits. The artefacts observed in the beachrock deposits were all flakes and blades. The small assemblage previously reported from the conglomerate at Bats Cave was composed almost entirely of these artefact types (Deacon 1966). In contrast, the artefacts discovered in the aeolianites were predominantly the waste products of knapping, including small flaking debris, an overshot flake, a core and a possible core. This suggests that humans were carrying out different activities in these parts of the coastal zone. It would appear that the production of stone tools was primarily taking place away from the beaches (e.g. among the dunes), but that the tools were mainly utilised in the intertidal or lower supratidal zones.

The lithic artefacts in the (intertidal and lower supratidal) Phase 2 deposits are relatively lightly weathered and display very little to no abrasion on their edges. The majority of the limited visible weathering is due to their current exposure within the intertidal zone. This contrasts markedly with the highly abraded and rounded natural clasts in these deposits. The size ranges of the artefacts and the natural clasts also differ notably. These differences indicate that the artefacts were not accumulated by the same agent as the natural clasts and that they were not moved significantly by natural processes (e.g. waves, swash and backwash) after their discard by the humans who made and/or used them (Shea 1999; Walter *et al*. 2000). Therefore, they can be considered to be broadly *in situ* within these deposits. Although some movement of artefacts may have occurred after discard, this appears to have been very limited. Therefore, their presence within these deposits suggests human activity within the intertidal and supratidal zones during Phase 2. This indicates that people were entering the intertidal zone and the lower parts of the supratidal zone, probably to collect shellfish or marine molluscs and/or to scavenge from carcasses of marine mammals that had washed up on the shore.

These sites represent the oldest evidence in South Africa for coastal occupation and the exploitation of marine food resources outside of the Greater Cape Floristic Region (Figure 3.4). They are also the only known case in southern Africa where human activity in the intertidal zone is evidenced by *in situ* artefacts rather than by shells and bones that were discarded at occupation sites after the organisms had been removed from the intertidal zone, processed and eaten. Only a single comparable occurrence has been reported, that of the archaeological sites within the Abdur Reef on Eritrea's Red Sea coast, where stone tools were found in intertidal deposits dated to 125 ± 7 ka (Walter *et al*. 2000; Bruggemann *et al*. 2004; Buffler *et al*. 2010). Coincidentally, this also dates to MIS 5e.

The dating and the geological context of the Blind River archaeological deposits (Wang *et al*. 2008) indicate that they can be considered contemporaneous with the Phase 2 deposits in the study area. MSA lithic artefacts, animal bone fragments and a partial human femur have been recovered from two sedimentary units at the site: a lower estuarine calcarenite and an upper storm beach gravel deposit (Laidler 1933; Wells 1935; MacFarlane 1937; Wang *et al*. 2008). Only very rudimentary analysis has been conducted on the lithics, and the results reveal little about human behaviour at the site (Laidler 1933, 1934; MacFarlane 1937). What, if any, role humans played in accumulating the animal bones is unknown.

The artefacts in the estuarine calcarenite are fresh and un-abraded (Laidler 1933), suggesting they were discarded on the edge of a lagoon or estuary and are in fairly pristine context (Shea 1999; Walter *et al*. 2000; Wang *et al*. 2008). These artefacts indicate human activity in this environment during late MIS 5e. The artefacts found in the gravels are relatively heavily abraded and rounded, having been rolled prior to their deposition (Laidler 1933). They are very similar to the natural clasts in the deposit in this regard. This is in sharp contrast to the abrasion state of the lithics in the beachrock in the study area. This may be due to movement from an initial point of discard (which may have been in either the intertidal zone or the supratidal zone) during the formation of the storm beach deposit (Shea 1999; Wang *et al*. 2008). As these artefacts have been reworked and are *ex situ*, they are not indicative of human activity in this immediate environment.

None of the archaeological evidence indicates the existence of an occupation site at the archaeological sites within the study area or at Blind River. This is not surprising, as strong winds and spray in the open areas along the shoreline would have made these areas unattractive for campsites. People are more likely to have camped in relatively sheltered areas beyond the dunes and walked to various locations to access different resources.

The evidence from the study area and Blind River indicates human utilisation of a number of different environments within the coastal zone during Early MIS 5. These include the intertidal and supratidal zones, coastal dunes, and riverine environments (estuaries or lagoons). Potential sources of food and other vital resources in these palaeoenvironments are considered in the following sub-section.

6.6.2. Coastal resource availability and exploitation

The shellfish and mollusc species composition of intertidal ecosystems is determined by a number of environmental variables including water temperature, wave action and substrate (McLachlan & Hanekom 1979; Kilburn & Rippey 1982; McQuaid & Branch 1984; Bustamente & Branch 1996; McLachlan 1996; Bustamente *et al*. 1997; Nel *et al*. 2001; Sink *et al*. 2005; Branch *et al*. 2007; Langejans *et al*. 2017). Substrate – the properties of the sediment or rock within the intertidal zone – has a very significant impact on the suitability of a location for different mollusc species (McLachlan & Hanekom 1979; McQuaid & Branch 1984; McLachlan 1996; Bustamente *et al*. 1997; Sink *et al*. 2005; Branch *et al*. 2007; Jerardino & Marean 2010). Different species are adapted to various sandy, rocky or mixed substrates and may be rare or absent when the substrate falls outside of their requirements (McLachlan & Hanekom 1979; Kilburn & Rippey 1982; McLachlan 1996; Sink *et al*. 2005; Branch *et al*. 2007; Langejans *et al*. 2017).

The sedimentary and geomorphic evidence from the study area indicates the existence of several distinct intertidal environments at various times during Phase 2. The beachrock facies represent beaches which had differing mixes of sand and clasts and thus, different substrate properties (Section 6.1.2). The raised benches and platforms cut into the aeolianite, and the exposed dolerite in several parts of the study area would both have provided very different substrates than the beach

deposits during the periods when they were exposed within the intertidal zone. Therefore, it is likely that a variety of different marine shellfish and mollusc species would have been available in the study area, with significant changes in the ecology of the intertidal zone over time and/or space.

Deacon (1966) suggested that the beachrock conglomerates could have been a source of raw material for lithic production prior to the cementation of the deposits. This is plausible, although the majority of the clasts are dolerite and sandstone, while the lithic artefacts found in the study area are predominantly hornfels, with some quartzite pieces being present (Section 5.1.3). The hornfels (which Mountain [1945, 1974] refers to as Lydianite, a once common term seldom used today) was formed by contact metamorphosis of Beaufort Series mudstone during the intrusion of the dolerites in the area, while the quartzite formed through metamorphosis of the sandstones of the same series (Mountain 1945, 1974). Outcrops of both of these lithologies have been reported within several kilometres of the study area (Mountain 1945, 1974). Therefore, suitable raw material for stone tool production would have been readily available to human populations occupying the area around East London.

A number of rivers flow into the sea in the vicinity of the study area. They are deeply entrenched, and have followed roughly the same courses for much of the Quaternary (Mountain 1974; Rust *et al*. 1985; Reddering & Esterhuysen 1987; Wiseman *et al*. 1993). Therefore, these rivers almost certainly existed during Early MIS 5, although the morphologies of their estuaries may have been very different than they are today. For instance, the calcarenite deposit at Blind River indicates the presence of an estuary or lagoon at this location during the late MIS 5e highstand (Wang *et al*. 2008). This contrasts strongly with the river today, which has no mouth or lagoon. Research conducted in the area indicates that significant changes in estuary morphology, and resulting effects on biodiversity, can occur relatively rapidly (Rust *et al*. 1985; Reddering & Esterhuysen 1987; Wiseman *et al*. 1993).

The rivers would have been vital sources of fresh water for both humans and terrestrial fauna living in the area. A variety of fish and marine invertebrate species have been reported from various parts of the river courses (Wiseman *et al*. 1993).

Waterfowl are also commonly observed, especially in the estuaries (Wiseman *et al*. 1993).

The previously-published (Section 2.2) and newly-discovered (Section 6.1.2) tracks at the Footprint Site indicate the presence of a number of vertebrate species in the study area. These include as-yet unidentified ungulate species of a range of different sizes. Many mammalian species have been reported in the East London area in historical and recent times (Wiseman *et al*. 1993). These include a number of potential prey species, such as hares and bovids of all size classes (e.g. duiker, bushbuck and buffalo).

It cannot be assumed that the terrestrial and marine species known from the study area today were present during Early MIS 5, as the climatic and environmental changes that occurred during this period would have affected the ecology of the area to varying degrees. However, given the broad similarities between the global climates of MIS 5e and the present day (Shackleton *et al*. 2003; NEEM Community Members 2013; Govin *et al*. 2015), it is likely that ecosystems had a similar level of biodiversity to those of today although the species composition of the ecosystems may not have been identical. Faunal remains, along with a growing number of trace fossils in aeolianites, indicate the existence of a number of now extinct (or locally extirpated) megafauna on (or near, in the case of anthropogenic accumulations of bones) the southern coast during Early MIS 5 (refs e.g. Klein 1976; Van Pletzen 2000; Roberts *et al*. 2008; Rector & Reed 2010; Helm *et al*. 2018a, b, 2019). It is possible (but by no means certain) that some of these species could have been present around East London at this time,

Whilst it is clear that a variety of species would have been available in the various marine and terrestrial environments in and around the study area, it cannot simply be assumed that human populations at this time had the capacity to exploit them. However, archaeological research into human subsistence practices provides a means to assess this.

A significant increase in human diet breadth, linked to changes in subsistence behaviours, occurred in South Africa between MIS 6 and early MIS 4 (Dusseldorp 2010; Clark & Kandel 2013; Marean 2014, 2016; Marean *et al*. 2014). A major

aspect of this was the appearance of a distinct “coastal adaptation” lifestyle at coastal archaeological sites which relied (in part at least) on the collection and consumption of “dense and predictable” (Marean 2016: 1) marine food resources from the intertidal zone. However, even at coastal sites, terrestrial mammal species of a range of sizes appear to have constituted the major faunal part of the human diet (Dusseldorp 2010; Clark & Kandel 2013; Marean 2014, 2016; Marean *et al*. 2014).

The available data from the study area do not allow the identification of what species humans were exploiting, or what specific strategies they employed in hunting or collecting them. However, the archaeological evidence for human subsistence in the southern Cape during Early MIS 5 indicates that people would have had the ability to exploit (at varying degrees of effectiveness) a variety of the many marine and terrestrial species that may have lived in the different environmental zones in the area (Dusseldorp 2010; Clark & Kandel 2013; Marean 2014, 2016).

7. CONCLUSIONS

The conclusions of this study are split into three sections. The first, which relates to the stratigraphy of the deposits in the study area, is linked to Aim 1 of the study (Section 1.2.2). The second section details the reconstructed Early MIS 5 palaeoenvironments for the study area, and is thus linked to Aims 2 and 3 (Section 1.2.2) and the Research Question (Section 1.2.1). The final section includes the conclusions reached about human presence and behaviour in the area during Early MIS 5 based on the available archaeological and palaeoenvironmental evidence.

7.1. STRATIGRAPHY & CHRONOLOGY

The profiles logged for this study record three distinct Late Pleistocene stratigraphic phases across the study area. Two periods of aeolian deposition (and the cementation of these deposits) are separated by a major unconformity/disconformity. This feature is associated with both marine deposits and intertidal erosional landforms. The stratigraphically lower aeolianite deposits are grouped within Phase 1, while the younger ones are assigned to Phase 3. The marine depositional and erosional features, which formed between the two aeolian phases, fall within Phase 2.

Three Optically Stimulated Luminescence (OSL) dates, one for each of the three phases, have been published for the study area by Jacobs & Roberts (2009). The error margins on the dates are wide, but they still provide reasonable chronological context for the deposits. The Phase 1 deposits (124 ± 4 ka) appear to have formed in mid-MIS 5e, during the relative sea-level lowstand between the two known MIS 5e highstands. The Phase 2 marine deposits (117.3 ± 6.2 ka) date to the second MIS 5e highstand. Finally, the Phase 3 sediments (115.8 ± 7.5 ka) were deposited in terminal MIS 5e and early MIS 5d during regression from the previous highstand.

7.2. PALAEOENVIRONMENTS

The major aeolian landform in the study area is a shore-parallel cordon, the main body of which is to the south-west of Nahoon Point. During Phase 1, palaeo-dunes and interdune deposits of a variety of different types coalesced to form the cordon. After the Phase 2 sea-level highstand, which eroded the cordon and cut benches

into the aeolianite, cordon growth continued with the deposition of Phase 3 aeolianites. In both Phases 1 and 3 a lack of accommodation space, which prevented landward transgression, and the growth of relatively dense vegetation on the dunes resulted in vertical accretion. Parabolic dunes formed from blow-outs in the vegetated dunes as a result of onshore winds. After a significant hiatus in the development of the cordon, growth resumed during the Holocene, with unconsolidated dune deposits forming unconformably on the eroded upper surfaces of the palaeo-dune deposits.

Whilst the cordon is the most obvious aeolianite landform in the study area, other significant features were also observed. A number of shore-parallel dunes, some fixed and some prograding landward, formed on Nahoon Point during Phase 1. In the same period, sand sheets were deposited on Nahoon Point and to the west of the cordon. During Phase 3, dunes which prograded or migrated along the coast formed on Nahoon Point and to the west of the cordon. Sand sheets and interdune deposits (sometimes interbedded with migrating dune deposits) were also common in both locations.

The Phase 1 deposits, both in the cordon and outside of it, became increasingly vegetated over time, indicating increasing landscape stability and/or wetter conditions. The same pattern was observed in the Phase 3 deposits, which were notably more highly vegetated than the Phase 1 deposits. This is very likely due to the significant and fairly rapid sea-level regression during late MIS 5e and MIS 5d, which resulted in the shoreline moving considerably further away than it did during the mid-MIS 5e lowstand.

Palaeo-wind regimes in the study area during Phases 1 and 3 were fairly similar to each other and to the modern winter wind patterns around East London. Alongshore winds from between the west and south-west made the dominant contribution to dune formation. Onshore winds, from the south and south-east, played a significant but considerably lesser role. North-easterly winds, which are most common in summer today, did not form dunes during either phase. It is also likely that rainfall seasonality was fairly similar to present patterns, with relatively dry winters and wetter summers, as this would have amplified the influence of the south-westerlies

on dune formation whilst simultaneously retarding the geomorphic effects of the north-easterlies.

Sea level during Phase 1 was lower than present, but near enough to modern levels for coastal dune formation to take place. The intertidal and supratidal beachrock deposits and raised marine benches and platforms assigned to Phase 2 indicate stepped sea level rise from a level similar to present up to a maximum of between 7.00 m and 8.64 m above mean sea level. This maximum level falls comfortably within the global range of sea level maxima during the second MIS 5e highstand, and is also very similar to maxima reported for this event from the southern coast. During Phase 3, sea level dropped below present levels again, but remained high enough for dune formation to occur in the area for some time. The cessation of dune formation in the study area suggests an eventual significant drop in sea level in MIS 5d. Dune formation only resumed during the Holocene.

7.3. HUMAN-ENVIRONMENTAL INTERACTIONS

The human footprints at Nahoon Point (Mountain 1966; Roberts 2008) are within Phase 1 deposits, as is a single lithic artefact found at Profile 16. The previously reported stone tools from Bats Cave (Deacon 1966) and East Beach (Jacobs & Roberts 2009) and newly discovered lithics in conglomerates around Nahoon Point all fall within Phase 2. Two small lithic assemblages in the upper aeolianites indicate human presence during Phase 3.

Despite the environmental changes that occurred in the study area during Early MIS 5, there appears to have been at least occasional human occupation (of unknown intensity) throughout this period. This is very likely due to the presence of reliable resources which were available for human exploitation. Hornfels and quartzite, the two raw material types identified in the small artefactual assemblages, are both readily available in various outcrops and exposures around East London. The many deeply-entrenched rivers in the area would have provided sources of fresh water for humans and animals alike. A variety of species suitable for human consumption were likely to have lived in the area during this period of time. This includes unidentified ungulate species of a range of sizes, whose presence in the study area is evidenced by previously unreported tracks within Phase 1 aeolianite.

The lithic artefacts in the intertidal deposits indicate human utilisation of this environment in the study area during MIS 5e. This is the only known evidence in South Africa for the exploitation of intertidal marine resources during this period that comes from a site outside of the Greater Cape Floristic Region in the southern and south-western Cape. This suggests that coastal resource use was more widespread during MIS 5e than previously thought.

REFERENCES

Abegg, F.E., Loope, D.B. & Harris, P.M. 2001. Carbonate eolianites – depositional models and diagenesis. In: Abegg, F.E., Loope, D.B. & Harris, P.M (eds) *Modern and ancient carbonate eolianites: sedimentology, sequence stratigraphy, and diagenesis.* SEPM Special Publication 71: 17 – 30.

Adams, A.E. & MacKenzie, W.S. 1998. *A Colour Atlas of Carbonate Sediments and Rocks under the Microscope*. London: Masson Publishing Ltd.

Admiralty. 2005. Approaches to East London. *International Chart Series* No. 4162.

Allen, J.R.L. 1982. *Sedimentary Structures, Their Character and Physical Basis Volume 1*. Amsterdam: Elsevier.

Allen, J.R.L. 1989. Fossil vertebrate tracks and indenter mechanics. *Journal of the Geological Society, London* 146: 600 – 602.

Allen, J.R.L. 1997. Subfossil mammalian tracks (Flandrian) in the Severn Estuary, S.W. Britain: mechanics of formation, preservation and distribution. *Philosophical Transactions of the Royal Society of London, B* 352: 481 – 518.

Andrefsky, W. 2005. *Lithics: Macroscopic approaches to analysis, second edition*. Cambridge: Cambridge University Press.

Anthony, E.J. 2009. *Shore Processes and their Palaeoenvironmental Applications*. Amsterdam: Elsevier.

Avery, D.M. 1987. Late Pleistocene Coastal Environment of the Southern Cape Province of South Africa: Micromammals from Klasies River Mouth. *Journal of Archaeological Science* 14: 405 – 421.

Avery, D.M. 1992. The environment of early modern humans at Border Cave, South Africa: micromammalian evidence. *Palaeogeography, Palaeoclimatology, Palaeoecology*, 91(1-2): 71 – 87.

Avery, D.M. 1993. Last Interglacial and Holocene altithermal environments in South Africa and Namibia: micromammalian evidence. *Palaeogeography, Palaeoclimatology, Palaeoecology* 101: 221 – 228.

Avery, G., Halkett, D., Orton, J., Steele, T., Tusenius M. & Klein, R.G. 2008. The Ysterfontein 1 Middle Stone Age Rock Shelter and the evolution of coastal foraging. *South African Archaeological Society Goodwin Series* 10: 66 – 89.

Avis, A.M. & Lubke, R.A. 1996. Dynamics and succession of coastal dune vegetation in the Eastern Cape, South Africa. *Landscape and Urban Planning* 34(3-4): 237 – 253.

Bada, J.L. & Deems, L., 1975. Accuracy of dates beyond the 14C dating limit using the aspartic acid racemisation reaction. *Nature* 255(5505): 218 – 219.

Bagnold, R.A. 1941. *Physics of blown sand and sand dunes*. New York: William Morrow and Co.

Bagnold, R.A. & Barndorff-Nielsen, O.E. 1980. The pattern of natural size distributions. *Sedimentology* 27: 199 – 207.

Baker, V.R. 2014. Uniformitarianism, earth system science, and geology. *Anthropocene* 5: 76 – 79.

Bard, E., Hamelin, B., Arnold, M., Montaggioni, L., Cabioch, G., Faure, G. & Rougerie, F. 1996. Deglacial sea-level record from Tahiti corals and the timing of global meltwater discharge. *Nature* 382(6588): 241 – 244.

Barham, L.S. & Mitchell, P.J. 2008. *The First Africans: African Archaeology from the Earliest Tool Makers to Most Recent Foragers*. Cambridge: Cambridge University Press.

Barwis, J.H. & Tankard, A.J. 1983. Pleistocene shoreline deposition and sea-level history at Swartklip, South Africa. *Journal of Sedimentary Research* 53(4): 1281 – 1294.

Bateman, M.D., Holmes, P.J., Carr, A.S., Horton, B.P. & Jaiswal, M.K. 2004. Aeolianite and barrier dune construction spanning the last two glacial-interglacial cycles from the southern Cape coast, South Africa. *Quaternary Science Reviews* 23: 1681 – 1698.

Bateman, M.D., Carr, A.S., Dunajko, A.C., Holmes, P.J., Roberts, D.L., McLaren, S.J., Bryant, R.G., Marker, M.E. & Murray-Wallace, C.V. 2011. The evolution of coastal barrier systems: a case study of the Middle-Late Pleistocene Wilderness barriers, South Africa. *Quaternary Science Reviews* 30: 63 – 81.

Bauer, B.O., Davidson-Arnott, R.G.D., Hesp, P.A., Namikas, S.L., Ollerhead, J. & Walker, I.J. 2009. Aeolian sediment transport on a beach: Surface moisture, wind fetch, and mean transport. *Geomorphology* 105: 106 – 116.

Bednarik, R.G. 2003. The earliest evidence of palaeoart. *Rock art research* 20(2): 89 – 136.

Beaumont, P.B. & Vogel, J.C. 2006. On a timescale for the past million years of human history in central South Africa. *South African Journal of Science* 102: 217 – 228.

Beaumont, P.B. & Bednarik, R.G. 2013. Tracing the emergence of palaeoart in sub-Saharan Africa. *Rock Art Research*: 30(1): 1 – 22.

Bezerra, F.H., Barreto, A.M. & Suguio, K. 2003. Holocene sea-level history on the Rio Grande do Norte State coast, Brazil. *Marine Geology* 196(1-2): 73 – 89.

Bird, E. 2008. *Coastal geomorphology: an introduction, second edition*. Chichester: Wiley.

Blanchon, P. & Shaw, J. 1995. Reef drowning during the last deglaciation: evidence for catastrophic sea-level rise and ice-sheet collapse. *Geology* 23 (1): 4 – 8.

Blanchon, P., Eisenhauer, A., Fietzke, J. & Liebetrau, V. 2009. Rapid sea-level rise and reef back-stepping at the close of the last interglacial highstand. *Nature* 458(7240): 881 – 884.

Blott, S.J. & Pye, K. 2001. Gradistat: A Grain Size Distribution and Statistics Package for the Analysis of Unconsolidated Sediments. *Earth Surface Processes and Landforms* 26: 1237 – 1248.

Bluck, B.J. 1967. Sedimentation of beach gravels; examples from South Wales. *Journal of Sedimentary Research* 37: 128 – 156.

Bluck, B.J. 1999. Clast assembling, bed-forms and structure in gravel beaches. *Earth and Environmental Science Transactions of The Royal Society of Edinburgh* 89(4): 291 – 323.

Bluck, B.J. 2011. Structure of gravel beaches and their relationship to tidal range. *Sedimentology* 58(4): 994 – 1006.

Bluck, B.J., Ward, J.D. & Spaggiari, R. 2001. Gravel beaches of southern Namibia. In: Packham, J.R., Randall, R.E., Barnes, R.S.K. & Neal, A. (eds) *Ecology and Geomorphology of Coastal Shingle.* Westbury: Otley: 56 – 76.

Boggs, S. 2014. *Principles of Sedimentology and Stratigraphy, fourth edition*. Upper Saddle River, NJ: Pearson Prentice Hall.

Branch, G.M., Griffiths, C.L., Branch, M.L. & Beckley, L.E. 2007. *Two Oceans: a Guide to the Marine Life of Southern Africa*. Cape Town: Struik.

Bricker, O.P., 1971. Introduction: beachrock and intertidal cement. In: Bricker, O.P. (ed.) *Carbonate Cements.* Baltimore: Johns Hopkins Press: 1 – 13.

Bridge, J. & Demicco, R. 2008. *Earth surface processes, landforms and sediment deposits*. Cambridge: Cambridge University Press.

Botha, G.A. 2018. Lithostratigraphy of the late Cenozoic Maputaland Group. *South African Journal of Geology* 121(1): 95 – 108.

Brink, J.S. 1987. The archaeozoology of Florisbad, Orange Free State. *Memoirs of the National Museum (Bloemfontein)* 24: 1 – 155.

Brooke, B. 2001. The distribution of carbonate eolianite. *Earth-Science Reviews* 55: 135 – 164.

Brookfield, M.E. 1977. The origin of bounding surfaces in ancient eolian sandstones. *Sedimentology* 24: 303 – 332.

Bruggemann, J.H., Buffler, R.T., Guillaume, M.M.M., Walter, R.C., von Cosel, R., Ghebretensae, B.N. & Berhe, S.M. 2004. Stratigraphy, palaeoenvironments and model for the deposition of the Abdur Reef Limestone: context for an important archaeological site from the last interglacial on the Red Sea coast of Eritrea. *Palaeogeography, Palaeoclimatology, Palaeoecology* 203: 179 – 206.

Buffler, R.T., Bruggemann, J.H., Ghebretensae, B.N., Walter, R.C., Guillaume, M.M., Berhe, S.M., McIntosh, W. & Park, L.E. 2010. Geologic setting of the Abdur archaeological site on the Red Sea coast of Eritrea, Africa. *Global and Planetary Change* 72(4): 429 – 450.

Bullock, P., Fedoroff, N., Jongerius, A., Stoops, G. & Tursina, T. 1985. *Handbook for soil thin section description*. Wolverhampton: Waine Research.

Bursey, M. & Wooldridge, T. 2002. Diversity of benthic macrofauna of the flood-tidal delta of the Nahoon Estuary and adjacent beach, South Africa. *African Zoology* 37(2): 231 – 246.

Bustamante, R. & Branch, G. 1996. Large scale patterns and trophic structure of southern African rocky shores: the roles of geographic variation and wave exposure. *Journal of Biogeography* 23(3): 339 – 351.

Bustamante, R.H., Branch, G.M. & Eekhout, S. 1997. The influences of physical factors on the distribution and zonation patterns of South African rocky-shore communities. *South African Journal of Marine Science* 18(1): 119 – 136.

Butzer, K.W. 1978. Sediment Stratigraphy of the Middle Stone Age Sequence at Klasies River Mouth, Tsitsikama Coast, South Africa. *South African Archaeological Bulletin* 33: 141 – 151.

Butzer, K.W. 1988. Sedimentological interpretation of the Florisbad spring deposits, South Africa. *Palaeoecology of Africa* 19: 181 – 189.

Butzer, K.W. 2004. Coastal eolian sands, paleosols, and Pleistocene geoarchaeology of the Southwestern Cape, South Africa. *Journal of Archaeological Science* 31: 1743 – 1781.

Calvet, F., Cabrera, M.C., Carracedo, J.C., Mangas, J., Perez-Torrado, F.J., Recio, C. & Trave, A. 2003. Beachrocks from the island of La Palma (Canary Islands, Spain). *Marine Geology* 197 (1–4): 75 – 93.

Camoin, G.F., Seard, C., Deschamps, P., Webster, J.M., Abbey, E., Braga, J.C., Iryu, Y., Durand, N., Bard, E., Hamelin, B. & Yokoyama, Y. 2012. Reef response to sea-level and environmental changes during the last deglaciation: Integrated Ocean Drilling Program Expedition 310, Tahiti Sea Level. *Geology* 40(7): 643 – 646.

Caputo, M.V. 1995. Sedimentary architecture of Pleistocene eolian calcarenites, San Salvador Island, Bahamas. In: Curran, H.A. & White, B. (eds) *Terrestrial and Shallow Marine Geology of the Bahamas and Bermuda.* Boulder: Geological Society of America: 63 – 76.

Caron, V., 2011. Contrasted textural and taphonomic properties of high-energy wave deposits cemented in beachrocks (St. Bartholomew Island, French West Indies). *Sedimentary Geology* 237(3-4): 189 – 208.

Carr, A.S., Bateman, M.D. & Holmes, P.J. 2007. Developing a 150 ka luminescence chronology for the barrier dunes of the southern Cape, South Africa. *Quaternary Geochronology* 2: 110 – 116.

Carr, A.S., Bateman, M.D., Roberts, D.L., Murray-Wallace, C.V., Jacobs, Z. & Holmes, P.J. 2010. The last interglacial sea-level high stand on the southern Cape coastline of South Africa. *Quaternary Research* 73: 351 – 363.

Carr, A.S., Chase, B.M. & Mackay, A. 2016. Mid to Late Quaternary Landscape and Environmental Dynamics in the Middle Stone Age of Southern South Africa. In: Jones, S.C. & Brian A. Stewart, B.A. (eds) *Africa from MIS 6-2: Population Dynamics and Paleoenvironments.* Dordrecht: Springer Science and Business Media: 23 – 47.

Cawthra, H.C. 2012. The Cenozoic evolution of the Durban Bluff and adjacent continental shelf. *Council for Geoscience Bulletin* 142. Pretoria. 119 pp.

Cawthra, H. & Uken, R. 2012. Modern beachrock formation in Durban, KwaZulu-Natal. *South African Journal of Science* 108: 107 – 112.

Cawthra, H.C. & Bateman, M.D. 2016. Sandy coasts. In: Knight, J. and Grab, S. (eds) *Quaternary environmental change in southern Africa: physical and human dimensions*. Cambridge: Cambridge University Press: 203 – 218.

Cawthra, H.C., Uken, R. & Ovechkina, M. N. 2012a. New Insights into the Geological Evolution of the Durban Bluff and adjacent Blood Reef, South Africa. *South African Journal of Geology* 115: 291 – 308.

Cawthra, H.C., Neumann, F.H., Uken, R., Smith, A.M., Guastella, L.A. & Yates, A. 2012b. Sedimentation on the narrow (8 km wide), oceanic current-influenced continental shelf off Durban, Kwazulu-Natal, South Africa. *Marine Geology* 323–325: 107–122.

Cawthra, H.C., Bateman, M.D., Carr, A.S., Compton, J.S. & Holmes, P.J. 2014. Understanding Late Quaternary change at the land-ocean interface: a synthesis of the evolution of the Wilderness coastline, South Africa. *Quaternary Science Reviews* 99: 210 – 223.

Cawthra, H.C., Compton, J.S., Fisher, E.C., MacHutchon, M.R. & Marean, C.W. 2016. Submerged shorelines and landscape features offshore of Mossel Bay, South Africa. In: Harff, J., Bailey, G. & Lüth, F. (eds) *Geology and Archaeology: Submerged Landscapes of the Continental Shelf*. Geological Society, London, Special Publications 411: 219 – 233.

Cawthra, H.C., Jacobs, Z., Compton, J.S., Fisher, E.C., Karkanas, P. & Marean, C.W. 2018. Depositional and sea-level history from MIS 6 (Termination II) to MIS 3 on the southern continental shelf of South Africa. *Quaternary Science Reviews* 181: 156 – 172.

Chase, B.M. & Thomas, D.S.G. 2006. Late Quaternary dune accumulation along the western margin of South Africa: distinguishing forcing mechanisms through the analysis of migratory dune forms. *Earth and Planetary Science Letters* 251: 318 – 333.

Chen, J.H., Curran, H.A., White, B. & Wasserburg, G.J. 1991. Precise chronology of the last interglacial period: ^{234}U-^{230}Th data from fossil coral reefs in the Bahamas. *Geological Society of America Bulletin* 103(1): 82 – 97.

Clark, J.L. 2011. The evolution of human culture during the later Pleistocene: using fauna to test models on the emergence and nature of 'modern' human behavior. *Journal of Anthropological Archaeology* 30: 273 – 291.

Clark, J.L. & Kandel, A.W. 2013. The evolutionary implications of variation in human hunting strategies and diet breadth during the Middle Stone Age of southern Africa. *Current Anthropology* 54: S269 – S287.

Clifton H.E. 1976. Wave-formed sedimentary structures-a conceptual model. In: Davis, R.A. & Ethington, R.L. (eds) *Beach and Nearshore Sedimentation*. SEPM Special Publication 24: 126 – 148.

Clifton, H.E., Hunter, R.E. & Phillips, R.L. 1971. Depositional structures and processes in the non-barred high-energy nearshore. *Journal of Sedimentary Research* 41(3): 651 – 670.

Cohen, K.M., Finney, S.C., Gibbard, P.L. &Fan, J.X. 2013. The ICS international chronostratigraphic chart. *Episodes* 36(3): 199 – 204.

Compton, J.S. 2011. Pleistocene sea-level fluctuations and human evolution on the southern coastal plain of South Africa. *Quaternary Science Reviews* 30: 506 – 527.

Compton, J.S. 2016. Quaternary environmental change on the southern African coastal plain. In: Knight, J. & Grab, S. (eds) *Quaternary environmental change in Southern Africa: Physical and human dimensions.* Cambridge: Cambridge University Press: 88 – 98.

Cooper, J.A.G. 2001. Geomorphological variability among microtidal estuaries from the wave-dominated South African coast. *Geomorphology* 40: 99 – 122.

Cooper, J.A.G. 2013. Sea Level Studies: Sedimentary indicators of relative sea-level changes - high energy coasts. In: Elias, S.A. (ed) *Encyclopedia of Quaternary Science, second edition.* Amsterdam: Elsevier: 385 – 395.

Cooper, J.A.G. & Flores, R.M. 1991. Shoreline deposits and diagenesis resulting from two Late Pleistocene highstands near +5 and +6 metres, Durban, South Africa. *Marine Geology* 97: 325 – 343.

Cooper, J.A.G., Green, A.N. & Wiles, E.A. 2017. Beachrock morphology and genesis on a paraglacial beach. *Sedimentary Geology* 360: 47 – 53.

Cooper, J.A.G., Green, A.N. & Compton, J.S. 2018. Sea-level change in southern Africa since the Last Glacial Maximum. *Quaternary Science Reviews* 201: 303 – 318.

Cornelis, W.M. & Gabriels, D. 2003. The effect of surface moisture on the entrainment of dune sand by wind: an evaluation of selected models. *Sedimentology* 50: 771 – 790.

Davidson-Arnott, R. 2010. *Introduction to coastal processes and geomorphology*. Cambridge: Cambridge University Press.

Davidson-Arnott R.G.D. & Greenwood B. 1976. Facies relationships on a barred coast, Kouchibouguac Bay, New Brunswick, Canada. In: Davis, R.A. & Ethington, R.L. (eds) *Beach and Nearshore Sedimentation*. SEPM Special Publication 24: 149 – 168.

Davidson-Arnott, R.G.D., MacQuarrie, K. & Aagaard, T. 2005. The effects of wind gusts, moisture content and fetch length on sand transport on a beach. *Geomorphology* 68: 115 – 129.

Davies, O. 1970. Pleistocene beaches of Natal. Annals of the Natal Museum 20: 403 – 442.

Davies, O. 1971. Pleistocene shorelines in the southern and south-eastern Cape Province. *Annals of the Natal Museum* 21: 183 – 279.

Davies, O. 1972. Pleistocene shorelines in the southern and south-eastern Cape Province (Part 2). *Annals of the Natal Museum* 21(2): 225 – 279.

Davies, O. 1973. Pleistocene shorelines in the western cape and South-West Africa. *Annals of the Natal Museum* 21(3): 719 – 765.

Davies, O. 1980. Last Interglacial shorelines in the south Cape. *Palaeontologia africana* 23: 153 – 171.

Deacon, H.J. 1966. The dating of the Nahoon Footprints. *South African Journal of Science* 62: 111 – 113.

Deacon, H.J. & Geleijnse, V.B. 1988. The Stratigraphy and Sedimentology of the Main Site Sequence, Klasies River, SouthAfrica. *South African Archaeological Bulletin* 43: 5 – 14.

d'Errico, F. & Henshilwood, C.S. 2007. Additional evidence for bone technology in the southern African Middle Stone Age. *Journal of Human Evolution* 52: 142 – 163.

d'Errico, F., Vanhaeren, M. & Wadley, L. 2008. Possible shell beads from the Middle Stone Age layers of Sibudu Cave, South Africa. *Journal of Archaeological Science* 35: 2675 – 2685.

Desruelles, S., Fouache, E., Ciner, A., Dalongeville, R., Pavlopoulos, K., Kosun, E., Coquinot, Y. & Potdevin, J.-L. 2009. Beachrocks and sea level changes since Middle Holocene: comparison between the insular group of Mykonos–Delos–Rhenia (Cyclades, Greece) and the southern coast of Turkey. *Global and Planetary Change* 66: 19 – 33.

Dias, K.A. 2014. *High-Resolution Methodology for Particle Size Analysis of Naturally Occurring Sand Size Sediment Through Laser Diffractometry WITH Application to Sediment Cores: Kismet, Fire Island, New York*. Unpublished MSc Thesis. Stony Brook University, USA.

Doe, T.W. & Dott, R.H., JR. 1980. Genetic significance of deformed cross bedding—with examples from the Navajo and Weber Sandstones of Utah. *Journal of Sedimentary Petrology* 50: 793 – 812.

Doucette, J.S. 2000. The distribution of nearshore bedforms and effects on sand suspension on low-energy, micro-tidal beaches in Southwestern Australia. *Marine Geology* 165(1-4): 41 – 61.

Dravis, J.J. 1996. Rapidity of freshwater calcite cementation – implications for carbonate diagenesis and sequence stratigraphy. *Sedimentary Geology* 107: 1 – 10.

Dumas, B., Hoang, C.T. & Raffy, J. 2006. Record of MIS 5 sea-level highstands based on U/Th dated coral terraces of Haiti. *Quaternary International* 145: 106 – 118.

Dunham, R.J. 1971. Meniscus cement. In: Bricker, O.P. (ed) *Carbonate Cements.* Baltimore: Johns Hopkins Press: 297 – 300.

Dusseldorp, G.L. 2010. Prey choice during the South African Middle Stone Age: avoiding dangerous prey or maximising returns? *African Archaeological Review* 27: 107 – 133.

Dusseldorp, G.L. 2012. Tracking the influence of technological change on Middle Stone Age hunting strategies in South Africa. *Quaternary International* 270: 70 – 79.

Dutton, A. & Lambeck, K. 2012. Ice volume and sea level during the last interglacial. *Science* 337(6091): 216 – 219.

Fairbridge, R.W. & Johnson, D.L. 1978. Eolianite. In: Fairbridge, R.W. & Bourgeois, J. (eds) *The Encyclopedia of Sedimentology.* Stroudsburg, PA: Dowden, Hutchinson and Ross: 279 – 282.

Faith, J.T. 2008. Eland, buffalo and wild pigs: were Middle Stone Age humans ineffective hunters? *Journal of Human Evolution* 55: 24 – 36.

Faith, J.T. 2011. Ungulate biogeography, statistical methods, and the proficiency of Middle Stone Age hunters. *Journal of Human Evolution* 60(3): 315 – 317.

Feathers, J.K. 2002. Luminescence dating in less than ideal conditions: case studies from Klasies River main site and Duinefontein, South Africa. *Journal of Archaeological Science* 29: 177 – 194.

Fisher, E.C., Bar-Matthews, M., Jerardino, A. & Marean, C.W. 2010. Middle and Late Pleistocene paleoscape modeling along the southern coast of South Africa. *Quaternary Science Reviews* 29: 1382 – 1398.

Fisher, E.C., Albert, R.M., Botha, G., Cawthra, H.C., Esteban, I., Harris, J., Jacobs, Z., Jerardino, A., Marean, C.W., Neumann, F.H. & Pargeter, J. 2013. Archaeological reconnaissance for middle stone age sites along the Pondoland Coast, South Africa. *PaleoAnthropology* 2013:104 – 137.

Fisher, E.C., Cawthra, H.C., Esteban, I., Jacobs, Z., Jerardino, A., Miller, C., Neumann, F.H., Oertle, A., Pargeter, J., Saktura, R., Schefuss, E. & Szabo, K. 2019. Coastal occupation and foraging during the Late Pleistocene and early Holocene at Waterfall Bluff, eastern Pondoland, South Africa. *22nd Biennial Congress of the Southern African Society for Quaternary Research, Mossel Bay, 29 – 31 January 2019*.

Flemming, B.W. 1978. Underwater sand dunes along the southeast African continental margin-observations and implications. *Marine Geology* 26: 177 – 198.

Flemming, B,W. 1980. Sand transport and bedform patterns on the continental shelf between Durban and Port Elizabeth (southeast African continental margin). *Sedimentary Geology* 26: 179 – 205.

Flemming, B.W. 1981. Factors controlling shelf sediment dispersal along the southeast African continental margin. *Marine Geology* 42: 259 – 277.

Flügel, E. 2004. *Microfacies of Carbonate Rocks: Analysis, Interpretation and Application*. Berlin: Springer-Verlag.

Folk, R.L. 1966. A review of grain-size parameters. *Sedimentology* 6: 73 – 93.

Folk, R.L. 1971. Longitudinal dunes of the northwestern edge of the Simpson Desert, Northern Territory, Australia, 1. Geomorphology and grain size relationship. *Sedimentology* 16: 5 – 54.

Fornos, J.J., Bromley, R.G., Clemmensen, L.A. & Rodriguezperea, A. 2002, Tracks and trackways of *Myotragus balearicus* Bate (Artiodactyla, Caprinae) in Pleistocene aeolianites from Mallorca (Balearic Islands, Western Mediterranean). *Palaeogeography, Palaeoclimatology, Palaeoecology* 180: 277 – 313.

Frankel, E. 1968. Rate of formation of beach rock. *Earth and Planetary Science Letters* 4: 439 – 440.

Frébourg, G., Hasler, C.A., Le Guern, P. & Davaud, E. 2008. Facies characteristics and diversity in carbonate eolianites. *Facies* 54(2): 175 – 191.

Friedman, G.M. 1964. Early diagenesis and lithification in carbonate sediments. *Journal of Sedimentary Petrology* 34: 777 – 813.

Fryberger, S.G., Ahlbrandt, T.S. & Andrews, S. 1979. Origin, sedimentary features, and significance of low-angle aeolian 'sand sheet' deposits, Great Sand Dunes National Monument and vicinity, Colorado. *Journal of Sedimentary Petrology* 49: 733 – 746.

Gardner, R.A. & McLaren, S.J. 1994. Variability in early vadose carbonate diagenesis in sandstones. *Earth-Science Reviews* 36: 27 – 45.

Gischler, E. 2007. Beachrock and intertidal precipitates. In: Nash, D.J. & McLaren, S.J. (eds) *Geochemical Sediments and Landscapes.* Malden, MA: Blackwell: 365 – 390.

Gischler, E. 2014. Quaternary reef response to sea-level and environmental change in the western Atlantic. *Sedimentology* 62(2): 429 – 465.

Gischler, E. & Lomando, A.J. 1997. Holocene cemented beach deposits in Belize. Sedimentary Geology 110 (3–4): 277 – 297.

Goldsmith, V. 1985. Coastal dunes. In: Davis, R.A. (ed) *Coastal sedimentary environments.* New York: Springer: 303 – 378.

Goudie, A.S. 1983. Calcrete. In: Goudie, A.S. & Pye, K. (eds) *Chemical Sediments and Geomorphology.* London: Academic Press: 93 – 131.

Govin, A., Capron, E., Tzedakis, P.C., Verheyden, S., Ghaleb, B., Hillaire-Marcel, C., St-Onge, G., Stoner, J.S., Bassinot, F., Bazin, L. & Blunier, T. 2015. Sequence of events from the onset to the demise of the Last Interglacial: Evaluating strengths and limitations of chronologies used in climatic archives. *Quaternary Science Reviews* 129: 1 – 36.

Grün, R., Brink, J.S., Spooner, N.A., Taylor, L., Stringer, C.B., Franciscus R.G. & Murray, A.S. 1996. Direct dating of Florisbad hominid. *Nature* 382: 500 – 501.

Grün, R., Beaumont, P.B., Tobias, P.V. & Eggins, S.M. 2003. On the age of the Border Cave 5 human mandible. *Journal of Human Evolution* 45: 155 – 167.

Halkett, D.J, Hart, T., Yates, R.J., Volman, T.P., Parkington, J.E., Orton, J., Klein, R.G., Cruz-Uribe, K. & Avery, G. 2003. First excavation of intact Middle Stone Age layers at Ysterfontein, Western Cape Province, South Africa: implications for Middle Stone Age ecology. *Journal of Archaeological Science* 30: 955 – 971.

Hanor, J.S. 1978. Precipitation of beachrock cements: mixing of marine and meteoric waters vs. CO2-degassing. *Journal of Sedimentary Petrology* 48: 489 – 501.

Haslett, S.K. & Curr, R.H. 2001. Stratigraphy and palaeoenvironmental development of Quaternary coarse clastic beach deposits at Plage de Mezpeurleuch, Brittany (France). *Geological Journal* 36(2): 171 – 182.

Hearty, P.J. 2002. The Kaena highstand on Oahu, Hawaii: further evidence of Antarctic Ice collapse during the middle Pleistocene. *Pacific Science* 56 (1): 65 – 82.

Hearty, P.J. & Neumann, A.C. 2001. Rapid sea level and climate change at the close of the Last Interglaciation (MIS 5e): evidence from the Bahama Islands. *Quaternary Science Reviews* 20(18): 1881 – 1895.

Hearty, P.J., Kindler, P., Cheng, H. & Edwards, R.L. 1999. A+20m middle Pleistocene sea-level highstand (Bermuda and the Bahamas) due to partial collapse of Antarctic ice. *Geology* 27: 375 – 378.

Hearty, P.J., Hollin, J.T., Neumann, A.C., O'Leary, M.J. & McCulloch, M. 2007. Global sea-level fluctuations during the Last Interglaciation (MIS 5e). *Quaternary Science Reviews* 26: 2090 – 2112.

Heiri, O., Lotter, A.F. & Lemcke, G. 2001. Loss on ignition as a method for estimating organic and carbonate content in sediments: reproducibility and comparability of results. *Journal of Paleolimnology* 25: 101 – 110.

Helm, C.W., Anderson, R.J., Buckley, L.G., Cawthra, H.C. & de Vynck, J.C. 2017. Biofilm assists recognition of avian trackways in Late Pleistocene coastal aeolianites, South Africa. *Palaeontologia africana* 52: 78 – 84.

Helm, C., Cawthra, H., Cowling, R., De Vynck, J., Marean, C., McCrea, R. & Rust, R. 2018a. Palaeoecology of giraffe tracks in Late Pleistocene aeolianites on the Cape south coast. *South African Journal of Science* 114(1-2): 1 – 8.

Helm, C.W., McCrae, R.T., Lockley, M.G., Cawthra, H.C., Thesen, G.H. & Mwankunda, J.M. 2018b. Late Pleistocene vertebrate trace tossils in the Goukamma Nature Reserve, Cape South Coast, South Africa. *Palaeontologia africana* 52: 89 – 101.

Helm, C.W., McCrea, R.T., Cawthra, H.C., Lockley, M.G., Cowling, R.M., Marean, C.W., Thesen, G.H., Pigeon, T.S. & Hattingh, S. 2018c. A New Pleistocene Hominin Tracksite from the Cape South Coast, South Africa. *Scientific Reports* 8(1): 3772. https://doi.org/10.1038/s41598-018-22059-5.

Helm, C.W., Cawthra, H.C., De Vynck, J., Lockley, M.G., McCrae, R.T. & Venter, J. 2019. The Pleistocene fauna of the Cape south coast revealed through ichnology at two localities. *South African Journal of Science* 115 (1-2): 1 – 9.

Henshilwood, C.S. 2007. Fully symbolic Sapiens behaviour: innovation in the middle stone age at Blombos cave, South Africa. In: Mellars, P., Boyle, K., Bar-Yosef, O. & Stringer, C. (eds) *Rethinking the human revolution: new behavioural and biological perspectives on the origin and dispersal of modern humans.* Cambridge: McDonald Institute for Archaeological Research: 123 – 132.

Henshilwood, C.S. & Marean, C.W. 2003. The Origin of Modern Human Behavior: Critique of the Models and Their Test Implications. *Current Anthropology* 44(5): 627 – 651.

Henshilwood, C.S. & Lombard, M. 2013. Becoming Human: Archaeology of the Sub-Saharan Middle Stone Age. In: Renfrew, C. & Bahn, P. (eds) *The Cambridge World Prehistory, Volume 1.* Cambridge: Cambridge University Press: 106 – 130.

Henshilwood, C.S., d'Errico, F., Marean, C.W., Milo, R.G. & Yates, R. 2001. An early bone tool industry from the Middle Stone Age at Blombos Cave, South Africa: implications for the origins of modern human behaviour, symbolism and language. *Journal of Human Evolution* 41: 631 – 678.

Henshilwood, C.S., d'Errico, F., Yates, R., Jacobs, Z., Tribolo, C., Duller, G.A.T., Mercier, N., Sealy, J., Valladas, H., Watts, I. & Wintle, A.G. 2002. The emergence of modern human behaviour: Middle Stone Age engravings from South Africa. *Science* 295: 1278 – 1280.

Henshilwood, C.S., d'Errico, F., Vanhaeren, M., van Niekerk, K. & Jacobs, Z. 2004. Middle Stone Age shell beads from South Africa. *Science* 304: 404.

Henshilwood, C.S., d'Errico, F. & Watts, I. 2009. Engraved ochres from the Middle Stone Age levels at Blombos Cave, South Africa. *Journal of Human Evolution* 57: 27 – 47.

Henshilwood, C.S., d'Errico, F., van Niekerk, K.L., Coquinot, Y., Jacobs, Z., Lauritzen, S.-E., Menu, M. & García-Moreno, R. 2011. A 100,000-year-old ochre-processing workshop at Blombos Cave, South Africa. *Science* 334: 219 – 222.

Henshilwood, C.S., d'Errico, F., van Niekerk, K.L., Dayet, L., Queffelec, A. & Pollarolo, L. 2018. An abstract drawing from the 73,000-year-old levels at Blombos Cave, South Africa. *Nature* 562(7725): 115 – 118.

Herries, A.I. 2011. A chronological perspective on the Acheulian and its transition to the Middle Stone Age in southern Africa: the question of the Fauresmith. *International Journal of Evolutionary Biology* 2011: 1 – 25.

Hesp, P. 1988. Morphology, dynamics and internal stratification of some established foredunes in southeast Australia. *Sedimentary Geology* 55(1-2): 17 – 41.

Hesp, P. 2002. Foredunes and blowouts: initiation, geomorphology and dynamics. *Geomorphology* 48(1-3): 245 – 268.

Hesp, P. 2004. Coastal dunes in the tropics and temperate regions; location, formation, morphology and vegetation processes. In: Martinez, M.L. & Psuty, N.P. (eds) *Coastal Dunes, Ecology and Conservation.* Berlin: Springer-Verlag: 29 – 49.

Hillestad-Nel, T., Wurz, S. & Henshilwood, C.S. 2018. Small mammals from marine isotope stage 5 at Klasies River, South Africa–reconstructing the local palaeoenvironment. *Quaternary International* 471: 6 – 20.

Hopley, D. 1986. Beachrock as a sea-level indicator. In: van de Plassche, O. (ed) *Sea-Level Research.* Dordrecht: Springer: 157 – 173.

Horowitz, D.H. 1982. Geometry and origin of large-scale deformation structures in some ancient windblown sand deposits. *Sedimentology* 29: 155 – 180.

Hunter, R.E. 1977a. Basic types of stratification in small eolian dunes. *Sedimentology* 24: 361 – 387.

Hunter, R.E. 1977b. Terminology of cross-stratified sedimentary layers and climbing-ripple structures. *Journal of Sedimentary Petrology* 47(2): 697 – 706.

Hunter, R.E. 1981. Stratification styles in eolian sandstones: some Pennsylvanian to Jurassic examples from the western interior U.S.A. In: Ethridge, F.G. & Flores, R.M. (eds) *Recent and Ancient Nonmarine Depositional Environments: Models for Exploration.* SEPM Special Publication 31: 315 – 332.

Hunter, R.E., Clifton, H.E. & Phillips, R.L. 1979. Depositional processes, sedimentary structures, and predicted vertical sequences in barred nearshore systems, southern Oregon coast. *Journal of Sedimentary Research* 49(3): 711 – 726.

Huntley, D.J. 2002. Comment on ‘‘Luminescence dating of coastal sands: overcoming changes in environmental dose rate’’ by J.C. Vogel, A.G. Wintle and S.M. Woodborne. *Journal of Archaeological Science* 29: 559 – 560.

Illenberger, W.K. 1992. *Sediment dynamics of the Sundays River mouth area, Algoa Bay*. Unpublished PhD thesis. University of Port Elizabeth.

Illenberger, W.K. 1996. The geomorphologic evolution of the wilderness dune cordons, South Africa. *Quaternary International* 33: 11 – 20.

Jackson, D.W.T., Cooper, J.A.G. & Green, A.N. 2014. A preliminary classification of coastal sand dunes of KwaZulu-Natal. *Journal of Coastal Research* 70: 718 – 722.

Jacobs, Z. 2010. An OSL chronology for the sedimentary deposits from Pinnacle Point Cave 13B – A punctuated presence. *Journal of Human Evolution* 59: 289 – 305.

Jacobs, Z. & Roberts, D.L. 2009. Last Interglacial Age for aeolian and marine deposits and the Nahoon fossil human footprints, Southeast Coast of South Africa. *Quaternary Geochronology* 4: 160 – 169.

Jacobs, Z., Roberts, R. G., Lachlan, T. J., Karkanas, P., Marean, C. W. & Roberts, D. L. 2011. Development of the SAR TT-OSL procedure for dating Middle Pleistocene dune and shallow marine deposits along the southern Cape coast of South Africa. *Quaternary Geochronology* 6: 491 – 513.

James, N.P. & Ginsburg, R.N., 1990. Extracts from the Seaward margin of the Belize barrier and atoll reefs. In: Tucker, M.E. & Bathurst, R.G.C. (eds) *Carbonate Diagenesis.* Oxford: Blackwell Scientific Publications: 55 – 80.

Jerardino, A. 2016. On the origins and significance of Pleistocene coastal resource use in southern Africa with particular reference to shellfish gathering. *Journal of Anthropological Archaeology* 41: 213 – 230.

Jerardino, A. & Marean, C.W. 2010. Shellfish gathering, marine paleoecology and modern human behaviour: perspectives from cave PP13B Pinnacle Point, South Africa. *Journal of Human Evolution* 59: 412 – 424.

Jouzel, J., Masson-Delmotte, V., Cattani, O., Dreyfus, G., Falourd, S., Hoffmann, G., Minster, B., Nouet, J., Barnola, J.M., Chappellaz, J. & Fischer, H. 2007. Orbital and millennial Antarctic climate variability over the past 800,000 years. *Science* 317(5839): 793 – 796.

Kelletat, D. 2006. Beachrock as sea-level indicator? Remarks from a geomorphological point of view. *Journal of Coastal Research* 22 (6): 1555 – 1564.

Kelly, C.S., Green, A.N., Cooper, J.A.G. & Wiles, E. 2014. Beachrock facies variability and sea level implications: a preliminary study. *Journal of Coastal Research*, 70: 736 – 742.

Kilburn, R. & Rippey, E. 1982. *Sea Shells of Southern Africa*. Johannesburg: Macmillan South Africa.

Kindler, P. & Bain, R.J. 1993. Submerged upper Holocene beachrock on San Salvador Island, Bahamas: implications for recent sea-level history. *Geologische Rundschau* 82: 241 – 247.

Kindler, P. & Mazzolini, D. 2001. Sedimentology and petrography of dredged carbonate sands from Stocking Island (Bahamas); implications for meteoric diagenesis and aeolianite formation. *Palaeogeography, Palaeoclimatology, Palaeoecology* 175: 369 – 379.

Klappa, C.F. 1980. Rhizoliths in terrestrial carbonates: classification, recognition, genesis and significance. *Sedimentology* 27(6): 613 – 629.

Klein, R.G. 1976. The Mammalian Fauna of the Klasies River Mouth Sites, Southern Cape Province, South Africa. *South African Archaeological Bulletin* 31: 75 – 98.

Klein, R.G. 1979. Stone Age exploitation of animals in southern Africa. *American Scientist* 67(2): 151 – 160.

Klein, R.G. 2001. Southern Africa and Modern Human Origins. *Journal of Anthropological Research* 57: 1 – 16.

Klein, R.G. 2008. Out of Africa and the evolution of human behavior. *Evolutionary Anthropology: Issues, News, and Reviews* 17: 267 – 281.

Klein, R.G. & Cruz-Uribe, K. 1996. Exploitation of large bovids and seals at Middle and Later Stone Age sites in South Africa. *Journal of Human Evolution* 31(4): 315 – 334.

Klein, R.G. & Edgar, B. 2002. *The Dawn of Human Culture*. New York: John Wiley and Sons, Inc.

Klein, R.G. & Bird, D.W. 2016. Shellfishing and human evolution. *Journal of Anthropological Archaeology* 44: 198 – 205.

Klein, R.G., Avery, G., Cruz-Uribe, K., Halkett, D., Parkington, J.E., Steele, T., Volman, T.P. & Yates, R. 2004. The Ysterfontein 1 Middle Stone Age site, South Africa, and early human exploitation of coastal resources. *Proceedings of the National Academy of Sciences of the United States of America* 101: 5708 – 5715.

Knight, J. 2007. Beachrock Reconsidered. Discussion of: Beachrock as Sea-Level Indicator? Remarks from a Geomorphological Point of View. Journal of Coastal Research, 22 (6), 1558–1564. *Journal of Coastal Research* 23(4): 1074 – 1078.

Knight, J. & Harrison, S. 2014. Limitations of uniformitarianism in the Anthropocene. *Anthropocene* 5: 71 – 75.

Knight, J. & Grab, S. 2015. Rocky Shorelines of the Wild Coast. In: Grab, S. & Knight, J. (eds) *Landscapes and Landforms of South Africa.* Cham: Springer: 57 – 63.

Kocurek, G. 1981. Significance of interdune deposits and bounding surfaces in aeolian dune sands. *Sedimentology* 28(6): 753 – 780.

Kocurek, G. 1988. First-order and super bounding surfaces in eolian sequences – bounding surfaces revisited. *Sedimentary Geology* 56: 193 – 206.

Kocurek, G. 1991. Interpretation of ancient eolian sand dunes. *Annual Review of Earth and Planetary Sciences* 19: 43 – 75.

Kocurek, G. 1996. Desert aeolian systems. In: Reading, H.G. (ed) *Sedimentary Environments: Processes, Facies and Stratigraphy, third edition.* Malden, MA: Blackwell: 125 – 153.

Kocurek, G. & Dott, R.H. 1981. Distinctions and uses of stratification types in the interpretation of eolian sand. *Journal of Sedimentary Research* 51(2): 579 – 595.

Konert, M. & Vandenberghe, J. 1997. Comparison of laser grain size analysis with pipette and sieve analysis: a solution for the underestimation of the clay fraction. *Sedimentology* 44: 523 – 535.

Kopp, R.E., Simons, F.J., Mitrovica, J.X., Maloof, A.C. & Oppenheimer, M. 2009. Probabilistic assessment of sea level during the last interglacial stage. *Nature* 462(7275): 863 – 867.

Kopp, R.E., Simons, F.J., Mitrovica, J.X., Maloof, A.C. & Oppenheimer, M. 2013. A probabilistic assessment of sea level variations within the last interglacial stage. *Geophysical Journal International* 193(2): 711 – 716.

Kuman, K.A., Inbar, M. & Clarke, R.J. 1999. Palaeoenvironments and cultural sequence of the Florisbad Middle Stone Age hominid site, South Africa. *Journal of Archaeological Science* 26: 1409 – 1426.

Kyriacou, K., Parkington, J.E., Will, M., Kandel, A.W. & Conard, N.J. 2015. Middle and Later Stone Age shellfish exploitation strategies and coastal foraging at Hoedjiespunt and Lynch Point, Saldanha Bay, South Africa. *Journal of Archaeological Science* 57: 197 – 206.

Laidler, P.W. 1933. Dating evidence concerning the Middle Stone Ages and a Capsio-Wilton culture, in the south-east Cape. *South African Journal of Science* 30(7): 530 – 542.

Laidler, P.W. 1934. The archaeological and geological sequence in the Transkei and Ciskei. *South African Journal of Science* 31(7): 535 – 546.

Lambeck, K., Esat, T.M. & Potter, E.K. 2002. Links between climate and sea levels for the past three million years. *Nature* 419(6903): 199 – 206.

Lambeck, K., Purcell, A. & Dutton, A. 2012. The anatomy of interglacial sea levels: the relationship between sea levels and ice volumes during the Last Interglacial. *Earth and Planetary Science Letters* 315: 4 – 11.

Lancaster N. 1993. Origins and sedimentary features of supersurfaces in the northwestern Gran Desierto sand sea. In: Pye, K. & Lancaster, N. (eds) *Aeolian Sediments: Ancient and Modern.* Oxford: Blackwell Scientific: 71 – 83.

Langejans, G.H.J., van Niekerk, K.L., Dusseldorp, G.L. & Thackeray, J.F. 2012. Middle Stone Age shellfish exploitation: potential indications for mass collecting and resource intensification at Blombos Cave and Klasies River, South Africa. *Quaternary International* 270: 80 – 94.

Langejans, G.H., Dusseldorp, G.L. & Thackeray, J.F. 2017. Pleistocene molluscs from Klasies River (South Africa): Reconstructing the local coastal environment. *Quaternary International* 427: 59 – 84.

Le Roux, F.G. 1989a. Lithostratigraphy of the Nahoon Formation (Algoa Group). *South African Committee for Stratigraphy, Lithostratigraphic Series* 9. Pretoria: South African Geological Survey.

Le Roux, F.G. 1989b. *The lithostratigraphy of Cenozoic deposits along the south-east cape coast as related to sea-level changes*. Unpublished MSc thesis. University of Stellenbosch.

Le Roux, F.G. 1991. Lithostratigraphy of the Salnova Formation (Algoa Group). *South African Committee for Stratigraphy, Lithostratigraphic Series* 11. Pretoria: South African Geological Survey.

Lea, P.D. 1996. Vertebrate tracks in Pleistocene eolian sand-sheet deposits of Alaska. *Quaternary Research* 45: 226 – 240.

Lipar, M., Webb, J.A., Cupper, M.L. & Wang, N. 2017. Aeolianite, calcrete/microbialite and karst in southwestern Australia as indicators of Middle to Late Quaternary palaeoclimates. *Palaeogeography, Palaeoclimatology, Palaeoecology* 470: 11 – 29.

Livingstone, I. & Warren, A. 1996. *Aeolian geomorphology: an introduction*. Harlow: Longman.

Lockley, M. 1991. *Tracking Dinosaurs*. Cambridge: Cambridge University Press.

Loizeau, J-L., Arbouille, D., Santiago, S. & Vernet, J-P. 1994. Evaluation of a wide range laser diffraction grain size analyser for use with sediments. *Sedimentology* 41: 353 – 361.

Lombard, M. 2005. Evidence of hunting and hafting during the Middle Stone Age at Sibudu Cave, KwaZulu-Natal, South Africa: a multianalytical approach. *Journal of Human Evolution* 48: 279 – 300.

Lombard, M. 2007a. Evidence for change in Middle Stone Age hunting behaviour at Blombos Cave: results of a macrofracture analysis. *South African Archaeological Bulletin* 62(185): 62 – 67.

Lombard, M. 2007b. The gripping nature of ochre: the association of ochre with Howiesons Poort adhesives and Later Stone Age mastics from South Africa. *Journal of Human Evolution* 53(4): 406 – 419.

Lombard, M. & Phillipson, L. 2010. Indications of bow and stone-tipped arrow use 64 000 years ago in KwaZulu-Natal, South Africa. *Antiquity* 84: 635 – 648.

Lombard, M., Wadley, L., Deacon, J., Wurz, S., Parsons, I., Mohapi, M., Swart, J. & Mitchell, P. 2012. South African and Lesotho Stone Age sequence updated (I). *South African Archaeological Bulletin* 67: 123 – 144.

Long, A.J., Barlow, N.L.M., Busschers, F.S., Cohen, K.M., Gehrels, W.R. & Wake, L.M. 2015. Near-field sea-level variability in northwest Europe and ice sheet stability during the last interglacial. *Quaternary Science Reviews* 126: 26 – 40.

Longman, M.W. 1980. Carbonate diagenetic textures from nearsurface diagenetic environments. *AAPG Bulletin* 64: 461 – 487.

Loope, D.B., 1986. Recognizing and utilizing vertebrate tracks in cross-section: *PALAIOS* 1: 141 – 151.

MacFarlane, D.R. 1937. On the East London levallois. *South African Journal of Science* 33(3): 893 – 903.

Mackay, A. & Welz, A. 2008. Engraved ochre from a Middle Stone Age context at Klein Kliphuis in the Western Cape of South Africa. *Journal of Archaeological Science* 35: 1521 – 1532.

Manger, G.E. 1963. Porosity and bulk density of sedimentary rocks. *Geological Survey Bulletin* 1144-E: 1 – 55.

Marean, C.W. 2010. Pinnacle Point Cave 13B (Western Cape Province, South Africa) in context: The Cape Floral kingdom, shellfish, and modern human origins. *Journal of Human Evolution* 59: 425 – 443.

Marean, C.W. 2014. The origins and significance of coastal resource use in Africa and Western Eurasia. *Journal of Human Evolution* 77:17 – 40.

Marean, C.W. 2016. The transition to foraging for dense and predictable resources and its impact on the evolution of modern humans. *Philosophical Transactions of the Royal Society B* 371: 20150239. http://dx.doi.org/10.1098/rstb.2015.0239.

Marean, C.W., Bar-Matthews, M.,Bernatchez, J., Fisher, E., Goldberg, P., Herries, A.I.R., Jacobs, Z., Jerardino, A., Karkanas, P., Minichillo, T.,Nilssen, P.J., Thompson, E., Watts, I. & Williams, H.M. 2007. Early human use of marine resources and pigment in South Africa during the Middle Pleistocene. *Nature* 449: 905 – 908.

Marean, C.W., Cawthra, H.C., Cowling, R.M., Esler, K.J., Fisher, E., Milewski, A., Potts, A.J., Singels, E. & De Vynck, J. 2014. Stone age people in a changing South African greater Cape Floristic Region. In: Allsopp, N., Colville, J.F. & Verboom, G.A. (eds) *Fynbos: ecology, evolution, and conservation of a megadiverse region.* Oxford: Oxford University Press: 164 – 199.

Marker, M.E. 1984. Marine benches of the Eastern Cape, South Africa. *South African Journal of Geology* 87(1): 11 – 18.

Marker, M.E. 1987. A note on marine benches of the southern Cape. *South African Journal of Geology* 90(2): 120 – 123.

Martin, A.K. & Flemming, B.W. 1987. Aeolianites of the South African coastal zone and continental shelf as sea-level indicators. *South African Journal of Science* 83: 507 – 508.

Martin, A.K. & Flemming, B.W. 1988. Physiography, structure, and geological evolution of the Natal continental shelf. In: Schumann, E.H. (ed.) *Coastal Ocean Studies off Natal, South Africa.* Lecture Notes on Coastal and Estuarine Studies 26: 11 – 46.

Matthews, T., Rector, A., Jacobs, Z., Herries, A.I. & Marean, C.W. 2011. Environmental implications of micromammals accumulated close to the MIS 6 to MIS 5 transition at pinnacle Point cave 9 (Mossel Bay, Western Cape Province, South Africa). *Palaeogeography, Palaeoclimatology, Palaeoecology* 302(3-4): 213 – 229.

Maud, R.R. 1968. Quaternary geomorphology and soil formation in coastal Natal. *Zeitschrift für Geomorphologie*, Supplement 7: 155 – 199.

Mauz, B., Vacchi, M., Green, A., Hoffmann, G. & Cooper, A. 2015. Beachrock: a tool for reconstructing relative sea level in the far-field. *Marine Geology* 362: 1 – 16.

McBrearty, S. 2007. Down with the Revolution. In: Mellars, P., Boyle, K., Bar-Yosef, O. & Stringer, C. (eds) *Rethinking the human revolution: new behavioural and biological perspectives on the origin and dispersal of modern humans.* Cambridge: McDonald Institute for Archaeological Research: 133 – 151.

McBrearty, S. & Brooks, A. 2000. The revolution that wasn't: a new interpretation of the origin of modern human behavior. *Journal of Human Evolution* 39: 453 – 563.

McKee, E.D. & Bigarella, J.J. 1972. Deformational structures in Brazilian coastal dunes. *Journal of Sedimentary Petrology* 42: 670 – 681.

McKee E.D. & Ward W.C. 1983. Eolian environment. In: Scholle, P.A., Bebout, D.G. & Moore, C.H. (eds) *Carbonate Depositional Environments.* Tulsa: American Association of Petroleum Geologists: 132 – 170.

McKee, E.D., Douglass, J.R. & Rittenhouse, S. 1971. Deformation of lee-side laminae in eolian dunes. *Geological Society of America Bulletin* 82: 359 – 378.

McLachlan, A. 1996. Physical factors in benthic ecology: effects of changing sand particle size on beach fauna. *Marine Ecology Progress Series* 131: 205 – 217.

McLachlan, A. & Hanekom, N. 1979. Aspects of the biology, ecology and seasonal fluctuations in biochemical composition of Donax serra in the East Cape. *South African Journal of* Zoology 14: 183 – 193.

McLaren, S. 1993. Use of cement types in the palaeoenvironmental interpretation of coastal aeolianite sequences. In: Pye, K (ed) *The Dynamics and Environmental Context of Aeolian Sedimentary Systems*. Geological Society of London, Special Publication 72: 235 – 246.

McLaren, S.J. 1995. The role of sea spray in vadose diagenesis in Late Pleistocene coastal deposits. *Journal of Coastal Research* 11: 1075 – 1088.

McLaren, S.J. 2001. Effects of sea spray on vadose diagenesis of late Quaternary aeolianites, Bermuda. *Journal of Coastal Research* 17: 228 – 240.

McLaren, S.J. 2007. Aeolianite. In: Nash, D.J. & McLaren, S.J. (eds) *Geochemical Sediments and Landscapes.* Oxford: Blackwell: 144 – 172.

McLaren, S. & Gardner, R. 2004. Late quaternary vadose carbonate diagenesis in coastal and desert dune and beach sands: Is there a palaeoclimatic signal? *Earth Surface Processes and Landforms* 29: 1441 – 1458.

McQuaid, C.D. & Branch, G.M. 1984. The influence of sea temperature, substratum and wave exposure on rocky shore intertidal communities: an analysis of faunal and flora biomass. *Marine Ecology Progress Series* 19: 145 – 151.

Melgarejo, J.C. & Martin, R.F. 2011. *Atlas of non-silicate minerals in thin section*. The Canadian Mineralogist, Special Publication 7. 522 pp.

Meyers, J.H. 1987. Marine vadose beachrock cementation by cryptocrystalline magnesian calcite- Maui, Hawaii. *Journal of Sedimentary Petrology* 57: 558 – 570.

Miall, A.D. 1977. Lithofacies Types and Vertical Profile Models in Braided River Deposits: A Summary. *Fluvial Sedimentology* – Memoir 5: Pages 597 – 604.

Miall, A. D. 1996. *The Geology of Fluvial Deposits: Sedimentary Facies, Basin Analysis and Petroleum Geology*. Heidelberg: Springer-Verlag Inc.

Miall, A.D. 2014. Updating uniformitarianism: stratigraphy as just a set of 'frozen accidents'. In: Smith, D.G., Bailey, R.J., Burgess, P.M. & Fraser, A.J. (eds) *Strata and Time: Probing the Gaps in Our Understanding.* Geological Society, London, Special Publications 404: 11 – 36.

Milan, J. & Bromley, R.G. 2006. True tracks, undertracks and eroded tracks, experimental work with tetrapod tracks in laboratory and field: *Palaeogeography, Palaeoclimatology, Palaeoecology* 231: 253 – 264.

Milan, J., Bromley, R. G., Titschack, J. & Theodorou, G. 2007. A diverse vertebrate ichnofauna from a Quaternary eolian oolite from Rhodes, Greece. In: Bromley, R. G., Buatois, L. A., Mángano, M. G., Genise, J. F. & Melchor, R. N. (eds) *Sediment-Organism Interactions: A Multifaceted Ichnology.* SEPM Special Publications 88: 332 – 343.

Milàn, J., Theodorou, G., Loope, D.B., Panayides, I., Clemmensen, L.B. & Gkioni, M. 2015. Vertebrate tracks in Late Pleistocene–Early Holocene (?) carbonate aeolianites, Paphos, Cyprus. *Annales Societatis Geologorum Poloniae* 85(3): 507 – 514.

Miller, W.R. & Mason, T.R. 1994. Erosional Features of Coastal Beachrock and Aeolianite Outcrops in Natal and Zululand. *Journal of Coastal Research* 10: 374 – 394.

Miller, D.E., Yates, R.J., Parkington, J.E. & Vogel, J.C. 1993. Radiocarbon-dated evidence relating to a mid-Holocene relative high sea-level on the south-western Cape coast, South Africa. *South African Journal of Science* 89: 35 – 44.

Miller, G.H., Beaumont, P.B., Deacon, H.J., Brooks, A.S., Hare, P.E. & Jull, A.J.T. 1999. Earliest modern humans in southern Africa dated by isoleucine epimerization in ostrich eggshell. *Quaternary Science Reviews* 18: 1537 – 1548.

Milliman, J.D. 1974. *Marine Carbonates*. Berlin: Springer-Verlag.

Milo, R.G. 1998. Evidence for hominid predation at Klasies River Mouth, South Africa, and its implications for the behaviour of early modern humans. *Journal of Archaeological Science* 25: 99 – 133.

Moore, C.H. 1973. Intertidal carbonate cementation in Grand Cayman, West Indies. *Journal of Sedimentary Petrology* 43: 591 – 602.

Moore, C.H. 1989. *Carbonate Diagenesis and Porosity*. Developments in Sedimentology 46. Amsterdam: Elsevier.

Moslow, T.F., 1984. *Depositional models of shelf and shoreline sandstones* (No. 27). Tulsa: American Association of Petroleum Geologists.

Mountain, E.D. 1945. The geology of East London, CP. *South African Journal of Geology* 48: 31 – 42.

Mountain, E.D. 1966. Footprints in calcareous sandstone of Nahoon Point. *South African Journal of Science* 66: 103 – 111.

Mountain, E.D. 1974. *The Geology of the area around East London, Cape Province: An explanation of sheet map 3227D (East London), 3228C (Kei Mouth)*. Pretoria: Geological Survey.

Mourre, V., Villa, P. & Henshilwood, C.S. 2010. Early use of pressure flaking on lithic artifacts at Blombos Cave, South Africa. *Science* 330: 659 – 662.

Muller, G. 1971. Petrology of the Cliff Limestone (Holocene) North Bimini, The Bahamas. *Neues Jarhbuch für Mineralogie Monatschefte* 11: 507 – 523.

Murray-Wallace, C.V. & Woodroffe, C.D. 2014. *Quaternary sea level changes: A global perspective*. Cambridge: Cambridge University Press.

Namikas, S.L. & Sherman, D.J. 1995. A review of the effects of surface moisture content on aeolian sand transport. In: Tchakerian, V.P. (ed) *Desert Aeolian Processes*. London: Chapman and Hall Ltd. 269 – 293.

NEEM Community Members. 2013. Eemian interglacial reconstructed from a Greenland folded ice core. *Nature* 493: 489 – 494.

Nel, R. McLachlan, A. & Winter, D.P.E. 2001. The effect of grain size on the burrowing of two *Donax* species. *Journal of Experimental Marine Biology and Ecology* 265: 219 – 238.

Neumann, A.C. & Hearty, P.J. 1996. Rapid sea-level changes at the close of the Last Interglacial (stage 5e) recorded in Bahamian Island geology. *Geology* 24: 775 – 778.

Neumeier, U. 1998. *The Role of Microbial Activity in Early Cementation of Beachrocks (Intertidal Sediments)*. Unpublished PhD thesis. University of Geneva.

Neumeier, U. 1999. Experimental modelling of beachrock cementation under microbial influence. *Sedimentary Geology* 126: 35 – 46.

Nicholl, J.A.L., Hodell, D.A., Naafs, B.D.A., Hillaire-Marcel, C., Channell, J.E.T. & Romero, O.E. 2012. A Laurentide outburst flooding event during the last interglacial period. *Nature Geoscience* 5: 901 – 904.

Nichols, G. 2009. *Sedimentology and stratigraphy*, second edition. Oxford: Wiley-Blackwell.

Oak, H.L. 1984. The boulder beach: a fundamentally distinct sedimentary assemblage. *Annals of the Association of American Geographers* 74(1): 71 – 82.

O'Leary, M.J., Hearty, P.J., Thompson, W.G., Raymo, M.E., Mitrovica, J.X. & Webster, J.M. 2013. Ice sheet collapse following a prolonged period of stable sea level during the last interglacial. *Nature Geoscience* 6(9): 1 – 5.

Omoto, K. 2004. Radiocarbon ages and isotope fractionations of beachrock samples collected from the Nansei Islands, southwestern Japan. *Radiocarbon* 46(2): 539 – 550.

Orford, J.D., Carter, R.W. & Jennings, S.C. 1991. Coarse clastic barrier environments: evolution and implications for Quaternary sea level interpretation. *Quaternary International* 9: 87 – 104.

Parkington, J.E. 2003. Moderns and middens: shellfishing and the Middle Stone Age of the Western Cape. *South African Journal of Science* 99: 243 – 247.

Pettijohn, F.J., Potter, P.E. & Siever, R. 1973. *Sand and Sandstones*. New York: Springer Verlag.

Plummer, L.N. 1975. Mixing of seawater with calcium carbonate groundwater. In: Whitten, H.T. (ed) *Quantitative Studies in the Geological Sciences*. Geological Society of America Memoirs 142: 219 – 236.

Porat, N. & Botha, G. 2008. The luminescence chronology of dune development on the Maputaland coastal plain, southeast Africa. *Quaternary Science Reviews* 27: 1024 – 1046.

Postma, G. & Nemec, W. 1990. Regressive and transgressive sequences in a raised Holocene gravelly beach, southwestern Crete. *Sedimentology* 37(5): 907 – 920.

Potter, P.E. & Pettijohn, F.J. 1962. Paleocurrents and paleogeography. *AAPG Bulletin* 46(8): 1468 – 1493.

Potter, P.E. & Pettijohn, F.J. 1977. *Paleocurrents & Basin Analysis*, second edition. Berlin: Springer-Verlag.

Potts, A.J., Bond, W.J. & Cowling, R.M. 2015. Understanding biome boundaries in South Africa. *South African Journal of Botany* 101: 1 – 4.

Pye, K. 1983. Coastal dunes. *Progress in Physical Geography* 7: 531 – 557.

Railsback, L.B., Gibbard, P.L., Head, M.J., Voarintsoa, N.R.G. & Toucanne, S. 2015. An optimized scheme of lettered marine isotope substages for the last 1.0 million years, and the climatostratigraphic nature of isotope stages and substages. *Quaternary Science Reviews* 111: 94 – 106.

Ramsay, P.J. 1991. *Sedimentology, coral reef zonation, and late Pleistocene coastline models of the Sodwana Bay continental shelf, northern Zululand*. Unpublished PhD thesis. University of Natal.

Ramsay, P.J. 1995. 9000 years of sea-level change along the southern African coastline. *Quaternary International* 31: 71 – 75.

Ramsay, P.J. & Cooper, J.A.G. 2002. Late Quaternary sea-level change in South Africa. *Quaternary Research* 57: 82 – 90.

Ranwell, D. 1959. Newborough Warren, Anglesey: I. The dune system and dune slack habitat. *The Journal of Ecology* 47(3): 571 – 601.

Reading, H.G. & Collinson, J.D. 1996. Clastic coast. In: Reading, H.G. (ed) *Sedimentary environments: Processes, facies and stratigraphy, third edition.* Malden, MA: Blackwell: 154 – 231.

Rector, A.L. & Reed, K.E. 2010. Middle and late Pleistocene faunas of Pinnacle Point and their paleoecological implications. *Journal of Human Evolution* 59(3-4): 340 – 357.

Reddering, J.S.V. & Esterhuysen, K. 1987. The effects of river floods on sediment dispersal in small estuaries: a case study from East London. *South African Journal of Geology* 90(4): 458 – 470.

Reeckman, S.A. & Gill, E.D. 1981. Rates of vadose diagenesis in Quaternary dune and shallow marine calcarenites, Warrnambool, Victoria, Australia. *Sedimentary Geology* 30(3): 157 – 172.

Reynard, J., Van Pletzen-Vos, L. & Wurz, S. 2017. The human-environmental relationship at Klasies River during MIS 5c-e. *2017 Conference of the Association for Southern African Professional Archaeologists (ASAPA). Pretoria, 5 – 7 July.*

Roberts, D.L. 2008. Last Interglacial Hominid and Associated Vertebrate Fossil Trackways in Coastal Eolianites, South Africa. *Ichnos* 15: 190 – 207.

Roberts, D.L. & Berger, L. 1997. Last interglacial (c.117 kyr) human footprints from South Africa. *South African Journal of Science* 93: 349 – 350.

Roberts, D. L., Botha, G. A., Maud, R. R. & Pether, J. 2006. Coastal Cenozoic deposits. In: Johnson, M. R., Anhaeusser, C. R. & Thomas, R. J. (eds) *The Geology of South Africa.* Johannesburg: Council for Geoscience: 605 – 628.

Roberts, D.L., Bateman, M.D., Murray-Wallace, C.V., Carr, A.S. & Holmes, P.J. 2008. Last interglacial fossil elephant trackways in coastal eolianites, Still Bay, South Africa. *Palaeogeography, Palaeoclimatology, Palaeoecology* 257: 261 – 279.

Roberts, D.L., Bateman, M.D., Murray-Wallace, C.V., Carr, A.S. & Holmes, P.J. 2009. West coast dune plumes: climate driven contrasts in dunefield morphogenesis along the western and southern South African coasts. *Palaeogeography, Palaeoclimatology, Palaeoecology* 271: 24 – 38.

Roberts, D.L., Karkanas, P., Jacobs, Z., Marean, C.W. & Roberts, R.G. 2012. Melting ice sheets 400,000 yr ago raised sea level by 13 m: Past analogue for future trends. *Earth and Planetary Science Letters* 357: 226 – 237.

Roberts, D., Cawthra, H. & Mesekiwa, C. 2014. Dynamics of late Cenozoic aeolian deposition along the South African coast: a record of evolving climate and ecosystems. In: Martini, I. P. & Wanless, H. R. (eds) *Sedimentary Coastal Zones from High to Low Latitudes: Similarities and Differences.* Geological Society Special Publication 338: 353 – 387.

Roep, T.B. 1986. Sea-level markers in coastal barrier sands: examples from the North Sea coast. In: van de Plassche, O. (ed) *Sea-Level Research.* Dordrecht: Springer: 97 – 128.

Rohling, E.J., Grant, K., Bolshaw, M., Roberts, A.P., Siddall, M., Hemleben, C. & Kucera, M. 2009. Antarctic temperature and global sea level closely coupled over the past five glacial cycles. *Nature Geoscience* 2: 500 – 504.

Romano, M. 2015. Reviewing the term uniformitarianism in modern Earth sciences. *Earth Science Reviews* 148: 65 – 76.

Rossetti, D.D.F. 1999. Soft-sediment deformation structures in late Albian to Cenomanian deposits, São Luís Basin, northern Brazil: evidence for palaeoseismicity. *Sedimentology* 46(6): 1065 – 1081.

Rowe, M.P. & Bristow, C.S. 2015. Landward-advancing Quaternary eolianites of Bermuda. *Aeolian Research* 19: 235 – 249.

Rubin, D.M. & Hunter, R.E. 1982. Bedform climbing in theory and nature. *Sedimentology* 29(1): 121 – 138.

Russell, R.J. 1963. Beach rock. *Journal of Tropical Geography* 17: 24 – 27.

Rust, I.C., Esterhuysen, K. & Reddering, J.S.V. 1985. *Sedimentation in the Nahoon Estuary. Research on sedimentation in estuaries*. *ROSIE Report* No*.* 10. Port Elizabeth: Department of Geology, University of Port Elizabeth.

Rutherford, M.C., Mucina, L. & Powrie, L.W. 2006. Biomes and bioregions of southern Africa. *Strelitzia* 19: 30 – 51.

Salzmann, L., Green, A. & Cooper, J.A.G. 2013. Submerged barrier shoreline sequences on a high energy, steep and narrow shelf. *Marine Geology* 346: 366 – 374.

Schmalz, R.F. 1971. Formation of beachrock at Eniwetok Atoll. In: Bricker, O.P. (ed) *Carbonate Cements.* Baltimore: Johns Hopkins Press: 17 – 24.

Schroeder, J.H. 1988. Spatial variations in the porosity development of carbonate sediments and rocks. *Facies* 18: 181 – 204.

Shackleton, N.J. 1969. The last interglacial in the marine and terrestrial records. *Proceedings of the Royal Society B* 174(1034): 135 – 154.

Shackleton, N.J. 1982. Stratigraphy and chronology of the Klasies River Mouth deposits: oxygen isotope evidence. In: Singer, R. & Wymer, J. (eds) *The Middle Stone Age at Klasies River Mouth in South Africa.* Chicago: University of Chicago Press: 194 – 199.

Shackleton, N.J., Sánchez Goñi, M., Pailler, D. & Lancelot, Y. 2003. Marine Isotope Substage 5e and the Eemian Interglacial. *Global and Planetary Change* 36: 151 – 155.

Shaw, A., Holmes, P. & Rogers, J. 2001. Depositional landforms and environmental change in the headward vicinity of Dias Beach, Cape Point. *South African Journal of Geology* 104: 101 – 114.

Shea, J.J. 1999. Artifact abrasion, fluvial processes, and “living floors” from the Early Paleolithic site of’Ubeidiya (Jordan Valley, Israel). *Geoarchaeology* 14(2): 191 – 207.

Shillito, L.M., Almond, M.J., Nicholson, J., Pantos, M. & Matthews, W. 2009. Rapid characterisation of archaeological midden components using FT-IR spectroscopy, SEM–EDX and micro-XRD. *Spectrochimica Acta Part A: Molecular and Biomolecular Spectroscopy* 73(1): 133 – 139.

Shipp, R.C. 1984. Bedforms and depositional sedimentary structures of a barred nearshore system, eastern Long Island, New York. In: Greenwood, B. & Davis, R.A. (eds) *Hydrodynamics in Wave-Dominated Coastal Environments*. Developments in Sedimentology 39: 235 – 259.

Siddall, M., Chappell, J. & Potter, E-K. 2007. Eustatic sea level during past interglacials. *Developments in Quaternary Sciences* 7: 75 – 92.

Sink, K.J., Branch, G.M. & Harris, J.M. 2005. Biogeographic patterns in rocky intertidal communities in KwaZulu-Natal, South Africa. *African Journal of Marine Science* 27(1): 81 – 96.

Skinner, J.D. & Chimimba, C.T. 2005. *The mammals of the southern African sub-region.* Cape Town: Cambridge University Press.

Skrivanek, A., Li, J. & Dutton, A. 2018. Relative sea-level change during the Last Interglacial as recorded in Bahamian fossil reefs. *Quaternary Science Reviews* 200: 160 – 177.

Smith, B.C. 2011. *Fundamentals of Fourier Transform Infrared Spectroscopy*. Boca Raton: CRC Press.

South African Weather Service. 2012. Climate data: East London, viewed January 2017, from https://web.archive.org/web/20120304032441/http://old.weathersa.co.za/Climat/Climstats/EastLondonStats.jsp

Sperazza, M., Moore, J.N. & Hendrix, M.S. 2004. High-resolution particle size analysis of naturally occurring very fine-grained sediment through laser diffractometry. *Journal of Sedimentary Research* 74(5): 736 – 743.

Steele, T. & Klein, R.G. 2008. Intertidal shellfish use during the Middle and Later Stone Age of South Africa. *Archaeofauna* 17: 63 – 76.

Steele, T. & Klein, R.G. 2009. Late Pleistocene subsistence strategies and resource intensification in Africa. In: Hublin, J.-J. & Richards, M.P. (eds) *The Evolution of Hominin Diets: Integrating Approaches to the Study of Palaeolithic Subsistence.* New York: Springer: 113 – 126.

Stephenson, W.J. 2000. Shore platforms: a neglected coastal feature? *Progress in Physical Geography* 24(3): 311 – 327.

Stoops, G. 2003. *Guidelines for the analysis and description of soil and regolith thin sections*. Madison, Wisconsin: Soil Science Society of America.

Stynder, D.D. 1997. The use of faunal evidence to reconstruct site history and Hoedjiespunt 1 (HDP1), Western Cape. Unpublished MA Dissertation, University of Cape Town.

Swales, A., Oldman, J.W. & Smith, K. 2006. Bedform geometry on a barred sandy shore. *Marine Geology* 226(3-4): 243 – 259.

Tankard, A.J. 1976. The Pleistocene history and coastal morphology of the Ysterfontein-Elands Bay area, Cape Province. *Annals of the South African Museum* 69: 73 – 119.

Texier P.-J., Porraz, G., Parkington, J.E., Rigaud, J.-P., Poggenpoel, C., Miller, C.E., Tribolo, C., Cartwright, C., Coudenneau, A., Klein, R.G., Steele, T. & Verna, C. 2010. Howiesons Poort tradition of engraving ostrich eggshell containers dated to 60,000 years ago at Diepkloof Rock Shelter, South Africa. *Proceedings of the National Academy of Sciences of the United States of America* 107: 6180 – 6185.

Thackeray, J.F. 1988. Molluscan fauna from Klasies River, South Africa. *South African Archaeological Bulletin* 43 (147): 27 – 32.

Thackeray, A.I. 1992. The Middle Stone Age south of the Limpopo River. *Journal of World Prehistory* 6: 385 – 431.

Theron, A.K. *Sediment Transport Regime at East London*. Unpublished M.Eng Thesis. University of Stellenbosch.

Thompson, J.C. 2010. Taphonomic analysis of the Middle Stone Age faunal assemblage from Pinnacle Point Cave 13B, Western Cape, South Africa. *Journal of Human Evolution* 59: 321 – 339.

Thompson, J.C. & Henshilwood, C.S. 2011. Taphonomic analysis of the Middle Stone Age larger mammal faunal assemblages from Blombos Cave, Southern Cape, South Africa. *Journal of Human Evolution* 60: 746 – 767.

Thompson, W.G., Curran, H.A., Wilson, M.A. & White, B. 2011. Sea-level oscillations during the last interglacial highstand recorded by Bahamas corals. *Nature Geoscience* 4(10): 684 – 687.

Tinley, K.L. 1985. *Coastal dunes of South Africa. South African National Scientific Programmes report 109.* Pretoria: CSIR.

Toffolo, M.B., Brink, J.S., van Huyssteen, C. & Berna, F. 2017. A microstratigraphic reevaluation of the Florisbad spring site, Free State Province, South Africa: Formation processes and paleoenvironment. *Geoarchaeology* 32(4): 456 – 478.

Tsoar, H. 2001. Types of aeolian sand dunes and their formation. In: Balmforth, N.J. & Provenzale, A. (eds) *Geomorphological fluid mechanics.* Berlin: Springer: 403 – 429.

Tucker. M. 1986. *The field description of sedimentary rocks*. Geological Society of London Handbook Series. Milton Keynes: John Wiley & Sons.

Tucker, M.E. & Bathurst, R.G.C. 1990a. Marine diagenesis: modern and ancient. In: Tucker, M.E. & Bathurst, R.G.C. (eds) *Carbonate Diagenesis.* Oxford: Blackwell Scientific Publications: 1 – 9.

Tucker, M.E. & Bathurst, R.G.C. 1990b. Meteoric diagenesis. In: Tucker, M.E. & Bathurst, R.G.C. (eds) *Carbonate Diagenesis.* Oxford: Blackwell Scientific Publications: 181 – 183.

Tucker M.E. & Wright V.P. 1990. *Carbonate Sedimentology*. Oxford: Blackwell Scientific Publications.

Underhill, D. 2011. The study of the Fauresmith: A review. *The South African Archaeological Bulletin* 66: 15 – 26.

Van Andel, T.H. 1989. Late Pleistocene sea levels and the human exploitation of the shore and shelf of southern South Africa. *Journal of Field Archaeology* 16(2): 133 – 155.

Van Niekerk, K.L. 2011. Marine Fish Exploitation during the Middle and Later Stone Age of South Africa. Unpublished Ph.D. Thesis. University of Cape Town.

Van Pletzen, L. 2000. *The large mammal fauna from Klasies River*. Unpublished MA dissertation, University of Stellenbosch.

Vieira, M.M. & De Ros, L.F. 2006. Cementation patterns and genetic implications of Holocene beachrocks from northeastern Brazil. *Sedimentary Geology* 192: 207 – 230.

Villa, P., Soressi, M., Henshilwood, C.S. & Mourre, V. 2009. The Still Bay points of Blombos Cave (South Africa). *Journal of Archaeological Science* 36: 441 – 460.

Vogel, J.C. 2001. Radiometric dates for the Middle Stone Age in South Africa. In: Tobias, P.V., Raath, M.A., Maggi-Cecchi, J. & Doyle, G.A. (eds) *Humanity from African Naissance to Coming Millennia-Colloquia in Human Biology and Palaeoanthropology.* Florence: Florence University Press: 261–268.

Vogel, J.C., Wintle, A.G. & Woodborne, S.M. 1999. Luminescence dating of coastal sands: overcoming changes in environmental dose rate. *Journal of Archaeological Science* 26: 729 – 733.

Vogel, J.C., Wintle, A.G. & Woodborne, S.M. 2002. Reply to comment by D.J. Huntley on ‘‘Luminescence dating of coastal sands: overcoming changes in environmental dose rate’’ by J.C. Vogel, A.G. Wintle and S.M. Woodborne. *Journal of Archaeological Science* 29: 561.

Von den Driesch, A. 2004. The middle stone age fish fauna from the Klasies River main site, South Africa. *Anthropozoologica* 39 (2): 33 – 59.

Vousdoukas, M.I., Velegrakis, A.F. & Plomaritis, T.A. 2007. Beachrock occurrence, characteristics, formation mechanisms and impacts. *Earth-Science Reviews* 85: 23 – 46.

Wiles, E., Green, A.N. & Cooper, J.A.G. 2018. Rapid beachrock cementation on a South African beach: Linking morphodynamics and cement style. *Sedimentary Geology* 378: 13 – 18.

Williams, A.T. & Caldwell, N.E. 1988. Particle size and shape in pebble-beach sedimentation. *Marine Geology* 82(3-4): 199 – 215.

Wadley, L. 1993. The Pleistocene Later Stone Age south of the Limpopo River. *Journal of World Prehistory* 7(3): 243 – 296.

Wadley, L. 2001. What is cultural modernity? A general view and a South African perspective from Rose Cottage Cave. *Cambridge Journal of Archaeology* 11: 201 – 221.

Wadley, L. 2010. Were snares and traps used in the Middle Stone Age and does it matter? A review and a case study from Sibudu, South Africa. *Journal of Human Evolution* 58: 179 – 192.

Wadley, L. 2015. Those marvellous millennia: the Middle Stone Age of Southern Africa. *Azania: Archaeological Research in Africa* 50: 155 – 226.

Wadley, L., Williamson, B. & Lombard, M. 2004. Ochre in hafting in Middle Stone Age southern Africa: a practical role. *Antiquity* 78(301): 661 – 675.

Wadley, L., Hodgskiss, T. & Grant, M. 2009. Implications for complex cognition from the hafting of tools with compound adhesives in the Middle Stone Age, South Africa. *Proceedings of the National Academy of Sciences of the United States of America* 106: 9590 – 9594.

Walker, M., Johnsen, S., Rasmussen, S.O., Popp, T., Steffensen, J.P., Gibbard, P., Hoek, W., Lowe, J., Andrews, J., Björck, S. & Cwynar, L.C. 2009. Formal definition and dating of the GSSP (Global Stratotype Section and Point) for the base of the Holocene using the Greenland NGRIP ice core, and selected auxiliary records. *Journal of Quaternary Science* 24(1): 3 – 17.

Walter, R.C., Buffler, R.T., Bruggemann, J.H., Guillaume, M.M.M., Behre, S.M., Negassi, B., Libsekal, Y., Cheng, H., Edwards, R.L., von Cosel, R., Neraudeau, D. & Gagnon, M. 2000. Early human occupation of the Red Sea coast of Eritrea during the last interglacial. *Nature* 405: 65 – 69.

Wang, Q., Tobias, P.V., Roberts, D.L. & Jacobs, Z. 2008. A re-examination of a human femur found at the Blind River Site, East London, South Africa: Its age, morphology, and breakage pattern. *Anthropological Review* 71: 43 – 61.

Ward, W.C. 1973. Influence of climate on the early diagenesis of carbonate eolianites. *Geology* 1: 171 – 174.

Ward, W.C. 1975. Petrology and diagenesis of carbonate eolianites of north eastern Yucatan Peninsula. *American Association of Petroleum Geologists Studies in Geology* 2: 500 – 571.

Watts, N.L. 1980. Quaternary pedogenic calcrete from the Kalahari (southern Africa): mineralogy, genesis and diagenesis. *Sedimentology* 27: 661 – 686.

Watts, I. 2009. Red ochre, body-painting, and language: interpreting the Blombos ochre. In: Botha, R & Knight, C (eds) *The Cradle of Language.* Oxford: Oxford University Press: 62 – 92.

Watts, I. 2010. The pigments from Pinnacle Point Cave 13B, Western Cape, South Africa. *Journal of Human Evolution* 59: 392 – 411.

Weaver, T.D., Steele, T. & Klein, R.G. 2011. The abundance of eland, buffalo, and wild pigs in Middle and Later Stone Age sites. *Journal of Human Evolution* 60: 309 – 314.

Webb, G.E., Jell, J.S. & Baker, J.C. 1999. Cryptic intertidal microbialites in beachrock, Heron Island, Great Barrier Reef: implications for the origin of microcrystalline beachrock cement. *Sedimentary Geology* 126(1–4): 317 – 334.

Weiner, S., Goldberg, P. & Bar-Yosef, O. 2002. Three-dimensional distribution of minerals in the sediments of Hayonim Cave, Israel: diagenetic processes and archaeological implications. *Journal of Archaeological Science* 29(11): 1289 – 1308.

Wells, L.H. 1935. A fossilized human femur from East London. *South African Journal of Science* 32(7): 596 – 600.

Wentworth, C.K. 1922. A Scale of Grade and Class Terms for Clastic Sediments. *The Journal of Geology* 30: 377 – 392.

Whillier, A. 1962. Ocean currents at East London. *Civil Engineering* 4: 1 – 7.

Whittle, G.L., Kendall, C.G.S.C., Dill, R.F. & Rouch, L. 1993. Carbonate cement fabrics displayed: a traverse across the margin of the Bahamas Platform near Lee Stocking Island in the Exuma Cays. *Marine Geology* 110 (3–4): 213 – 243.

Wilkins, J., Schoville, B.J. Brown, K.S. & Chazan, M. 2012. Evidence for early hafted hunting technology. *Science* 338: 942 – 846.

Will, M., Parkington, J.E., Kandel, A.W. & Conard, N.J. 2013. Coastal adaptations and the Middle Stone Age lithic assemblages from Hoedjiespunt 1 in the Western Cape, South Africa. *Journal of Human Evolution* 64: 518 – 537.

Will, M., Kandel, A.W., Kyriacou, K. & Conard, N.J. 2016. An evolutionary perspective on coastal adaptations by modern humans during the Middle Stone Age of Africa. *Quaternary International* 404: 68 – 86.

Wilson, M.A., Curran, H.A. & White, B. 1998. Paleontological evidence of a brief global sea-level event during the last interglacial. *Lethaia* 31(3): 241 – 250.

Wiseman, K.A., Burns, M.E.R. & Vernon, C.J. 1993. *Estuaries of the Cape: Part II: Synopses of available information on individual systems. Report No. 42. Nahoon (CSE 44), Qinira (CSE 45) and Gqunube (CSE 46). CSIR Research Report 441*. Stellenbosch: CSIR.

Wright, P.V. 2007. Calcrete. In: Nash, D.J. & McLaren, S.J. (eds) Geochemical Sediments and Landscapes. Oxford: Blackwell: 10 – 45.

Wurz, S. 1999. The Howiesons Poort backed artefacts from Klasies River: an argument for symbolic behaviour. *The South African Archaeological Bulletin* 54: 38 – 50.

Wurz, S. 2013. Technological trends in the Middle Stone Age of South Africa between MIS 7 and MIS 3. *Current Anthropology* 54(Supplement 8): S305 – S319.

Wurz, S. 2016. Development of the archaeological record during the middle stone age. In: Knight, J. & Grab, S. (eds) *Quaternary Environmental Change in Southern Africa: Physical and Human Dimensions.* Cambridge: Cambridge University Press: 371 – 384.

Zazo, C. 1999. Interglacial sea levels. *Quaternary International* 55(1): 101 – 113.